Investigating novel platelet immunoreceptor ‘CEACAM2’ in contact-dependent events that modulate platelet thrombus formation

By

Musaed Mohammed Alshahrani. BSc, MSc

Submitted in total fulfilment of the requirements of the degree of

Doctor of Philosophy

Discipline of Laboratory Medicine

School of Medical Sciences

College of Science, Engineering and Health

December 2014

RMIT UNIVERSITY

Declaration

I certify that except where due acknowledgement has been made, the work is that of the author alone; the work has not been submitted previously, in whole or in part, to qualify for any other academic award; the content of the thesis/project is the result of work which has been carried out since the official commencement date of the approved research program; any editorial work, paid or unpaid, carried out by a third party is acknowledged; and, ethics procedures and guidelines have been followed.

Name: Musaed Mohammed Alshahrani

Signed:

Date: 12.12.2015

Acknowledgements

I would first like to express my sincere gratitude to my supervisor, Professor Denise E. Jackson, for giving me the opportunity to do my PhD in her laboratory at RMIT University. I would like to thank her for his help, continual guidance and constant encouragement throughout my PhD. I would also like to thank her for being extremely patience while she was teaching me valuable research techniques. Professor Jackson has provided me with invaluable training and skill sets that I will require for my future endeavors. I also would like to thank her for his guidance in designing my research at all times.

I also wish to sincerely thank Dr Cindy O'Malley who co-supervised my PhD project. I sincerely appreciate her help, guidance, advice, and encouragement that she has given me throughout my PhD studies. I would like to thank Dr Fatemeh Moheimani for providing so much help in the earlier half of my PhD candidature. I sincerely thank Professor Sonia Najjar our collaborator from Centre for Diabetes and Endocrine Research, Department of Physiology and Pharmacology, College of Medicine and Life Sciences, University of Toledo, Toledo, USA, for generated *Cc2*$^{-/-}$ mice, supplied the anti-mouse CEACAM2 antibody and her support during my PhD studies.

I would like to thank the great people at Prince Sultan Medical Military City (PSMMC), in particular Maj. Gen. Dr Saeed M. Alasmari (Current Director of General Directorate of Medical Service of the Armed Forces in Saudi Arabia) and Maj. Gen. Dr Humod M. Alshahrani (Current Director of PSMMC) and Maj. Gen. Saleh Alshumrani (Previous Assistant Director of PSMMC for administrative affairs, 2009). I also thank the many other leaders in the PSMMC for nominating and trusting me to pursue my higher degrees and to join the fascinating professionals at PSMMC, and I thank PSMMC and

Ministry of Higher Education in Saudi Arabia for providing me with full funding for my academic and research scholarship. For providing funds to support my attendance at the Platelets 2012 International Conference in USA and the 20th Annual Scientific conference of Australian Vascular Biology Society (AVBS) in Australia, I thank the Laboratory Medicine Department of the School of Medical Sciences and School of Graduate Research at RMIT University.

Not to forget my special friend, sorry he not my special friend only but my closest brother Dr Hussain Aldera for his positive attitude, care, support, encouragement and sincere advices since we were in the undergrad period. So, thanks a lot. I also thank my closest brother Mubarak Alshalan for his constant support and encouragement from when I was in high school until now. I also sincerely appreciate my close relatives and special friends, whose attitudes are so noble and honorable towards me.

My deepest gratitude goes to my family. I am very much indebted to my wife who gave me her full support. She shared every single moment with me throughout my PhD studies, and often took the brunt of my frustrations. I sincerely thank her from the bottom of my heart; thank you for your encouraging, understanding, trust, and belief in me.

Last but certainly not least, I would sincerely like to express my great love, appreciation and gratitude to my parents. To my mother whose love is boundless, and who gave me everything; love, affection, care, and support. She was full of hope that I could do more and more. I will never forget that she didn't sleep till very late at night while I was preparing for my exams. My father was my role model, but sadly he passed away in the second year of my BSc studies. My PhD was his dream. He sacrificed so much for me and taught me courage, honesty, respect, and how to think positively. In late 1996, he said go and do it because you can do it!

Acknowledgment in Arabic Language

بِسْمِ اللَّهِ الرَّحْمَنِ الرَّحِيمِ

(شَهِدَ اللَّهُ أَنَّهُ لَا إِلَهَ إِلَّا هُوَ وَالْمَلَائِكَةُ وَأُولُو الْعِلْمِ قَائِمًا بِالْقِسْطِ لَا إِلَهَ إِلَّا هُوَ الْعَزِيزُ الْحَكِيمُ)

الحمد لله حمدا يليق بجلال ووجهه وعظيم سلطانه، الحمد لله ان منّ علي بفضله و توفيقه و احسانه، الحمد لله ان شرفني و جعلني من المسلمين. و الصلاة والسلام على سيد المرسلين و إمام المعلمين سيدنا محمد المبعوث رحمة للعالمين. اللهم أخرجنا من ظلمات الجهل و الوهم إلى انوار المعرفة و العلم، و من وحول الشهوات إلى جنات القربات.

اما بعد ،

لقد كرم الله عز وجل الانسان (وَلَقَدْ كَرَّمْنَا بَنِي آدَمَ) وفضّله وميزه بنعمة العقل على سائر المخلوقات، بل وخلقه في أحسن خلق (لَقَدْ خَلَقْنَا الْإِنسَانَ فِي أَحْسَنِ تَقْوِيمٍ). ثم امرنا الحق تبارك وتعالى ان نتفكر ونتأمل روعة هذا الخلق البديع اذ يقول سبحانه (وَفِي أَنْفُسِكُمْ أَفَلا تُبْصِرُونَ) و يقول جل شأنه (سَنُرِيهِمْ آيَاتِنَا فِي الْآفَاقِ وَفِي أَنْفُسِهِمْ).

يأتي هذا الأمر الإلهي لأسباب عدة من أهمها أن نتعبد الله عز وجل بالتأمل في صور هذا الإعجاز الإلهي في دقة الوظيفة وتعقيد التركيب لهذا الخلق فتبارك الله احسن الخالقين. والسبب الآخر هو توجيه لأهل العلم بالبحث والتحقيق في التركيب والوظيفة معاً و من ثم تقديم الدواء وإصلاح الإعتلال في حال المرض لعله بعد مشيئة الله يمكن احياء هذه النفس اذ يقول (وَمَنْ أَحْيَاهَا فَكَأَنَّمَا أَحْيَا النَّاسَ جَمِيعاً).

بعد توفيق الله أخترت تخصص الجلطات الدموية بدافع ذاتي وطموح شخصي لغور اسبار هذا العلم في محاوله متواضعة لفهم الجسم البشري من خلال تحليل التعقيد التركيبي وشرح آلية الوظيفة لعلني بهذا استطيع اقتفاء اثر اهل العلم و المعرفة ولسان الحال يلهج بالدعاء والرجاء من المولى عز وجل ان يقبل مني هذا العمل خالصا لوجهه الكريم و أن يمنّ علي ويرحمني و يشملني بمن رفع درجتهم بالإيمان والعلم يوم القاه، يقول جل شأنه (يَرْفَعِ اللَّهُ الَّذِينَ آمَنُوا مِنكُمْ وَالَّذِينَ أُوتُوا الْعِلْمَ دَرَجَاتٍ). فاللهم ارحم ضعفي وعافني واعفو عني، اللهم امين.

إهداء ،،

إلى من أوصاني ربي بهم خيرا، الى من كانت دعواتهما لي في نومي ويقظتي في ليلي ونهاري في صحتي وسقمي خير زاد.

إلى مقام والدي طيب الله ثراه واقول الحمد لله بأن وفقني بوفاء العهد وصدق الوعد.

إلى مقام والدتي والذي يعجز اللسان عن شكرها اطال الله في عمرها على طاعته.

إلى زوجتي الغالية التي تحملت غربتي طوال فترة دراستي.

إلى وطني الشامخ المملكة العربية السعودية ،،،،

Abstract

Platelets are small fragments that are derived from megakaryocytes. They are released into the blood stream, where they prevent excessive blood loss at sites of tissue injury by sticking together and forming a haemostatic plug. However, excessive platelet clumping in diseased blood vessels can lead to blockages and cause thrombotic diseases such as heart attack and stroke In Australia, cardiovascular disease (CVD) and stroke are the two leading causes of death. In 2012, CVD accounted for 30% of all deaths and affected more than 3.72 million Australians [1]. The cost to the Australian community for CVD-associated disability is approximately 7.8 billion dollars per year. In the Aboriginal and Torres Strait Island population, CVD is the most common cause of death [2-4].

CVD is the general term for a class of heart diseases involving heart and blood vessels. Whilst the term commonly refers to any form of disorder affecting the cardiovascular system, it is most typically linked to atherosclerosis. The mortality rates for CVD have increased in the past few years within high-income countries and it is now the leading cause of death in the Western world [5]. Thrombi are formed in response to damage to the endothelial lining of the blood vessels, which causes platelets to clump together and activate at the site of damage. In the pathological sequelae of atherosclerosis, rupture of collagen-rich plaques leads to *in vivo* platelet activation, adhesion and thrombus formation. In a physiological context, Ig-ITIM superfamily members negatively regulate the initial phase of contact-dependent events involving platelet-collagen GPVI interactions, thereby limiting the *in vivo* growth of thrombi. Few examples of naturally occurring inhibitors of platelet-collagen interactions have been described [6]. Prostacyclin and nitrous oxide (NO) are natural inhibitors released from the endothelium [7], while Ig-ITIM members appear to be the first identified natural inhibitors that serve an autoregulatory role when platelets come into contact with each other following exposure to collagen [8].

Platelet adhesion to the vascular endothelium is a crucial component of normal haemostasis and of pathological thrombus formation. Therefore, a full understanding of the regulation of *in vivo* platelet signalling pathways and thrombus formation will depend on elucidation of the nonredundant roles of Ig-ITIM superfamily members, including CEACAM2. These receptors appear to regulate specific intracellular effector pathways and to recognise distinct ligands where localisation may differ. They are also differentially expressed during activation of platelets.

Carcinoembryonic antigen-related cell adhesion molecule-2 (CEACAM2) is a cell surface glycoprotein expressed on blood, epithelial and vascular cells. CEACAM2 possesses adhesive and signalling properties mediated by immunoreceptor tyrosine-based inhibitory motifs. In this study, we demonstrate that CEACAM2 is expressed on the surface and in intracellular pools of platelets. Functional studies of platelets from *Ceacam2*$^{-/-}$ deficient mice (*Cc2*$^{-/-}$) revealed that CEACAM2 serves to negatively regulate collagen GPVI-FcRγ–chain and the C-type lectin-like receptor 2 (CLEC-2) signalling. *Cc2*$^{-/-}$ platelets displayed enhanced GPVI and CLEC-2-selective ligands, collagen related peptide (CRP), collagen and rhodocytin (Rhod)-mediated platelet aggregation. They also exhibited increased adhesion on type I collagen, and hyper-responsive CRP and CLEC-2-induced alpha and dense granule release compared to wild-type platelets. Furthermore, using intravital microscopy to ferric chloride ($FeCl_3$) injured mesenteric arterioles and laser induced injury of cremaster muscle arterioles, we herein show that thrombi formed in *Cc2*$^{-/-}$ mice were larger and more stable than wild-type controls *in vivo.* Thus, CEACAM2 is a novel platelet immunoreceptor that acts as a negative regulator of platelet GPVI-collagen interactions and of ITAM receptor CLEC-2 pathways.

Previous studies have implicated that the Ig-ITIM superfamily member, CEACAM1 may regulate integrin function. As CEACAM2 is the twin of CEACAM1, it is possible that

CEACAM2 may also have a physiologic role in integrin $\alpha_{IIb}\beta_3$-mediated platelet function. In this project, we investigated the functional importance of CEACAM2 in murine platelets. Using *Ceacam2*-deficient mice, we showed that they have prolonged tail bleeding times and volume of blood lost. *Cc2*$^{-/-}$ platelets have moderate integrin $\alpha_{IIb}\beta_3$ mediated functional defects with impaired kinetics of platelet spreading on fibrinogen and type I collagen and delayed kinetics in retraction of fibrin clots *in vitro*. This functional integrin $\alpha_{IIb}\beta_3$ defect could not be attributed to altered integrin $\alpha_{IIb}\beta_3$ expression. *Cc2*$^{-/-}$ platelets displayed normal 'inside-out' signalling properties as demonstrated by normal agonist-induced binding of soluble FITC-fibrinogen and JON/A antibody binding. This project provides direct evidence that CEACAM2 is essential for normal integrin $\alpha_{IIb}\beta_3$-mediated platelet function and that disruption of mouse CEACAM2 induced a moderate integrin $\alpha_{IIb}\beta$3-mediated platelet functional defects.

Based on these results, it appears likely that CEACAM2 functions in similar way to its closely related family member, CEACAM1. Therefore, CEACAM2 can be viewed as a novel platelet immunoreceptor that act as a negative regulator of platelet-collagen interactions and as a positive regulator of integrin $\alpha_{IIb}\beta$3-mediated platelet functions.

Publications and awards arising from this thesis

I. Published scientific papers:

- **Alshahrani, M.,** Yang, E., Yip, J., Ghanem, S., Abdallah, S., deAngelis, A., O'Malley, C., Moheimani, F., Najjar, S. and Jackson, D. E. CEACAM2 negatively regulates hemi (ITAM-bearing) GPVI and CLEC-2 pathways and thrombus growth *in vitro* and *in vivo*. **Blood.** 2014;124(15):2431-2441.

- **Alshahrani, M.,** Najjar, S. and Jackson, D. E. The Ig-ITIM superfamily CEACAM2 positively regulates integrin $\alpha_{IIb}\beta_3$–mediated function in platelets. Thrombosis and Haemostasis, 2015 **(In press).**

- Yip J., **Alshahrani M.,** Beauchemin N., and Jackson D. E. CEACAM1 regulates integrin $\alpha_{IIb}\beta_3$–mediated functions in platelets. Platelets, 2015 **(Accepted June, 2015).**

II. Awards:

- **Alshahrani, M.,** Yang, E., Yip, J., Ghanem, S., Abdallah, S., deAngelis, A., O'Malley, C., Moheimani, F., Najjar, S. and Jackson, D. E. CEACAM2 negatively regulates hemi (ITAM-bearing) GPVI and CLEC-2 pathways and thrombus growth *in vitro* and *in vivo*. **Blood.** 2014;124(15):2431-2441.

  Award type: Excellence in Postgraduate Research Publications.

- **Alshahrani, M.,** Yang, E., Yip, J., Moheimani, F., Najjar, S. and Jackson, D. CEACAM2 regulates platelet-collagen interactions and thrombus growth *in vitro* and *in vivo* (Abstract: The Australian Vascular Biology Society (AVBS) 20th Annual Scientific conference, Gold Coast, Australia, 2012).

  Award type: Best oral presentation prize.

Accepted conference abstracts

I. International conference:

- Platelet International Conference (from June 7th -11th, 2012) held at Endicott College, Beverly, Massachusetts, USA.

Contribution type: Oral and poster presentation.

II. National and local conferences:

- The Australian Vascular Biology Society (AVBS) 20th Annual Scientific conference (September 13th – 16th, 2012) held at Hyatt Sanctuary Cove, Gold Coast, Australia.

Contribution type: Oral and poster presentation.

- Higher Degree Research Student Conference (Friday 19th October, 2012) held at RMIT University, Bundoora West campus, Melbourne, Australia.

Contribution type: Oral and poster presentation.

- Higher Degree Research Student Conference 2011 (Friday 21 October, 2011) at RMIT University, Bundoora West campus, Melbourne, Australia.

Contribution type: Poster presentation.

Abbreviations

ADP	Adenosine diphosphate
ANOVA	Analysis of variance
BSA	Bovine serum albumin
CEACAM	Carcinoembryonic antigen-related cell adhesion molecule
CLEC-2	C-type lectin-like receptor 2
cM	Centimorgan
CNBr	Cyanogen bromide
CPD	Critical point drying
CRP	Collagen related peptide
DAG	Diacylglycerol
DIC	Differential interference contrast
DMSO	Dimethyl sulfoxide
ECL	Enhanced chemiluminescence
ECM	Extra-cellular matrix
EDTA	Ethylenediamine tetra-acetic acid
FACS	Flow activated cell sorting
FcR	Fc receptor
$FeCl_3$	Ferric chloride
FITC	Fluorescein isothiocyanate
GP	Glycoprotein
GPCRs	G-protein coupled receptors

GPVI	Glycoprotein VI
HCl	Hydrochloric acid
HRP	Horseradish peroxidase
Ig	Immunoglobulin
IP	Immunoprecipitation
IP_3	Inositol-1,4,5-trisphosphate
ITAM	Immunoreceptor tyrosine based activation motif
ITIM	Immunoreceptor tyrosine based inhibition motif
ITSM	Immunoreceptor tyrosine based switch motif
IVM	Intravital microscopy
kDa	Kilodalton
KO or -/-	Knockout
LAT	Linker for activation of T-cells
mAb	Monoclonal antibody
MFI	Mean fluorescence intensity
NRS	Normal rabbit serum
PAR	Protease activated receptor
PBS	Phosphate buffered saline
PECAM-1	Platelet endothelial cell adhesion molecule-1
PGI_1	Prostaglandin I_1
PGS	Protein G sepharose
PKC	Protein kinase C
PLC	Phospholipase C

PMA	Phorbol myristate acetate
PRP	Platelet rich plasma
PPP	Platelet poor plasma
PS	Phosphatidyl serine
PVDF	Polyvinylidene difluoride
RCD	Ringers citrate dextrose
SDS-PAGE	Sodium dodecyl sulphate polyacrylamide gel electrophoresis
SEM	Scanning electron microscope
SH2	Src homology 2
SH3	Src homology 3
SLP-76	SH2 containing leukocyte protein of 76 kDa
TBS	Tris buffered saline
TPO	Thrombopoietin
TXA_2	Thromboxane A2
vWF	von Willebrand factor
WT or +/+	Wild-type
α	Alpha
β	Beta
γ	Gamma
µM	Micromolar

Table of Contents

List of Figures

List of Tables

1 Chapter One: Literature review

1.1 Platelet overview

Platelets are small, disc-shaped cell fragments, derived from a precursor megakaryocyte that circulates in the blood system of mammals [9, 10]. They are required for clot formation, haemostasis and wound healing. Platelets are also involved in angiogenesis both in the embryo and the adult [9, 11]. Insufficiency of platelets, a condition known as thrombocytopenia can lead to excessive bleeding [10]. On the other hand, platelets are involved in diseases such as thrombophlebitis and atherosclerosis [12, 13]. Interestingly, the angiogenic properties of platelets, were found to promote metastatic diseases such as spreading of tumours. Anti-platelet therapies are used to prevent excessive clotting and myocardial infarction.

Platelets were first described by Osler as disc-like objects that circulated singly in the blood but quickly aggregated when removed from circulation [14]. At the time Osler was not able to determine whether they were natural blood constituents, or contaminating organisms. Just a few years later, in 1881, Bizzozero reported some important facts about platelets including their importance to haemostasis and their aggregation in areas of damaged blood vessels [15, 16]. In addition, Bizzozero was probably the first to notice bone marrow-derived megakaryocytes, but did not connect them to platelets at the time [16]. However, about 20 years later, Wright showed the similar staining pattern between megakaryocytes and platelets [17]. Wright's stain is one of the Romanowsky stains still used today for the identification of formed elements in the blood.

Platelets are a rich source of growth factors used in wound healing that includes platelet-derived growth factor (PDGF), transforming growth factor beta (TGF-β), insulin-like growth factor 1 (IGF-1), epidermal growth factor (EGF) and vascular endothelial growth factor (VEGF). During the process of clot formation, platelets are shedding and these growth factors are released along with chemotactic signals to induce white blood cell

(WBC) migration to the wound site. Platelet enriched plasma has been used medically to speed the healing of ulcers and other wounds [18, 19].

1.1.1 Platelet formation

The megakaryocytes (MKs), from which platelets are formed, are descended from multi-potent haematopoietic stem cells that give rise to all circulating blood cells [20]. MKs reside in the bone marrow and are the largest (50-100 μm) and also the rarest cell in the bone marrow accounting for approximately 0.01% of all cells [21]. Platelets are released from the MKs after a unique process called endomitosis; where the DNA is replicated many times without division [20]. This is followed by a rapid expansion in the amount of cytoplasm and the elaboration of a membrane demarcation system, as well as the synthesis of granules and proteins necessary for platelet function [22].

Platelets are produced from long cytoplasmic extensions called proplatelets. A detailed model of this process is provided by Italiano [22]. After endomitosis, during cytoplasmic expansion phase, the megakaryocyte synthesises platelet specific proteins and organelles. Microtubules are assembled at the centrosome, radiate out towards the periphery of the cell and then run in parallel with the cell membrane [20]. Before proplatelet formation initiates, the microtubules the cell surface. The microtubules help to form large pseudopods that elongate to become proplatelet processes. Organelles are moved along the microtubule tracks to the ends of the proplatelets where platelets are being assembled. Proplatelets become constricted in places, leading to a beaded appearance. Eventually, almost all of the megakaryocyte cytoplasm is converted into proplatelets [20]. These pinch off, and further subdivide to become individual platelets (Figure 1-1). 2000 to 5000 new platelets are produced per cell when the megakaryocyte cytoplasm is transformed into proplatelets [23]. About 10^{11} platelets are produced per day in the average human with circulating concentration of around 150-400x10^{9}/litre [9, 20]. A reserve pool of platelets is stored in the

spleen-splenectomy was first proposed in 1916 as way of increasing circulating concentrations of platelets [24] and is still used to treat some cases of idiopathic thrombocytopenia purpura.

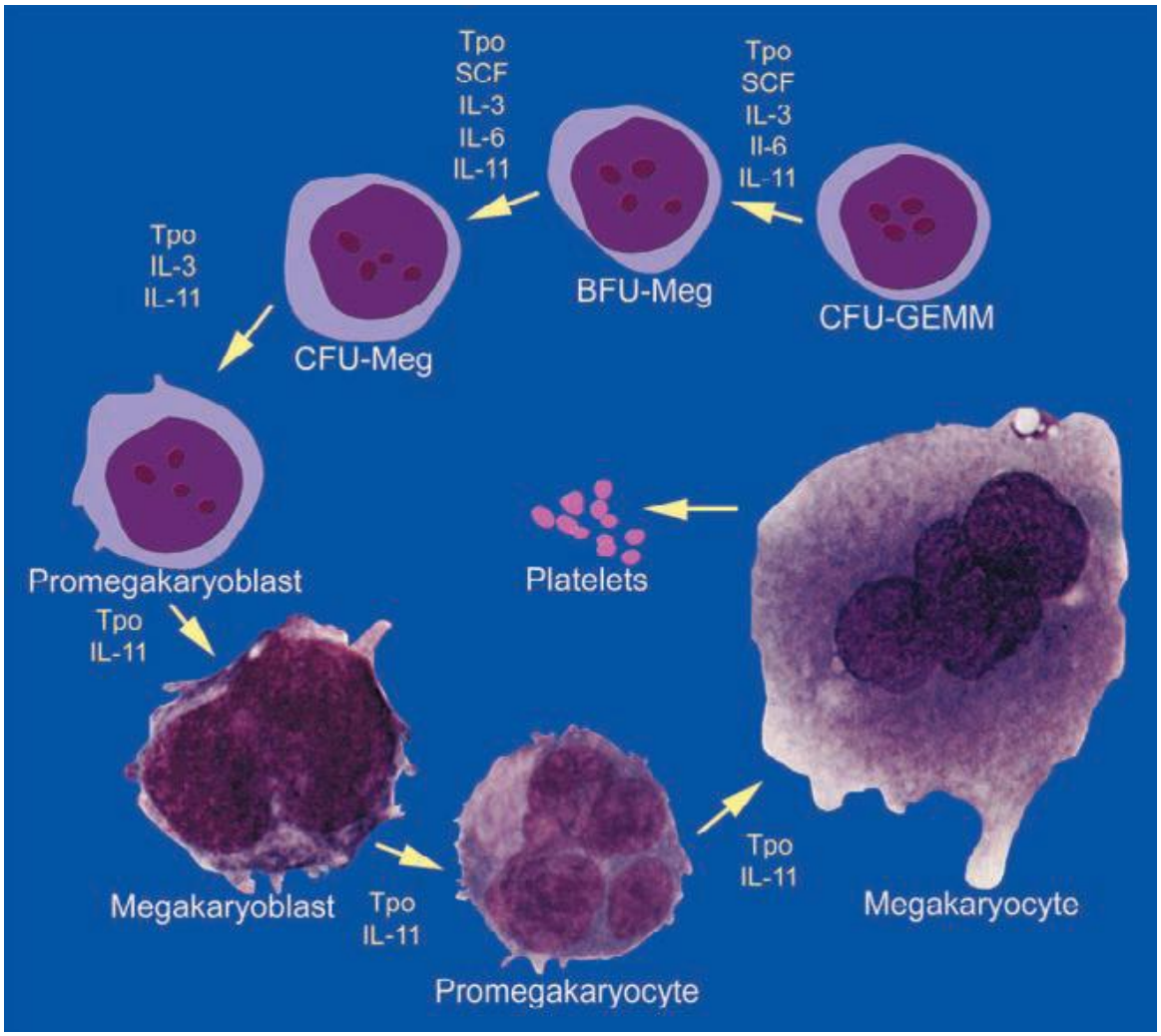

Figure 1-1: Schematic diagram representing the process of platelet development. The burst-forming unit, BFU-Meg is the first cell specifically committed to megakaryocyte development. Thrombopoietin (Tpo) is the principle regulator of platelet production and affects all stages of development. Adapted from [22].

1.1.2 Platelet production and apoptosis

As mentioned, platelets bud off from cytoplasmic extensions called proplatelets [25]. The events leading up to platelet release in megakaryocyte, i.e cytoskeletal reorganisation, ruffling, and membrane condensation, resemble those of a cell undergoing apoptosis [22]. The remnant megakaryocyte does, in fact, undergo apoptosis, but not until after platelet release.

1.1.3 The Process of Apoptosis and Platelet Assembly

In megakaryocytes, the sequence of remodelling events behind platelet formation and release shares a number of functions associated with apoptotic programmed cell death. These areas of overlap include cytoskeletal rearrangement and disruption, and the condensation and ruffling of nuclear and plasma membranes. Naturally, these similarities suggest that apoptosis influences platelet biogenesis in the megakaryocyte progenitors. Apoptosis in degenerating megakaryocytes destroys the cell nuclei [26], and research has suggested that the process affects proplatelet formation and the final release of platelets into the bloodstream. Cell destruction is relatively well understood in the myeloid megakaryocytic cells [27], and there is a positive correlation between the action of apoptosis and cell maturation [28, 29]. In megakaryocytes, previous research identified a number of proapoptotic and antiapoptotic factors distributed according to the maturity of the cell [30]. Megakaryocytes in the early stages of maturation contain a number of apoptosis inhibitor proteins, including Bcl-2 and Bcl-x_L, which restrict the formation of proplatelets [31, 32]. Furthermore, mature blood platelets lack Bcl-2, while aging megakaryocytes lack Bcl-x_L [33], suggesting that apoptosis affects the platelet assembly and release processes in senescent megakaryocytes. Further research into the caspase proteins involved in the formation of proplatelets showed that two members of the family, caspase-3 and caspase-9, are particularly active in mature megakaryocytes, and that blocking these factors restricts

proplatelet development [31]. Similarly, the proapoptotic factor, nitric oxide (NO), is also found in megakaryocytes. In the genetically distinct cell line Meg-01, NO may influence the release of platelet-sized objects, acting in conjunction with a haematopoietic growth factor, thrombopoietin (TPO), to facilitate the expression and release of platelets [34, 35]. Finally, proapoptotic TGF-β_1 and SMAD proteins are also present in megakaryocytes [36]. Further research investigated how these apoptotic factors interact during megakaryocyte and platelet maturation [37]. Caspase-3 and caspase-9 proteins are both active in terminally-differentiated megakaryocytes, but only caspase-3 is found in platelets [37, 38]. Like caspase-9, caspase-12 is present in megakaryocytes but absent in platelets [39]. The changing location and activity of apoptotic factors in megakaryocytes and platelets according to maturation implies variation in the apoptosis mechanisms. During the proplatelet stage of biogenesis, apoptotic factors in younger platelets are modulated.

1.1.4 Platelet anatomy

Platelets are the smallest of circulating cell fragments; they are disc-shaped with a diameter of 2-5 µm, a thickness of 0.5 µm and a volume of only 6-10 femtoliters [9, 16, 40, 41]. Despite their small size, platelets are quite complex. It consists of a plasma membrane, cytoskeletal elements, and a thick external glycocalyx (Figure 1-2). The Sol-Gel zone is the matrix of platelet cytoplasm, responsible for contraction and contains the open canalicular system (OCS), microtubules and microfilaments [42]. The organelle zone has platelet organelles, including mitochondria, lysosomes, alpha granules and glycogen granules, as well as stores of catecholamine, adenosine diphosphate (ADP), serotonin, calcium, platelet factor 4 (PF4), platelet mitogenic factor, fibrinogen, and β-thromboglobulin [43, 44].

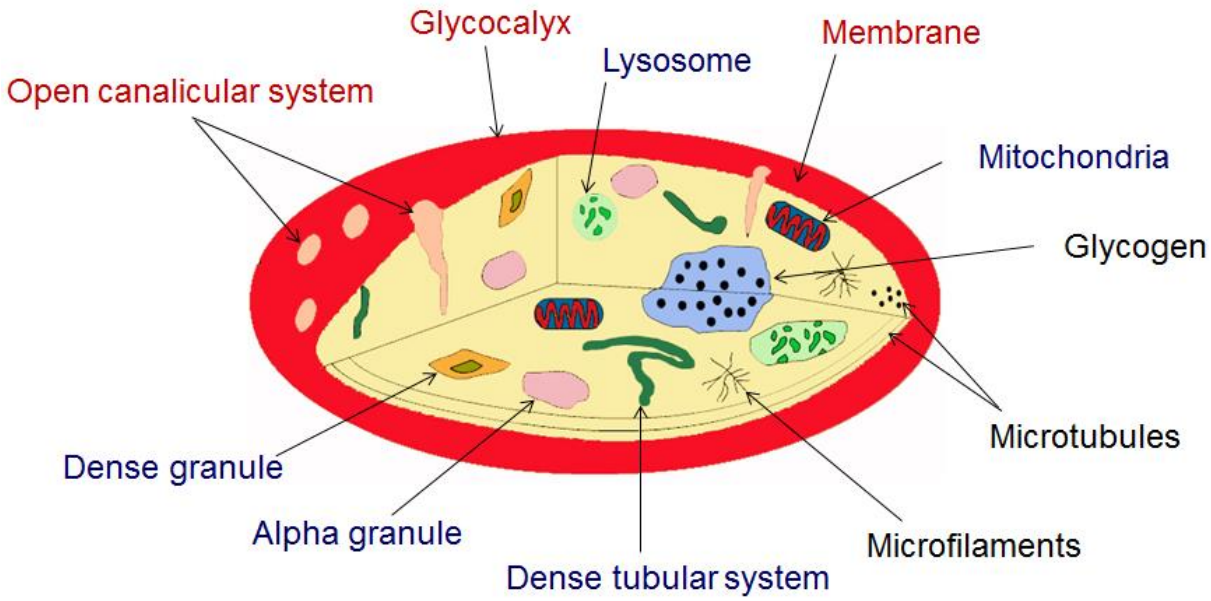

Figure 1-2: Diagrammatic structure of platelets showing different zones including the peripheral zone, the sol-gel zone, and the organelle zone. Platelet structure is depicting the presence of mitochondria, OCS, dense tubular system, microtubules, microfilaments, glycogen, membrane, glycocalyx and lysosome. Also shows the most important platelet granules, alpha and dense granules. Adapted from [45].

1.1.4.1 The Peripheral Zone

The peripheral zone is the outer layer of the disc-like platelets, and includes the plasma membrane, sub-membranous areas, and a thick glycoprotein layer called the glycocalyx.

1.1.4.2 The Plasma Membrane

The plasma membrane of the platelet is derived from the megakaryocyte and is not morphologically distinct from that of other cell types. However, the membrane contains functional features relevant to the role of platelets in initiating haemostasis. Platelets contain tissue factor within cholesterol-rich "islands" within the plasma membrane [40]. Tissue factor initiates clotting by serving as a co-factor for factor VIIa, which converts factor X to

Xa. The latter, in association with Va converts prothrombin to thrombin. This conversion requires an anionic phosphatidyl serine surface found on the unit membrane of platelets. The conversion of tissue factor to an active form seems to require the formation of microparticles on the surface of the membrane [46].

1.1.4.3 The Submembrane Area

The submembrane area is a distinct zone from which platelet organelles are excluded. It is here that the cytoplasmic domains of transmembrane receptors interact. Some of these, including the cytoplasmic portions of GPIIb and GPIIIa, as well as filamin, an actin binding protein that also binds to the GPIb-IX-V complex, are associated with cytoskeletal elements like calmodulin, myosin, and actin filaments [40]. The submembrane area contains an extensive network of cytoplasmic filaments.

1.1.4.4 The Glycocalyx

The glycocalyx is not just a barrier but its dynamic structure is charged with sensing environmental changes that might require a haemostatic response and then initiating aggregation, which promotes thrombus formation. There are about 25,000 copies of GPIb-IX-V complex and about copies of 80,000 integrin $\alpha_{IIb}\beta_3$ on the outside surface and in channels of the open OCS. Both types of receptor are mobile, which is important for their function in haemostasis [40]. Exposure of the subendothelium to the platelet because of a wound in the endothelial layer results in the immediate attachment (from nano to microseconds) of GPIb-IX-V receptor complex to the von Willebrand factor (vWF) that is attached to collagen. Collagen receptors, glycoprotein VI (GPVI) and the integrin $\alpha_2\beta_1$ help make the attachment more stable. The binding of GPIb-IX-V to vWF causes actin filament and cytoskeletal rearrangements in newly attached platelets.

1.1.5 The sol-gel zone

The cytoplasmic matrix is viscous network of fibrous material called the sol-gel zone, in which various organelles are embedded. The following subsections briefly describe the sol-gel zone contents.

1.1.5.1 Microtubules and microfilaments

Platelets contain rings of microtubules located deep in the submembrane region that help to maintain the shape of the resting platelet. When platelets are activated, the microtubules contract into tight rings around clusters of organelles. Surprisingly, the microtubule ring is not actually a network, but a single microtubule that coils on itself many times [40]. Disappearance of the microtubule ring due to low temperatures [47] or treatment with microtubule dissociating drugs, like colchicine [48], result in the loss of the typical discoid shape of the platelet.

In the resting platelet, about 30-40% of actin molecules are assembled into filaments, portions of which are in the sol-gel zone, making up the matrix that surrounds the organelles. In activated platelets, actin in association with myosin makes up contractile filaments which pull on the microtubule ring and drive alpha granules and dense bodies together in the platelet centre. Strong contractions result in the secretion of granule and dense body contents to the outside via the OCS.

1.1.5.2 Glycogen

Glycogen particles are randomly distributed in the sol-gel zone, sometimes encircled by membranes. White [49] has referred to these membrane-bound glycogen particles as glycosomes, a particular organelle involved in glycogen metabolism. Biochemical evidence suggests that platelets can synthesise glycogen given a primer and can also perform glycogenolysis. Some glycogen particles seem to be associated with the OCS.

1.1.6 Organelle zone

The organelle zone contains three types of secretory granules: alpha granules, dense bodies and lysosomes (Table 1). Alpha granules and dense bodies secrete their products after platelet activation by calcium dependent exocytosis. Also present are small mitochondria which provide for the energy needs of the platelet. There are also glycosomes, tubular inclusions as well as multivesicular bodies derived from the Golgi apparatus of the megakaryocyte.

Table 1-1. The contents of organelles of platelets [44].

Granules	Contents of Granule
1. Dense granules	Secretion of ions Guanine: GTP, GDP. Nucleotides: Adenine: ATP, GTP, ADP, GDP Serotonin (Transmitters), Histamine, Bivalent cations, Amines.
2. Alpha-granules	**Adhesion molecules*:*** P-selectin (CD62P), Glycoprotein IIb/IIIa (GPIIb/IIIa, integrin $\alpha_{IIb}\beta_3$, CD41/CD61), Platelet endothelial cell adhesion molecule-1 (PECAM-1/CD31), vWF, Thrombospondin-1 (TSP1), Vitronectin, Fibronectin. **Mitogenic factors*;*** TGF-ß, PDGF, **Protease inhibitors***;* Plasminogen activator inhibitor-1 (PAI-1), Tissue factor pathway inhibitor (TFPI), C1 inhibitor. **Coagulation factors*:*** Fibrinogen, Kininogen, Factors V, VII, XI, XIII.
3. Lysosomes	Glycosidases, Proteases. Cationic proteins. Digestive enzymes. Acid hydrolases, cathepsins D, LAMP-1, LAMP-2 and WAMP-1.
4. Glycosomes	Glycogen.

1.1.6.1 Alpha Granules

Alpha granules are the most numerous of the secretory granules, with about 40 to 80 granules present per platelet, depending on the site of the platelets. The granules are usually oval-shaped and 200-500 nm in diameter. They are more electron dense in the centre than in the periphery. They contain vWF that is generally contained in tube-like inclusions. Alpha granules also contain a bewildering variety of molecules within them, including adhesion factors, chemokines, molecules in the coagulation and fibrinolytic pathways, an array of growth factors, some immunologic molecules including IgG, and others that are not platelet specific, including albumin and histidine-rich glycoprotein [50]. The large number of proteins found in alpha granules lead to speculation that there may be more than one type of alpha granule [51], but so far the alpha granules have resisted functional subdivision. However, there are a so-called giant granules are present some times in normal individuals and can arise by fusion during long term storage of platelets *in vitro*. Giant alpha granules are also characteristic of several disease states of platelets [40, 52, 53]. Using electron tomography to create three-dimensional maps, van Nispen tot Pannerden and colleagues recognised four alpha granule types based on morphological criteria: 1) spherical granules containing 12-nm vWF tubules, 2) subtypes containing many luminal vesicles, 3) 50 nm-wide tubular organelles and 4) a population with 18.4-nm crystalline cross-striations [54]. Clathrin coated areas were noted both on spherical and tubular granules.

1.1.6.2 Dense granules

Dense granules are so named because of an electron dense, nearly opaque spherical centre, which is clearly separated from the surrounding membrane. There are about ten-fold fewer dense bodies relative to alpha granules. Some dense bodies have granule-like particles in the space between the central opacity and membrane and some have filamentous structures radiating from the central core [40]. Though usually ovoid or spherical, some

dense bodies have long tail-like extensions. The electron density of dense bodies is probably due to calcium complexed with pyrophosphate and serotonin. Relative to the alpha granules, they contain fewer proteins and more small molecule secretion products (Table 1). Dense bodies are slightly acidic and contain some membrane proteins usually associated with lysosomes, such as LAMP-2 and LAMP-3, but not LAMP-1 [55, 56].

1.1.6.3 Lysosomes

Lysosomes are formed early in megakaryocyte development, but platelets have a small number of lysosomes, 1-3 per platelet. These lysosomes contain acid hydrolases, cathepsin D and, LAMP-1, LAMP-2, WAMP-1 and stain for acid phosphatase. The functional significance of lysosomes in platelets is unclear. Levin (2007) made the point that some of the nucleated thrombocytes in non-mammalian species have a phagocytic role, so perhaps it is not surprising to find lysosomes in platelets. Lysosomes can expel their contents when platelets are stimulated *in vitro*, but it is not clear that this is physiologically relevant. White (2007) suggested that lysosomes in platelets are essentially vestigial. However, defective platelet lysosomes (as well as defective dense bodies) are associated with Hermansky–Pudlak syndrome, a genetic bleeding disorder [57].

1.1.6.4 Mitochondria

Platelets have a few mitochondria that are relatively small with uncomplicated structures. Drugs that block anaerobic glycolysis do not lead to a significant drop in ATP concentrations, therefore it is believed that mitochondria supply most of the energy requirements of the platelet [40]. Jobe and colleagues demonstrated that formation of the mitochondrial permeability transition pore (MPTP), a feature associated with apoptosis in nucleated cells, regulates early platelet activation events, including phosphatidylserine externalisation, membrane vesiculation and procoagulant activity [58].

1.1.6.5 Membrane Systems

Platelets have very complicated membrane systems for such small cells, including the surface connected OCS, the dense tubular system, and membrane complexes as well as occasional appearances of the Golgi apparatus.

1.1.6.6 Golgi Apparatus

In the megakaryocyte, the Golgi apparatus consists of the typical flattened membranes or saccules that function in the development of dense bodies, alpha granules, and lysosomes. However, Golgi complexes have almost disappeared by the time that proplatelets develop. Membranes of the Golgi apparatus are undetectable in most platelets, but can be found in 0.2 to 1% by thin section analysis [40]. Most likely, these are adventitious remnants rather than functional organelles. However, Golgi zones are common in patients with certain platelet hypogranular syndromes, in particular white platelet syndrome [59].

1.1.6.7 The Surface Connected OCS

The OCS is a serpentine collection of membranes that is open to the surface of the platelets. It is essentially long invaginations of the plasma membrane that anastomose and form a labyrinthine system within the cell. As these are open to the surrounding plasma, they greatly increase the surface area of the platelet, allowing signalling molecules access to the interior of the cell. The OCS may be the route by which plasma proteins such as fibrinogen are taken up by the platelet and then are transferred to the alpha granules, which as mentioned previously, contain proteins of non-platelet origin. The passageways of the OCS are also the means by which platelet stores are secreted during platelet activation. The OCS also serves as the source of surface membrane when a platelet binds to a damaged blood vessel. The platelet can increase its surface area to four fold after adhesion to the vascular surface by evaginating the OCS. Membranes of the OCS are also used to surround

bacteria taken up by platelets [40]. Finally, the OCS seems to be the source of membrane for the long tethers that form during platelet adhesion [54].

1.1.6.8 Dense tubular systems

The dense tubular system (DTS) originates from the rough endoplasmic reticulum of the megakaryocyte but functions as smooth endoplasmic reticulum within the platelet [40]. It consists of thin elongated membranes which contain calcium binding sites and enzymes for prostaglandin synthesis. It does not communicate with the open canilicular system, but some channels appear to associate with the microtubule ring surrounding the inner platelet. Much like the sarcoplasmic reticulum in muscle, the dense tubular system stores calcium and releases it upon platelet activation [60]. Within seconds of the platelets contact with thrombin, the DTS rounds up into vesicular form. This morphological change appears to be associated with discharge of calcium which facilitates exocytosis of granule contents.

1.1.6.9 Membrane complexes

Although the DTS and OCS do not seem to be physically communicating [54], they are physically associated with each other, similar to the arrangement between sarcoplasmic reticulum and T-tubules in the muscles. Small channels of the DTS are interspersed between open canaliculi. Freeze fracture studies reveal a very intimate relationship between the two.

1.2 Platelet physiology

The principal role of platelets in the body is to maintain haemostasis by controlling bleeding through thrombus, or clot formation at the site of damaged blood vessels endothelium.

1.2.1 Platelet function in haemostasis

Under normal circumstances, platelets circulate independently in the blood. Aged or damaged platelets are removed by phagocytosis in the spleen and also by Kupffer cells, specialised resident macrophages in the liver. Platelets help maintain haemostasis by initiating and participating in thrombus (clot) formation to control bleeding. Thrombi are formed in response to damage to the endothelial lining of the blood vessels, which causes platelets to clump together and activate at the site of damage. Under normal conditions, the endothelial cells inhibit activation of platelets by the production of proactive NO, prostaglandin and ADPase, which break down adenosine diphosphate, a platelet activator. The endothelial cells also produce vWF, which aids the platelet adhesion to collagen within the extracellular matrix.

When an injury occurs to the endothelial cell layer, which may be the result of exogenous trauma, or due to the insult of ageing, the collagen in the extracellular matrix, along with vWF and tissue factor (factor III) are exposed to the blood. When the platelets contact any of protein, they are activated and clumped together. Platelets can also be activated by thrombin in combination with tissue factor. Platelets have within them granulated stores of vWF and tissue factor, which are excreted and thus have positive feedback effect on clotting activity as the platelets are activated. Activated platelets release a number of other active molecules including PF4, the growth factors TGF beta and PDGF, the matrix protein fibronectin, and the clotting proteins beta thromboglobulin, fibrinogen, and coagulation factors V and XIII. Activation of platelets also initiates the arachidonic acid pathway to convert prostaglandin H2 to thromboxane A_2 (TXA_2), which further facilitates platelet aggregation.

In platelet aggregation, the platelets use the proteins fibrinogen, fibronectin, vitronectin, thrombospondin and vWF as connecting bridges. Important aggregation

receptors include integrin $\alpha_{IIb}\beta_3$ (GPIIb/IIIa), the GPIb-IX-V complex, integrin $\alpha_2\beta_1$ and GPVI. The two latter are specific for collagen [61].

Aggregation of the platelets and their adhesion to damaged surfaces of the blood vessel act together to form the platelet aggregate. The contractile myosin and actin filaments in platelets are stimulated to contract during formation of the thrombus, retracting the clot (Figure 1-3). Clots consist not only of platelets, but most importantly fibrin, as well as other blood cell types which are caught in the nest of fibrin fibres (Figure 1-4). Blood fibrinogen is a soluble plasma glycoprotein that is converted to fibrin by the serine protease thombin. Fibrin is then cross-linked by activated clotting factor XIII to form a stable clot (Figure 1-5). Haemostasis is important but only a temporary solution. Active wound repair is needed. As previously mentioned, platelets secrete growth factors that stimulate the invasion of fibroblasts and the repair of connective tissue.

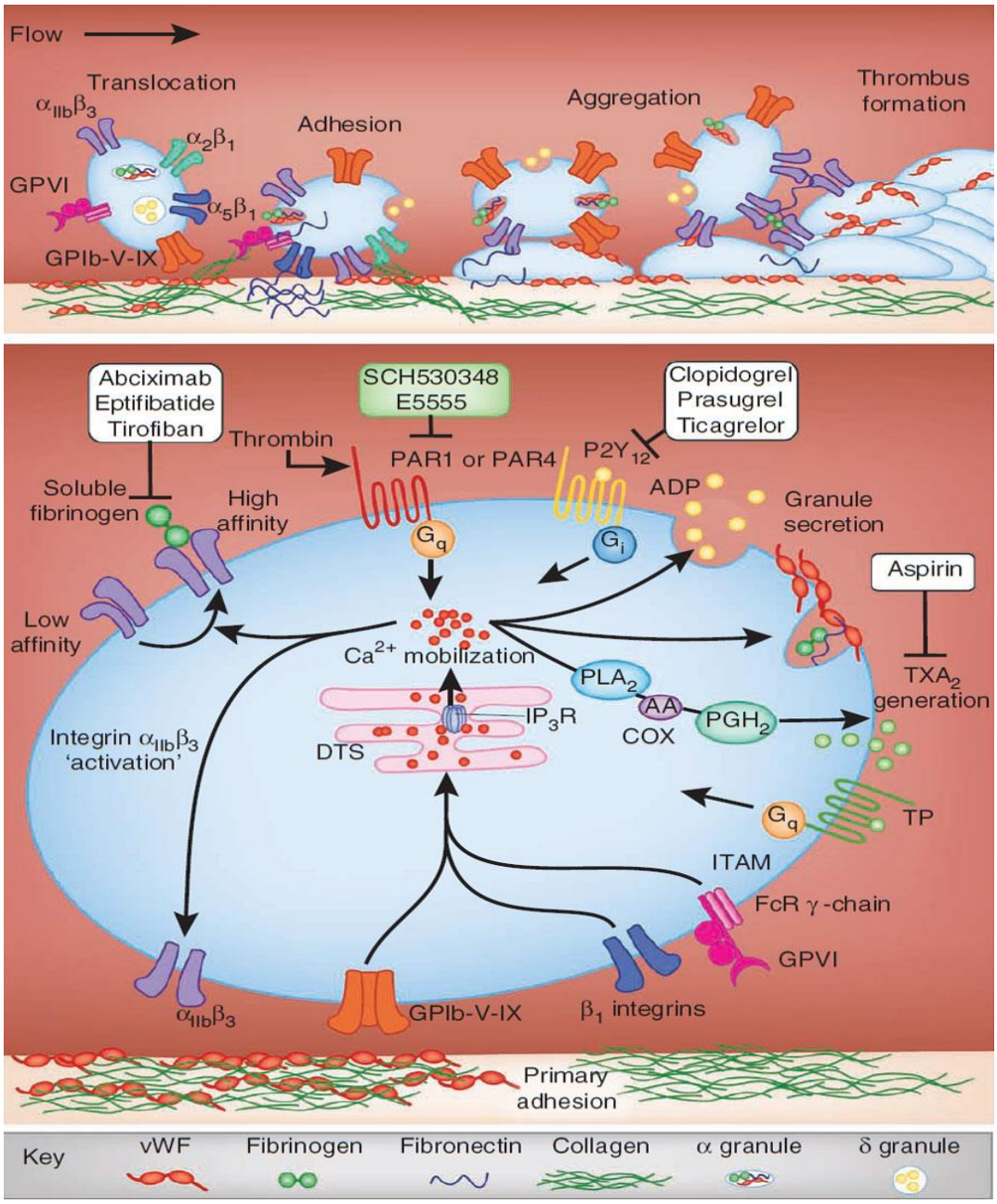

Figure 1-3: Adhesion and activation mechanisms supporting the haemostatic and prothrombotic function of platelets. Platelet adhesion mediated through GPIb coupling. This binding process induces differential expression and thus the formation of complex. GPIb interacts with the A_1 domain of vWF and mediates platelet tethering, allowing further interaction between GPVI and collagen. This process switches the integrin $\alpha_{IIb}\beta_3$ from low-affinity to high-affinity binding state leading to fibrinogen binding and platelet-platelet aggregation. Then the activation process leads to activation of GPCRs, and secretion of ADP and TXA_2, which bind to their ligands, the $P2Y_{12}$ and TP receptors, respectively. Thrombus formation is also triggered by tissue factor (TF), which plays a crucial role in platelet activation by binding to the platelet protease activated receptors (PAR-1 and PAR-4). Adapted from [62].

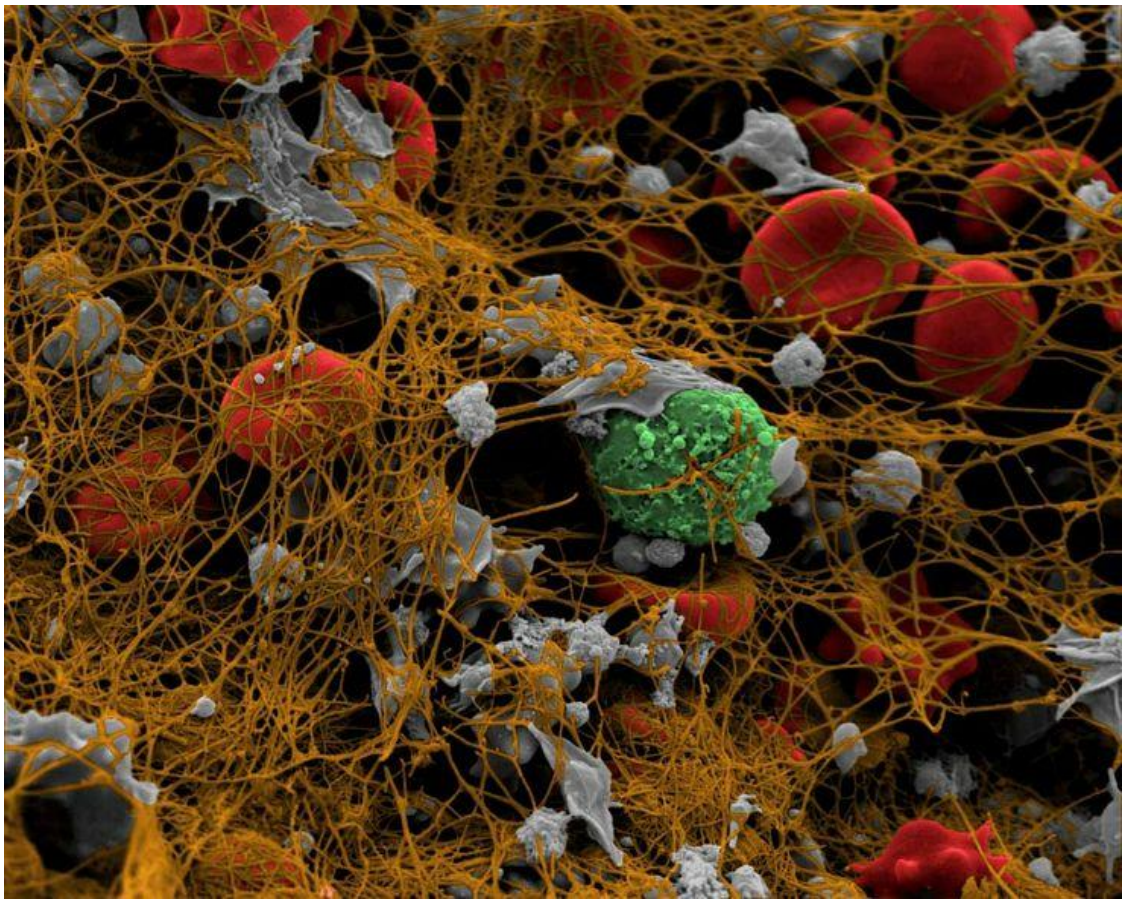

Figure 1-4: Clot formation. Colorised electron micrograph. Red blood cells = red. Leuckocytes= green. Platelets = grey. Fibrin=brown. **The Fibrin mesh of Clot.** Colourised electron micrograph of fibrin clot enclosing platelets, red blood cells and fibrin fibers. Red blood cells = red. Fibrin fibers = light green. aggregation = purple. Adapted from [63].

1.2.2 Platelet activation

When the endothelial layer is injured, as when blood vessel is cut or damaged, vWF and collagen become available to platelets which then adhere to the site of injury, are activated and begin to clump. Platelets can also be activated by thrombin, the formation of which is aided by tissue factor from the subendothelium.

Activated platelets change shape, developing pseudopods, and stretch to cover the damaged endothelium. The contents of alpha granules and dense bodies are secreted through the OCS into the plasma. Dense bodies secrete ADP, serotonin, and calcium. ADP further stimulates aggregation [64, 65]. Likewise, serotonin weakly accelerates platelet aggregation separately but also potentiates the response to ADP [66] and increases overall procoagulant activity. Calcium helps in aggregation as well by enabling binding of glycoprotein receptors to various agents. Alpha granules secrete, among other proteins, the fibrous adhesion proteins fibrinogen, vWF, fibronectin and thrombospondin which serve as connecting agents in further aggregation. Integrin $\alpha_{IIb}\beta_3$ on the platelet surface is a calcium-dependent receptor for fibrinogen, vWF, fibronectin, and thrombospondin, as well as vitronectin. The GPIb-V-IX complex also binds vWF, GPVI and GPIa binds collagen, locking the platelets to damaged endothelium. The activated, aggregated platelets form a plug in the wound site to stem the flow of blood.

Platelet activation through ADP also initiates the arachidonic acid pathway, leading to the synthesis of TXA_2, which provides a positive feedback mechanism to yield more platelet aggregation [67, 68]. This pathway is dependent upon phosphoinositol 3-kinase. A complex series of events involving tissue factor (the extrinsic pathway) or other various clotting factors (the intrinsic pathway) result in prothrombin being converted to thrombin (Figure 1-5) [69]. The latter cleaves fibrinogen to make fibrin, which polymerises into long strand.

Fibrin strands are cross-linked by factor XIII to form a stable network that strengthens the platelet plug [70-72].

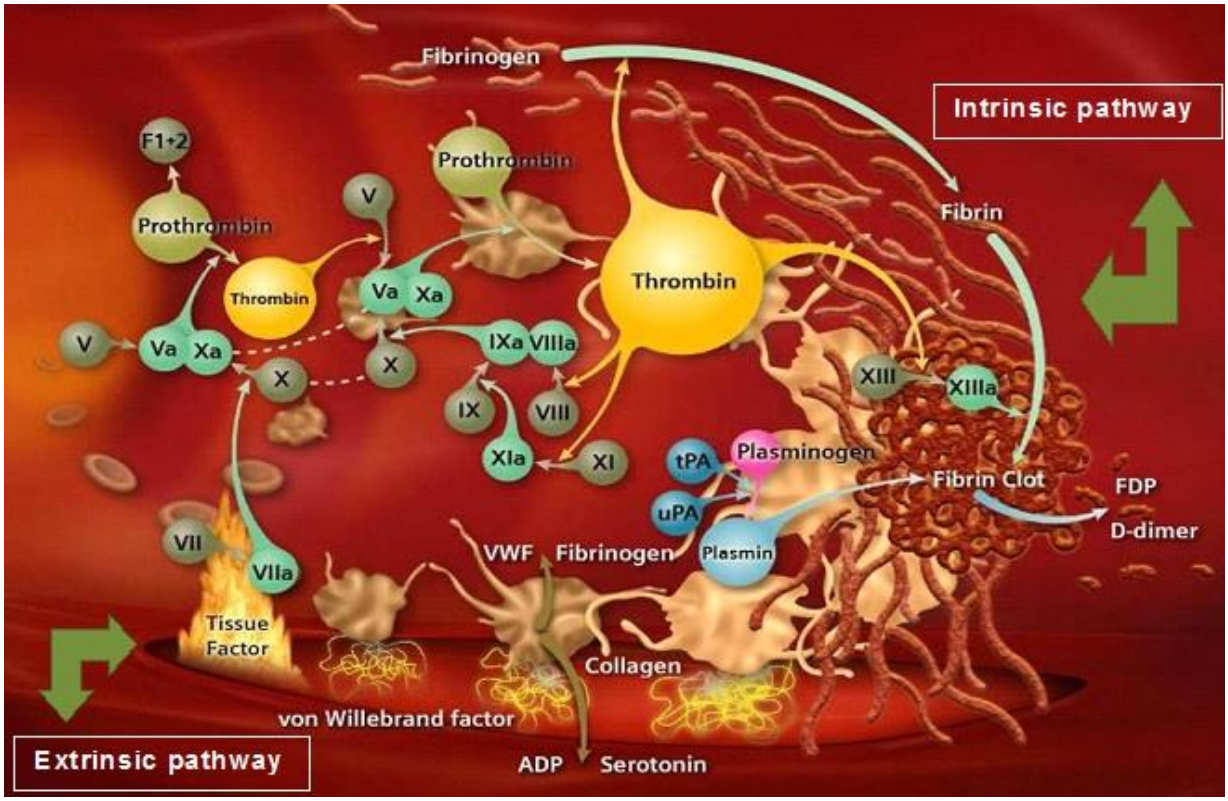

Figure 1-5: Blood coagulation cascade. The coagulation cascade is initiated via intrinsic pathway at the site of blood vessel damage by activating factor XII or via extrinsic pathway at the site of trauma when tissue factor is exposed. Adapted from [69-73].

1.2.3 Endogenous mechanisms of inhibition of platelet function

As long as the endothelium remains healthy and undamaged, platelets circulate in a largely resting and quiescent state. Dangerous arterial thrombi can occasionally occur when atherosclerotic plaques form at lipid rich sites in otherwise healthy blood vessels [74]. There is homeostatic balance between prothrombotic and anti-thrombotic mediators within the blood.

The main endogenous inhibitors of platelet function, all produced by endothelial cells include NO, endothelial ADPase (also called ectonucleotidase CD39) and the eicosanoid prostacyclin [74, 75]. Endothelial nitric oxide synthase (eNOS), located in the plasma membrane of endothelial cells, generates NO, a gaseous locally-active hormone. NO passively diffuses across the platelet plasma membrane where it stimulates soluble guanylyl cyclase (sGC) [74, 76]. This enzyme catalyses the formation of cyclic GMP which in turn inhibits platelet adhesion, activation and aggregation [76]. NO also causes smooth muscles surrounding the blood vessel to relax, leading to dilation of the vessels. NO is also produced by the platelet itself shortly after activation [77]. This inhibits further platelet recruitment into aggregates, unless the stimulus is sufficiently strong.

In animal models of atherosclerosis, treatment with L-arginine, which is an eNOS substrate, inhibits atherosclerotic lesions [78]. An L-arginine supplement given to human subjects inhibits ADP-dependent aggregation of platelets. NO effects are concentration dependent, under normal circumstances, NO is produced in the nanomolar range, which is sufficient to prevent platelet adhesion. Excessive NO, in the micromolar range, can lead to vascular injury.

Prostacyclin is an arachidonic acid derivative that inhibits platelet aggregation, platelet activation and vasoconstriction. Prostacyclin synthase, the last enzyme in the prostacyclin pathway is found in the endoplasmic reticulum of endothelial cells and smooth

muscle cells, but is not present in platelets. Prostacyclin's effects on platelets and smooth muscle cells are mediated by prostacyclin receptor. It is a G-protein coupled membrane receptor of the prostanoid family (see section 1.5.1.3). Insufficient or poorly regulated prostacyclin concentrations have been implicated in a wide variety of cardiovascular conditions including hypertension, stroke, atherosclerosis and myocardial infarction [79].

Endothelial CD39 is one of a family of Ecto-nucleoside triphosphate diphosphohydrolases that hydrolyse the terminal phosphates in nucleotide di- and triphosphates [80, 81]. It is an integral cell membrane protein with its active site on the external side. Thus, it can hydrolyse ADP and ATP that is in the blood plasma. These nucleotides act as signalling molecules as well as potential energy sources for chemical reactions. Excess ADP in the plasma, released from platelets or from damaged vascular tissue can have prothrombotic effects, through ADP receptors on platelets. The activity of endothelial CD39 inhibits the critical platelet recruitment phase [82].

1.2.4 Pharmaceutical inhibitors of platelet activation

When endogenous inhibitors of thrombus formation are insufficient, people are prone to dangerous clot formation that can cause cerebrovascular accidents (stroke) or induce myocardial infarction by blocking coronary arteries. There are three classes of drugs that have been used to protect patients from overactive platelets: nonsteroidal anti-inflammatory drugs (particularly aspirin); thienopyridines; and GPIIb/IIIa inhibitors [83].

The production of TXA_2 is inhibited by aspirin and other cyclooxygenase inhibitors [83]. TXA_2 is produced by activated platelets and functions as a positive feedback agent, increasing the activation of platelets. Aspirin treatment has been demonstrated to have significantly reduced heart disease by inhibiting thrombus formation in patients with atherosclerosis [83, 84].

Thienopyridines, such as Ticlopidine and Clopidogrel block the $P2Y_{12}$ receptor on platelets, which is the receptor for ADP [82, 83] (see section 1.5.1.2). Clopidogrel is usually favoured, because Ticlopidine treatment has the side-effect of thrombocytopenia. These drugs are prescribed for people with atherosclerosis, post myocardial infraction, and those who have just undergone coronary angioplasty.

GPIIb/IIIa (integrin $\alpha_{IIb}\beta_3$) inhibitors prevent the cross-linking of platelets through the binding of the glycoproteins to fibronectin, vWF, vitronectin and other large proteins [83]. Inhibitors in clinical use include Abciximab (a monoclonal antibody), Eptifibatide (isolated from snake venom) and Tirofiban [85].

1.3 Integrins

Integrins mediate attachment of cells to surfaces, extracellular matrix or other cells. They are receptors involved in cell signalling in the sense that they can help inform the cell about ligands, matrix proteins and conditions on the exterior of the cell by 'outside-in' signalling [86]. Integrins are also be involved with 'inside-out' signalling-influencing the outside environment on the basis of biochemical changes within the cell [86, 87].

Integrins link the cell surface to extracellular matrix proteins, such as fibronectin, collagen and laminin. Thus, they may help to regulate cell shape, cell movement and even the cell cycle [87]. Integrins work alongside other cell adhesion molecules as well as members of immunoglobulin superfamily to mediate intercellular communication and cell to basement membrane interactions. Integrins are heterodimers consisting of an α and a β subunits. In mammals, there are eighteen known α chains and only eight β chains. The subunits can be mixed and matched depending on a cell's requirements so that there are 24 distinct integrins in mammals [87]. Both subunits span the plasma membrane and both have tails that extend into the cytoplasm. The various subunits vary in size from 90-160

kilodaltons. Several α subunits contain the αA domain near the N-terminal which is similar to the A1 domain in vWF that mediates binding to collagen proteins. The A1 domain may contain divalent cation binding sites that are occupied when integrin is interacting with arginine-glycine-aspartic acid (RGD) sites on matrix proteins.

The major integrins of interest in platelet biology are $\alpha_{IIb}\beta_3$, $\alpha_v\beta_3$, $\alpha_2\beta_1$ and $\alpha_5\beta_1$. Integrin $\alpha_{IIb}\beta_3$ will be described in some detail and other integrins will be described briefly.

1.3.1 β_3 Family of integrins

There are two β_3 integrins, so named because they share the same beta subunit. Integrin $\alpha_{IIb}\beta_3$ and $\alpha_v\beta_3$, are both expressed on platelets. Their alpha subunits share 36% sequence homology. Knockout experiments in mice show the importance of these integrins to platelet function. In the absence of β_3 gene there is essentially no platelet aggregation with resultant haemorrhagic effects [87].

1.3.1.1 Integrin $\alpha_{IIb}\beta_3$

Integrin $\alpha_{IIb}\beta_3$ is the main platelet integrin, with about 80,000 copies per platelet. It is the crucial receptor required in physiological processes such as clot retraction, platelet spreading, cytoskeletal reorganisation, irreversible platelet adhesion, platelet aggregation and thrombus stability [88]. Platelet aggregation is mediated by integrin $\alpha_{IIb}\beta_3$ which is also known as GPIIb-IIIa. This protein is normally expressed only on megakaryocytes and platelets. On the latter, it is the major integral protein of plasma membrane and is also expressed on the membranes of alpha granules.

This receptor goes from low-affinity resting state to an active state wherein it has high-affinity for extracellular ligands vWF and fibrinogen [89, 90], which cross-link platelets together. It also is able to bind thrombospondin, vitronectin, plasminogen and fibronectin [90]. The binding of most proteins by integrin $\alpha_{IIb}\beta_3$ is via the RGD recognition

sequence. However fibrinogen contains RGD, a different amino acid sequence in its recognition of integrin for fibrinogen, K-Q-A-G-D-V [91-93].

The various domains of the alpha and beta chains are depicted in Figure 1-6 and 1-7 [89]. The A domain of the beta chain is the one principally involved in the binding of RGD sequences. The A domain also has three metal binding sites called MIDAS, ADMIDAS and LIMBS (for ligand-induced metal binding site) [94, 95]. The beta subunit has four EGF domains so named because of their resemblance to Epidermal Growth Factor. The propeller domain in the alpha chain, which interacts with the A domain of the beta chain, has a series of seven amino-acid repeats (the 'blades') that are involved in binding divalent cations. The calf and thigh domains of integrin α_{IIb} are primarily in the form of beta pleated sheets [96] and both have similar, immunoglobulin-like, β-sandwich folds [97]. Both subunits have tail domains that extend into cytoplasm and interact with a multitude of intracellular proteins. There is small acidic region between the thigh and first calf domain called genu (latin for knee) which binds to calcium. Another genu exists in the beta subunit involving the hybrid, PSI and EGF domains [96].

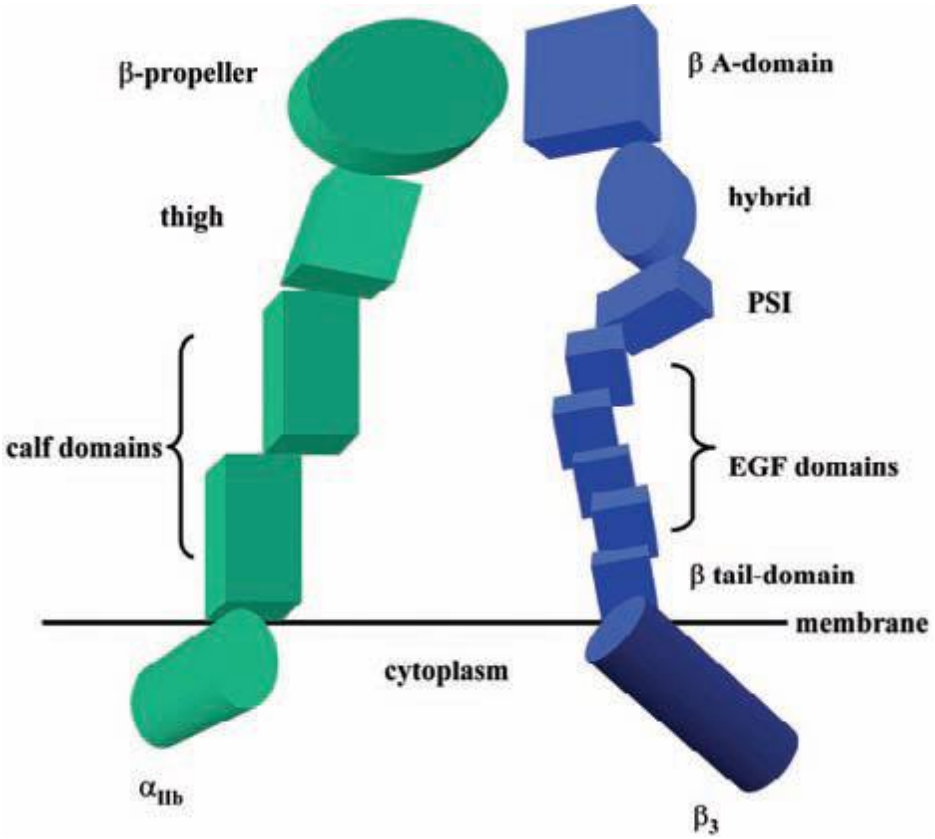

Figure 1-6: Depiction of Structure of integrin $\alpha_{IIb}\beta_3$ complex. This cartoon showing the α_{IIb} (green) domains and β_3 (blue) subunits in an extended conformation Adapted from [89].

The presence of the genu in both subunits allows a conformational shift to occur from bent to an extended state in a calcium-dependent manner [98]. When the receptor binds to the ligand, the protein changes to an extended form. Crystal structure of the pure receptor shows the bent state. The activation of integrin $\alpha_{IIb}\beta_3$ is termed 'inside-out' signalling, because the events that regulate it are intracellular in nature but result in changes that occur on the extracellular surface. During 'inside-out' signalling, changes in conformation of the extracellular domains increase the affinity for its ligand. The same integrin also participates in 'outside-in' signalling, where external events lead to widespread biochemical events within the cell [99]. This type of signalling happens after the ligand is bound. In this case, changes in conformation of the cytoplasmic tails create interaction sites for cytoskeletal proteins as well as protein kinases. Inside-out signalling is mediated through the GPVI and the GPIb-IX-V complexes and G-Protein coupled receptors (GPCRs) (Figure 1-7) [89]. Binding of polymeric collagen, exposed during vascular injury to the GPVI complex causes clustering of GPVI receptor (see section 1.6.1) and its associated Fc receptor gamma subunit which ultimately results in the activation of phospholipase C. That enzyme catalyses the formation of inositol 1,4,5 trisphosphate (IP_3) and diacylglycerol. IP_3 mobilises Ca^{2+}, whereas diacylglycerol activates protein kinase C, which phosphorylates a number of different intracellular proteins. Both events appear to be involved in activation of the integrin. Binding of vWF to the GPIb-IX-V complex initiates a similar set of events.

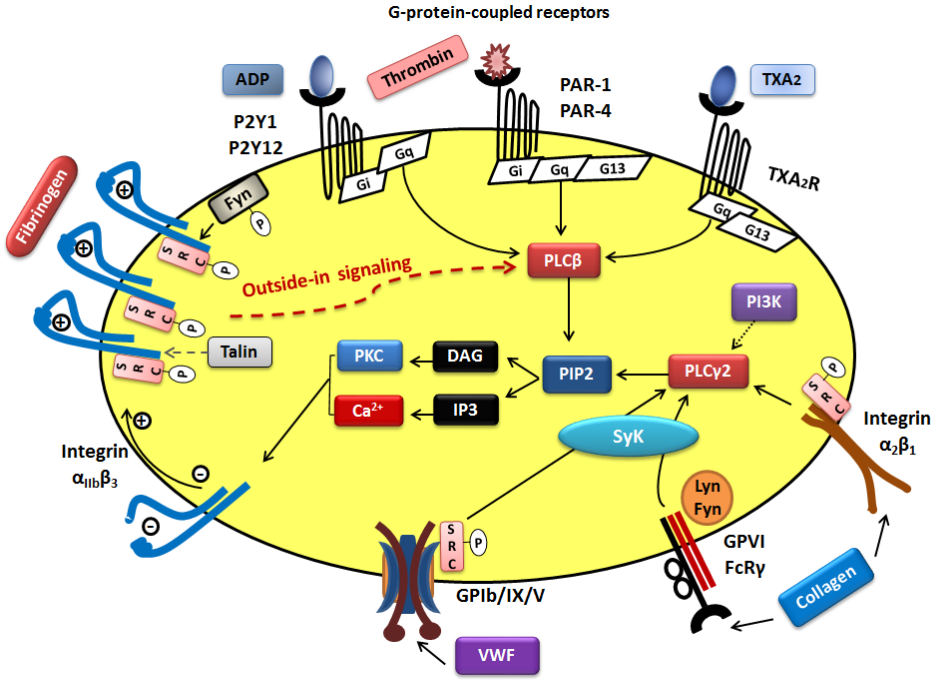

Figure 1-7: Inside-out and 'outside-in' integrin $\alpha_{IIb}\beta_3$ signalling events mediated by GPCRs, GPVI and GPIb-IX-V. This carton explains different platelet signalling pathways. Firstly, 'inside-out' integrin $\alpha_{IIb}\beta_3$ signalling is initiated via one of the GPCRs, collagen receptors, integrin $\alpha_2\beta_1$ and GPVI which all converge via release of PIP_2 from the membrane and lead to mobilisation of calcium. 'Inside-out' integrin $\alpha_{IIb}\beta_3$ signalling brings about a separation of the transmembrane domains of the two subunits of integrin $\alpha_{IIb}\beta_3$. This separation is thought to allow the tail units to interact with specific cellular proteins involved in 'outside-in' signalling shown here as phosphorylated Src.

Ultimately, the cytoplasmic tails of the integrin subunit are bound by one or more proteins, resulting in an "unclasping" of the tail region and a conformational shift which results in an increase in affinity of the extracellular domains for RGD and other ligands. The exact sequence of events is not known with precision. The integrin tails interact with 20 or more different cytoplasmic proteins. The best candidate for the activating protein is the head domain of Talin [89, 100]. Talin is an abundant cytoplasmic protein that mediates the interaction of integrins (β_3 cytoplasmic tail) with actin microfilaments of the cytoskeleton.

Platelet aggregation occurs in two phases, first reversible aggregation that depends on inside-out signals, and then irreversible aggregation that occurs in response to outside-in signalling [101]. Inside-out signalling brings about separation of the trans-membrane domains of the two subunits. This separation is thought to allow the tail units to interact with specific cellular proteins involved in outside-in signalling. On larger scale, a factor that seems to be involved is clustering of the integrin in membrane brought about by cross-linking of their extracellular domains through their ligands proteins such as fibrinogen. Artificial cross-linking of the dimers using chemicals is sufficient to bring about the activation of two protein kinases associated with outside-in signalling, c-Src and Syk [102].

Binding of fibrinogen to integrin $\alpha_{IIb}\beta_3$ causes protein tyrosine phosphatase (PTP-1B) to associate with a complex between the integrin, c-Src, and c-Src kinase (CSK). The latter is a protein kinase that phosphorylates c-Src to keep it in a normally inactive state. Upon the association of PTP-1B, CSK dissociates from the complex, and c-Src is dephosphorylated and becomes active. c-Src is a tyrosine kinase with a multitude of substrates that are involved in downstream signalling associated with other kinases including Syk, Tec tyrosine kinases, integrin linked kinase, protein kinase C, and phosphatidylinositol 3-kinase [101]. The kinase cascade results in many of the effects associated with irreversible platelet aggregation and activation.

Glanzmann's thrombasthenia (GT) is a disease of platelets in which integrin $\alpha_{IIb}\beta_3$ is either absent from the platelets or defective [103, 104]. In many cases, expression of the protein is normal but its binding properties are compromised (Type II GT). The condition can be inherited or acquired through autoimmune responses. Platelet numbers and morphology are normal but integrin $\alpha_{IIb}\beta_3$ cross-linking of platelets by fibrinogen does not occur, and bleeding times are quite prolonged [103, 105]. Nose bleeds, heavy menstrual flow, and excessive post-operative bleeding are common symptoms [105]. GT, along with

mouse knockout experiments, demonstrates the key role for integrin $\alpha_{IIb}\beta_3$ in platelet activation and aggregation [106].

Through its role in cross-linking platelets through fibrinogen and other ligand proteins, integrin $\alpha_{IIb}\beta_3$ plays a direct role in initial platelet aggregation. The bidirectional signalling and the resulting kinase cascade mediates many of the activities leading to irreversible platelet aggregation, thrombus formation and clot retraction.

1.3.1.2 Integrin $\alpha_v\beta_3$

The integrin $\alpha_v\beta_3$ has two subunits, alpha v and beta 3. It serves as receptor for vitronectin on platelets and is also found on endothelial cells, monocytes, macrophages, dendritic cells, chondrocytes and fibroblasts. This integrin is involved in the binding of platelets to endothelial cells during inflammatory processes. It is also known to play a role in angiogenesis and tumour metastasis which may be related to its presence on platelets, as these are a source of tumour growth factors and angiogenic factors. $\alpha_v\beta_3$, however, is likely to exert only a minor influence as there only about 50 copies of the protein on the platelet surface as compared to about 50,000-80,000 copies for integrin $\alpha_{IIb}\beta_3$ [107].

1.3.2 Integrin $\alpha_2\beta_1$

The integrin $\alpha_2\beta_1$, also known as GPIa-IIa on platelets or VLA-2 on lymphocytes, is present on a wide variety of cells. Its ligands include collagen and the laminin family of proteins, but it does not appear to function as a laminin receptor on platelets. Per platelet, there are around 2000-4000 copies of integrin $\alpha_2\beta_1$.

The alpha subunit has the typical seven amino acid repeats in the propeller domain. This domain can also interact with three to four Ca^{2+} ions. The structure of integrin $\alpha_2\beta_1$ is shown in Figures 1-8 and 1-9. There is an I domain sandwiched between the second and third repeats that binds to the GFOGER amino acid sequence on collagen or collagen related

peptide (CRP) [108]. Currently, it is believed that this integrin increases its affinity for the collagen ligand after the platelet is activated by interaction between collagen and the platelet GPVI. This interaction alone is insufficient to activate the platelet under high shear conditions. Another platelet glycoprotein (GPIb), and the presence of vWF in plasma are necessary for this to occur.

Integrins are responsible for firm adhesion of the activated platelet to the subendothelium. Since Glanzmann's thrombasthenia platelets still adhere, even though they lack integrin $\alpha_{IIb}\beta_3$, it is likely that integrin $\alpha_2\beta_1$ interaction is sufficient for adherence albeit not for creation of an effective plug.

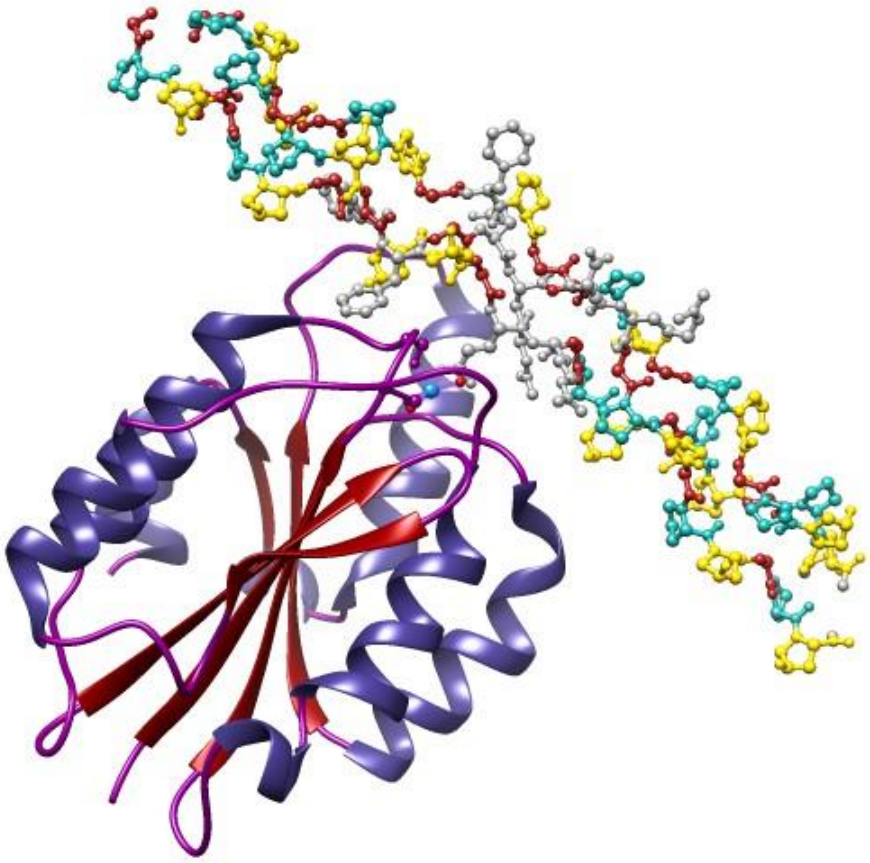

Figure 1-8: Integrin alpha2-beta1/collagen complex containing Gly-Phe-Hyp-Gly-Glu-Arg motif. Protein chains are coloured from the N-terminal to the C-terminal using a rainbow (spectral) colour gradient. Adapted from [109, 110].

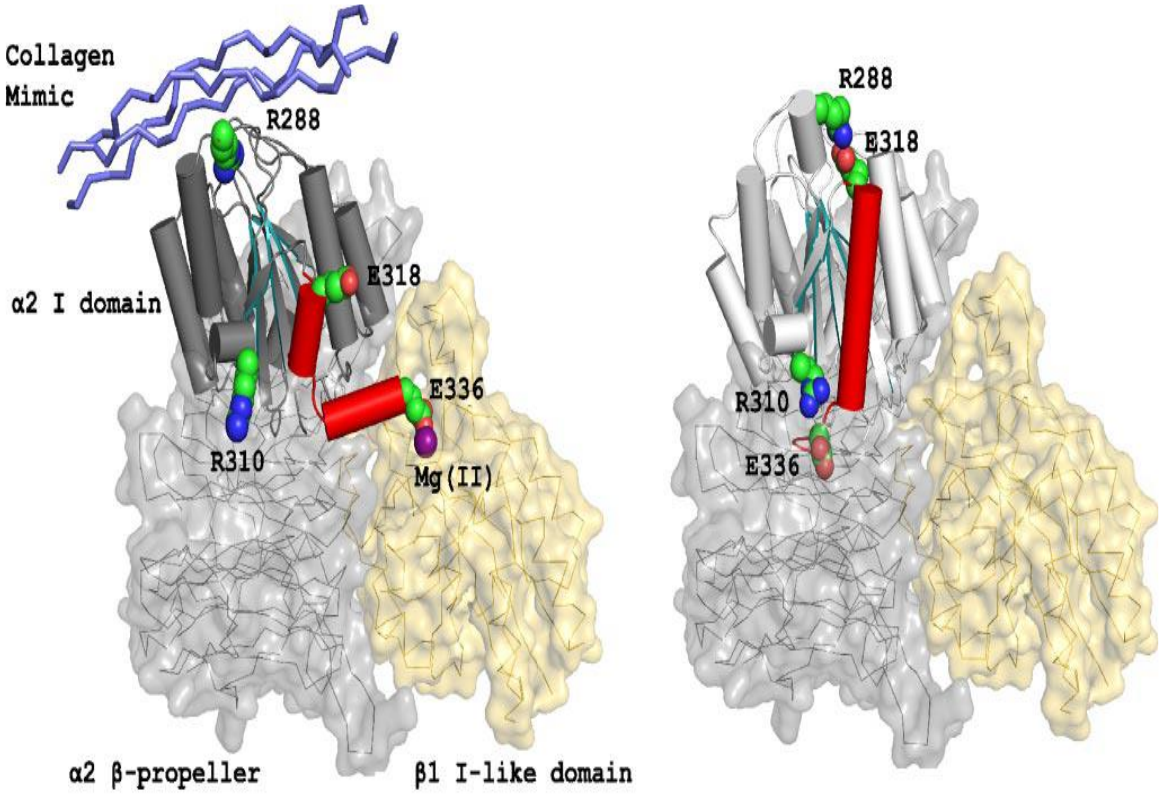

Figure 1-9: Functional and structural mode of integrin $\alpha_2\beta_1$ activation. Activation of integrin $\alpha_2\beta_1$ necessitates the involvement of $\alpha_2\beta_1$ propeller, Beta-1 I-like domain and other alpha-2 domains. All these differential activation reactions occur with the binding of collagen and actin with the integrin. Adapted from [111].

1.3.3 Other Integrin family members

The integrin $\alpha_5\beta_1$ is present on many cell types including platelets. Its function in platelets is not well defined but its general role is to bind the extracellular matrix protein fibronectin as well as some proteinases. The integrin may have a role in stabilising adhesion of the platelets to injury sites on the vasculature.

The integrin $\alpha_6\beta_1$ is also present on many cell types including platelets. Its general role is binding to the laminin family and other extracellular matrix proteins. It may also have a role in stabilising platelet adhesion to sites of injury.

The β_2 family of integrins consists of $\alpha_L\beta_2$ and $\alpha_M\beta_2$. The former is present on activated but not resting platelets, whereas the latter has yet to be detected. The usual ligands for $\alpha_L\beta_2$, which is also expressed in T-lymphocytes, are cell adhesion molecules ICAM1 and ICAM2. The former is expressed on endothelial cells. Gene knockout studies have discovered that platelets in mice without the β_2 gene have much shorter half-lives and that caspase activities (which are frequently associated with apoptosis) were elevated [112].

1.4 Leucine rich repeat family

A leucine rich repeat (LRR) is fairly common protein motif called the α/β horseshoe fold that is present in many proteins but is not necessarily related in function. Within platelets, leucine rich repeats are found in two important receptors, the GPIb-IX-V complex (also known as CD42) and the Toll-like receptors.

1.4.1 GPIb-IX-V complex

The GPIb-IX-V is non-covalent multimeric complex composed of GPIbα, GPIbβ, GPIX and GPV subunits. It serves as receptor for vWF, thrombospondin I and P-selectin, which is found both on activated platelets and on endothelial cells [113]. It also interacts with α-thrombin, factors XI and XII, and kininogen, all of which are involved in coagulant

activity. There are about 50,000 copies of the GPIb-IX-V complex found on an average sized platelet. This complex is essential for platelet adhesion under conditions of high shear.

Bernard-Soulier syndrome, or haemorrhagiparous thrombocytic dystrophy, is a genetic bleeding disorder caused by absence of the GPIb-IX-V complex or a defect in its activity. It is characterised by the inability of platelets to bind to or aggregate at sites of vascular injury. It is one of the giant platelet syndromes; the normal attachment of GPIb-IX-V to the cytoskeleton through filamen help to regulate the size of the platelet [113].

Immune thrombocytopenic purpura is sometimes caused by autoantibodies to GPIb-IX-V or integrin $\alpha_{IIb}\beta_3$. The structure of GPIb-IX-V (hereinafter called 'the complex') is shown in Figure 1-10. All four subunits are transmembrane membrane proteins with tails protruding into the cytoplasm. Leucine rich repeats are found in three of four subunits with the exception being GPIbβ which is linked by disulphide bonds to GPIbα. GPIbα has an unusual region of sulphated tyrosines adjacent to a long section with associated sialomucin. Most of the ligand binding sites are located in the N-terminal loop of the GPIbα with the notable exception of collagen, which binds to GPV. Calmodulin associates with the cytoplasmic tails of GPIbβ and GPV which may help regulate surface expression of the complex. Filamin binds to the cytoplasmic tail of GPIbα, linking it to the cytoskeleton.

The GPIb-IX-V complex acts as an 'outside-in' signalling receptor to activate the platelet integrins $\alpha_{IIb}\beta_3$ and $\alpha_2\beta_1$, which in turn mediate stable platelet adhesion, aggregation and clot retraction. The mechanisms by which this signalling works have not yet been completely clarified but they involve both G-proteins coupled and tyrosine kinases. Key elements include c-Src, which is a tyrosine kinase, phospholipase γ2 (PLCγ2) which raises Ca^{2+} in the cytosol by generating IP_3; and PI-3 kinase, which generates signals that activate integrin $\alpha_{IIb}\beta_3$. Extracellular signal regulated kinase 1/2 (Erk-1/2) and Syk kinase also appear to be involved.

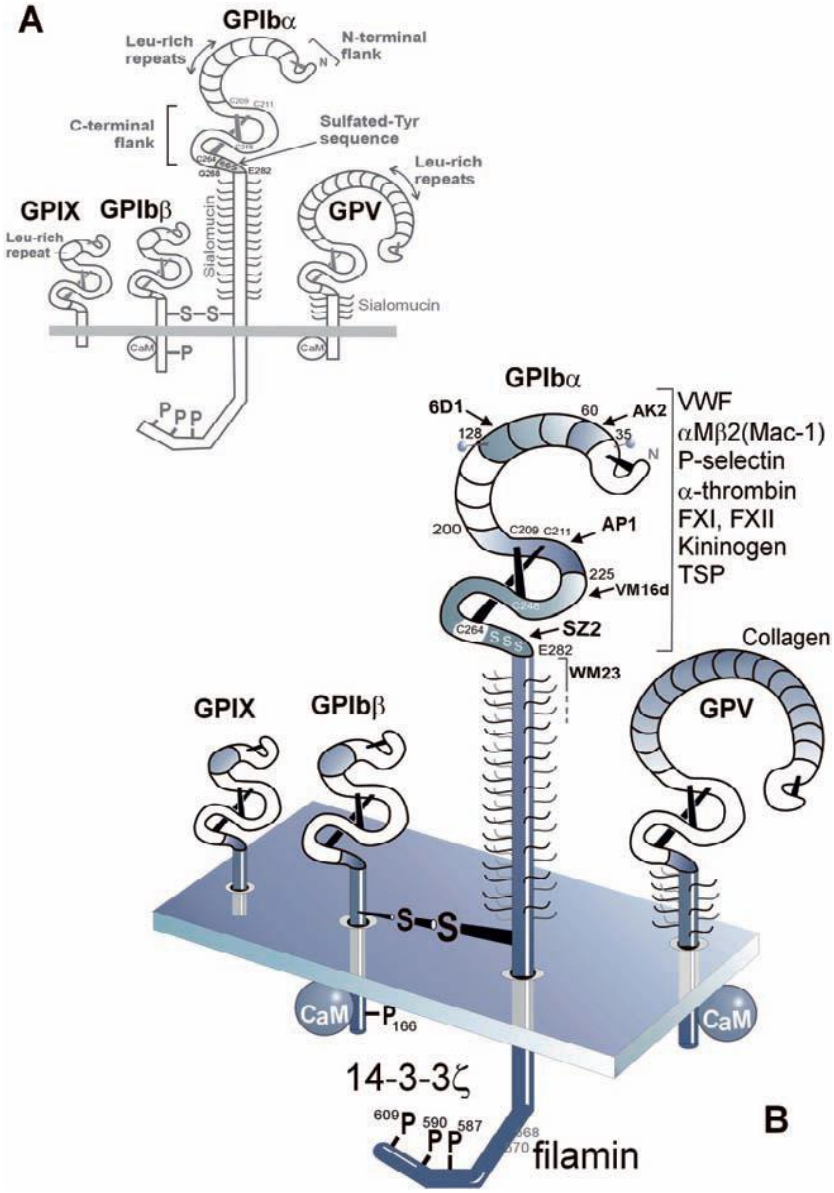

Figure 1-10: Structure of GPIb-IX-V. Panel (A) shows the leucine-rich repeats, the sulphated tyrosine residues and the sialomucin regions. Protein binding sites are indicated in panel (B). The C-terminal region of GB1bα alpha region interacts with filamin. The GPV and GPIb beta chain carboxy-terminals interact with calmodulin. Adapted from [113].

1.4.2 Toll-like receptors

This class of receptors are the proteins, which play a crucial role in the innate immune system. These single, membrane-spanning and non-catalytic receptors identify the structurally conserved molecules obtained from microbes. The Toll-like receptors have two sections of 9-11 leucine rich domains connected by a linker region, transmembrane domain, glycosylated double loop domain and a cytoplasmic Toll/Interleukin-1 signalling domain. A small molecule, MD-2 associates with the extracellular terminus. Toll-like receptors interact with lipopolysaccharides and some endotoxins. Experiments in mice have suggested a role for Toll-like receptor-4 in that treatment with lipopolysaccharide caused platelets to adhere more tightly to fibrinogen whereas mice which genetically lacked the receptors did not show the same response [114].

1.5 Seven transmembrane receptor family

The seven transmembrane domain receptors are mostly GPCRs, and are widely used mechanisms in eukaryocytes to sense the presence of extracellular ligands, such as hormones or neurotransmitters or significant extracellular peptide. These receptors activate intracellular signalling modalities such as the cAMP system or the phosphatidylinositol signal transduction pathway, leading frequently to complex cellular responses. They are tightly linked to cellular metabolism and can have very general effects. Therefore, if several GPCRs act through cAMP, they are generally affecting the same cytosolic pool of cAMP and therefore are likely to have similar effects, regardless of the initial stimulus. Additive results may occur when more than one type of stimulus is used.

There are generally seven transmembrane domains with three intracellular and three extracellular loops in these long proteins (Figure 1-11). There is also long cytoplasmic tail which may interact with protein kinase C, protein kinase A or GPCR kinase. GPCRs are

generally highly conserved. Of the 367 human and 392 mouse GPCRs studied by Vesalius and colleagues, 343 were common to both species [115].

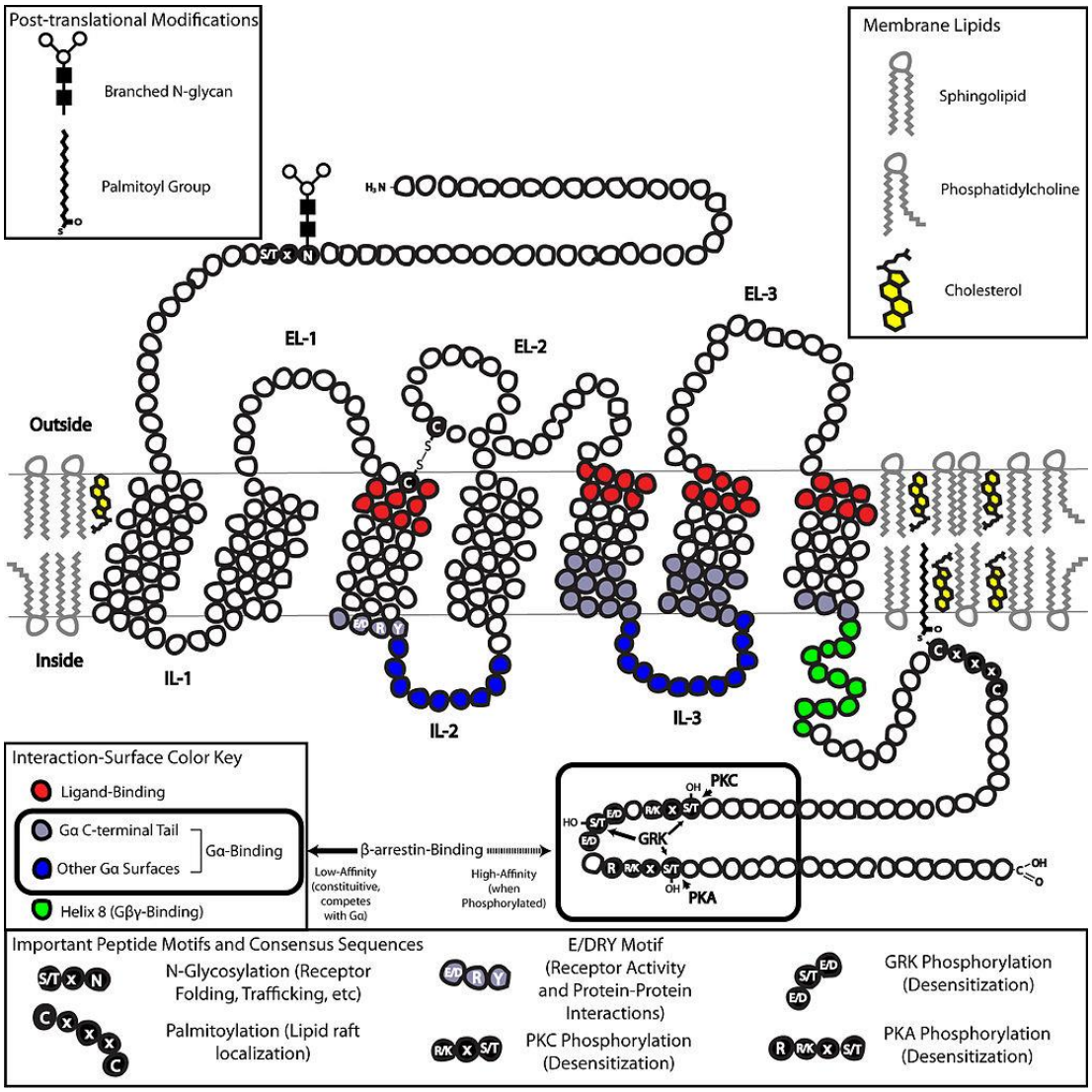

Figure 1-11: Structure of generic GPCR. IL=intracellular loop. EL=extracellular loop. Filled black squares=N-acetyl glucosamine. Unfilled circles=mannose. N=Asparagine. X=any amino acid. C=cysteine. E/D=glutamate or aspartate. Y=Tyrosine. R/K=arginine or lysine. G alpha=alpha subunit of G protein. G beta/gamma=subunits of heterodimeric G protein. PKC=Protein Kinase C. PKA= Protein kinase A. GRK=GPCR kinase. Adapted from [116].

1.5.1 GPCRs expressed in platelets

In the platelet, there are various GPCRs, including thrombin receptors, ADP receptors, the prostacyclin receptor, the thromboxane receptor, receptors for the neurotransmitters serotonin, dopamine and epinephrine, vasopressin receptor, an adenosine receptor, and possibly chemokine receptors. These are considered in more detail below.

1.5.1.1 Thrombin receptors

Thrombin receptors are called protease activated receptors (PARs) because they are activated by specific cleavage of the N-terminal domain (Figure 1-12). This results in new N-terminus which by rearrangement of the protein acts as a tethered ligand [109, 117]. This is an unusual situation for a GPCR; whereas most of these receptors can be turned on and off depending on the concentrations of their respective ligands, thrombin receptors can only be activated once. In terms of platelets, this is no particular disadvantage given their short lifespan, and the fact platelets themselves are single-use mechanisms for generating thrombi. However, PARs are not just restricted to platelets, though expression of PAR mRNA is mainly found in cells involved in the vasculature, including endothelial cells and smooth muscle cells.

There are four PARs, numbered 1-4. PAR-2 is not a thrombin receptor since it is activated by trypsin and related proteases. PAR-1 seems to be important in human platelets which have 2500 copies per platelet, with about two thirds present on the plasma membrane. PAR-1 signalling however is apparently insignificant in mouse platelets. The lack of PAR-1 gene in mice caused 50% embryonic lethality but the survivors had no haemorrhagic diseases and their platelets could be activated normally [118]. Humans and mice both have signalling systems that utilise two PARs. In humans, the pair is PAR-1 and PAR-4 but in mice it appears to be PAR-3 and PAR-4 [117]. Mouse platelets express PAR-3, but in human platelets the expression is insignificant [117]. In the absence of PAR-3, PAR-4 is

sensitive to thrombin at high (30 nM) levels but not low (1 nM) levels. On the other hand, PAR-3 by itself does not activate platelets in response to thrombin, even when overexpressed. PAR-3 appears to act as a co-factor to PAR-4, increasing its sensitivity to thrombin [119]. Mouse PAR-4 is required for platelet thrombus propagation but not juxtamural thrombus formation or fibrin generation [120]. Although platelets isolated from PAR-4-deficient mice are not responsive to thrombin, they can be activated by other agonists. Also, there is no evidence that the mice bleed spontaneously indicating that thrombus propagation is not required for haemostasis in the absence of injury [121].

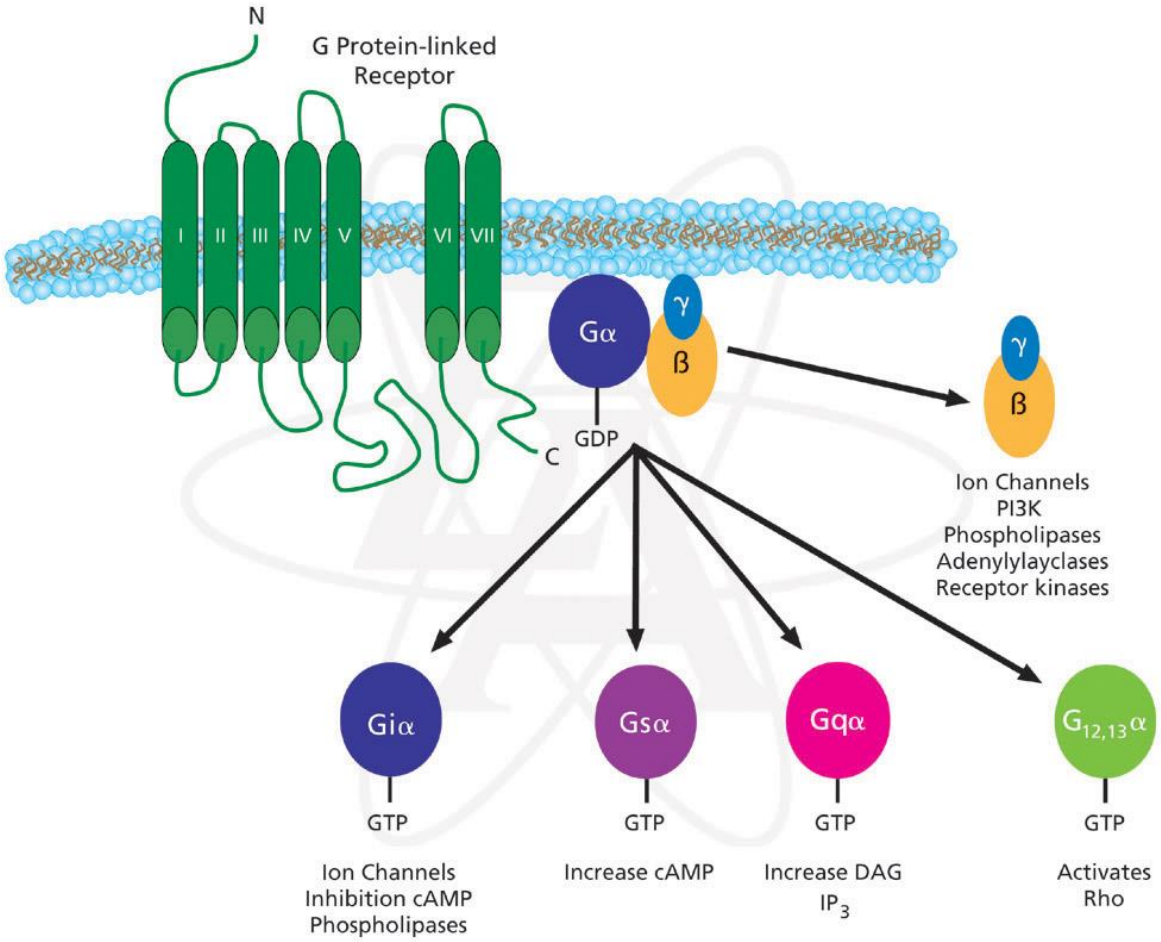

Figure 1-12: Structure of G-Protein coupled receptors. GPCRs display a common structure consisting of seven transmembrane domains with three intracellular and three extracellular loops in these long proteins. GPCRs also contain a long cytoplasmic tail which may interact with protein kinase C, protein kinase A or GPCR kinase. GPCRs are generally highly conserved. Of the 367 human and 392 mouse GPCRs studied by Vassilatis and colleagues, 343 were found to be common to both species [115]. This figure illustrates the GPCRs signalling pathways via Gα protein. Adapted from [122].

1.5.1.2 ADP receptors

ADP was the first known small molecule platelet agonist. ADP and other nucleotides may be released from damaged cells or may be secreted from intact cells or activated platelets. There are two platelet ADP receptors of the seven transmembrane family $P2Y_1$ and $P2Y_{12}$ (Figure 1-13) [64, 83, 123]. They are part of a family of 14 such receptors that have been cloned, although not all members of the family are known to respond to nucleotides. ADP is a platelet aggregating agent, it can trigger reversible aggregation and shape change, whereas secondary aggregation and secretory activities are dependent upon TXA_2.

$P2Y_1$ is expressed on platelets as well as most other human tissues. It is present on the plasma membrane but also in membranes of the OCS and those of the alpha granules. In the presence of $P2Y_{12}$ antagonists, ADP induced transient aggregation and shape change, suggesting that these can be mediated by the $P2Y_1$ receptor alone [83]. Similar results were achieved for platelets from mice engineered to lack the gene for $P2Y_{12}$ and from humans who were congenitally deficient in $P2Y_{12}$ [64].

Activation of platelet $P2Y_1$ by ADP leads to activation of phospholipase C mediated by a specific G protein, Gq [83, 123]. The resultant increase in cytosolic calcium is mediated by IP_3. Some of the calcium is released from intracellular stores, though some may also influx from the extracellular medium. Platelets from mice lacking the G_q gene do not undergo shape change in response to ADP [83, 124] but still undergo partial aggregation.

$P2Y_{12}$ expression is restricted to platelets, vascular smooth muscle cells and to some regions of the brain. It has the structure of classic GPCR sequence. It is stimulated by ADP and its analogues whereas ATP is an antagonist [123]. $P2Y_{12}$ has the major responsibility for platelet aggregation. It is coupled to adenyl cyclase inhibition through the G protein subtype $G_{\alpha i2}$ [64]. Adenyl cyclase inhibition does not directly cause activation of integrin

$\alpha_{IIb}\beta_3$ and platelet aggregation but does counteract inhibitory prostaglandins, which works through increasing cAMP. $P2Y_{12}$ amplifies intracellular calcium mobilisation induced through the $P2Y_1$ receptor and the secretion of dense granules stimulated by TXA_2 or thrombin [83]. The details of $P2Y_1$ receptor signal transduction have yet to be totally elucidated but it appears to involve the phosphoinosotide 3-phosphate activation of Rap1-B and phosphorylation of serine/threonine protein kinase B/Akt. Metabolites of the antithrombotic thienopyridine drugs ticlopidine and clopidogrel are antagonists of $P2Y_{12}$ [125].

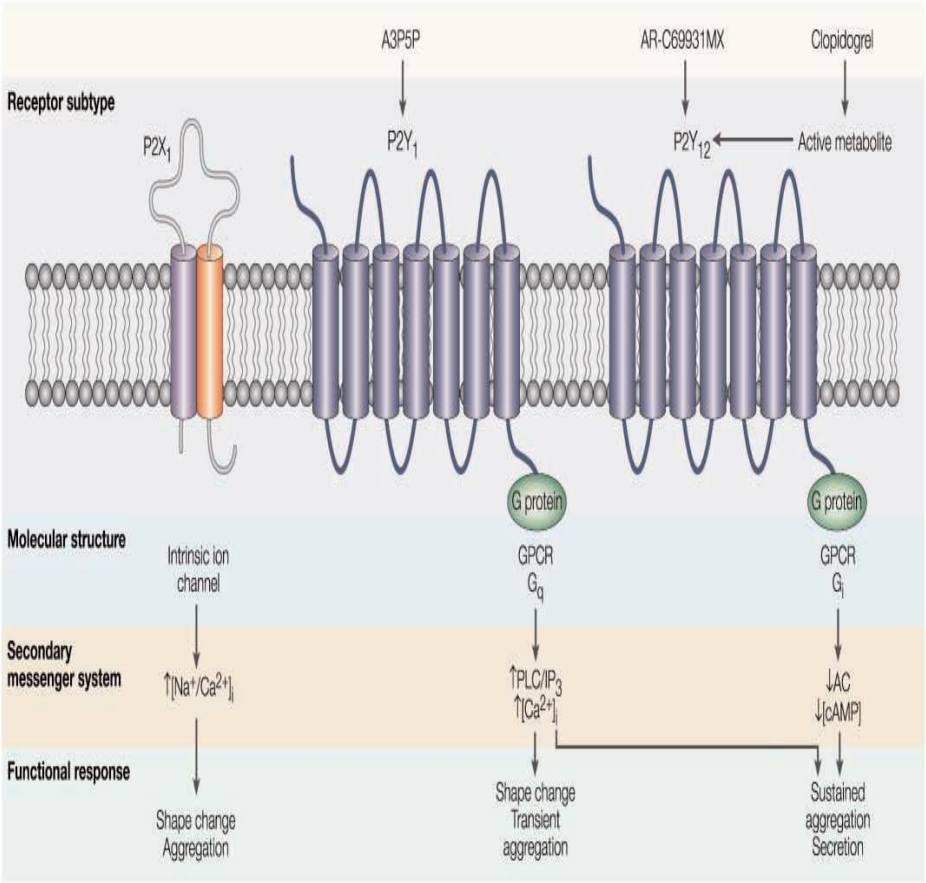

Figure 1-13: Different subtypes of ADP receptors. $P2Y_1$ and $P2Y_{12}$ are GPCRs. There are two main ADP receptors. The $P2Y_{12}$ receptor leads to inhibition of adenylyl cyclase (AC) and a decrease in cyclic AMP (cAMP), resulting in platelet secretion of thrombotic mediators and in platelet aggregation. The $P2Y_1$ receptor leads to improved calcium influx (Ca^{2+}), resulting in platelet shape change. Adinosine-3-phosphate-5phosphate (A3P5P) and Cangrelor (formerly AR-C9931MX) are two specific $P2Y_1$ and $P2Y_{12}$ antagonists, respectively. Adapted from [83].

1.5.1.3 Prostaglandin family receptors

There are ten known prostaglandin receptors, all are GPCRs of the seven transmembrane family. Five have been detected on platelets: receptors for TXA_2, PGI_2 (prostacyclin) PGD_2, PGE_1 and PGE_2. TXA_2 and prostacyclin are important physiological regulators of platelet function.

Thromboxane A_2 receptor: TXA_2 is a short-lived autocrine factor that amplifies aggregation and activation of platelets after they have been stimulated by agonists such as thrombin or ADP. It also functions as a vasoconstrictor and mitogenic agent, hastening the proliferation of cells involved in vascular repair [126]. Signals initiated at the TXA_2 receptor in response to binding facilitate integrin $\alpha_{IIb}\beta_3$ activation and subsequent secretion of dense granule contents. There are two forms of TXA_2 receptors on platelets, TPα and TPβ, which appear to arise in humans from differential splicing of a single gene [68]. Both mRNA transcripts are present in platelets. There is some evidence that TPβ heterodimerise with other GCPRs such as the prostacyclin receptor which may have functional significance [127]. In mice, most of the known TXA_2 functions also seem to be mediated through a single gene, the deletion of which results in a mild bleeding disorder [128]. The mouse gene seems to be organised similarly to the human gene with the entire coding region in exons two and three [128, 129].

The activated TPα in platelets couples through the G proteins Gq and $G_{12/13}$ [109] and possibly G_i [68]. The former stimulates protein phospholipase C-β which acts to raise intracellular calcium as well as activating protein kinase C signalling pathways. $G_{12/13}$ indirectly regulates the phosphorylation of myosin light chain through the Rho kinase. Both forms of TP appear to be coupled to adenyl cyclase, however TPα activates adenyl cyclase, whereas TPβ inhibits it. An Arg^{60} to Leu mutation in TPα in human patients leads to a

bleeding disorder [68]. This mutation decreases phospholipase C activation but does not affect adenyl cyclase inhibition.

Prostacyclin receptor: Prostacyclin (PGI_2), a prostaglandin secreted by endothelial cells, inhibits platelet aggregation through the PGI_2 receptor. This receptor called the IP receptor [74], activates adenyl cyclase through the G protein protein $G_{\alpha s}$ resulting in an increase in cyclic AMP [75]. The C-terminal portion of the IP receptor is substituted with a C-15 farnesyl isoprenoid chain at Cys383. The isoprenoid substitution is not required for prostacyclin binding but is necessary for efficient coupling to both adenyl cyclase and phospholipase C activation [126].

PGD_2 receptor: Prostaglandin D_2 has an anti-aggregatory activity on platelets through its receptor, of which there about 200 copies per average human platelet. There are a decreased number of these receptors in patients with type IIa hyperlipoproteinemia which may account for the thrombotic disorders that occur in such people [130].

PGE_1 and PGE_2 receptor: PGE_1 induces cAMP accumulation in platelets through the IP receptor. PGE_2 is a bimodal regulator of platelet aggregation: at high concentration it is an inhibitor but at low concentrations it potentiates the response of platelets to collagen or ADP. There are two receptors for PGE_2, called EP3 and EP4 in the mouse. EP3 inhibits adenyl cyclase whereas EP4 does the opposite [131]. EP3 is also a receptor for PGE_1 but EP4 is not. IP is not receptor for PGE_2.

1.5.2 Chemokine receptors

Platelets are the source for several chemokines including PF4, β thromboglobulin, epithelial/neutrophil activation peptide 78 (ENA-78) and the regulated upon activation, normal T-cell expressed and secreted (RANTES) chemokine. Platelets also have chemokine receptors including CCR1, CCR3, CCR4, CX3CR1, and CXCR4 [109, 132]. The latter is

the receptor for stromal cell factor 1 and for TARC (thymus and activation related chemokine). CXCR4 is also found on megakaryocytes and may have a role in their maturation [22]. CCR3 and CCR4 are receptors for RANTES which is released during platelet activation and so is likely to be involved in autocrine feedback regulation. CCR4 is also a receptor for some megakaryocyte produced cytokines and TARC which is also found in alpha granules. CX3CR1 is the receptor for fractalkine, known to be involved in atherosclerosis [133].

1.5.3 Other seven transmembrane receptors

There are a number of other GPCR with seven transmembrane regions expressed in platelets. These include the vasopressin receptor, the adenosine receptor, a β2-adrenergic receptor, the serotonin receptor, and D5 and D6 receptors for dopamine [109]. Vasopressin (anti-diuretic hormone) is a platelet agonist in the presence of adenosine, as the two receptors act in a synergistic manner. Serotonin is a major component of dense granules, so the presence of the receptor is another example of platelet autocrine regulation; serotonin functions as an agonist. The actions of dopamine on platelet function are still unclear.

1.6 ITAM-coupled receptors in platelets

The consensus immune receptor tyrosine based activation motif (ITAM) is YxxI/Lx(6–12)YxxI/L whereas the consensus immunoreceptor tyrosine based inhibitory motif (ITIM) is S/I/V/LxYxxI/V/L with 25-30 amino acid spacing between tyrosine residues [134]. In both cases, the tyrosines are phosphorylated by Src family kinases after ligand recognition and receptor clustering. However, in some cases ITAMs can mediate inhibitory signals and ITIMs can mediate positive signals [134].

As previously discussed, both the GPVI-associated FcRγ, the FcγRIIa and CLEC-2 (sections 1.6.1, 1.6.2 and 1.6.3) are ITAM coupled immunoreceptors that upon

phosphorylation leads to platelet activation events. Both have dual consensus ITAM sequences in their cytoplasmic regions and are also associated with calmodulin. Curiously, activation through either ITAM leads to the proteolytic cleavage and shedding of both [135] though the intramembranous region of FcγRIIa is protected.

The immunoglobulin (Ig) superfamily is a group of proteins that are structurally related as they all contain a specific region called the 'immunoglobulin domain'. The superfamily includes both soluble and membrane proteins, many of which are involved in recognition phenomena. The superfamily includes proteins of the immune system including antibodies, membrane proteins involved in antigen presentation and co-receptors, as well as some cell adhesion molecules, cytokine receptors, growth factor receptors and even the large intracellular muscle protein titin. The immunoglobulin superfamily is probably the largest family of proteins known with 700 plus members.

Among the members of the immunoglobulin superfamily found in platelets are GPVI, PECAM-1, the carcinoembryonic antigens CEACAM1 and CEACAM2, G6B, signal regulatory protein α (SIRPα) and the ITAM and ITIM coupled receptors. The carcinoembryonic antigens are discussed in a separate section (see section 1.8); the remainder is discussed below.

1.6.1 GPVI

GPVI is a platelet membrane receptor for collagen. It is 58 kilodalton glycoprotein that functions primarily as a signalling molecule through the FcRγ chain. Ablation of the FcRγ gene results in loss of GPVI from the platelets probably because FcRγ acts as a chaperone and required to trafficking GPVI to surface membrane [3]. The collagen binding domain resides in two immunoglobulin (Ig) C2 loops at the end of a long mucin-like stalk

(Figure 1-14). The cytoplasmic tail contains binding sites for calmodulin and The Src family of tyrosine kinases. The extreme C terminal end is absent in the mouse.

Of the macromolecules in the exposed extracellular matrix, collagen is the most thrombogenic; binding leads first to adhesion of platelets followed by the secretion of alpha and dense granule contents then platelet aggregation. This leads to further autocrine stimulation of thrombus formation.

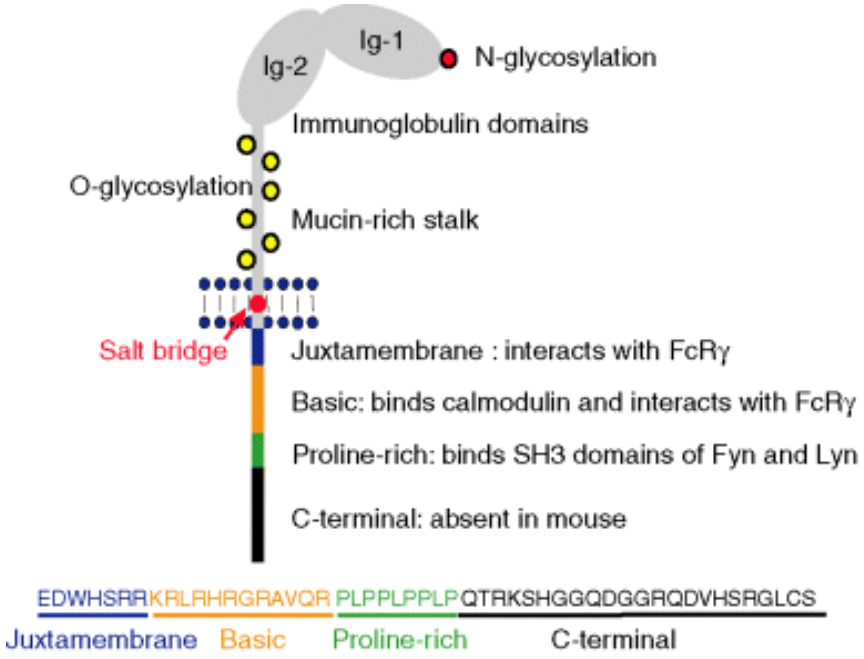

Figure 1-14: Structure of GPVI. Immunoglobulin domains, glycosylation sites, the mucin-rich stalk and the juxtamembrane region are shown. The proline rich region binds the src homology domains of Fyn and Lyn. A basic region in the C-terminal region binds to calmodulin and interacts with FcR γ-chain. Adapted from [136].

Collagen binds not only to GPVI but also to integrin $\alpha_2\beta_1$ (Figure 1-15), but there are CRPs that bind only to GPVI [136], therefore the contribution by each to thrombus formation can be experimentally separated. The snake venom toxin convulxin is also very

powerful activator of signalling processes through GPVI. Since it is tetrameric, the toxin is able to cross-link the GPVI receptor, which presumably collagen does as well, since it presents multiple binding sites in its highly repetitive structure. These agents have allowed the dissection of activation through GPVI from that of other receptors. Also, collagen-induced thrombus formation under shear conditions is deficient in platelets lacking GPVI [137].

Cross-linking of GPVI receptors leads to the phosphorylation of the ITAM of FcRγ by Src-like kinases Fyn and Lyn (Figure 1-15). The kinases are bound to the proline rich cytoplasmic region of GPVI. Syk kinase binds to the phosphorylated ITAM portion of FcRγ, leading to Src kinase mediated and autophosphorylation of Syk. Syk initiates a series of down-stream events which include the formation of a Linker of Activation T cells (LAT) signalosome and activation of PLCγ2. PLCγ2 is also activated by integrin $\alpha_2\beta_1$ and GPIb-IX-V but signalling through GPVI is considerably more powerful. Src kinase inhibitors completely inhibit aggregation and limit adhesion on collagen/vWF surfaces under conditions of high shear. Similar results are obtained in platelets deficient in PLCγ2 [136, 138].

Some idea of the complexity of signalling processes is given by Figure 1-15. However, it is probably even more complicated. For instance, GPIb-IX-V and GPVI are physically and functionally connected. Note the presence of Btk/Tec (Bruton's tyrosine kinase) in the signalosome adjacent to PLCγ2. Btk and other kinases of Tec family are non-receptor tyrosine kinases which frequently are involved in PLC activation and calcium mobilisation. An inhibitor of Btk was shown to prevent collagen-induced thromboembolism in an experimental mouse model [139].

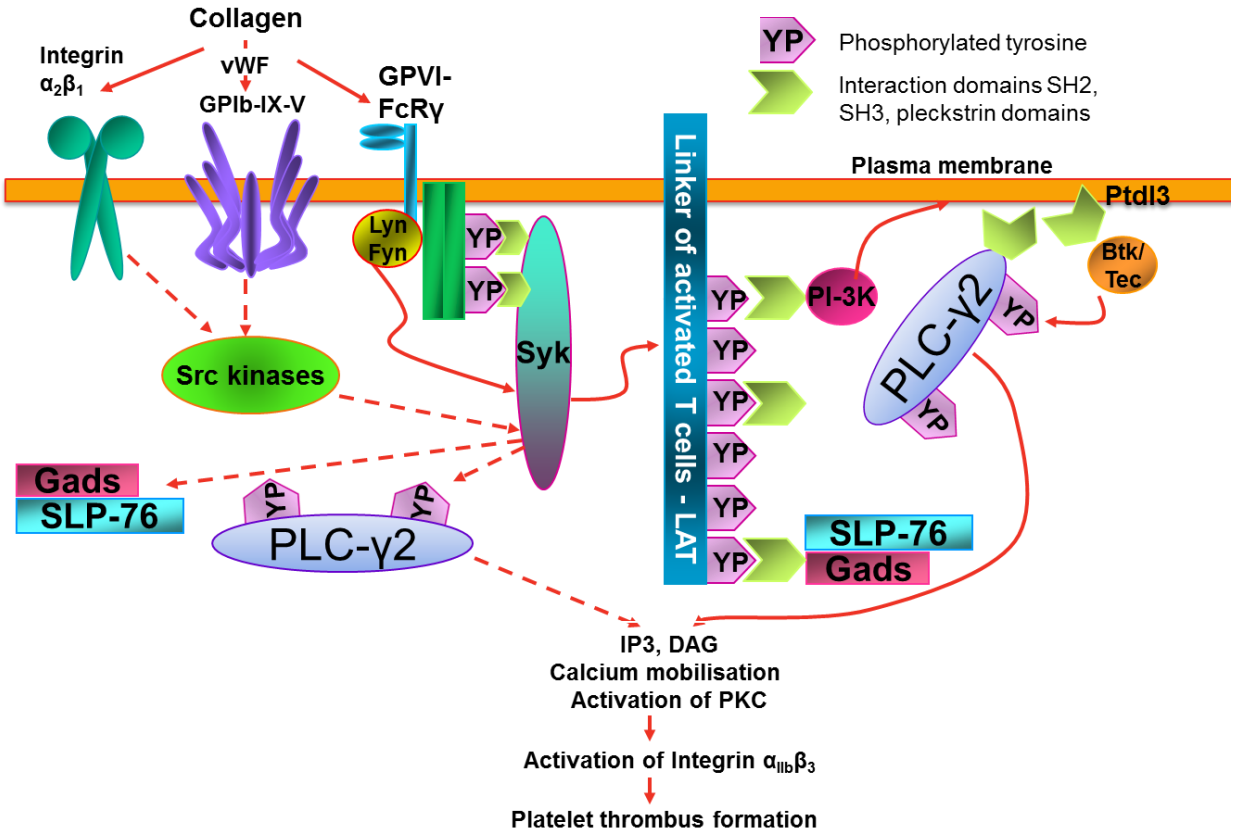

Figure 1-15: Signalling through GPVI and the LAT signalosome. Collagen interacts directly with GPVI/FcR γ-chain and integrin $\alpha_2\beta_1$. Also collagen interacts indirectly to GPIb-IX-V complex via the A1 domain of vWF. The ITAM regions of the latter interact with Src homology regions after phosphorylation and lead to platelet thrombus formation. Adapted from [136].

1.6.2 FcγRIIa- A second platelet ITAM receptor

Another member of the immunoglobulin superfamily found in human platelets but not mouse is FcγRIIa [140]. It has molecular weight of 42 kilodaltons and contains two C-2 type Ig loops, similarly to GPVI. On its cytoplasmic tail it has two ITAMs. FcγRIIa is complexed with GPIb-IX-V and can be activated on the surface by vWF or from within by G-protein-coupled receptors.

FcγRIIa is involved in immunological defences to a variety of pathogens; it is present on macrophages and neutrophils. By binding to antibody complexes, it may promote interaction between platelet and pathogens. Its presence on platelets is problematic however, since clustering of the protein is induced by many antibodies in immune disorders. Similarly to GPVI, clustering of FcγRIIa activates platelets. This is particularly difficult in heparin induced thrombocytopenia wherein antibodies to complexes of heparin with PF4 activate platelets through FcγRIIa, leading to deficiency of platelets and thrombus formation [141].

1.6.3 The C-type lectin CLEC-2 in platelets

Exploring how C-type lectin 2 (CLEC-2) activates platelets through a signalling process that uses the single YxxL sequence, down to the molecular level, is crucial for further understanding its role in platelet function. As a result, this section will explore the historical research describing CLEC-2, which led to the modern understanding of how this receptor is an important mediator of the platelet activation process. This will include a description of the structure of CLEC-2 and their signalling pathways.

CLEC-2 was the subject of research by Suzuki-Inoue et al. when researching rhodocytin (aggretin), a toxin found in snake venom [142]. The group observed that CLEC-2 acted as a rhodocytin receptor in platelets. Subsequent assays conducted by Chaipan et al. and Kerrigan et al. showed that CLEC-2 belongs to the V (non-classical) C-type lectin receptor group [143, 144]. High levels of the receptor are expressed in human

and mouse platelets and low levels are found in mouse neutrophils and sinusoidal endothelial cells in the liver of rats. However, the two research programs found no evidence that CLEC-2 was expressed in human neutrophils. This research followed studies by Colonna et al. which highlighted the presence of CLEC-2-derived mRNA in a range of blood cell types, including dendritic cells, granulocytes, and monocytes [145]. However, they found no evidence of CLEC-2 protein in these cells. Previously, Weis et al. and Drickamer groups had proposed a likely structure for CLEC-2, suggesting that it included a single transmembrane section connected to a stalk region, alongside an N-terminal domain embedded in the cytoplasmic tail [146, 147]. The two research groups also discovered a C-type lectin-like domain (CTLD), specifically a C-terminal carbohydrate-like recognition domain (CRD). Through a process of elimination, the two research groups deduced that ligands must bind to the receptor site through a protein-based interaction, because the CTLD possessed none of the residues that are essential for the binding of carbohydrates. Following this line of reasoning, it is therefore possible to suggest that rhodocytin also uses this binding mechanism to bind, because it contains no glycosylated groups.

CLEC-2 contains only one signalling motif, a single YxxL motif incorporated in the cytoplasmic tail alongside a triple amino acid group (Figure 1-16). This singular motif separates CLEC-2 from similar proteins containing ITAM, because other members of this family incorporate a double YxxL sequence separated by between six and twelve amino acids. Although the receptor protein families containing ITIM and immunoreceptor tyrosine-based switch motif (ITSM) also incorporate a single YxxL group, it is structurally and, therefore, functionally different to the YxxL group found in CLEC-2. The CLEC-2 YxxL structure does not include the conserved amino acid sequence located before the YxxL motif. For the ITIM and ITSM receptor proteins, these YxxL motifs

perform an essential function in regulating the inhibition of ITAM. They achieve this by interacting with the SHP-1/SHP-2 tyrosine phosphatases or SHIP-1/SHIP-2 inositol phosphatases that form part of the SH2 domain.

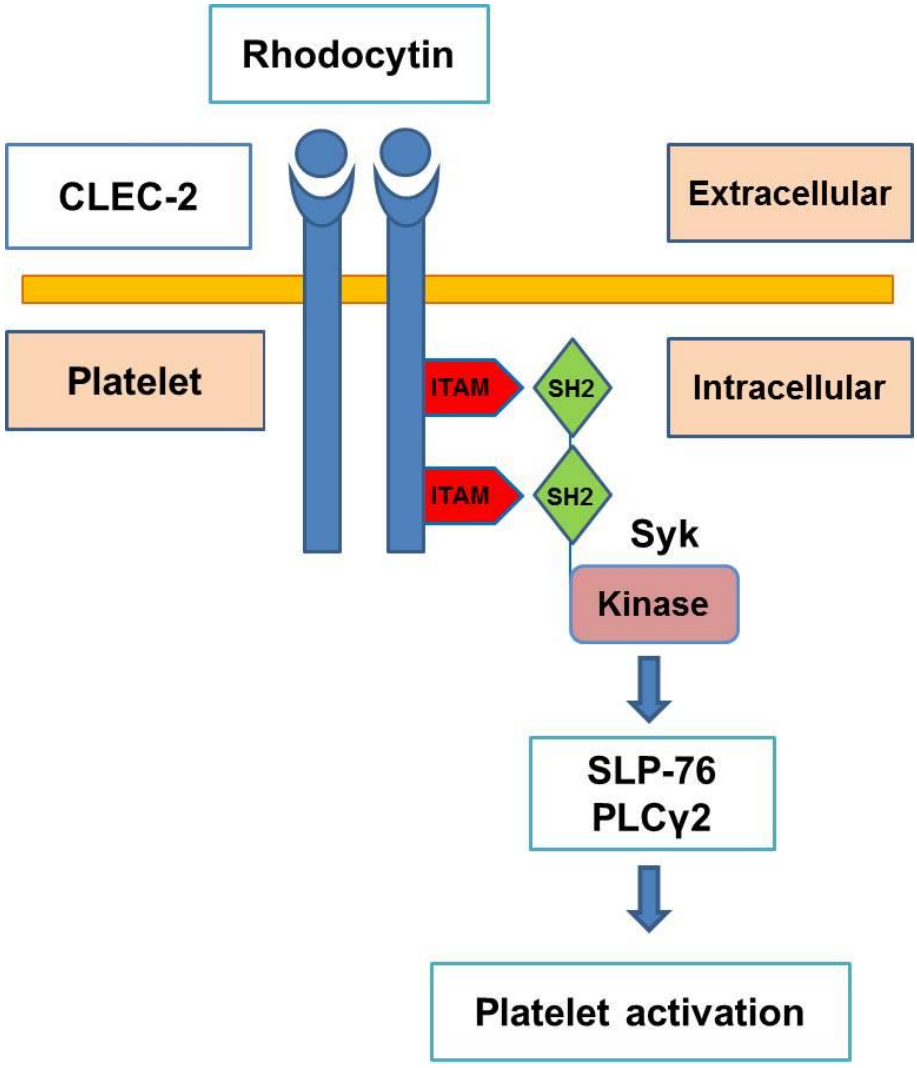

Figure 1-16: The CLEC-2 structure and signalling pathways. CLEC-2 signalling pathway is mediated after rhodocytin stimulation via atypical ITAMs leads to Syk activation and resulting in platelet activation. Red colour (ITAMs domains), Green colour (SH2 domains), Pink colour (Tyrosine kinase, Syk) and Blue colour (CLEC-2 structure). Adapted from [148].

1.6.3.1 Rhodocytin

To study the molecular basis of how haemotoxins promote clotting, Huang et al. and Shin and Morita purified venom extracted from the Malayan Pit Viper (*Calloselasma rhodostoma*) [149, 150]. The results showed that the major active toxin was rhodocytin, a C-type lectin [149, 150] which caused platelet activation and aggregation. Blocking of integrin $\alpha_2\beta_1$ by antibody inhibited the powerful aggregating action [149, 151]. Subsequently, Eble et al. argued that integrin $\alpha_2\beta_1$ could not be the mechanism behind clotting, because rhodocytin showed no affinity for recombinant integrin $\alpha_2\beta_1$ [152]. Conversely, simultaneous research by Clemetson suggested that integrin $\alpha_2\beta_1$ and GPIbα antibodies could restrict rhodocytin-induced platelet activation [153]. This contradicted research conducted by Shin and Morita, which suggested that cleaving GPIbα had no effect on rhodocytin-initiated platelet activation [150]. Bergmeier et al. added further complexity by showing that integrin $\alpha_2\beta_1$, GPIbα, and GPVI, a collagen receptor, were not necessary components of platelet activation in the presence of rhodocytin [154]. Their research involved depleting the GPIbα group of mice through the action of O-sialoglycoprotein endopeptidase, and the GPVI group via JAQ1, a GPVI monoclonal antibody, leaving no active integrin $\alpha_2\beta_1$ complex [154]. Thus, Bergmeier et al. proposed that the process by which rhodocytin stimulates powerful activation of platelets does not require integrin $\alpha_2\beta_1$, GPIbα, or GPVI [154].

To further explore the processes underpinning rhodocytin-induced platelet activation, Suzuki-Inoue et al. used rhodocytin affinity chromatography and mass spectrometry as part of a proteomic approach [142], showing that CLEC-2 was crucial. Research using activation with NFAT as a reporter construct to study expression in DT40 cells derived from chickens further supported this [142]. Finally, this line of research showed that the engagement of CLEC-2 was the only process needed to initiate human platelet activation by rhodocytin. This was achieved by showing that a polyclonal antibody to CLEC-2 instigated human

platelet activation without FcγRIIa, a platelet low-affinity IgG Fc receptor [142]. Fuller (2006) showed that integrin $\alpha_2\beta_1$ was not involved in the rhodocytin-CLEC-2 binding process, by showing that azide-free preparations of integrin $\alpha_2\beta_1$-blocking antibodies did not inhibit the action of rhodocytin on platelet activation. In conclusion, this part of research shows that the CLEC-2 receptor is responsible for facilitating platelet aggregation in the presence of rhodocytin.

1.6.3.2 The CLEC-2 signalling pathway

The CLEC-2 receptor was identified through cloning processes using a bio-informatic screen to look for receptors with a similar structure to C-type lectin [145]. Its exact function and ligands remained largely unknown until research showed that it was a signalling receptor located on the platelet surface, with the ability to instigate platelet aggregation [142]. Structural assay techniques were used to study the composition of CLEC-2, finding that the lectin-like receptor contained a YxxL motif in its cytoplasmic tail. The results also suggested that this motif was very similar to the YxxL-(X)10-12-YxxL found in ITAM, with one difference: CLEC-2 contains a single rather than a tandem motif. To make a distinction between the two motif types, CLEC-2's single motif arrangement is referred to as a half- or hemi-motif, in common with other similar receptors. It is known that the ITAM signalling motif, which is found in T-cell receptors as well as in the GPVI/FcRγ-chain complex collagen receptor in platelets, plays a highly significant role in immune responses. Investigation of the GPVI/FcRγ-chain's role in signalling events shows that GPVI cross-linking within the FcRγ-chain cytoplasmic domain induces tyrosine phosphorylation of the ITAM receptor through the action of Fyn and Lyn, members of the Src kinase family. At the next stage of the signalling cascade, the phosphorylated ITAM undergoes binding with the SH2 tandem domain, which initiates downstream signalling events that induce tyrosine phosphorylation of a number of Syk substrates, including the adaptor proteins LAT, SLP-

76, and Vav1/3. A number of effecter enzymes, including Bruton's Tyrosine Kinase (Btk); PI3-kinase; the Rho family members Rac and Cdc42; and PLCγ2, are also activated [155].

Suzuki-Inoue's research group investigated the rhodocytin signalling process, showing that the toxin prompts the single YxxL motif to undergo phosphorylation and, via a downstream cascade, bind with the Syk tandem SH2 domains. Crucially, the hemi-ITAM must be present for CLEC-2 signal transduction to occur [142, 156]. Further studies revealed the process by which the CLEC-2 domain's single YxxL motif binds with the SH2 domains of Syk. Research studies led by Watson and O'Callaghan suggested that CLEC-2 has a dimeric form in inactivated platelets, with a 2:1 stoichiometric binding ratio between the tandem SH2 domains of Syk and the phosphorylated domains of two CLEC-2 molecules [155, 157].

Studies using immunoprecipitation further revealed the potential processes behind the interaction of CLEC-2 and Syk tyrosine kinase. Firstly, phosphorylated CLEC-2 peptides could bind and precipitate Syk from mouse platelets and, in turn, CLEC-2 precipitation from platelets treated with rhodocytin is facilitated by the tandem SH2 domains of Syk tyrosine kinase [142]. Secondly, a number of point mutations that inhibit phosphotyrosine binding in the Syk N- and C-terminal SH2 domains blocked CLEC-2-induced signalling processes in transfected DT40 cells [156]. Added to this, Suzuki-Inoue et al. showed that the presence of both the Syk N- and the C- terminal SH2 domains is essential for an interaction to occur, because neither domain on its own was able to instigate the precipitation of CLEC-2 from platelets treated with rhodocytin [142]. Taken together, these research studies show that Syk tyrosine kinase regulation of CLEC-2 uses a unique process, with a pair of phosphorylated CLEC-2 receptors cross-linked across the N- and C-terminal SH2 domains.

Overall, the downstream elements of the CLEC-2 signalling pathway closely resemble the GPVI process, instigating the tyrosine phosphorylation of LAT, SLP-76, and Vav1/3, and the activation of Btk and PLCγ2 effector enzymes [142, 156]. Syk and PLCγ2 knockout murine platelets showed no response at all, even at extreme concentrations of rhodocytin, reinforcing the idea that Syk and PLCγ2 are crucial components of signal transduction mediated by CLEC-2. Conversely, murine platelets lacking LAT or SLP-76 adaptor proteins, or Vav1/3, a guanine nucleotide exchange factor, showed no reaction at low concentrations of rhodocytin but limited reaction at higher concentrations. Therefore, they have an essential compensatory function during CLEC-2 signalling [142]. Adaptor proteins are essential to the YxxL motif-containing receptor signalling process, because they create a protein framework around which PLCγ2 interacts with the platelet membrane. Many adaptor proteins, including the membrane adaptor LAT and the cytosolic adaptors SLP-76 and Gads, are present in platelets. The adaptor proteins LAT or SLP-76 play some role in the CLEC-2 signalling process, and GPVI-based signalling is inhibited if these proteins are deficient. However, the effect of SLP-76 is subtly different: mice with the SLP-76 protein knocked out have an inhibited GPVI signalling process, while CLEC-2 signalling is only partially inhibited, suggesting that the CLEC-2 complex has the ability to use other adaptor proteins to retain some functionality [142, 156]. Research also showed that Gads in platelets interacts with SLP-76 and tyrosine phosphorylated LAT, so must play a major role in recruiting PLCγ2 to the platelet membrane surface by creating links with the SLP-76 and LAT functional groups. In Gads-deficient mice, platelet activation in the presence of relatively low concentrations of CLEC-2 or GPVI is only slightly retarded, and full activation occurs in the presence of high concentrations of these agonists. This implies that Gads has a relatively minor role in the CLEC-2 and GPVI signalling pathways, and supports the existence of platelet activation processes independent of Gads further down involving LAT adaptor molecule

1.6.3.3 Endogenous CLEC-2 ligands

In a landmark study investigating how platelets interacted and bound with human immunodeficiency virus type 1 (HIV-1) particles, Chaipan et al. suggested that CLEC-2 possessed an endogenous ligand. The study showed that platelets had the ability to bind with HIV-1 particles, internalising them via a process using CLEC-2 and DC-SIGN receptors [143]. DC-SIGN was the main driver of this process, by binding with mannose sugar complexes within the HIV-1 viral envelope protein, Env [158]. However, the presence or absence of Env protein made little difference to CLEC-2 binding, indicating that the receptor used a protein derived from the host cell used by the virus during replication. If CLEC-2 and DC-SIGN were blocked, platelet binding to the viral particles was significantly inhibited, indicating that the proteins interacted and promoted the propagation of the HIV-1 virus throughout the infected host [143].

Suzuki-Inoue et al. building upon their affinity purification research that identified CLEC-2, showed that podoplanin was a CLEC-2 ligand [159]. Many types of tumour cells preferentially express podoplanin on their leading, invasive edge, and this ligand can play a role in platelet aggregation [160]. In turn, this tumour-cell induced platelet activation may prompt cancer metastasis through the release of metalloproteinases and growth factors, ultimately leading to tumour cell invasion and growth [161, 162]. Indeed, this tumour cell-induced activation resembles some of the features of the platelet activation process in the presence of rhodocytin, with a distinct, recognisable delay [163, 164]. This lag phase prompted Suzuki-Inoue et al. to hypothesise that CLEC-2 was the receptor responsible for mediating platelet activation in tumour cells through the action of podoplanin.

1.7 ITIM-coupled receptors in platelets

Probably the most important ITIM-bearing receptor in platelets is PECAM-1 which inhibits platelet responses to collagen binding. Phosphorylation of the ITIM regions result in the binding of protein-tyrosine phosphatase SHP-2 and with a lower affinity the related phosphatase SHP-1 (Figure 1-15). Both phosphatases have Src homology 2 (SH2) domains that bind to phosphorylated tyrosine ITIM Y663 and Y686 motif [165]. Also recruited is PP2A, which also contains the SH2 domain, which is an inhibitor of p38 MAP kinase. Phosphorylation of SHP-1 and 2 introduces docking sites for Grb2 which connects the complex to signalling processes through integrin $\alpha_{IIb}\beta_3$.

1.7.1 PECAM-1

PECAM-1 was first recognised as the leukocyte differentiation antigen CD31 present on platelets, monocytes and granulocytes [166]. Various investigators working on endothelial cells described this protein known as glycoprotein (GP) IIa, GPIIa', ENDOCAM, or the hec7 antigen that was particularly concentrated at cell/cell junctions. Cloning of the cDNA for the protein showed that it was of immunoglobulin superfamily and homologous to other cell adhesion molecules [167]. So the protein was renamed once again as the platelet/endothelial cell adhesion molecule-1 or PECAM-1. Among other activities, PECAM-1 interacts with neutrophil membrane glycoproteins to promote neutrophil transmigration through the endothelial layer [168, 169].

PECAM-1 is 130 kilodalton transmembrane glycoprotein with six type C2 Ig-Domains (6 Ig) [166, 170, 171]. Two ITIMs are in the cytoplasmic tail of the protein [166]. Both ITIMs become tyrosine phosphorylated after integrin $\alpha_{IIb}\beta_3$-mediated platelet aggregation and recruit the SH2 domain containing protein-tyrosine phosphatases, SHP-1 and SHP-2.

The cytoplasmic tail can be variously sized depending on differential splicing of exons 10-16 yielding isoforms of PECAM-1 that may have functionally different properties. The expression of PECAM-1 on the platelet surface varies between individuals from 5000 to 8800 copies per platelet [74, 172]. There are several allelic variations of PECAM-1 that have been described [173] some of which may be implicated in cardiovascular disease.

Despite the fact that PECAM-1 can interact with PECAM-1 molecules on other cells, it is not involved directly in platelet aggregation. However, engagement of Ig-Domain 6 of PECAM-1 using anti-PECAM-1 antibodies augmented platelet activation [174]. Despite its homology and activity in other cell types as a cellular adhesion molecule, its role in platelets is mostly related to signal transduction. It serves as a bidirectional signalling device.

Dephosphorylation of Syk and Btk kinases by SHP-1 leads to a decrease in their activity [175]. In turn, the decrease in kinase activity inhibits tyrosine phosphorylation of PLC, and hence a decrease in its activity, thus lowering the concentration of inositol (1,4,5) triphosphate and diacylglycerol (DAG). In principle, this could account for some of the inhibitory properties of signalling through PECAM-1. In fact, mutation of tyrosine to phenylalanine resides at ITIM sites prevents recruitment of SHP-2 by PECAM-1 [134, 176, 177].

PECAM-1 is a positive modulator of adhesion strengthening mediated by integrin $\alpha_{IIb}\beta_3$. It is a negative regulator of collagen and immune complex receptors that have ITAM-1 sequences like FcRγ which is complexed to GPVI. PECAM-1 deficient mice form larger thrombi that are more stable than wild-type mice (Figure 1-17), confirming an inhibitory role for PECAM-1 *in vivo* [178].

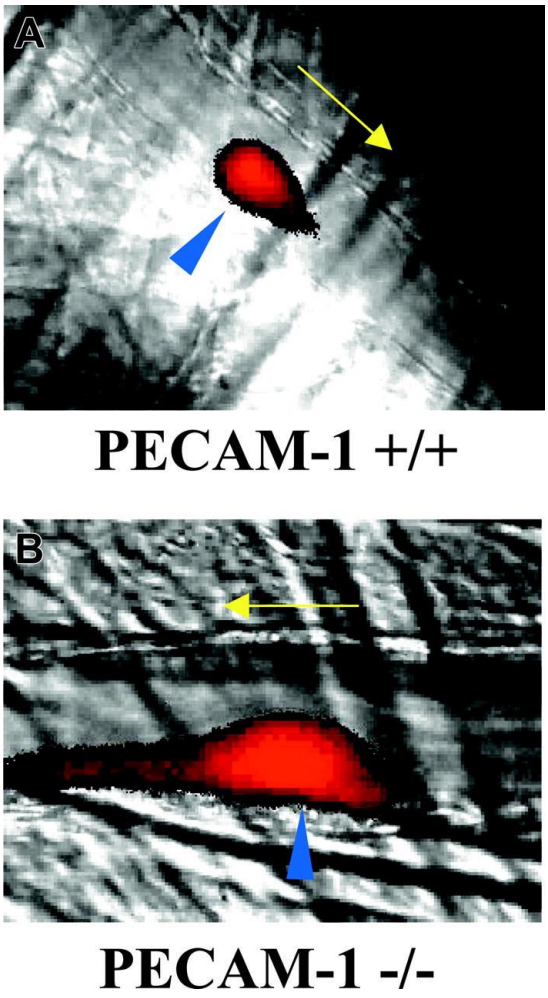

Figure 1-17: Difference in thrombus formation in PECAM-1$^{+/+}$ mice versus PECAM-1$^{-/-}$ mice by intravital microscopy (IVM). (A) Shows the Control and (B) The thrombus formation in cremaster muscle arteriole by using nitrogen dye laser. PECAM-1$^{-/-}$ mice were labelled with CD41 Ab (Fab fragment). After three minutes, thrombus formation was studied using bright field and florescence microscopy. The yellow arrows show the direction of blood flow while blue arrows specifically show the laser-induced damage position. The red blot indicates the size of the clot. Adapted from [178].

1.7.2 Other ITIM receptors

Another ITIM coupled receptor found in platelets is G6B, which contains single Ig domain and two ITIMs in its cytoplasmic tail [179]. Like PECAM-1, phosphorylation of the ITIMs produces sites for SHP-1 and SHP-2 binding. Cross-linking of G6B with antibodies causes an inhibition of platelet aggregation in response to such agonists as ADP and collagen-related peptides. This inhibition does not require calcium. Inhibition of signalling through CLEC-2 or GPVI seems to be independent of SHP-1 and SHP-2 and may involve inhibition of signalling through Src and Syk kinases [180].

Also found on platelets is another ITIM bearing immunoreceptor, TREM-like transcript 1 (TLT-1) [181]. TLT-1 also contains a proline rich region. TREM stands for triggering receptors expressed on myeloid cells and represents a family of at least five members. TLT-1 is found only on megakaryocyte and platelet alpha granules but relocates to the platelet surface upon stimulation with agonists [182]. The TLT-1 cytoplasmic tail binds to ezrin/moesin/radixin family of proteins which suggest that it maybe involved in linking to fibrinogen [183]. Unlike the other ITIM containing proteins, TLT-1 is involved in promoting platelet activation rather than inhibiting it. TLT-1 deficient mice have an extended bleeding time and develop inflammatory lesions and haemorrhage [183].

1.8 Carcinoembryonic antigen related cell adhesion molecule family

The original carcinoembryonic antigen (CEA) is a cell adhesion molecule expressed during embryogenesis but not normally found in adults [184]. Its presence in tumours of various types made it a valuable tumour marker. CEA-related molecules make up a family of at least 29 members, which are in turn a subset of the immunoglobulin superfamily (see section 1.6.1, 1.6.2 and 1.7.1).

Carcinoembryonic antigen-related cell adhesion molecule-1 (CEACAM1) contains 4 Ig-Domains, a transmembrane domain followed by a long (ITIM-containing) or short cytoplasmic domain (ITIM-less). CEACAM1 (also known as biliary glycoprotein and CD66a) was discovered first as a protein receptor of the hepatitis virus in the bile ducts within the liver [185]. CEACAM1 displays broad expression that is conserved in human and rodents and has since been recognised as a cell adhesion protein expressed on the surface of granulocytes, leukocytes, monocytes, dendritic cells, endothelial cells and in some epithelia [186].

CEACAMs preferentially form homodimers, i.e.: CEACAM1 binds itself (homophilic-homophilic interaction involving Ig-Domain 1), or heterodimers with CEA and CEACAM6. CEACAMl is a member of the Ig-ITIM superfamily that is a cousin of PECAM-1. These two receptors share similarities in structure and function in many biological systems, particularly in their ability to act as inhibitory co-receptors to modulate ITAM-associated signalling pathways.

In mice, there are two CEACAM genes designated as CEACAM1 and CEACAM2 [185]. While CEACAM2 is restricted to the mouse, functions of CEACAM2 in the mouse are taken over by CEACAM1 in humans based upon evolutionary conservations. CEACAM1 and CEACAM2 share some similarities in structure, but differ in the number of extracellular Ig-Domains (CEACAM1 contains 4 Ig-Domains while CEACAM2 contains 2 Ig-Domains, Figure 1-18) and in the ligand binding properties of their distal variable N-terminal Ig-Domain. CEACAM1 N-terminal variable Ig-Domain 1 mediates homophilic binding while CEACAM2 does not [186]. At this stage the only ligand identified for CEACAM2 is the murine coronavirus mouse hepatitis virus spike glycoprotein(s). Both CEACAM1 and CEACAM2 contain transmembrane receptors and contain *identical* ITIMs in their cytoplasmic domains.

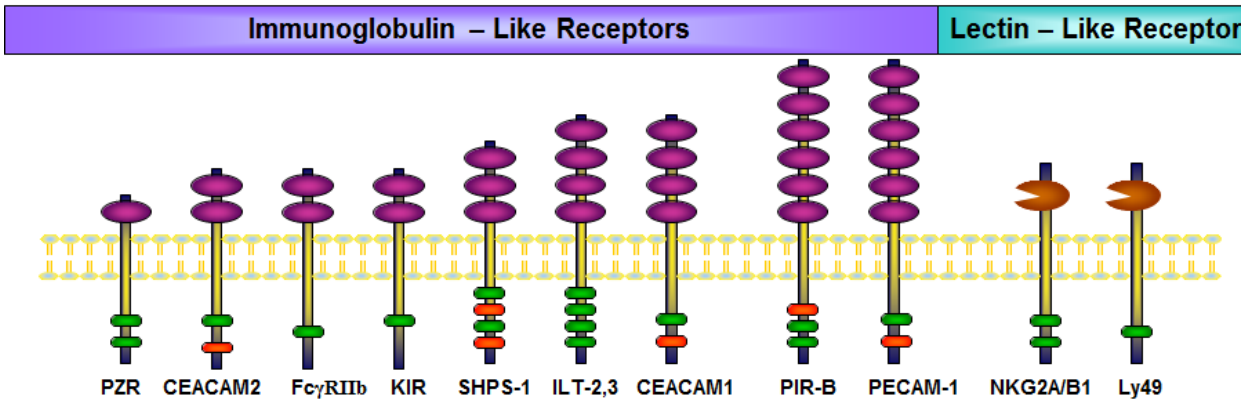

Figure 1-18: Immunoglobulin superfamily receptors and Lectin- like receptors. This figure shows comparison of the structures of PECAM-1, CEACAM1, and CEACAM2. CEACAM1 and CEACAM2 structures vary considerably at the N-terminus. The structures above represent the most common forms, although differential splicing leads to a number of isoforms. CEACAM1 and CEACAM2 have identical transmembrane and cytoplasmic regions including the ITIM. The cytoplasmic domain is only ten amino acids. Purple colour (Ig domains), Green colour (ITIM domains), Red colour (ITSM domains) and Orang colour (Lectin domains).

The role of CEACAM2 protein in platelet function is not clearly defined. Based upon previous studies, CEACAM1 is expressed on the surface of murine and human platelets and expression is upregulated by platelet activation. CEACAM1 is expressed modestly on the surface of resting platelets [187] but has prominent intracellular expression profile suggesting that like TLT-1 it is compartmentalised until platelet activation events occur. The fact that CEACAM2 has different ligand properties than CEACAM1 would suggest unique biological roles as the avidity of ligand interactions (activation versus clustering) appears fundamental to drive cell signalling responses (Figure 1-19). In preliminary studies, CEACAM2 appear to function in a similar way as CEACAM1 at least in the context of insulin metabolism [188].

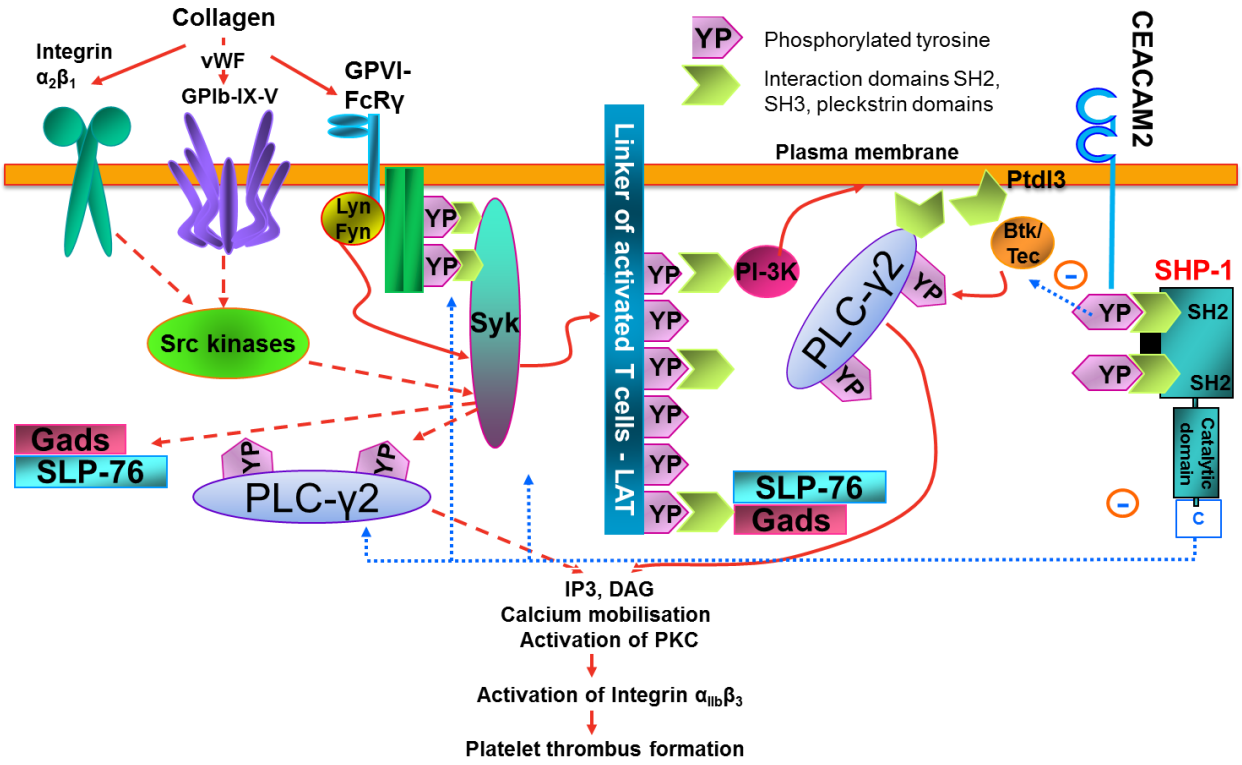

Figure 1-19: Model of the expected role of CEACAM2 in GPVI signalling pathway via LAT signalosome. The ITAM regions of the latter interact with Src homology regions after phosphorylation. ITIM residues of CEACAM2 interact with SH2 domains of SHP-1 resulting in a conformational change where the catalytic domain opens up. This event allows the catalytic domain to do dephosphorylation of ITAM signalling elements to downregulate the ITAM pathway components. Adapted from [136].

CEACAM1 is expressed on the surface of mouse and human platelets and inhibits platelet-collagen interactions as well as thrombus growth [187]. CEACAM1 is capable of homophilic reactions, which are critically dependent on amino acid residues 43 and 44 [189, 190]. Three C2 and one N-terminal V-type Ig domains are contained within the extracellular portion of CEACAM1 (Figure 1-18). The CEACAM1 gene contains a functional promoter and nine exons [191]. During mRNA processing, exon 7 is alternatively spliced which results in the expression of two isoforms, the short isoform (CEACAM1-4S) lacking 61 of the 71 amino acids of intracellular domain and the long isoform (CEACAM1-4L) which includes serine (Ser503) and tyrosine (Tyr488) phosphorylation sites [192]. The short isoform lacks the intracellular phosphorylation sites of 4L isoform [192]. CEACAM1 mediates various functions, including cell adhesion [193] and tumor suppression [194], and acts as a 12 mediator of angiogenesis [195] and T-lymphocyte signalling [196].

Platelets from mice lacking the CEACAM1 gene displayed enhanced reactivity to collagen and CRP and larger thrombus growth both *in vitro* and *in vivo*. The *Ceacam1*-deficient mice were more susceptible to collagen induced thromboembolism than wild-type mice [187].

The human CEACAM1 gene has two homologues in mice, termed CEACAM1 and CEACAM2, whereas only one is found in the rat [197]. The differences in the coding region between the CEACAM1 and CEACAM2 are mainly found in exon 2. As in the human, the mouse CEACAM1 gene is expressed abundantly in the liver, spleen, small intestine and prostate. In contrast, CEACAM2 is only found in the kidney, testis and to smaller extent in the spleen [188] (which is a repository for platelets). The differences in expression indicate that the two related proteins are not functionally redundant. Though the presence of CEACAM1 has been demonstrated in platelets [187], there appears to be no published data on the expression of CEACAM2 in platelets.

Interestingly, CEACAM1 is substrate of the insulin tyrosine kinase [198]. Deletion of CEACAM1 gene in mice results in insulin resistance, dyslipidemia and fatty liver due to elevated tryglyceride and cholesterol levels. CEACAM1 deficient mice are being investigated as model of metabolic syndrome and type II diabetes. It should be noted, however that deletion of CEACAM1 is not lethal nor does it appear to cause obvious developmental defects.

Like PECAM-1, phosphorylation of the ITIM of CEACAM1 is known to result in the recruitment of SHP-1, at least in T-cells [199]. Like PECAM-1, CEACAM1 contains ITIM sequences that when phosphorylated inhibit Src family kinases, probably through interaction with Src homology (SH) domains [200]. Platelets express at least six Src family kinases including Lyn, Fyn, Fgr, Src, and Yes. As previously discussed, Fyn and Lyn are known to be involved in platelet activation through the GPVI collagen receptor (see section 1.6.1) and Fyn and Src are involved in 'outside in' signalling through integrin $\alpha_{IIb}\beta_3$ (see section 1.3.1.1). Lyn is also implicated in vWF signalling through the GPIb-IX-V receptor. It seems likely that PECAM-1 and CEACAM1 and possibly CEACAM2 and other ITIM bearing inhibitors such as G6b achieve inhibition by down-regulating the activity of Src family kinases in the absence of strong signalling through collagen or vWF binding.

1.9 Mechanism of stable thrombus formation in mice

Mechanisms of platelet activation and aggregation are thought to have some similarities in mammals with minor differences in receptor repertoires. The small differences with respect to human platelets (containing 3 ITAM containing receptors) and mouse platelets (lacking FcγRIIa, while containing two ITAM receptors which are GPVI/FcR γ-chain and CLEC-2) need to be understood when exploring the formation of a thrombus [119]. The shorter GPVI cytoplasmic tail in mice, fall under the heading of

variations on a theme, rather than fundamental differences. Nevertheless, the following describes the situation in mice, in which researchers have the advantage of clean genetic techniques. First, it should be made clear that thrombus formation is not the only function of platelets. They are known to interact with and engulf pathogens. Animals or humans with thrombocytopenia have spontaneous bleeding events in the absence of obvious injury. Thus, platelets are involved in haemostasis on a non-emergency basis. Small vascular leaks that occur in the normal course of physiology do not require large clots. Platelets also appear to be actively involved in the both adult and embryonic regulation of angiogenesis [201-204].

In vivo mouse model of platelet thrombus formation have shown that this is a dynamic highly complex multi-step process. These studies include platelet activation, involvement of vWF, collagen, fibrinogen and fibronectin, various platelet aggregation accumulations, intracellular calcium mobilisation, and release of secondary wave mediators, ADP, and TXA_2. Thrombus formation initially involves platelet translocation and adhesion via platelet adhesive receptor–ligand interactions to exposed extracellular matrix (ECM) components; platelet accrual occurs, this may be followed by fragments of thrombus breaking off and embolising downstream [205-208]. Finally, a thrombus will grow and eventually occlude the vessel. Several factors influence thrombus stability, including platelet adhesive protein-ligand interactions, outside-in signalling events of integrins, particularly integrin $\alpha_{IIb}\beta_3$, stable platelet adhesion, signalling molecules involving Src family kinases and secondary wave mediators, ADP, TXA_2 and their receptors $P2Y_{12}$ and TP [209]. Numerous studies confirm the role of other platelet receptors on the stability of thrombus formation *in vivo*, including CD40L, Gas6, semaphorin 4D and contact-dependent signalling events [210-212]. Mechanisms of stable thrombus formation are explained in Figure 1-20.

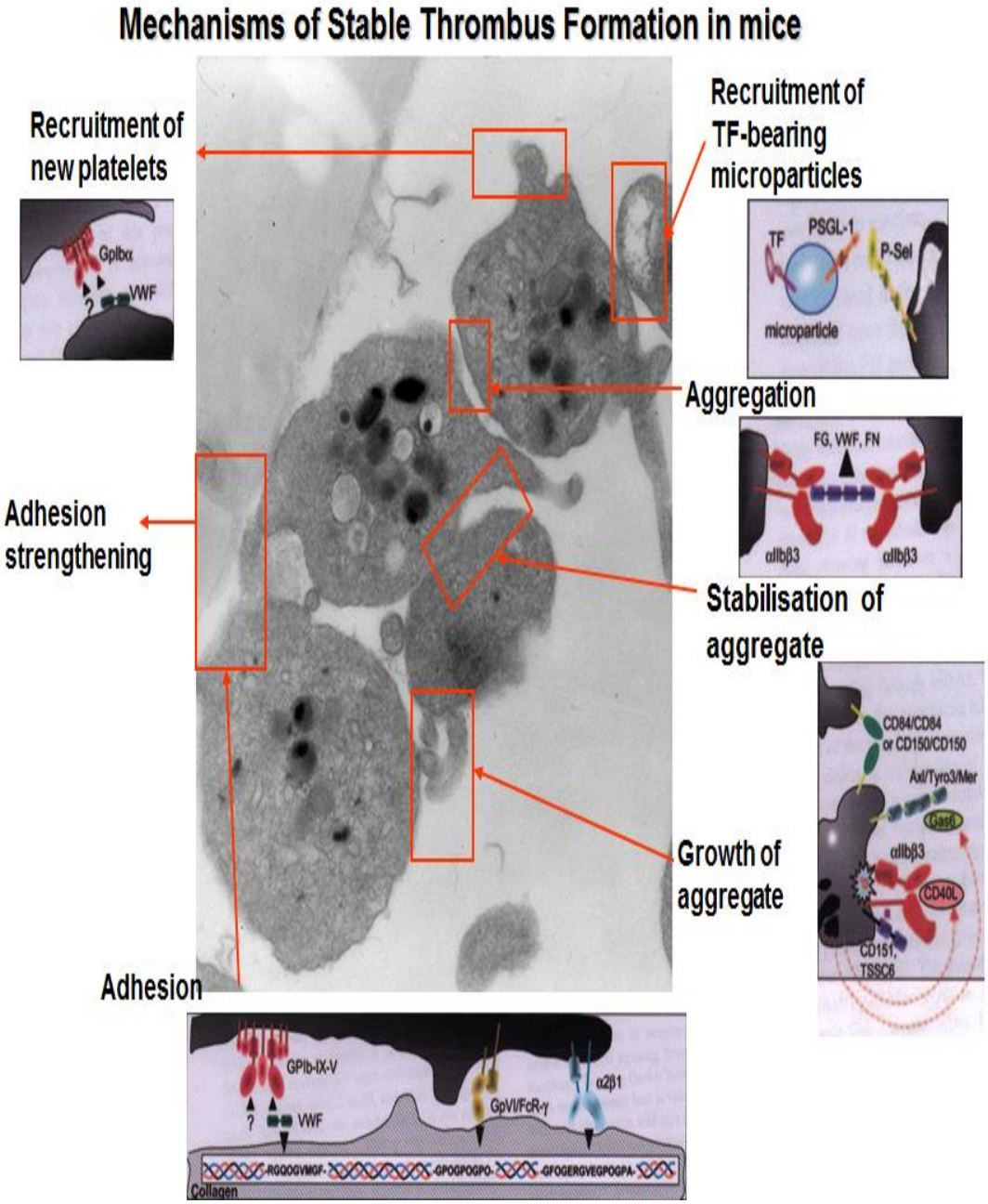

Figure 1-20: Mechanisms of stable thrombus formation in mice. Transmission electron microscope image of activated platelets. Mechanisms involved in formation of stable thrombus include recruitment of new platelets, adhesion, adhesion strengthening, recruitment of TF-bearing microparticles, aggregation, stabilisation of aggregation, and growth of aggregate. Adapted from [211].

1.10 Aims of the thesis

The main aim of the project is to investigate the different roles of the novel platelet immunoreceptor 'CEACAM2' in contact-dependent events that modulate platelet function *in vitro* and on thrombus formation *in vivo.*

- To determine the functional role of CEACAM2 in GPVI contact-dependent platelet activation (Chapter 3).

- To define if CEACAM2 negatively regulates platelet function via CLEC-2 mediated mechanisms (Chapter 4).

- To investigate the contribution of CEACAM2 in contact-dependent platelet adhesion under *in vitro* flow conditions using type I collagen as the ECM. Furthermore, to investigate the contribution of CEACAM2 in contact-dependent platelet adhesion under *in vivo* flow conditions. Three different mouse models of ferric chloride ($FeCl_3$)-induced vascular injury of mesenteric arterioles, laser induced injury of cremaster muscle arterioles and $FeCl_3$-induced injury upon GPVI depletion were used in CEACAM2 knockout (*Cc2*$^{-/-}$) compared to wild-type mice (Chapter 5).

- To determine the role of CEACAM2 in 'outside-in' integrin $\alpha_{IIb}\beta_3$-mediated signalling pathways (Chapter 6).

2 Chapter Two: General materials and methods

2.1 Materials

2.1.1 Antibodies and chemicals

Rabbit anti-mouse CEACAM2 was provided by Professor Sonia Najjar (Toledo, OH). Rabbit anti-mouse CEACAM1 was provided by Dr. Nicole Beauchemin (Goodman Cancer Research Centre, McGill University, Montreal, Canada). PECAM-1 antibody (Anti-mouse, 390) was provided by Dr Steve Albelda (University of Pennsylvania, Philadelphia, PA). The specific anti-rabbit fluorescein isothiocyanate (FITC) and rabbit anti-mouse phycoerythrin (PE) were purchased from Dako (Botany, Australia). Antiphosphotyrosine- horseradish peroxidase (HRP)-conjugated, RC20, anti-mouse CD3e, rat anti-mouse CD44, anti-mouse integrin β_3 (CD61), FITC-conjugated anti-mouse CD62P antibodies and FITC-Annexin V were obtained from BD Biosciences Pharmingen (Franklin Lakes, NJ). Antiphosphotyrosine HRP-conjugated, 4G10 antibody was purchased from Millipore (Billerica, MA). Anti-mouse GPVI [3], anti-mouse integrin $\alpha_2\beta_1$ (CD49b) [213], anti-mouse GPIbα-IX-V complex (CD42b) [2], anti-mouse GPVI (JAQ1) [137], anti-mouse CD9 and PE conjugated JON/A monoclonal antibodies were purchased from Emfret Analytics (Würzburg, Germany). Anti-phospho-Src-(Tyr416) and anti-Src-(36D10) antibodies were purchased from Cell Signalling Technology (Danves, MA). Anti-PLCγ2 (sc-407), Syk (c-20; sc-929), GAPDH (6C5; sc-32233) and Erk-2 antibodies were purchased from Santa Cruz Biotechnology (Dallas, TX).

Protease activated receptor-4 (PAR-4) agonist peptide (H-Ala-Tyr-Pro-Gly-Lys-Phe-NH_2; AYPGKF-NH_2) was purchased from GL Biochem Ltd. (Shanghai, China). Platelet agonists Adenosine diphosphate (ADP) and acid-soluble collagen were obtained from Chrono-Log Co. (Havertown, PA). Collagen-related peptide (CRP) was purchased from Dr. Richard W. Farndale (University of Cambridge, Cambridge, United Kingdom). Type I collagen fibrils were obtained from Nycomed (Linz, Austria). Rhodocytin (Rhod) agonist

was kindly provided by Professor Bernhard Nieswandt (University Clinic of Wuerzburg and Rudolf Virchow Centre, Germany). Thrombin, calcium ionophore (CI-A23187), Phorbol 12-myristate 13-acetate (PMA), epinephrine (Epi), sodium chloride (NaCl), dimethyl sulfoxide (DMSO), calcium chloride ($CaCl_2$), prostaglandin E_1 (PGE_1), bovine serum albumin (BSA) were purchased from Sigma Aldrich (St Louis, MO). Potassium chloride (KCL), $MgCl_2$-$6H_2O$, $NaHCO_3$, sodium citrate, glucose, HEPES, sodium dodecyl sulphate (SDS), polyacrylamide gel electrophoresis (PAGE), Tween 20, quinacrine, 2-Mercaptoethanol, paraformaldehyde, Osmium tetroxide (OsO4), glutaraldehyde, ethanol, acetone, iron (III) Chloride ($FeCl_3$) were purchased from Sigma Aldrich (St Louis, MO). PCR primers (107 [sense], 123 [anti-sense], SNeo9 [sense], Aneo8 [antisense]) and RED Extract-N-Amp were purchased from Sigma Aldrich (St Louis, MO). Enhanced chemiluminescence (ECL) system, protein G sepharose 4 fast flow and hyperfilm ECL were supplied from GE Healthcare Life Science (NSW, Australia). Polyvinylidene difluoride (PVDF) membrane and prestained SDS-PAGE standards (low range) were purchased from Bio-Rad laboratories (NSW, Australia). Fura-2-pentaacetyxymethylester (FURA-2/AM) was obtained from Molecular Probes (Eugene, OR).

2.1.2 Mice

The generation of *Cc2*$^{-/-}$ mice and breeding onto C57BL/6 background for 10 generations has been described [188]. Wild-type C57BL/6 mice were purchased from ARC animal facility (Perth, WA, Australia). Age- and sex-matched wild-type and *Cc2*$^{-/-}$ littermates were housed at RMIT University animal facility. All procedures were approved by the RMIT University animal ethics committee #0918 and #1239. The genotyping of *Cc2*$^{-/-}$ mice was confirmed by polymerase chain reaction (PCR) analysis of tail genomic DNA.

2.2 Methods

2.2.1 Genotyping

2.2.1.1 Purification of mouse tail genomic DNA

Using the DNeasy Protocol for Rodent tails to extract and separate genomic Deoxyribonucleic acid (DNA) samples for genotyping, tail clips of 3-weeks-old mouse tail tissue were assayed using DNeasy® blood and tissue kit handbook (Qiagen Pty.Ltd, Clifton Hill, Victoria).

2.2.1.2 PCR protocol

Standard Polymerase Chain Reaction (PCR) methodology was used to determine the CEACAM2 genotype and generated a number of primer sets used to facilitate genotyping of the DNA: primer 1) - 107 (sense) 5´ GCC CTT CTC TGG GAG GAG AAT CAA T 3´, primer 2) 123 (anti-sense) 5´ GCC TTC AGC AGC GTG GAG TGG A 3´, primer 3) SNeo9 (sense) 5´ GGA TCG GCC ATT GAA GAA GAT 3´, primer 4) Aneo8 (antisense) 5´ CGC CAA GCT CTT CAG CAA TAT 3´.

Following the PCR Genotyping Protocol, the -107 primer, situated in exon 2, is the promoter sequence for CEACAM2 and 123, and is exclusive to CEACAM2. To disrupt the functionality of the gene, SNeo9 and ANeo8 were delivered via a neomycin cassette for making CEACAM2 knockout. Using the protocol, it was predicted that ~1050 bp and ~750 bp of PCR products would be generated for CEACAM2 wild-type (WT) and knockout (KO) mice respectively.

PCR master mix including 1.0 µL of Milli-Q H_2O, 1.0 µL of 20 µM-107 [0.4 µM], 1.0 µL of 20 µM-123 [0.4 µM] and 5.0 µL of RED Extract-N-Amp was prepared to detect CEACAM2, wild-type allele. Moreover, to detect CEACAM2 knockout allele, another PCR master mix including 1.0 µL Milli-Q H_2O, 1.0 µL 20 µM-ANeo8 [0.4 µM], 1.0 µL 20 µM-

SNeo9 [0.4 µM] and 5.0 µL RED Extract-N-Amp-PCR was prepared. 3.0 µL of wild-type or *Cc2*$^{-/-}$ Qiagen purified genomic DNA was added to 8.0 µL of PCR master mix for each sample including control. Purified DNA mixture was amplified under the following cycling condition using Bio-Rad C1000™ thermal cycler PCR machine protocol (Pittsburgh, PA). The PCR conditions were based on the following cycles: 94°C for 15 minutes (Denaturation), (94°C for 30 seconds denaturation, 62°C for 30 seconds annealing, 72°C for 3 minutes extension) x 2 cycles, (94°C for 30 seconds denaturation, 55°C for 30 seconds annealing, 72°C for 3 minutes extension) x 40 cycles, 10 minutes in 72°C. Following these cycles, samples were kept at 4°C.

2.2.1.3 Agarose gel electrophoresis

The next stage of genotyping involved using gel electrophoresis to separate the PCR products. The assay used 2% (w/v) agarose gel as the medium and, for post-electrophoresis staining of the nucleic acid fragments, containing 1x Sybr Green, a sensitive, stable, and safe dye, was added. The first stage involved immersing the 2% (w/v) agarose gel in 1 × Tris-Acetic acid-EDTA buffer pH 8.5 (TAE), before loading the gel with 10 µl of each PCR product. To stain the DNA bands after electrophoresis, 4 µl of 2 log ladder of standard DNA marker was loaded onto the agarose gel. Electrophoresis, using a 120V power source, was run for 35 minutes, and the Bio-Rad Molecular Imager Gel Doc XR+ System facilitated DNA imaging. For each PCR assay, a number of DNA and non-DNA controls were assessed, to help confirm each genotype, and Milli-Q H_2O, highlighted any potential contamination of the PCR reagents with DNA. The known DNA controls included CEACAM2$^{+/+}$ (WT), CEACAM2$^{+/-}$ (Heterozygous), and CEACAM2$^{-/-}$ (KO), alongside three WT and three KO unknown DNA controls.

2.2.2 Blood collection and platelet preparation

Blood was drawn from anaesthetised wild-type and *Cc2*$^{-/-}$ mice by inhalation of 2% (v/v) isoflurane followed by cardiac puncture, using a 1-ml syringe with a 26-gauge needle. The blood was transferred to a microfuge tube containing 100 µl 3.2% (w/v) tri-sodium citrate and 50 ng/mL PGE_1 [8]. The top layer, platelet rich plasma (PRP) was isolated by centrifuging blood samples at 115 g for 8 minutes at room temperature without brake.

Washed platelets were generated by re-spinning PRP down in the presence of 50 ng/mL PGE_1 at 640 g for 10 minutes without brake, then resuspending the platelet pellet gently in 500 µL Ringer-citrate-dextrose, RCD (108 mM NaCl, 38 mM KCl, 1.7 mM $NaHCO_3$, 21.2 mM sodium citrate, 27.8 mM glucose, and 1.1 mM $MgCl_2.6H_2O$, pH 6.5). Washed platelets were then prepared for platelet count.

Platelet poor plasma (PPP) was obtained by centrifugation of the remaining blood after PRP collection at 800 g for 10 minutes at room temperature without brake. The top layer of the blood samples was separated and pooled into a separate tube as PPP.

2.2.3 Measurement of platelet aggregation

Platelet function was evaluated by turbidimetric aggregometry. Turbidimetric aggregation measures the increase in light transmission as platelets come out of suspension to form aggregates, in response to stimulation with a chemical agonist using a 4-channel light transmission aggregometer (Chrono-log, Havertown, PA). The data were recorded using AGGRO/LINK (8) software (Chrono-Log Co, Havertown, PA).

2.2.3.1 Murine PRP aggregation

Platelet aggregation responses were measured on a 4-channel light transmission aggregometer using PRP as previously described [214, 215]. Wild-type and *Cc2*$^{-/-}$ platelets were normalised to $100x10^9$/L in RCD buffer pH 7.4 by using a Cell-DYN Emerald

analyser (Abbott, Lake Forest, IL). The platelets were pre-incubated with 100 µg/mL fibrinogen and 1 mM $CaCl_2$ in a final volume of 250 µL for 5 minutes at 37°C and then stirred constantly (1000 rpm) for 1 minute at 37°C prior to addition of agonists. The platelet aggregation baseline was set using mouse PPP diluted 1:2 in RCD buffer pH 7.4. Platelet aggregation was initiated by addition of agonist including 125-500 µM PAR-4 agonist peptide (AYPGKF-NH_2), 2.5-10 µM ADP, 1.25-5 µg/mL CI-A23187, 1.25-5 µg/mL Collagen, and 0.625-2.5 µg/mL cross-linked CRP. For experiments related to CLEC-2 signalling, 0.12-0.48 µg/mL Rhodocytin (Rhod) was used to initiate platelet aggregation. The platelet aggregation response was monitored for 10 minutes.

2.2.3.2 Murine washed platelet aggregation

Platelet aggregation responses were measured on a 4-channel light transmission aggregometer using washed platelets as described in section 2.2.3.1. The only exception was that the platelet aggregation baseline was set using RCD buffer pH 6.5 instead of mouse PPP. Platelet aggregation was initiated by addition of agonist including 0.25-1 U/mL thrombin, 250-500 µM PAR-4 agonist peptide, and 5-10 µg/mL CRP.

2.2.4 Haematological parameters

Blood was collected from anaesthetised wild-type and *Cc2*$^{-/-}$ mice as described in section 2.2.2. Most of the haematopoietic cells were analysed from murine whole blood by using Cell-DYN Emerald analyser. In addition, neutrophils, lymphocytes and monocytes were quantified by a manual WBC differential count.

2.2.5 Static platelet adhesion assay

A time-course of normal static platelet adhesion assay was performed with 12 mm circular glass coverslips (Crown Scientific, Moorebank, New South Wales) placed into 4x24 well plates, with one plate used for each time point of 15 min, 30 min, 45 min and 60 min. The 12 mm circular glass coverslips were coated with ECM, 50 µg/mL type I collagen or

fibrinogen at 100 µg/mL for 2 hours at room temperature. After 2 hours incubation, plate wells were washed with RCD at pH 6.5 by using a vacuum pump to aspirate fluid. Plate coverslips were blocked with 10% (w/v) normal human serum supplemented with 50 µg/ml phenyl methyl sulphonyl fluoride (PMSF) for 60 minutes at room temperature, then washed with RCD pH 7.4 prior to the addition of platelets.

Washed platelets were normalised to $100x10^9$/L by using RCD pH 6.5, and $CaCl_2$ was added to platelet suspension to a final concentration of 1 mM. Platelets were added to plate wells containing coverslips and incubated together in a humidified chamber to adhere with ECMs for 15 min, 30 min, 45 min and 60 minutes at 37°C. The 24-well plates containing washed platelets were removed from the incubator after appropriate times, and then unbound platelets were washed gently with RCD pH 6.5. The adherent platelets were fixed with 3.7% (w/v) paraformaldehyde for 30 minutes at room temperature, and then fixed platelets washed with RCD pH 7.4.

The adherent platelets on coverslips were prepared on 76x26 mm glass microscope slides with a frosted end and 22x40 mm coverslips, then mounted by Vectashield (Australian Laboratory Service, Melbourne, Victoria) and sealed with nail polish. The adherent wild-type and *Cc2*$^{-/-}$ platelets were analysed at different time points using a Zeiss Axiovert microscope (Carl Zeiss, Gottingen, Germany) captured with an Axiocam MRm camera and analysed with Axiovision Rel 4.6 software and differential interference contrast microscopy at 63x magnification (DIC under oil). Finally, the number of adherent platelets per high-powered field were quantified for both wild-type and *Cc2*$^{-/-}$ platelets [214].

2.2.6 Platelet spreading studies

The 12 mm circular glass coverslips were placed in 24-well plates and coated with 50 µg/mL type I collagen or fibrinogen at 100 µg/mL, then blocked with 10% (w/v) normal human serum. Platelet preparation was carried out as described in section 2.2.5.

Intravital Microscopy - $100x10^9$/L washed platelets were allowed to adhere in the absence or presence of several agonists such as 0.5 mM PAR-4 agonist peptide, 20 µM ADP and 100 nM PMA, and then mixed gently. The washed platelets with appropriate agonist were then added to suitable ECMs. In addition, washed platelets without agonist were added to RCD pH 7.4 as a negative control. Adherent platelets were incubated in a humidified chamber to adhere with ECMs for 60 minutes at 37°C. Non-adherent platelets were washed away, and the coverslips and glass microscope slides were prepared as previously described in section 2.2.5. Finally, images of wild-type and *Cc2*$^{-/-}$ spread platelets were captured, saved and then the surface area of spread platelets was measured in μm^2 using a Zeiss Axio Image M1 motorised microscope on 63x oil DIC magnification (see section 2.2.5).

Scanning Electron Microscope (SEM) studies - Adherent platelets were fixed overnight (O/N) on a rotating wheel in 0.1M phosphate buffer pH 7.2 (11.5 mL of 0.2M NaH_2PO_4 H_2O [27.6 g/L] plus 38.5 mL of 0.2M Na_2HPO_4 [anhydrous; 28.4 g/L]) containing 1% (w/v) paraformaldehyde and 1.5% (v/v) glutaraldehyde, then samples were rinsed 5 times for 4 hours in 0.175M phosphate buffer (19.25 mL of 0.2M NaH_2PO_4 H_2O plus 68.25 mL of 0.2M Na_2HPO_4 anhydrous; pH 7.2). Samples were post fixed for 1h with 0.175M phosphate buffer pH 7.2 containing 1% (v/v) OsO4, and then rinsed in Milli-Q water three times for 10 minutes on a rotating wheel. 12 mm coverslips were taken out into 12 mm coverslips holder, and then samples were dehydrated in a series of ethanol 50, 70, 90, 95, 2x100% for 10 minutes each, 50/50 ethanol/acetone and 100% acetone for 10 minutes. The samples were loaded onto an automated critical point drying machine (CPD) using Leica EM CPD300 (Leica Microsystems, NSW, Australia). The samples were prepared for SEM imaging and coated with gold sputter using Emscope SC500 Sputter Coaters (Quorum Technologies, East Sussex, United Kingdom). SEM high resolution images were captured

using a JCM-6000 Benchtop-SEM at 10kV (JEOL, NeoScope, Portsmouth, NH) equipped with digital camera, high and low vacuum mode. Finally, the number of filopodia per platelet was counted in 3 different categories (0, 1-3 and >3) and analysed on SEM images from random fields involving the percentage of 100 platelets counted.

2.2.7 Mouse tail bleeding assay

Wild-type and *Cc2*$^{-/-}$ mice were sex and age-matched (6-8 weeks). Mice were anesthetised by Isotec 3 machine using 2% (v/v) isoflurane and 2 litres/min of oxygen (O_2). Once anesthetised, mice were laid in lateral recumbency on a firm surface and under gravity. The tail was laid horizontally with the tip over the edge. Tails were transected at 2 mm diameter of tail tip with a sharp scalpel blade. A stopwatch was started immediately upon transection and blood drops were collected into an Eppendorf tube containing 100 µL of 3.2% (w/v) tri-sodium citrate. The tail bleeding time was recorded from until there was no more blood drops or for 15 minutes, whichever occurred first. When no blood was observed within 60 seconds of cessation, bleeding time was considered stopped. Volume of blood loss was recorded for each genotype [216].

2.2.8 Clot retraction assessment

PRP was derived from wild-type and *Cc2*$^{-/-}$ mice, then normalised to $100x10^9$/L in RCD buffer pH 7.4. 1 mL of platelet suspensions were prepared and corrected with PPP to the final volume 250 µL. Platelet mixtures were placed in siliconised glass tubes containing 6 µL of mouse erythrocytes to give colour contrast. Platelet clots were initiated by the addition of thrombin to the final concentration of 2.5 U/mL, then they were mixed gently. The reaction was allowed to proceed for 10 hours at 37 °C with a toothpick present. Photographic images of the clot retraction were recorded following appropriate time points (0-10 hours). At appropriate time points (0-24 hours), the blood clot was removed using the toothpick and the remaining serum volume was measured per percentage or µL [217, 218].

2.2.9 Flow cytometric immunophenotyping

2.2.9.1 Analysis of CEACAM2 and other platelet glycoprotein expression on mouse platelets

Surface and total expression of CEACAM2 in wild-type and *Cc2*$^{-/-}$ platelets was performed using washed platelets as previously described [99]. For surface expression, 50 µL of washed platelets (100x10^{9}/L) were pre-incubated for 1 hour at room temperature with a primary antibody such as anti-rabbit CEACAM1 antibody, 2457 (1/500), anti-rabbit CEACAM2 antibody, 2052 (1/100), anti-mouse PECAM-1 (10 µg/mL), pre-immune rabbit serum (1/100), anti-mouse GPVI (10 µg/mL) and anti-mouse CD9 (10 µg/mL). The platelet-antibody complex was washed with 0.2% (w/v) BSA-RCD pH 6.5, followed by FITC-conjugated anti-rat (1/200) or PE-conjugated anti-rat (1/100) or Streptavidin-PE (1/200) for 45 minutes at room temperature. For direct antibody conjugation, platelets were pre-incubated with anti-mouse integrin β_3, CD61 (10 µg/mL), anti-mouse integrin $\alpha_2\beta_1$, CD49b (15 µg/mL), anti-mouse GPIbα/IX/V, CD42b (10 µg/mL), and anti-mouse CD44 (10 µg/mL) for 45 minutes at room temperature.

To determine the total protein expression, platelets were pre-incubated with 0.1% (w/v) saponin in RCD buffer pH 6.5 and appropriate antibody for 1 hour at room temperature. The platelets were diluted by addition of 300 µL RCD buffer pH 7.4. 10,000 individual platelets were analysed on a FACS Canto II flow cytometer (BD Biosciences, San Jose, CA) and Weasel software Version 3.0.2 (Walter and Eliza Hall Institute of Medical Research, Victoria, Australia). The template was formatted for a platelet-specific FITC/PE protocol with forward scatter (FSC), side scatter (SSC), and fluorescent parameters in log scale. The main platelet population was selected prior to the acquisition of data.

Changes to the surface expression of CEACAM1 and CEACAM2 was also measured on wild-type and *Cc2*$^{-/-}$ platelets upon addition of several agonists such as 0.125-1.0 U/mL

thrombin, 100-300 µM PAR-4 agonist peptide and 1.0-4.0 µg/mL CRP. After addition of agonists, platelets were pre-incubated with either anti-rabbit CEACAM1, 2457 (1/500) or anti-rabbit CEACAM2 antibodies, 2052 (1/100) followed by PE conjugated anti-rat (1/200). The platelets were diluted by addition of 300 µL RCD buffer pH 7.4. 10,000 individual platelets were analysed on a FACS Canto II flow cytometer and Weasel software Version 3.0.2.

2.2.9.2 Analysis of alpha granule release (FITC-P-selectin)

Washed mouse platelets ($100x10^9$/L; 50 µL) were activated with several agonists including 0.1-0.2 U/mL thrombin, 100-300 µM PAR-4 agonist peptide and 0.5-2.0 µg/mL CRP or CLEC-2 selective agonist, Rhod at 0.6-1.2 µg/mL for 15 minutes at 37°C. The activated platelets were fixed with 1% (w/v) paraformaldehyde for 10 minutes at room temperature, and then terminated with RCD pH 6.5. Fixed platelets were then pre-incubated with 10 µg/mL P-selectin antibody (FITC-CD62P) for 30 minutes at room temperature, then washed with 0.2% (w/v) BSA-RCD pH 6.5, then spun at 640 g for 10 minutes without brake. The platelets were diluted by addition of 300 µL RCD buffer pH 6.5. Alpha granule exocytosis was identified using platelet population characteristic forward and side laser scatter and examined for expression of FITC-CD62P. 10,000 individual platelets were analysed on a FACS Canto II flow cytometer and Weasel software Version 3.0.2 [219].

2.2.9.3 Analysis of dense granule release using quinacrine uptake

Washed mouse platelets ($100x10^9$/L; 50 µL) were pre-stained with 100 µM of 500 µM quinacrine dye for 30 minutes at 37°C. Stained platelets were then terminated with 0.2% (w/v) BSA-RCD pH 6.5, and then spun at 640 g for 10 minutes without brake. The platelets were activated with several agonists including 0.125-1.0 U/mL thrombin, 100-300 µM PAR-4 agonist peptide and 0.25-4.0 µg/mL CRP or 0.4-1.2 µg/mL Rhod of CLEC-2 selective agonist, for 10 minutes at 37°C. The platelets were diluted by addition of 300 µL

RCD buffer pH 7.4. Dense granule exocytosis was recorded as the percentage decrease in quinacrine fluorescence intensity compared to resting platelets. 10,000 individual platelets were analysed on a FACS Canto II flow cytometer and Weasel software Version 3.0.2.

2.2.9.4 Analysis of soluble FITC-fibrinogen and JON/A-PE binding

FITC-conjugated fibrinogen was prepared by conjugating 20 mg human fibrinogen to FITC (Sigma Chemical, St Louis, MO) in 0.15 M carbonate buffer pH 9.0 for 1 hour at room temperature. The FITC-labelled fibrinogen was purified using a PD10 column (Amersham Pharmacia, Piscataway, NJ), and then the column was eluted with 15 mL (15 x 1 mL) of PBS and 1 ml fractions were collected [8, 220].

Measurement of FITC-labelled fibrinogen and PE-conjugated JON/A mAb binding to platelets via GPIIb/IIIa (integrin $\alpha_{IIb}\beta_3$) was performed. Washed mouse platelets (50 µL containing $100x10^9$/L in RCD pH 6.5) were pre-incubated with FITC-labelled fibrinogen at 1.2 µg/mL or PE-conjugated JON/A mAb (1:50 dilution) in the presence or absence of agonists. Platelets were activated with agonists including 0.125-1.0 U/mL thrombin, 100-300 µM PAR-4 agonist peptide, 10 µM ADP, mixture of 10 µM ADP plus 20 µM Epi, 20 µM PMA and 0.25-4.0 µg/mL CRP for 1 hour at 37°C in a dark room. Washing steps were performed using RCD pH 6.5 containing 0.2% (w/v) BSA after each step. The platelets were fixed with 1% (w/v) paraformaldehyde for 10 minutes at room temperature. They were then diluted by addition of 300 µL RCD buffer pH 6.5 and 10,000 individual platelets were analysed as described in section 2.2.9.1.

2.2.9.5 Phosphatidylserine exposure

PRP and washed platelets were generated as described in section 2.2.2. PRP was pre-incubated with 1 mM acetylsalicylic acid for 45 minutes at 37°C. Washed platelets were isolated and the pellet was gently resuspended in 500 µL Tyrode's buffer (10 mM HEPES, pH 6.5, containing 138 mM NaCl, 2.7 mM KCl, 1 mM $MgCl_2$, 3 mM NaH_2PO_4, 5 mM

glucose) containing 0.1 U/mL apyrase. 100x10^9/L washed platelets were pre-incubated with 2.5 mM $CaCl_2$ and 2 µL of FITC-labelled Annexin V, followed by agonist stimulation, 0.125-0.5 U/mL thrombin, 100-300 µM PAR-4 agonist peptide and 1-4.0 µg/mL CRP for 45 minutes at 37°C. The labelled platelets were then terminated with 0.2% (w/v) BSA-Tyrode's buffer pH 6.5, and then spun at 640 g for 10 minutes without brake. The platelets were diluted by addition of 300 µL Tyrode's buffer and 10,000 individual platelets were analysed on a FACS Canto II flow cytometer and Weasel software Version 3.0.2.

2.2.10 Western blot

Washed platelets from wild-type and *Cc2*$^{-/-}$ mice were stimulated with 10 µg/mL of CRP versus resting at different time points (0, 15-30 seconds, 1-3 minutes) to measure global tyrosine phosphorylation (pTyr). Reactions were terminated with an equal volume of Triton lysis buffer (15 mM HEPES, pH 7.4, containing 145 mM NaCl, 0.1 mM $MgCl_2$, 10 mM EGTA, 2 mM sodium orthovanadate, 0.2 mM leupeptin, 1 mM phenylmethylsulfonyl fluoride and 1% [v/v] Triton X-100) as previously described [8, 219]. Platelet lysates were mixed for 1 hour at 4°C on a rotator, and then centrifuged at 15,000 g for 15 minutes at 4°C. After platelet lysate separation, Triton-soluble supernatants were isolated, and retained protein concentration determined by Bio-Rad protein assay (section 2.2.12). 30 µg of protein was eluted with 30 µL of SDS reducing buffer for 10 minutes at 100°C, then eluted proteins were loaded onto a 10% SDS-PAGE. Proteins were transferred to PVDF membrane by Western blotting. PVDF membranes were blocked with blocking buffer (1 M Tris-HCl, pH 7.4, containing 3% [w/v] BSA and 0.05% [v/v] Tween 20) for 2 hours at room temperature. PVDF membranes were soaked in HRP-conjugated RC20 (1/5000; 0.25µg/µL) or 4G10 (1/20,000) antibodies for 2 hours at room temperature, and then washed three times with Tris-buffered saline (TBS; 20 mM Tris, pH 7.4, containing 150 mM NaCl and 0.05% [v/v] Tween 20) for 10 minutes. This blot was stripped with stripping buffer (62.5 mM Tris-

HCl, pH 6.7, containing 100 mM 2-Mercaptoethanol and 2% (v/v) SDS) and re-probed using anti-Erk-1/2 Ab for detection of Erk-1 and 2 antigens as aprotein loading control. Membranes were then developed with the ECL detection system.

To determine the GPVI depletion in mice, blood samples were collected through cardiac puncture from wild-type and *Cc2*$^{-/-}$ mice as described in section 2.2.2, 5 days after treatment with either 100 µg of anti-mouse GPVI (JAQ1) antibody or 100 µg isotype control. Washed platelets were generated as described in section 2.2.2. A platelet count was performed using Cell-DYN Emerald analyser to standardise platelet counts required for Western blotting. 100 µL of washed platelets ($100x10^9$/L) were mixed with an equal volume of 1% (v/v) Triton lysis buffer and incubated for 1 hour at 4°C on a rotator. Platelet lysates were generated as described in section 2.2.10. Equal amounts of protein (100 µg) were loaded on 10% SDS PAGE gel, transferred to a PVDF membrane, probed with immunoblotting: rabbit polyclonal anti-human GPVI (5 µg/mL) and HRP conjugated anti-rabbit antibodies (1/10,000) and visualised using the ECL development kit as described in section 2.2.10.

2.2.11 Immunoprecipitation and immunoblotting

For immunoprecipitation, the only differences from the method described for western blot were that the platelets were stimulated with 10 µg/mL of CRP, a GPVI selective agonist or with 1.2 µg/mL Rhod, a CLEC-2 selective agonist versus resting (0 and 90 seconds). Triton-soluble supernatants were prepared as described above and precleared twice with 50 µL of 50% (v/v) Cyanogen bromide (CNBr) activated sepharose beads followed by mixing for 15 minutes at 4°C, then centrifuged at 4000 g for 5 minutes at 4°C. After centrifugation, Triton-soluble supernatants were pre-incubated with either 1 µg of anti-PLCγ2, anti-Src-(36D10) or Syk (c-20) antibodies overnight at 4°C followed by the addition of 50 µL of 50% (w/v) protein G-sepharose beads for 1 hour at 4°C. Protein-antibody complexes were

then washed 5 times with immunoprecipitation buffer (50 mM Tris-HCl, pH 7.4, containing 150 mM NaCl and 1% [v/v] Triton X-100) followed by centrifuged at 4000 g for 5 minutes at room temperature. The protein-antibody complexes were eluted with 30 µL of SDS reducing buffer for 10 minutes at 100°C, then eluted proteins were loaded and separated on 10% SDS-PAGE. Protein transfer and membrane blocking were described as above. Membranes were coated with 4G10 (1/20,000) or anti-phospho-Src-(Tyr416; 1/2,000) antibodies for 2 hours at room temperature, and then washed three times with TBS for 10 minutes. A protein loading control blot was stripped and re-probed using anti-PLCγ2 (1/5,000), anti-Src-(36D10; 1/2,000), Syk (c-20; 1/2,000), then incubated with anti-rabbit HRP-conjugated secondary antibody diluted in TBS at 1/20,000. Membranes were washed with TBS and developed by ECL [215, 219].

2.2.12 Bio-Rad protein assay

The Bio-Rad protein assay was performed to estimate the protein concentration in the platelet lysate as described [221]. 800 µL of different dilutions of samples (1/80, 1/160 and 1/320) and BSA standard (1.25, 2.5, 5 and 10 µg/mL) or blank sample (water only) were prepared in Milli-Q water. 200 µL of Bio-Rad dye was added to protein, BSA standard and blank samples, followed by mixing and 5 minutes incubation at room temperature. The absorbance maximum for an acidic solution is determined when Bio-Rad dye binds to the protein and this binding leads to a shift in the wavelength from 465 to 595 nm. Protein concentration of BSA standard and samples was determined by measuring the fluorescence intensity at the wavelength 595 nm using a spectrophotometer analyser (Perkin Elmer, Waltham, MA). A standard curve was created by plotting OD 595 nm versus known amounts of BSA protein standard values, and then the protein concentration of the appropriate sample was calculated based on the X factor and dilution. To adjust the final concentration, the unknown sample concentration was calculated by multiplying the X

factor with dilution. The mean of protein concentrations was calculated and expressed as µg/mL to determine the appropriate protein concentration for each sample.

2.2.13 Analysis of murine platelet adhesion and thrombus formation under *in vitro* flow

Mouse blood was drawn as previously mentioned in section 2.2.2. A three channel µ-slide $III^{0.1}$ with dimensions (0.1 x 1.0 x 45 mm, H x W x L), (Microslides, ibidi, Martinsried, Germany) was pre-coated with 500 µg/mL type I fibrillar collagen (Nycomed, Linz, Austria) for 1 hour at 37°C, followed by washing with RCD pH 7.4 for 1 minute. Anticoagulated whole blood from wild-type and *Cc2*$^{-/-}$ mice was normalised to $300x10^9$/L platelets then pre-incubated with 0.05% (w/v) rhodamine 6G dye for 30 minutes at 37°C. Labelled blood was perfused through the collagen-coated µ-slide $III^{0.1}$ at a shear wall flow rate of 1800 $seconds^{-1}$ for 6 minutes. Nonadherent cells were washed at the same shear wall flow rate with RCD buffer pH 7.4. Thrombi were recorded in real-time for 6 minutes and imaged using Z-stack analysis and deconvolution of 3D reconstructions using a Zeiss Axiovert microscope equipped with an Axiocam MRm camera (Carl Zeiss, Thornwood, NY). Thrombus volume was calculated from the thrombus area (μm^2) multiplied by the thrombus height (µm) for wild-type and *Cc2*$^{-/-}$ thrombi at various time points.

2.2.14 $FeCl_3$-induced vascular injury of mesenteric arterioles *in vivo*

$FeCl_3$-induced vascular injury of mesenteric arterioles was performed according to the method described [187, 222]. Wild-type and *Cc2*$^{-/-}$ mice (4-6 weeks old) were anaesthetised with Ketamine (20 µl/g) /xylazine (1 µl/g) through intraperitoneal injection, to facilitate manipulation of the animal. The limbs were secured using masking tape and the teeth were tied to straighten the neck. An incision was then made between the clavicle and the neck, to expose the jugular vein. Two (10S) black threads were placed around the jugular vein, and a hole was created for cannula insertion at 15°C parallel to the vein to

deliver the rhodamine 6G dye or top up anaesthetic. The mesenteric arterioles were then located and visualised using a Zeiss Axiovert microscope equipped with an Axiocam MRm camera (Carl Zeiss). The diameter of arterioles (80-100 μm) was measured with the Axiovision Rel 4.6 program. A 1mm×4mm whatman filter paper strip was soaked in freshly prepared 7.5% (w/v) $FeCl_3$ solution for ~ 3 seconds, and then placed on the vessel at the required site for 4 minutes. The filter strip was then removed, and the injury site was flushed with some saline. The vessels were then checked and the injured area was located by phase contrast microscopy using the Axiovert microscope to detect the $FeCl_3$ deposits indicating oxidative damage. 75 μl of rhodamine 6G dye (0.05% w/v) was infused directly into the cannula, visualised by the brightness of the vein under the Axiovert microscope, then rhodamine fluorescent channel (at position 5) and Z-stack images were captured (90-120 slices). Real time thrombus growth was monitored on the rhodamine channel and Z-stack images were recorded over 10 minutes of 2-minute cycles.

2.2.15 Laser-induced injury of cremaster muscle arterioles *in vivo*

Laser-induced injury of cremaster muscle arterioles was performed according to the method described [222, 223]. The mice were prepared for the procedure as described in section (2.2.14). The mice were then transferred to the cremaster examination board and a small incision was made at the tip of the scrotum to loosen the membrane using a blunt forceps. A 10S thread was used to tie one testicle and the cremaster muscle located at the bottom of the testicle was located and removed. To avoid dryness of the muscle a few drops of superfusion buffer (saline) were added. A small hole was made at the tip using a cauteriser, and a fine forceps was placed into the hole. Another hole was made at the centre of the muscle. The cauda epididymis was held and the membrane between the muscle and the testis was hydrated using superfusion buffer (saline). The testis was then pushed back into the body. The right and left edges of the muscle were then held and tied using a 6S

thread that was later secured on the board using yellow waterproof tape. The cremaster arteriole was located under long-distance lens 20x, under bright field (TL shutter open, position 1, filter H) and viewed through a Zeiss Axiovert microscope equipped with an Axiocam MRm camera and Axiovision Rel4.6 software. The potential cremaster muscle arteries of diameter (30-40 μm) were measured using a gauge on the monitor of an intravital microscope.

Endothelial injury was induced in the cremaster muscle artery by the Micropoint Laser System, manufactured by Photonics Instruments (Photonic instrument, St. Charles, IL), with the resulting images displayed by Axiovision microscope technology. To create an injury at a specific parafocal location on the vessel wall, the laser was switched to laser channel (position 6) and concentrated through the objective lens of the microscope [224], with one or two pulses used to create an injury of sufficient size and severity with maximum of 10 pulses. To avoid any interference caused by previous thrombi developed in the subject mice, additional injuries were induced upstream. No noticeable trends related to size or formation characteristics were apparent across this sequence of multiple thrombi created in individual mice. Following laser injury, 100 μL of 0.05% (w/v) rhodamine 6G dye was infused and visualised by the brightness of the vein under the microscope, and rhodamine channel (position 5) and Z-stack images were captured (80-100 slices). Thrombus formation was monitored on rhodamine channel and Z-stack images for the vessel were captured. Real-time recording was determined over 10 minutes of 2-minute cycles.

2.2.16 Quantification of platelet thrombus parameters

Thrombus formation parameters were calculated according to the method described [187, 222]. Z-stack images were deconvolved and thrombus formation parameters of thrombus area (μm^2), thrombus height (μm), vessel length (μm), vessel diameter (μm), thrombus volume (μm^3), vessel volume, percentage of vessel occlusion and stability score

were determined using Axiovision Rel4.6 software. Thrombus area was calculated by drawing around selected thrombi using scaling outline in μm^2, and thrombus height and their length were also measured in µm. Thrombus volume was derived by multiplying thrombus area with thrombus height of the platelet clot. Vessel volume was calculated by the formula: [Vessel volume = π x (vessel diameter/2)^2 x vessel length]; Percentage (%) of vessel occlusion was calculated by the formula: [% of vessel occlusion = Thrombus volume/vessel volume x 100%].

To determine the thrombus formation characterisation, a specific formula for each parameter was used as follows:

I. Thrombus volume = Thrombus area x Thrombus height.

II. Vessel volume = π x (vessel diameter/2)^2 x vessel length.

III. Percentage (%) of vessel occlusion = Thrombus volume / vessel volume x 100%.

IV. Average for % vessel occlusion = (% Vessel occlusion at 6-8 min + % Vessel occlusion at 8-10 min) / 2.

V. Stability score = Average of the % vessel occlusion.

a) 0-10% is stability score equal to 1

b) 11-20% is stability score equal to 2

c) 21-30% is stability score equal to 3

d) 31-40% is stability score equal to 4

e) 41-50% is stability score equal to 5

f) 51-60% is stability score equal to 6

g) 61-70% is stability score equal to 7

h) 71-80% is stability score equal to 8

i) 81-90% is stability score equal to 9

j) 91-100% is stability score equal to 10, (complete vessel occlusion).

For time-lapse analysis, the number of emboli (<20 μm) was calculated over 2 minutes starting from the time of first thrombus. Size of embolus (<20 μm) was calculated by the length of each embolus just before it broke away from the vessel wall over 2 minutes starting from the time of first thrombus. Time to vessel occlusion was calculated as the time from the initial recording until blood had stopped flowing through the vessel. Data were plotted using GraphPad Prism software program version 6 (GraphPad, San Diego, CA).

2.2.17 Statistical analysis

Statistical analysis was carried out using GraphPad Prism software program version 6 (GraphPad, San Diego, CA). All data sets are expressed as mean ± standard error of mean (SEM). Statistical significance was determined using unpaired Student's *t* test or two-way analysis of variance (ANOVA). Data were checked for normal distribution using the Shapiro-Wilk normality test. *P*-value <0.05 was considered significant. To correct multiple comparisons for type I error, the Bonferroni post-test was performed.

3 Chapter Three: *In vitro* characterisation of CEACAM2 regulation of collagen GPVI/FcR gamma chain signalling pathway in platelets

3.1 Introduction

As one of the most important constituents of vessel wall, collagen contributes to platelet activation and adhesion in response to vascular damage. Platelets and collagen can interact directly via direct platelet collagen receptors expressed on the membrane surface. Alternatively, the interaction can be indirect, when immobilised vWF binds to one or both of the platelet receptors GPIb-V-IX and activated integrin $\alpha_{IIb}\beta_3$ [225]. Research has identified a number of collagen receptors expressed in platelets, with GPVI [226] and integrin $\alpha_2\beta_1$ the two most important [227]. The former is essential to platelets adhering to fibrillar collagen, whereas the latter is not essential, as shown by research using β_1 integrin-null platelets [228].

In platelets and megakaryocytes, the GPVI-FcRγ-chain complex is the most important collagen signalling receptor expressed on the surface [229, 230]. GPVI induces phosphorylation of a tandem YxxL sequence on the Fc receptor (FcR)–γ–chain, as part of a Src-dependent process involving the ITAM. In turn, the tyrosine kinase, Syk, is recruited and activated via its tandem SH2 domains, inducing a signalling cascade that creates a linker for T cell-dependent signalosome activation. In turn, this mediates PLCγ-2 activation, increasing the concentration of intracellular Ca^{2+} and activating protein kinase C, with increased platelet aggregation [231, 232].

Many negative regulatory mechanisms downregulate *in vivo* platelet-collagen interactions. Major regulators include nitric oxide and prostacyclin [74], released by the endothelium, and members of the immunoglobulin Ig-ITIM superfamily, contained within platelets. The latter group includes PECAM-1, and CEACAM1, which auto-regulate platelet interactions in the presence of collagen [219, 233-235]. Collagen plays a role in platelet adhesion and thrombus development, especially with GPVI/FcRγ–chain signalling. Thus,

natural inhibitors of the auto-regulatory mechanisms moderating signalling processes between the GPVI/FcRγ–chain and collagen must be present in platelets [224].

The ITIM-bearing receptor regulation of ITAM in leukocytes is well understood. However, less is known about regulation in platelets where Ig-ITIM–bearing receptors bind with multiple phosphatase types, including SH2-domain containing tyrosine phosphatase-1 and -2 (SHP-1, SHP-2), and SH2-domain containing inositol polyphosphate 5'-phosphatase (SHIP) [236]. Current theories suggest that Ig-ITIM bearing receptors undergo differential interaction with the distinct phosphatase groups, in a manner depending on cell conditions and activation status [237, 238].

Regulation of these complex inhibitory mechanisms is difficult to dissect because, under certain conditions, inhibitory ITAM signalling is mediated by ITAM-bearing receptors, via the FcRγ–chain or DAP12 adaptor [239, 240]. Switching between ITAM signalling activation and inhibition is governed by the strength of ligand binding to the receptor. Low-avidity ligand interactions may influence regulation of inhibitory signalling by phosphatases. Conversely, higher-avidity ligand cross linkages may activate ITAM-mediated signalling responses. Hence, understanding the complex relationship between activation and inhibition in platelets is crucial [239, 240].

Several studies imply that Ig-ITIM superfamily members in platelets regulate platelet-collagen interactions [8, 187]. Human and murine platelets do not contain the prototypic inhibitory Ig-ITIM superfamily member FcγRIIb, but instead, PECAM-1 and CEACAM1 are Ig-ITIM-superfamily members that are able to negatively regulate interactions [187, 219, 233]. Other Ig-ITIM superfamily members, including triggering receptors expressed on myeloid cells (TREM), transcript-1 (TLT-1), and G6B, are critical for modulating platelet function [179, 182]. Much remains to be investigated in order to assess the contribution of Ig-ITIM superfamily to platelet thrombus formation.

CEACAM2 (previously known as Bgp2) is a type I-transmembrane receptor from the CEACAM superfamily of genes that is expressed in several cell types, including intestinal tissue crypt epithelia, kidney cells, testis and several nuclei in the brain, including the ventromedial hypothalamus [188, 241, 242]. CEACAM1 and CEACAM2 proteins, are encoded by different genes containing 9 exons each [197], but share a similar overall structure in particular with respect to Ig-Domains in the extracellular segment and an almost identical ITIM-containing cytoplasmic tail. However, the two proteins differ by two important features. Firstly, CEACAM1 predominantly possesses four extracellular Ig-Domains (CEACAM1-4L), in contrast to CEACAM2 that has two extracellular Ig-Domains (N terminal, A2 domain) resulting from alternative splicing of exons 3 and 4 (CEACAM2-2L) [242]. This leads to a differential degree of glycosylation with CEACAM2 containing 5 out of the 16 N-linked glycans in CEACAM1. Secondly, the two receptors display differential ligand binding properties of the distal variable N-terminal Ig-Domain that promotes homophilic binding in CEACAM1, but not CEACAM2 [186]. The only ligand thus far identified for CEACAM2 is the murine coronavirus mouse hepatitis virus spike glycoprotein (s) [185]. In addition, CEACAM2 proteins utilise two ITIMs identical to CEACAM1 to recruit SHP-1, and to a lesser degree, SHP-2 protein-tyrosine phosphatase [243, 244]. With SHP-1 playing an important role in platelet activation by the collagen receptor GPVI [245], it is likely that SHP recruitment to the ITIM domains of CEACAM1 contributes to the regulatory role of CEACAM1 in platelet-collagen interactions [187].

The potential involvement of CEACAM2 in regulating platelet-collagen interactions is unknown. Thus, the aim of this chapter was to investigate whether CEACAM2 regulates platelet-collagen interactions *in vitro*.

3.2 Results

3.2.1 Genotyping of wild-type and CEACAM2 knockout mice

Before performing the functional studies, Northern blot and RT-PCR analysis methodologies allowed verification of the age/sex-matched wild-type and homozygous CEACAM2 knockout mice genotypes [188]. Following the technique developed by Professor Sonia Najjar's laboratory at Toledo University, USA, a number of primer combinations were used (Figure 3-1). Primer -107 (sense) acted as the forward primer for the wild-type allele, because it binds with exon 2 found in the murine CEACAM2 gene. For the CEACAM2 encoding genes, primer 123 (anti-sense) acted as a reverse primer because it binds with 3'-end of the encoding genes. These particular primers exclusively amplify the murine CEACAM2 wild-type allele, creating a 1050 bp fragment. Conversely, these primers cannot amplify the deleted CEACAM2 gene in the same way because the neomycin cassette replaces the CEACAM2 coding region through homologous recombination. Moving to the allele Knockout (KO) group, forward primer SNeo9 (sense), which binds with the neomycin cassette, was used. For the reverse primer, ANeo8 (anti-sense) was used, because it binds with 3´-end of the neomycin cassette. These particular primers amplify only the knockout allele and deliver a 750 bp fragment: they cannot amplify the wild-type CEACAM2 gene in the same way due to homologous recombination of the CEACAM2 coding region [188].

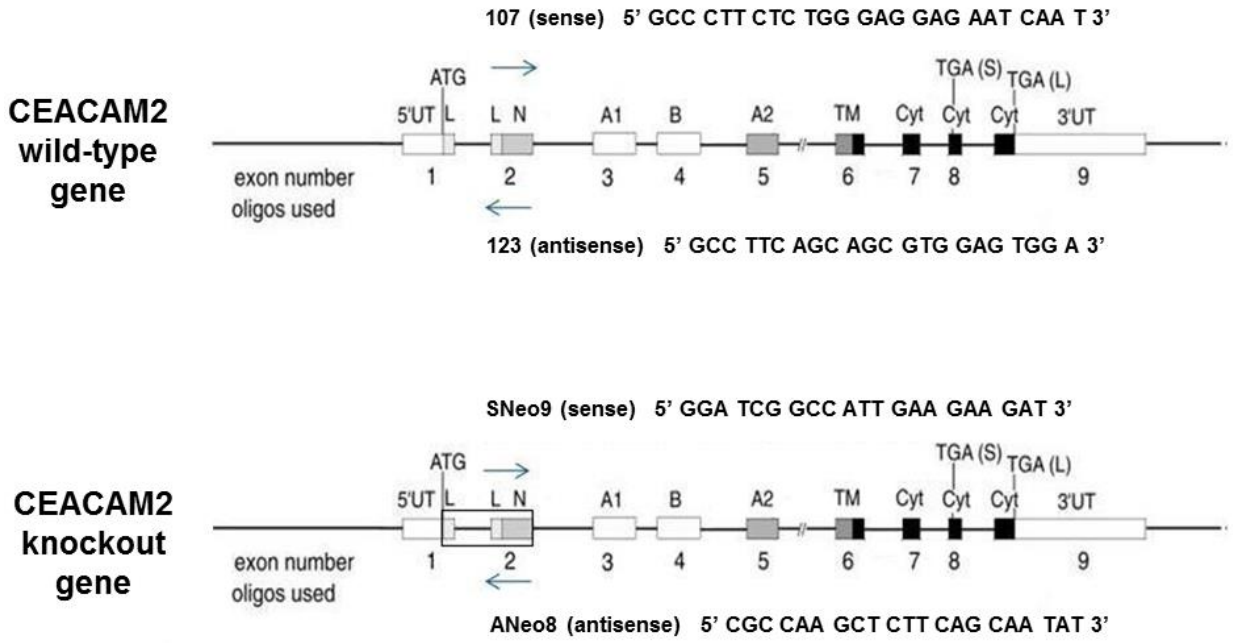

Figure 3-1: CEACAM2 primers map design to identify the wild-type and CEACAM2 knockout mice. CEACAM2 is located on chromosome 7 and found in exon 2. Specific sense and antisense primers are used for CEACAM2-wild-type (-107 and 123) and CEACAM2 knockout (-SNeo9 and ANeo9; respectively) genes. Adapted from [186]. CEACAM2 knockout gene was generated by replacing exon 1, including the translation initiation site in the *Ceacam2* gene with a gene encoding neomycin resistance. More details were provided in Chapter 2, section 2.2.1.2.

To image and examine the DNA fragments resulting from electrophoresis of the PCR products, Sybr safe DNA stain was added to 2% (w/v) agarose gel. Each PCR run included a number of DNA controls: known $Cc2^{+/+}$ (Wild-type), $Cc2^{+/-}$ (Heterozygous), and $Cc2^{-/-}$ (KO), alongside 3 unknown $Cc2^{+/+}$ and 3 unknown $Cc2^{-/-}$ DNA types. To eliminate any DNA recombination of PCR reagents and primers, Milli-Q H_2O acted as the non-DNA control. Wild-type and $Cc2^{-/-}$ mice generate different PCR products after amplification, namely 1050 bp and 750 bp fragments respectively. In these images, the DNA marker is in Lane 1, the $Cc2^{+/+}$, $Cc2^{+/-}$, and $Cc2^{-/-}$ DNA controls are in Lanes 2-4, and Milli-Q H_2O is in Lane 5. In Figure 3-2A, Lanes 6, 7, and 8 display amplified DNA products as 1050 bp

fragments that are specific to wild-type mice following electrophoresis with 123 and -107 primers. The lack of banding in the final three lanes (9-11) shows that these lanes belonged to the *Cc2*$^{-/-}$ mice and were not amplified by the wild-type mouse specific primers. Conversely, in Figure 3-2B, bands in Lanes 9-11 show the presence of 750 bp PCR fragments that are specific to *Cc2*$^{-/-}$ mice. Lanes 6–8 show no amplification, so the genomic DNAs extracted from these mice suggested that they belonged to the C57BL/6 and CEACAM2 KO groups.

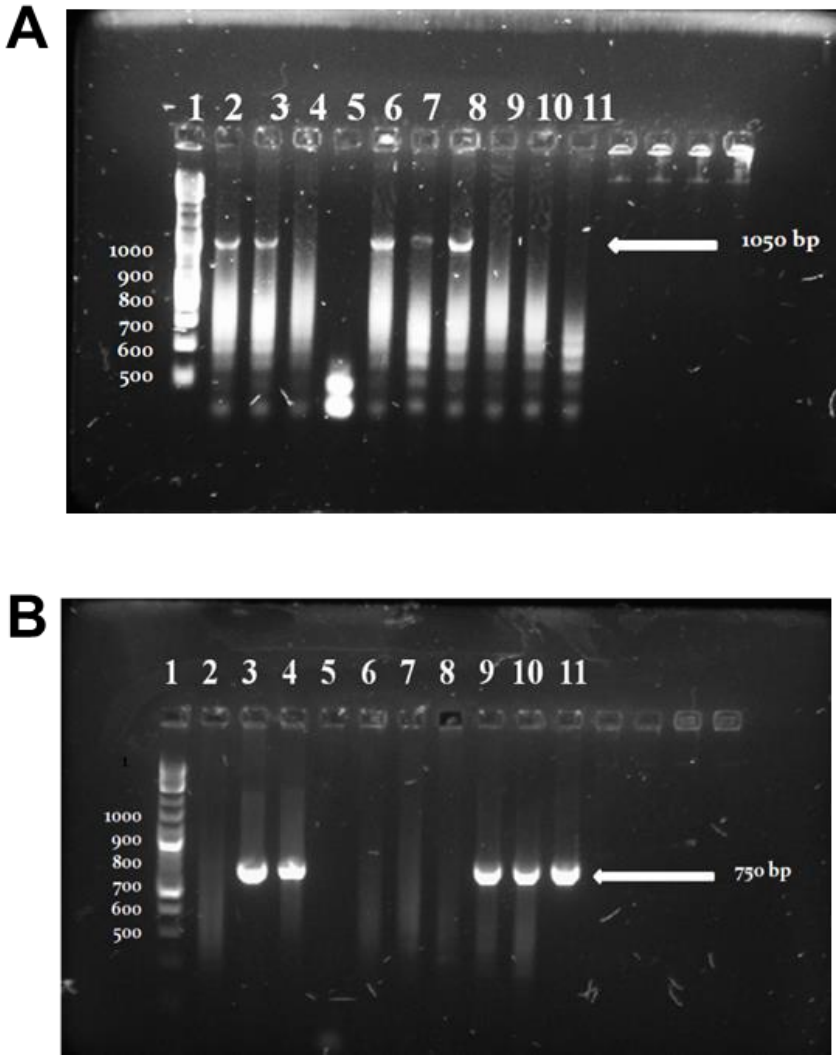

Figure 3-2: PCR CEACAM2 genotype for mouse tail DNA. (A) Wild-type mice displayed amplified DNA products as 1050 bp fragments in lane 6-8). **(B)** *Cc2*$^{-/-}$ showed the presence of 750 bp PCR fragments. Lane 1 (2-Log ladder DNA marker), lane 2 (Wild-type DNA), lane 3 (Heterozygous *Cc2* $^{+/-}$ DNA), lane 4 (*Cc2*$^{-/-}$ DNA), lane 5 (Milli-Q H_2O), lane 6-8 (wild-type DNA) and lanes 9-11 (*Cc2*$^{-/-}$ DNA).

3.2.2 *Cc2*$^{-/-}$ mice have normal haematological parameters

To determine whether CEACAM2 deletion affects production of haematopoietic cells such as platelets, a comparison of wild-type and *Cc2*$^{-/-}$ mice of the same sex and age was performed. All haematological parameters including WBC count, red blood cell (RBC) count, haemoglobin (Hb), packed cell volume (PCV), mean cell volume (MCV), mean cell haemoglobin (MCH), mean cell haemoglobin concentration (MCHC), red cell distribution width (RDW), neutrophils, lymphocytes and monocytes and platelet count (PLT) were determined. As Table 3-1 reveals, all haematological parameters including platelet count were normal in *Cc2*$^{-/-}$ compared to wild-type mice. The assays were run in triplicates, and the data shown are representative of 6 independent experiments, presented as mean fluorescence intensity (MFI) ± SEM ($P > 0.05$ is non-significant for all haematological parameters), using statistics Student *t*-test.

Table 3-1: Haematological parameters of wild-type and *Cc2*$^{-/-}$ mice. Results are expressed as MFI ± SEM. (P> 0.05 is non-significant for all haematologic parameters), using statistics Student *t*- test.

Haematological parameter	**Wild-type (n = 6)**	***Cc2*$^{-/-}$ (n = 6)**
WBC, $\times 10^9$/L	6.20 ± 1.03	5.25 ± 0.66
RBC, $\times 10^{12}$/L	9.07 ± 0.22	8.89 ± 0.46
HGB, g/L	132.33 ± 3.08	129.33 ± 6.90
PCV, L/L	0.43 ± 0.01	0.42 ± 0.02
MCV, fl	48.33 ± 0.55	48.00 ± 0.85
MCH, pg	14.61 ± 0.24	14.56 ± 0.23
MCHC, $\times 10^3$ g/L	302.00 ± 3.40	303.83 ± 3.21
RDW, %	13.25 ± 0.18	13.58 ± 0.19
PLT, $\times 10^9$/L	726.66 ± 23.10	741.00 ± 9.80
WBC/Neut/, %	8.58 ± 1.72	7.41 ± 1.50
WBC/Lymph, %	88.91 ± 2.34	90.00 ± 2.27
WBC/Mono, %	2.50 ± 0.65	3.08 ± 1.26
WBC/Neut, $\times 10^9$/L	0.55 ± 0.17	0.37 ± 0.07
WBC/Lymph, $\times 10^9$/L	5.47 ± 0.88	4.74 ± 0.65
WBC/Mono, $\times 10^9$/L	0.17 ± 0.06	0.16 ± 0.07

3.2.3 CEACAM2 is expressed on the surface and in intracellular pools of murine and human platelets

Next, we aimed to investigate whether CEACAM2 is expressed on the cell surface and in intracellular pools of resting murine platelets. To determine whether surface expression of CEACAM2 is increased after granule release, we examined the binding of a specific anti–mouse CEACAM2 polyclonal antibody to resting and agonist stimulated wild-type mouse platelets, detected by flow cytometry. As shown in Figure 3-3A, resting platelets incubated with the anti-mouse CEACAM2 antibody had a two-fold increase in surface expression compared to normal rabbit pre-immune serum (21.56 ± 1.754 vs 9.854 ± 1.597, respectively; $^{**}P<0.01$; n=5). This finding indicates the presence of CEACAM2 on the surface of mouse platelets. In addition, characterisation of the total distribution of CEACAM2 in mouse platelets was determined by permeabilisation of the platelet membrane with saponin. Saponin-treated platelets incubated with anti-CEACAM2 antibody had a 2.5-fold higher MFI than those incubated with normal rabbit pre-immune serum (83.66 ± 8.935 vs 33.08 ± 6.756, respectively; $^{**}P<0.01$; n=5; Figure 3-3A). This finding points to an additional intracellular CEACAM2 pool in mouse platelets. CEACAM2 is predominantly expressed in platelets as the commonly found CEACAM2-2L (CC2-2L) form of ~ 52 kDa (Figure 3-3B). CC2-2L of CEACAM2 contains 2 Ig-Domains (N terminal, A2 domain), a transmembrane domain and long ITIM-containing cytoplasmic domain. As shown in Figure 3-3B, there is no detectable protein expression in the platelet lysates from *Cc2*$^{-/-}$ mice, but significant expression in the wild-type mouse platelet lysate. Equivalence in protein loading was determined by stripping and reprobing the blot with anti-GAPDH. Cell surface expression of CEACAM2 was increased in a dose-responsive manner upon agonist stimulation with thrombin (0.12-1 U/mL), PAR-4 agonist peptide (100-300 µM) and CRP (1-4 µg/mL) compared to resting platelets ($^{***}P<0.001$; n=4; Figure 3-3C). In *Cc2*$^{-/-}$ platelets, the expression of several platelet glycoproteins, including

GPVI, PECAM-1, CEACAM1, integrin $\alpha_2\beta_1$, integrin $\alpha_{IIb}\beta_3$, GPIb-IX-V complex, CD44 and CD9 was similar to wild-type platelets (Figure 3-4A-B). In contrast, CEACAM2 was expressed in wild-type platelets but absent in *Cc2*$^{-/-}$ platelets (Figure 3-4A). Consistently, up-regulation of CEACAM1 surface expression was similar in wild-type versus *Cc2*$^{-/-}$ platelets upon a dose-responsive manner of agonist stimulation with thrombin (0.12-1 U/mL), PAR-4 agonist peptide (100-300 µM) and CRP (1-4 µg/mL) (Figure 3-2C). These data show that CEACAM2 protein is localised to both the surface and intracellular pools in resting mouse platelets.

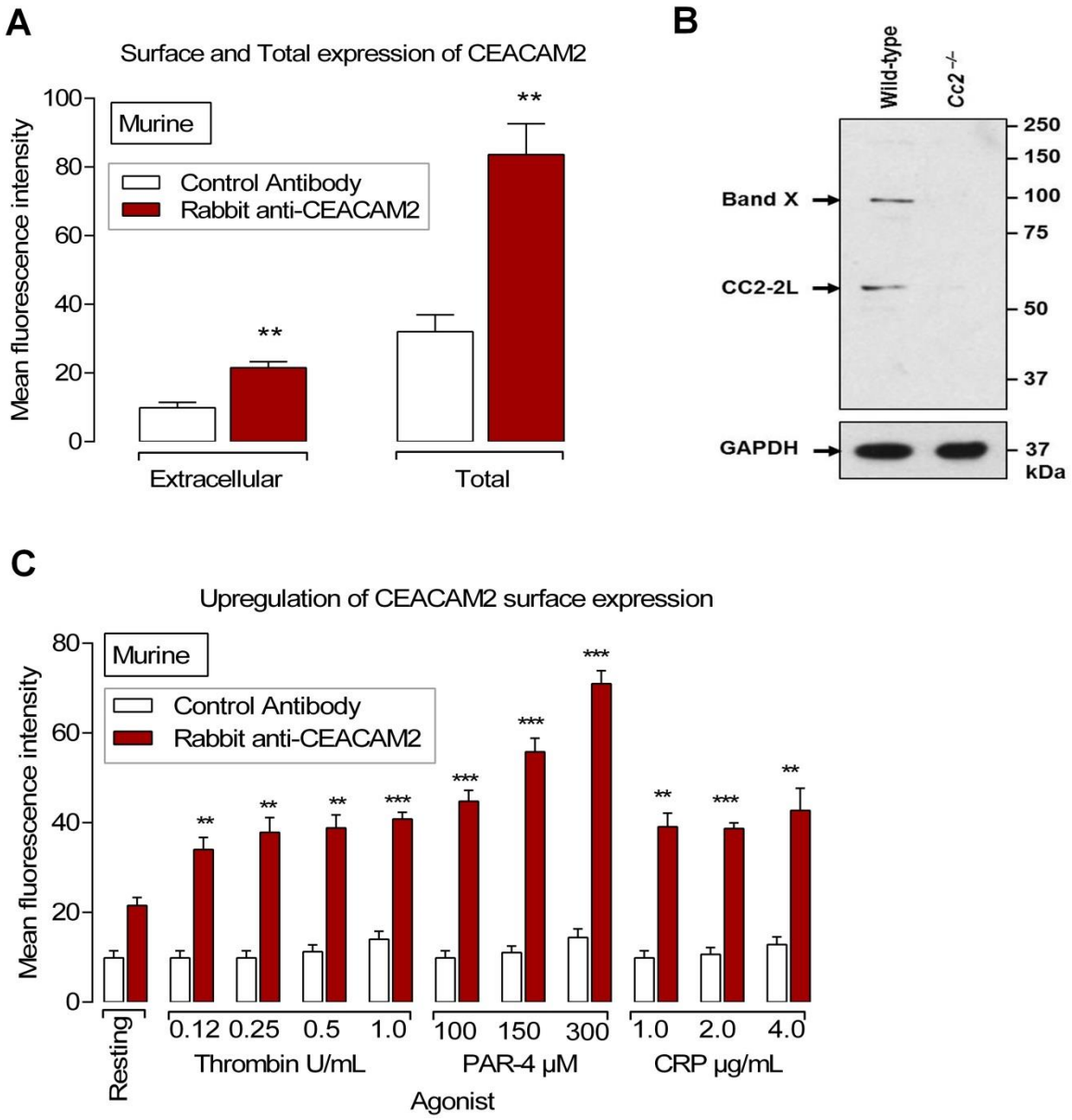

Figure 3-3: CEACAM2 is expressed on the surface and in intracellular pools in murine platelets. (A) Flow cytometric analysis of CEACAM2 surface and total expression on resting murine platelets. Platelets were stained with a polyclonal anti-murine CEACAM2 2052 antibody followed by a secondary PE conjugated anti-rabbit antibody. Normal rabbit serum was included as a negative control. For total expression, platelets were resuspended in 0.1% (w/v) saponin, and then washed with a combination of 0.1% (w/v) saponin and 0.2% (w/v) Bovine serum Albumin (BSA). Data were collected by a live platelet gate based on forward versus side scatter profiles on a FACS Canto II flow cytometer. Results are cumulative data derived from four independent experiments and represented as MFI ± SEM (***P*<0.01; n=4). **(B)** Platelet lysates from wild type and *Cc2*$^{-/-}$ mice were analysed by 10% SDS-PAGE and Western blotting using 1:2000 of rabbit anti–mouse CEACAM2 polyclonal antibody (2052) (upper panel), followed by reprobing with GAPDH antibody to control for protein loading (bottom panel). A ~52 kDa band representing CEACAM2 and another one (band X) at ~95kDa representing an unidentified protein were detected. **(C)** CEACAM2 surface expression was increased upon agonist stimulation of wild-type murine platelets using thrombin (0.125-1.0 U/mL), PAR-4 agonist peptide (100-300 µM) and collagen related peptide (CRP; 1.0-4.0 µg/mL) over a dose-dependent range (***P*<0.01 and ****P*<0.001; n=4). CEACAM2 surface expression was determined as described in panel A.

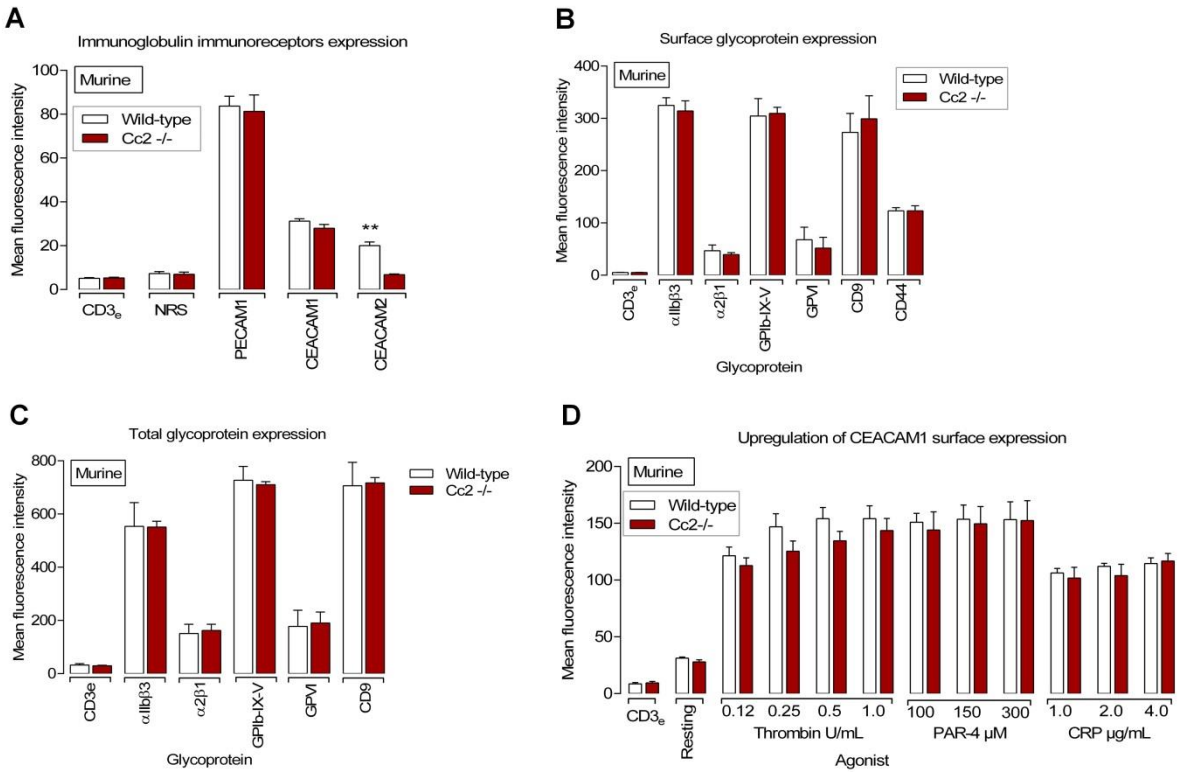

Figure 3-4: Immunoglobulin immunoreceptors expression in murine platelets. (A) Flow cytometric analysis of PECAM-1, CEACAM1 and CEACAM2 expression on resting wild-type versus *Cc2*$^{-/-}$ platelets. Wild-type and *Cc2*$^{-/-}$ platelets were stained with a monoclonal anti-murine PECAM-1 antibody, polyclonal anti-murine CEACAM1 2457 antibody or polyclonal anti-murine CEACAM2 2052 antibody followed by a secondary PE conjugated anti-rat or anti-rabbit antibody. Normal rabbit serum (NRS) and isotype control antibody CD3 were included as negative controls. Data were collected by a live platelet gate based on forward versus side scatter profiles on a FACS Canto II flow cytometer. Results are cumulative data derived from four independent experiments and represented as MFI ± SEM (**P<0.01; n=4). **(B)** Cell surface expression of platelet glycoproteins was monitored by flow cytometry using specific monoclonal antibodies for wild-type and *Cc2*$^{-/-}$ platelets. MFI was reported with a standard error of mean for at least four independent experiments and no significant difference was demonstrated. **(C)** Total expression of platelet glycoproteins on resting wild-type and *Cc2*$^{-/-}$ murine platelets was determined and antibodies concentrations were described in Methodology section. **(D)** Cell surface expression of CEACAM1 upon agonist stimulation of wild-type versus *Cc2*$^{-/-}$ murine platelets was determined as described in Figure 3-3, panel B.

3.2.4 *Cc2*$^{-/-}$ platelet response to GPVI-selective agonists

To determine whether CEACAM2 negatively regulates ITAM-bearing, collagen–GPVI–mediated platelet responses, platelet aggregation responses were evaluated using wild-type versus *Cc2*$^{-/-}$ mice platelets. PRP were stimulated using a range of G-protein-coupled agonists, PAR-4 agonist peptide (125–500 µM; Figure 3-3Aa–c), ADP (2.5–10 µM; Figure 3-5Ad–f) and CI-A23187 (1.25–5.0 µg/mL; Figure 3-5Ag–i), with acid-soluble type I collagen (1.25–5 µg/mL; Figure 3-6Aa–c) and the GPVI collagen receptor selective agonist, CRP (0.625–2.5 µg/mL; Figure 3-6Ad–f). In addition, washed platelets were stimulated using thrombin (0.5-1 U/mL; Figure 3-7Aa–b), PAR-4 agonist peptide (250–500 µM; Figure 3-7Ac–d) and CRP (5–10 µg/mL; Figure 3-7Ae–f). As shown in Figures 3-5 and 3-7A-B, similar platelet aggregation profiles were observed in wild-type and *Cc2*$^{-/-}$ platelets treated with thrombin, PAR-4 agonist peptide, ADP and CI. However, in response to collagen and CRP agonist (Figure 3-6A-B), enhanced platelet aggregation responses were observed in *Cc2*$^{-/-}$ platelets, particularly at subthreshold doses compared to wild-type platelets. These data suggest that lack of CEACAM2 leads to hyper-responsive tyrosine-kinase dependent signalling pathway in platelets upon collagen and CRP stimulation.

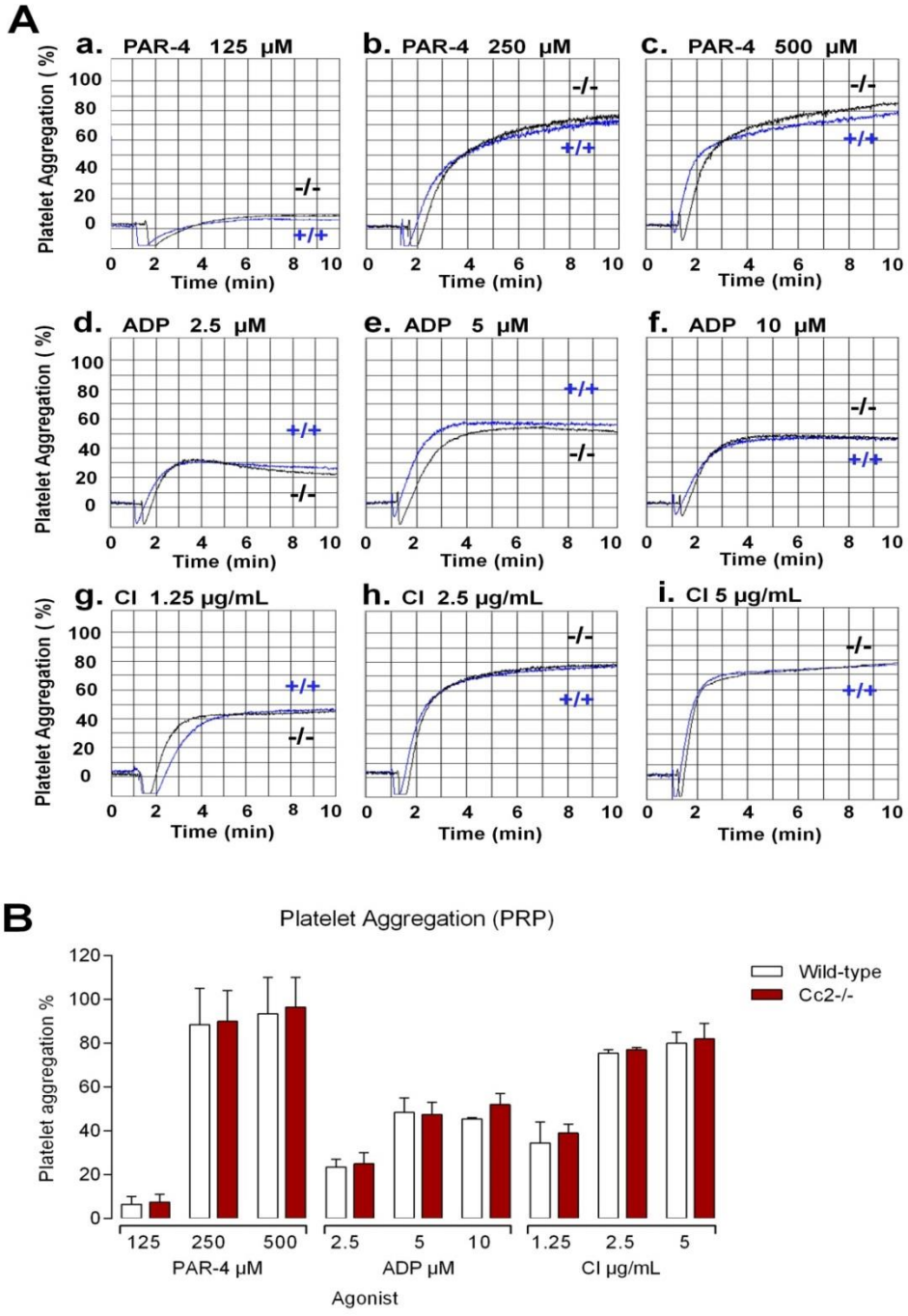

Figure 3-5: *Cc2*$^{-/-}$ platelets are normal after stimulation with GPCRs and calcium ion channel agonists. **(A-B)** Aggregation responses of PRP (platelet count adjusted to 100x10^9/L) for wild-type (+/+) and *Cc2*$^{-/-}$ mice were determined following stimulation with the following agonists: **(a-c)** PAR-4 agonist peptide (125-500 µM), **(d-f)** ADP (2.5-10 µM), **(g-i)** calcium ionophore (1.25-5 µg/mL). Note that *Cc2*$^{-/-}$ are comparable to wild-type platelets. These data are representative of at least four independent experiments (P>0.05; n=4).

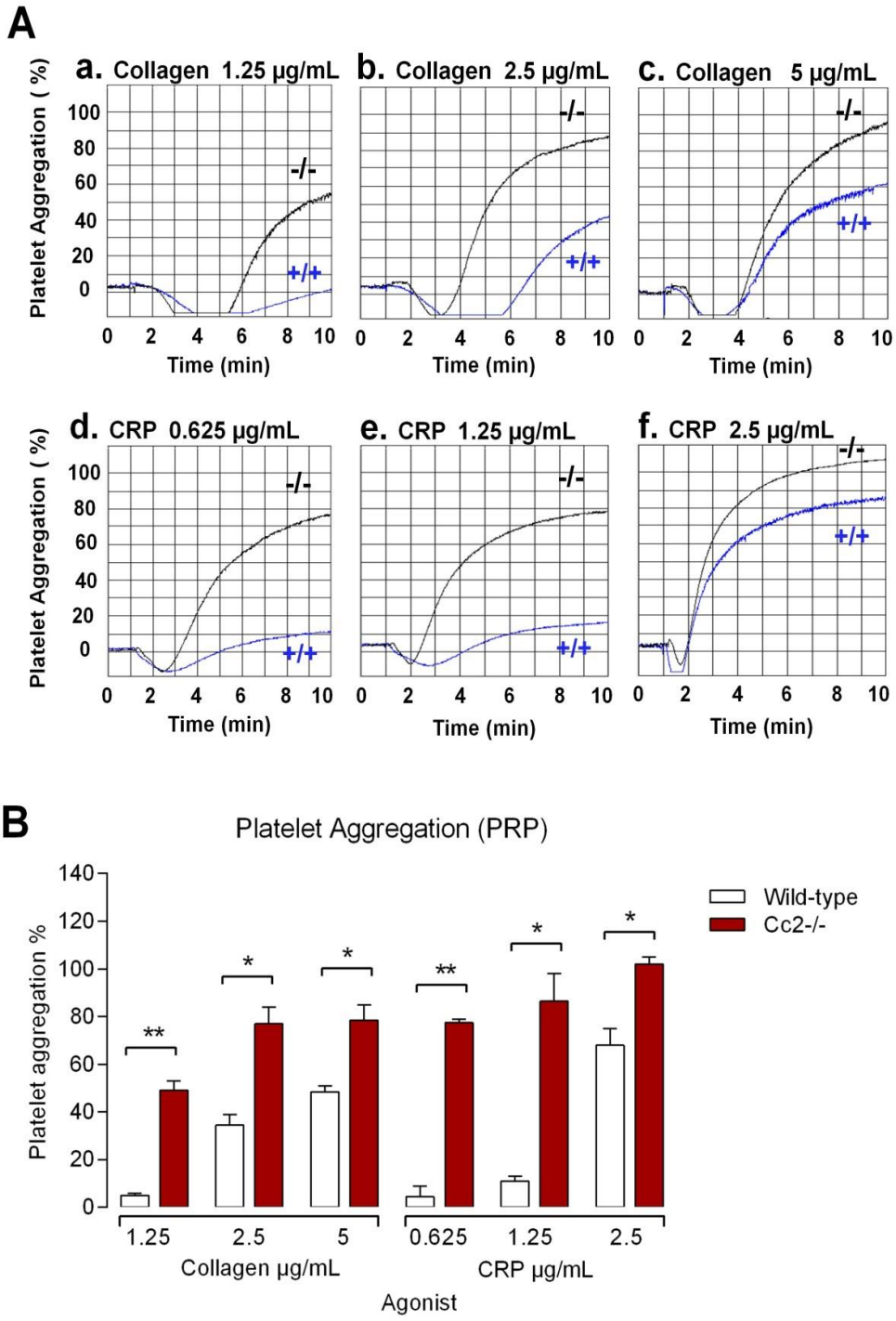

Figure 3-6: *Cc2*$^{-/-}$ platelets are hyper-responsive to stimulation with type I collagen and GPVI selective agonist, CRP. (A-B) Aggregation responses of PRP ($100x10^9$/L) for wild-type (+/+) and *Cc2*$^{-/-}$ mice were determined following stimulation with the following agonists: **(a-c)** type I collagen (1.25-5 µg/mL) and **(d-f)** CRP (0.625-2.5 µg/mL). Note that *Cc2*$^{-/-}$ platelets are hyper-responsive to stimulation by type I collagen and GPVI-selective agonist, CRP. These data are representative of at least four independent experiments (**P*<0.05 and ***P*<0.01; n=4).

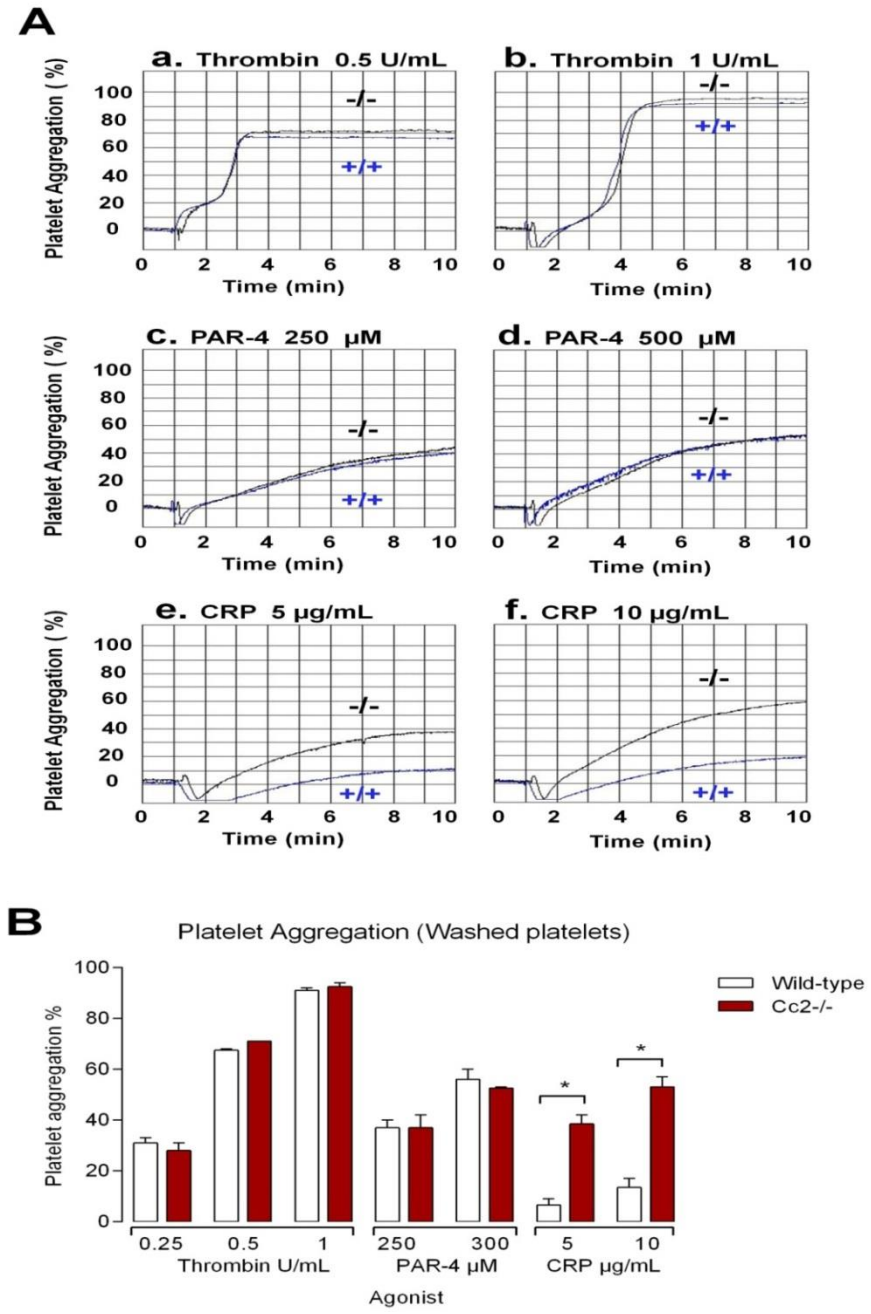

Figure 3-7: *Cc2*$^{-/-}$ washed platelets are hyper-responsive to stimulation with GPVI selective agonist, CRP. (A-B) Aggregation responses of murine washed platelets for wild-type (+/+) and *Cc2*$^{-/-}$ mice were determined following stimulation with the following agonists: **(a-b)** Thrombin (0.5-1 U/mL), **(c-d)** PAR-4 agonist peptide (250-500 µM) and **(e-f)** CRP (5-10 µg/mL). *Cc2*$^{-/-}$ platelets are hyper-responsive to stimulation by GPVI-selective agonist, CRP. These data are representative of at least four independent experiments performed (**P*<0.05; n=4).

3.2.5 *Cc2*$^{-/-}$ platelets display enhanced GPVI-mediated alpha and dense granule secretion

As *Cc2*$^{-/-}$ platelets exhibited hyper-responsive GPVI-mediated platelet aggregation responses, we investigated whether the absence of CEACAM2 affects the platelet-release reaction stimulated by GPVI-specific agonist, CRP (0.5-2 µg/mL), thrombin (0.1-0.2 U/mL) and PAR-4 agonist peptide (100-300 µM). The ability of wild-type and *Cc2*$^{-/-}$ platelets to secrete alpha (P-selectin) and dense granules (Quinacrine) upon GPVI and GPCRs stimulation was determined. As seen in Figures 3-8A and 3-9A, the release of alpha and dense granule contents from *Cc2*$^{-/-}$ platelets upon stimulation by GPCRs agonists including thrombin and PAR-4 agonist peptide was similar to wild-type platelets. Furthermore, the release of alpha granule contents from *Cc2*$^{-/-}$ platelets was similar to that from *Cc1*$^{-/-}$ platelets after CRP stimulation (Figure 3-8B). However, *Cc2*$^{-/-}$ platelets released more alpha and dense granules at all doses of CRP compared with wild-type platelets but not when treated with thrombin and PAR-4 agonist peptide at any dose (*P<0.05; **P<0.01; ***P<0.001; n=4; Figures 3-8B and 3-9B). These results support the hypothesis that CEACAM2 acts as a negative regulator specifically of GPVI-mediated platelet granule release.

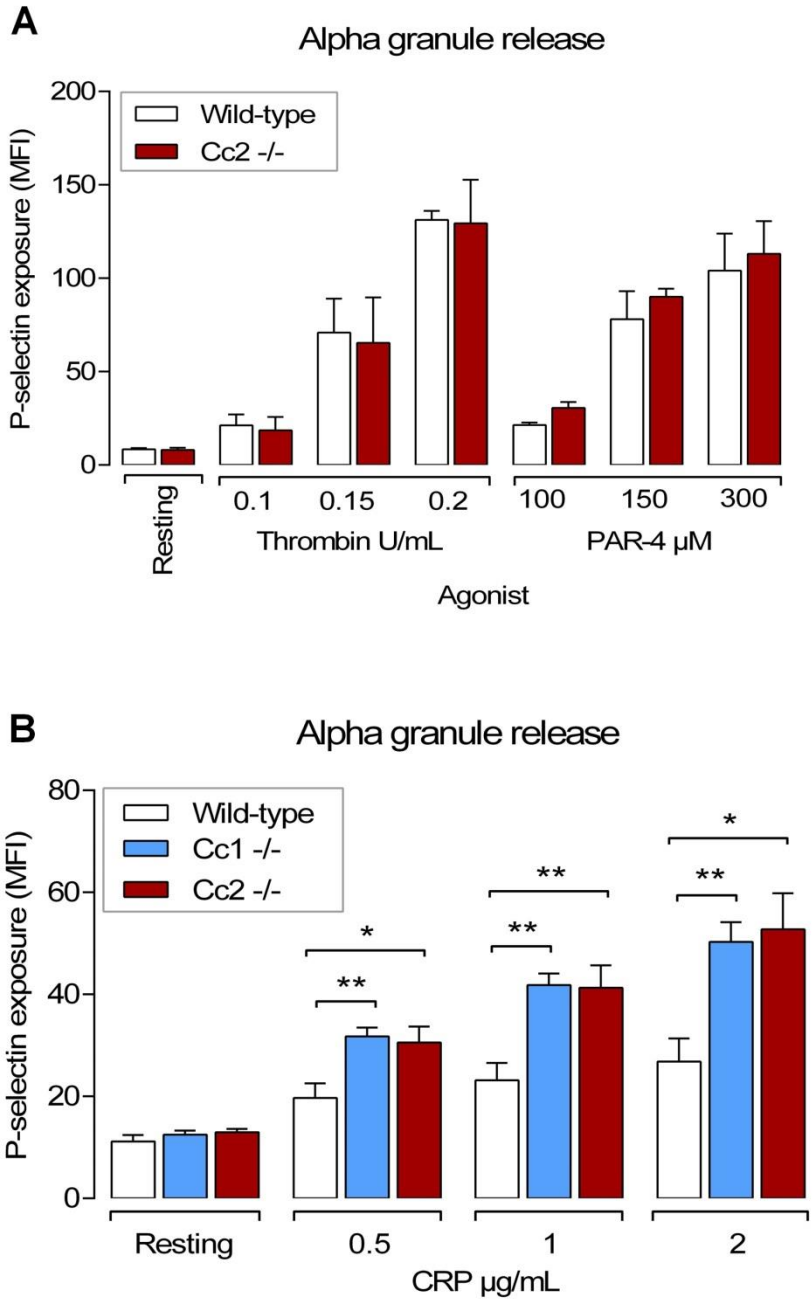

Figure 3-8: *Cc2*$^{-/-}$ platelets display enhanced alpha granule release following stimulation with GPVI-selective agonist, CRP. (A-B) Surface expression of P-selectin as a marker of alpha granule release was determined for washed platelets stimulated by thrombin (0.1-0.2 U/mL), PAR-4 agonist peptide (100-300 µM) and CRP (0.5-2.0 µg/mL) and then stained with either a buffer control and FITC-conjugated P-selectin mAb for both wild-type and *Cc2*$^{-/-}$ platelets **(A)** and *Cc1*$^{-/-}$ platelets **(B).** FITC-labelled samples were analysed on a FACS Canto II flow cytometer. Results are representative of three independent experiments (**P*<0.05 and ***P*<0.01; n=3).

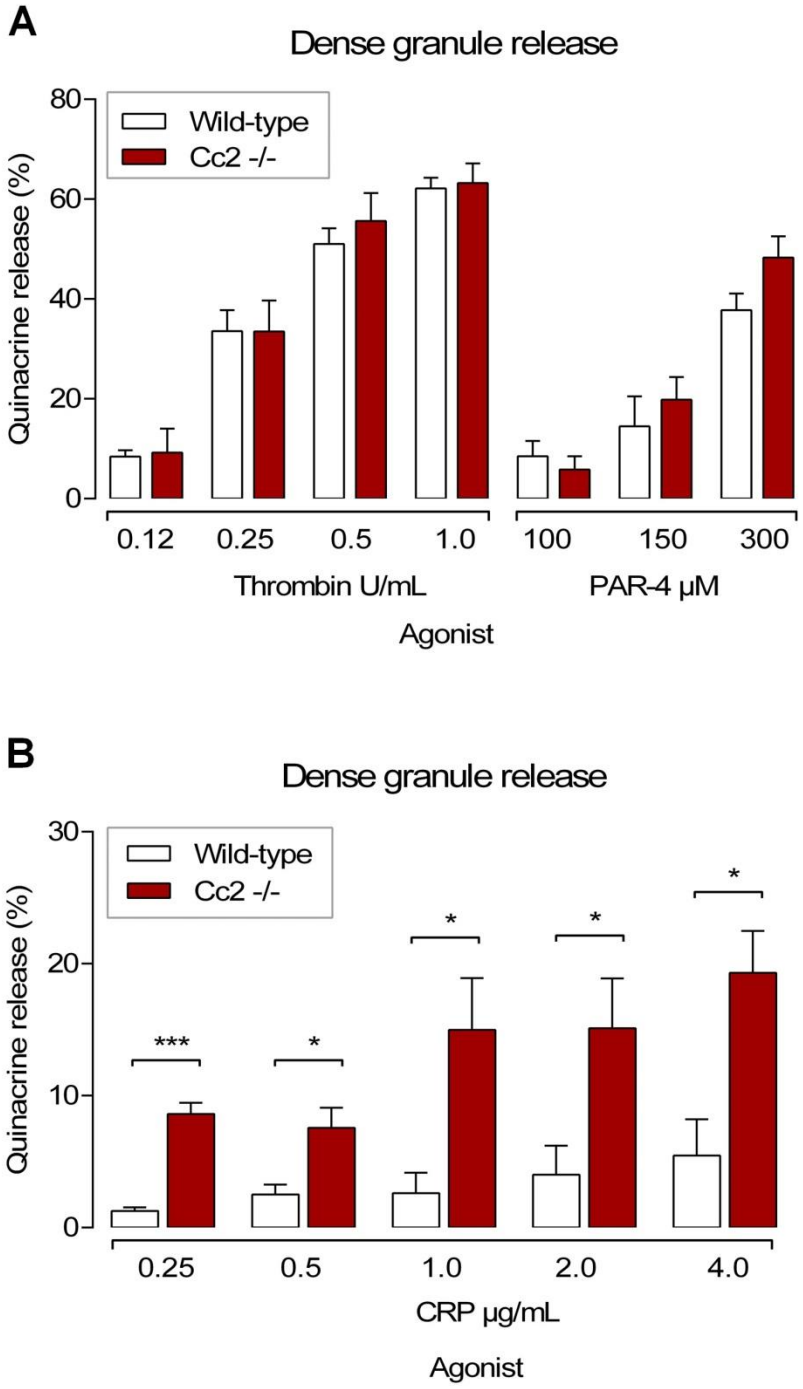

Figure 3-9: *Cc2*$^{-/-}$ platelets show enhanced dense granule release following GPVI-selective agonist, CRP stimulation. (A-B) Platelet dense granule exocytosis measured by release of fluorescent quinacrine by flow cytometry. Washed platelets ($100x10^9$/L) derived from both wild-type and *Cc2*$^{-/-}$ mice were stimulated with either no agonist, thrombin (0.12-1.0 U/mL), PAR-4 agonist peptide (100-300 µM) or CRP (0.25-4.0 µg/mL). Samples were analysed on a FACS Canto II flow cytometer. Data are reported as percentage quinacrine release and are representative of four independent experiments (*P<0.05 and ***P<0.001; n=4).

3.2.6 *Cc2*$^{-/-}$ platelets displayed enhanced static adhesion to immobilised type I fibrillar collagen

We examined whether CEACAM2 modulates collagen–GPVI–mediated platelet responses in a manner similar to other platelet Ig-ITIM immunoreceptors such as PECAM-1 and CEACAM1. Static platelet adhesion on type I fibrillar collagen was performed to determine the binding characteristics of platelets derived from wild-type and *Cc2*$^{-/-}$ mice over time. *Ceacam2*-null platelets bound more to immobilised type I fibrillar collagen but not to the negative control (RCD buffer, pH 7.4) compared to wild-type platelets at all time points (Figure 3-10). These data show that upon static adhesion to immobilised type I collagen, *Cc2*$^{-/-}$ platelets showed hyper-responsive platelet adhesion compared to wild-type platelets.

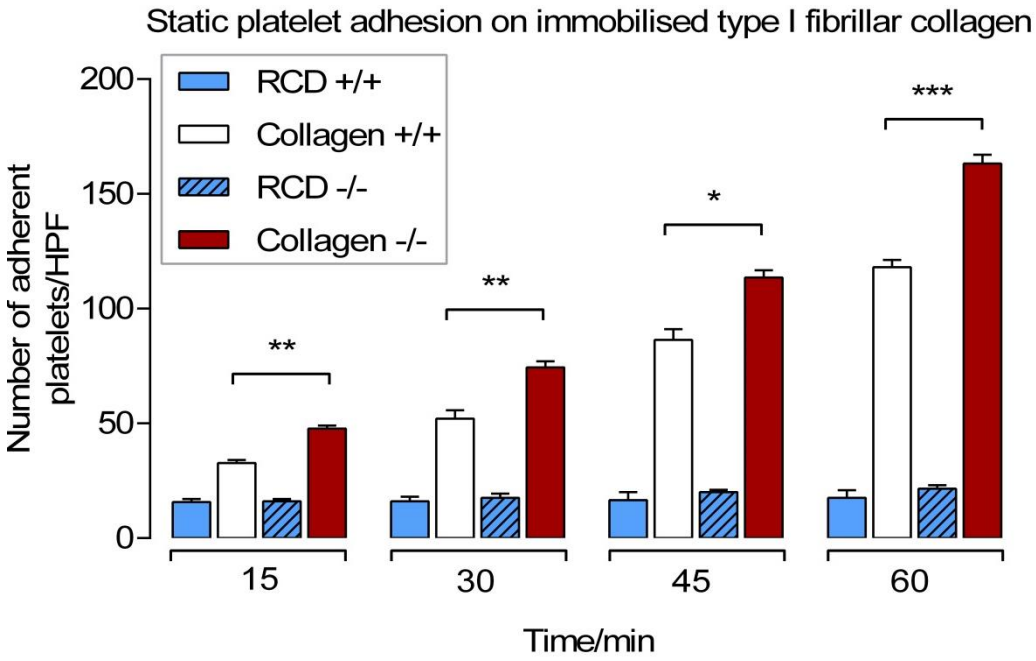

Figure 3-10: *Cc2*$^{-/-}$ platelets display enhanced static adhesion on immobilised type I collagen. Time course of wild-type (+/+) and *Cc2*$^{-/-}$ platelet adhesion to either buffer control or type I collagen (50 µg/mL) in the absence of magnesium for 15, 30, 45 and 60 minutes at 37°C. Non-adherent platelets were removed and adherent platelets were measured as described in Materials and Methods. Data represents four independent experiments. Note that *Cc2*$^{-/-}$ platelets show a higher level of number of adherent platelets in high-power field (HPF) to type I fibrillar collagen than wild-type platelets (+/+) at all time points (**P*<0.05, ***P*<0.01, ****P*<0.001; n=4).

3.2.7 Normal phosphatidylserine exposure in *Cc2*$^{-/-}$ platelets

A number of flow studies examining mouse and human blood suggest that GPVI, a signal receptor, is solely responsible for regulating any procoagulant activity of platelets induced by collagen, providing a bridge between the processes governing platelet activation and coagulation [228, 246, 247]. A long and powerful rise in cytosolic [Ca^{2+}]i regulates this procoagulant activity by changing the membrane location of the procoagulant phosphatidylserine (PS), a key coagulation regulator, on the outer surface of platelets [248]. As an example, membrane surfaces with high levels of exposed PS will significantly raise thrombin and factor Xa formation rates [249]. In order to determine the functional role of CEACAM2 in the regulation of the procoagulant activity of platelets, the effect on agonist-induced phosphatidylserine exposure (Annexin V) in wild-type, *Cc1*$^{-/-}$ and *Cc2*$^{-/-}$ platelets was determined. Washed platelets ($100x10^9$/L) were stimulated with G-protein coupled agonists, thrombin (0.12-0.5 U/ml) and PAR-4 agonist peptide (100-300 μM) and along with tyrosine kinase dependent GPVI-selective agonist, CRP (1-4 μg/ml). *Cc2*$^{-/-}$ platelets display a similar response of Annexin V-FITC binding in all GPCRs and GPVI agonists at all doses compared to wild-type platelets (Figure 3-11A). Moreover, *Cc1*$^{-/-}$ platelets showed a typical response of Annexin V-FITC binding with all agonists doses tested compared to *Cc2*$^{-/-}$ and wild-type platelets (Figure 3-11B).

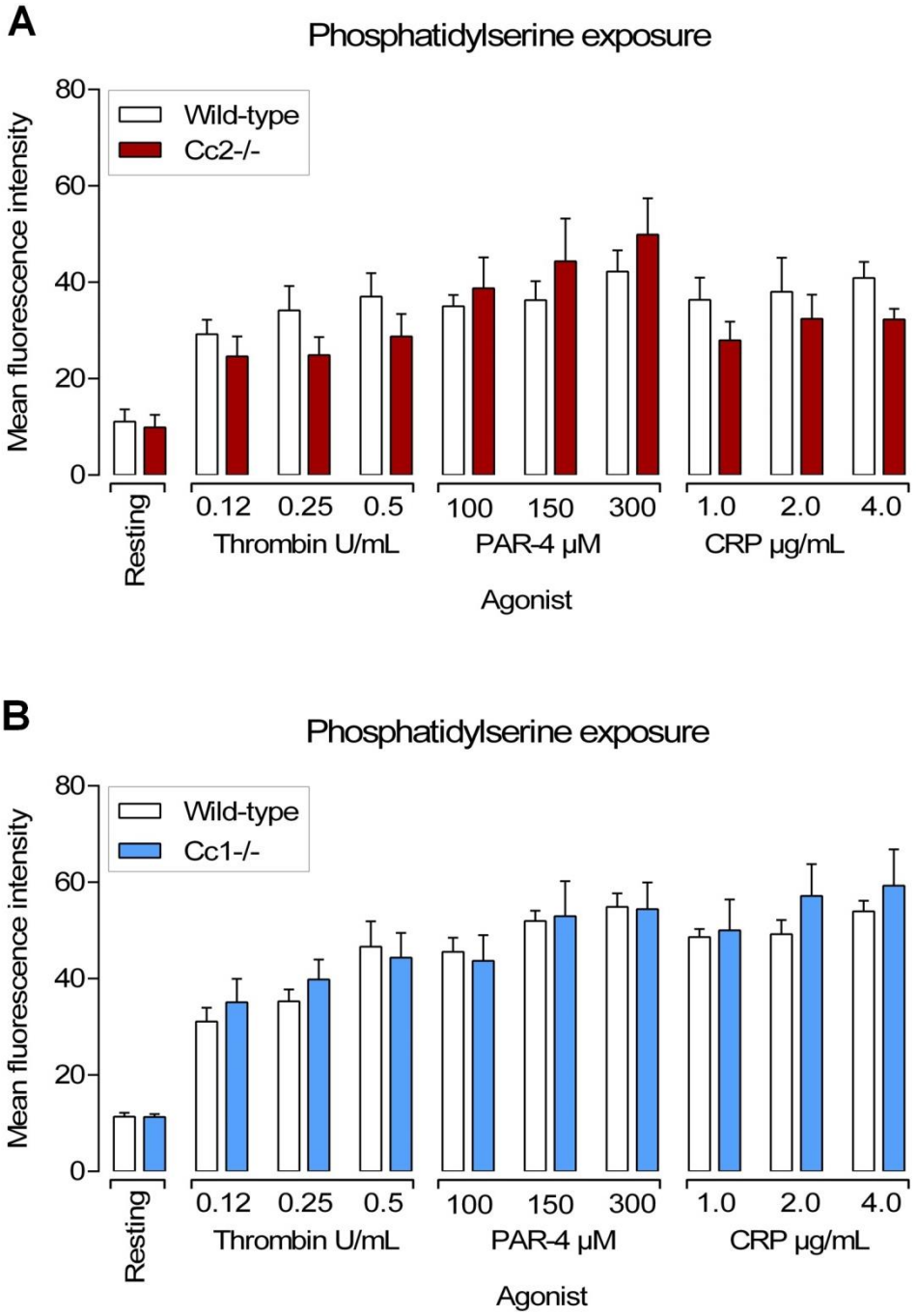

Figure 3-11: *Cc2*$^{-/-}$ platelets display normal phosphatidylserine exposure. (A-B) The influence of CEACAM1 And CEACAM2 on phosphatidylserine exposure (Annexin V) of murine washed platelets was examined following stimulation with thrombin (0.12-0.5 U/ml) and PAR-4 agonist peptide (100-300 µM) and the GPVI-selective agonist, CRP (1-4 µg/ml). **(A)** The MFI of Annexin V-FITC binding in wild-type versus *Cc2*$^{-/-}$ platelets was not significantly different to that in wild-type platelets. **(B)** MFI of PS exposure in wild-type versus *Cc1*$^{-/-}$ platelets was not significantly different to that in wild-type platelets. Data are reported as average of MFI Annexin V-FITC binding and are representative of six independent experiments (P>0.05; n=6).

3.2.8 Enhanced tyrosine phosphorylation in *Cc2*$^{-/-}$ platelets after GPVI- stimulation

To determine whether CEACAM2 plays a negative regulatory role in ITAM signalling pathways in platelets, wild-type and *Cc2*$^{-/-}$ platelets were stimulated using 10 µg/mL of CRP over a 3 minute-period. Global tyrosine phosphorylation of proteins in platelet lysates derived from CRP-stimulated *Cc2*$^{-/-}$ and wild-type mice was measured. Several tyrosine hyper-phosphorylated proteins of 54, 56, 65, 71, 74, 83 and 93kDa apparent molecular mass were detected in *Cc2*$^{-/-}$ in response to CRP stimulation for 15 seconds - 3 minutes by comparison to wild-type platelets (Figure 3-12A). Furthermore, PLCγ2, Src and Syk tyrosine phosphorylation was measured after CRP and Rhod-stimulation for 0-90 seconds by immunoprecipitation and Western blot analysis with anti-phosphotyrosine antibodies. As shown in Figure 3-12B, CRP-stimulated *Cc2*$^{-/-}$ platelets showed a 5-fold increase in PLCγ2 tyrosine phosphorylation (0.5230±0.014 vs 0.1340±0.004; ***P<0.001; n=3; Figure 3-12B.a), a 3-fold increase in Src tyrosine phosphorylation (0.4573±0.051 vs 0.2710±0.027; *P<0.05; n=3; Figure 3-12B.b), and a 3.5-fold increase in Syk tyrosine phosphorylation (0.5437±0.011 vs 0.1167±0.008; ***P<0.001; n=3; Figure 3-12B.c) compared to wild-type platelets. The equivalence of protein loading was determined by stripping and reprobing the blot with antibodies to the relevant protein (bottom panel). These data are consistent with the notion that CEACAM2 plays a role in attenuating platelet collagen GPVI/FcR γ-chain ITAM signalling pathways.

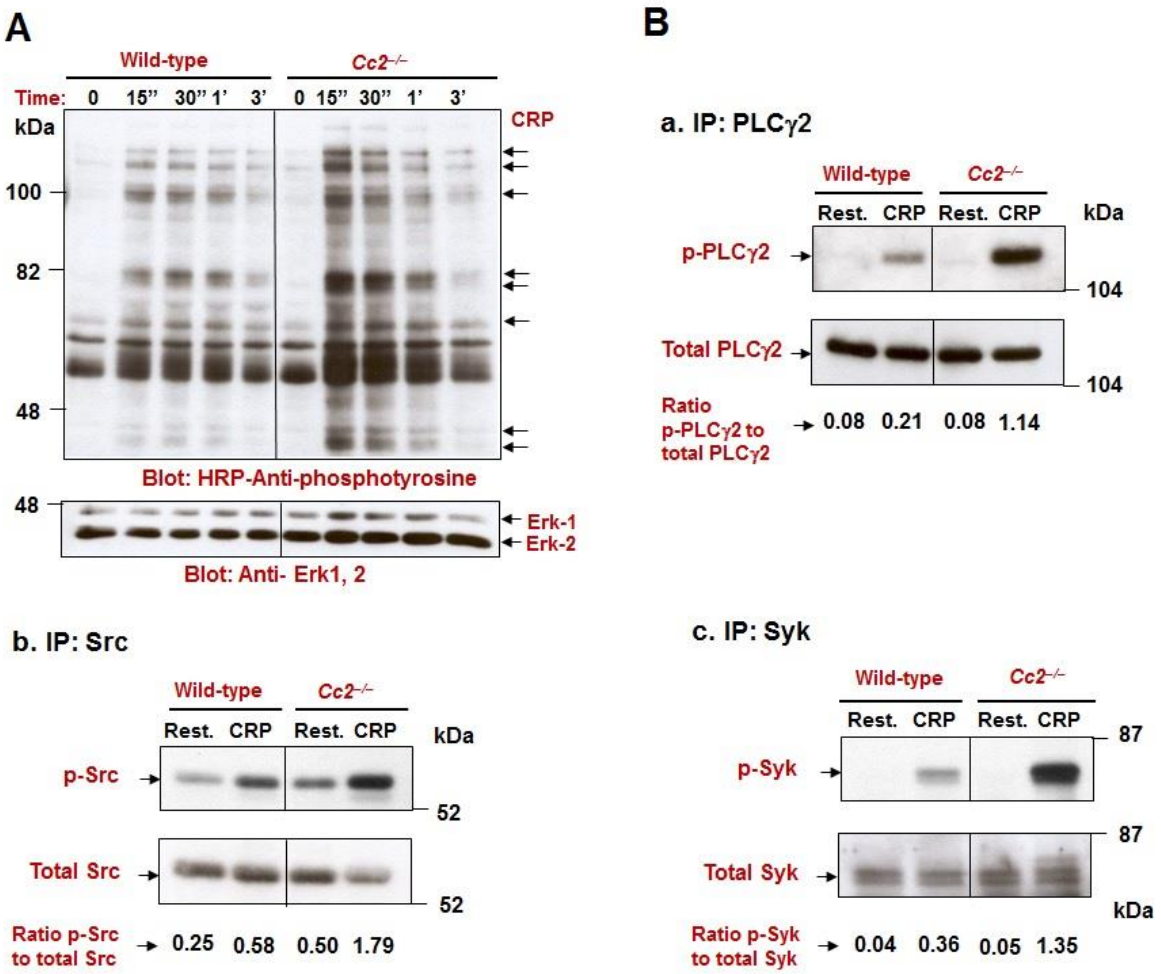

Figure 3-12: *Cc2*$^{-/-}$ platelets show hyper-tyrosine phosphorylated proteins after GPVI selective agonist, CRP stimulation over time. (A) Platelets (300x10^9/L) from wild-type and *Cc2*$^{-/-}$ mice were stimulated with 10 µg/mL of CRP at 37 °*C* for 3 minutes. Platelet lysate of 30 µg was then loaded onto a 10% (w/v) SDS-PAGE gel. Then Western blotting was performed to measure tyrosine phosphorylation, using 1/5000 of a HRP-conjugated anti-phosphotyrosine RC20 antibody. A protein loading control (bottom panel) blot was stripped and re-probed using anti-Erk-1/2 Ab for detection of Erk-1 and Erk-2 antigens. The data shown are a representative blot of similar results for 3 independent experiments. **(B)** Tyrosine phosphorylation of PLCγ2, Src and Syk was detected from platelet lysate after stimulation with 10 µg/mL of CRP versus resting at time 0 and 90 seconds. Immunoprecipitation of PLCγ2, Src and Syk from platelet lysates was performed followed by immunoblotting to detect **a.** p-PLCγ2, using 1/5000 of a HRP-conjugated anti-phosphotyrosine RC20 antibody. **b.** p-Src, using 1/2000 of anti-phospho Src and 1/20,000 of anti-rabbit. **c.** p-Syk, using 1/20,000 of a HRP-conjugated anti-phosphotyrosine 4G10 antibody. PLCγ2, Src and Syk antigens (bottom panel; a-c), loading control were confirmed by re-probing with polyclonal anti-PLCγ2, anti-Src and anti-Syk antibodies, respectively. The relative intensity of tyrosine phosphorelated PLCγ2, Src and Syk was quantified by ImageJ software Version 1.46r. The data shown are a representative blot of similar results for 3 independent experiments.

3.3 Discussion

Maintaining platelet quiescence requires a balance between activation and inhibition signalling events mediated by ITAM and regulated by ITIM-bearing receptor signalling. Healthy arterial endothelium is able to provide powerful inhibitory signalling to platelets via release of bioactive NO and PGI_2. However, upon endothelial damage or disease, where bioactive NO and PGI_2 concentrations are low, collectively platelet ITIM-bearing receptors play an important role as negative regulators [74]. In addition, similar to the immune system a homeostatic balance is required between activation and inhibition and this is provided in platelets through ITAM and ITIM bearing receptor pathways [74]. This stimulates the activation mechanisms to produce pathological thrombus formation. Under these circumstances, it is thought that platelets provide the inhibitory signalling mediated via cell contact events. Platelets contain at least five ITIM-bearing receptors, PECAM-1, CEACAM1, G6B, SIRPα and TREM-like transcript 1 [179, 182, 185, 187, 219, 233]. While individually, these exert moderate inhibition of collagen and thrombin signalling in platelets, collectively they are important to regulate the cell contact signalling events involved in the initiation of platelet-collagen interactions.

The key findings in this study is that CEACAM2 is expressed as the CC2-2L form in platelets (Figure 3-3BC), similar to other cell types such as ventromedial hypothalamus [188] and spermatids [242]. Moreover, CEACAM2 is expressed on the surface and in intracellular pools of resting murine platelets (Figure 3-3A). The current chapter suggests that under resting conditions, surface expression of CEACAM2 in murine platelets is low (Figure 3-3A), but undergoes a marked induction upon agonist stimulation with thrombin, PAR-4 agonist peptide, and CRP (Figure 3-3C). *In vitro* data show that CEACAM2 can negatively regulate the collagen GPVI ITAM-signalling pathway in platelets. Collectively, these findings of the initial characterisation of CEACAM2 in murine platelets and its ability

to negatively regulate platelet-collagen interactions *in vitro* are reminiscent of functions of the other related ITIM-bearing receptor, CEACAM1. These two receptors share similarities in structure and function in many biological systems, particularly in their ability to act as inhibitory co-receptors to modulate ITAM associated signalling pathways.

CEACAM2 restricts platelet-collagen GPVI interactions by disrupting the signalling processes that modulate the adhesion between platelets and collagen. In turn, this restricts pathological thrombus formation when vascular walls are damaged by atherosclerotic plaques, exposing the type-I collagen matrix. Other receptors in the Ig-ITIM superfamily, CEACAM1 and PECAM-1, also inhibit platelet-collagen GPVI interactions and thrombus formation. Under normal physiological conditions, NO and PGI_2 are produced in the vascular endothelium, negatively modulating the process, but their release is restricted when disease or injury occurs [74]. Rather than disrupting the interaction of platelets with the exposed collagen matrix, these mediators disrupt platelet aggregation via an auto-regulatory process. As a result, the normal negative mechanisms inhibiting platelet adhesion at the molecular level must include CEACAM2, CEACAM1 and PECAM-1 [74].

Based upon comparative studies of *Cc1*$^{-/-}$ [187] versus *Cc2*$^{-/-}$ platelets they appear to have similar functions in regulating GPVI dependent alpha and dense granule release (Figure 3-8B and 3-9B) and procoagulant activity of platelets via phosphatidylserine exposure (Figure 3-11A). It is possible that the dominant form of CEACAM1 in human platelets is the CC1-2L/2S [250], which is likely to be the "ortholog" of CEACAM2 in humans. In most tissues, the most dominant form of CEACAM2 is CC2-2S (even in spleen, kidney and testis where CEACAM2 is most highly expressed) [188, 241], except for the hypothalamus, where CC2-2L was cloned. In this case, CC2-4L/4S (with 4 Ig-Domain loops) was not found which is the most dominant form of CEACAM1. In addition, the same scenario in platelets would be expected, where it is likely that CEACAM2 is represented by

CC1-2L in human platelets, and that together with CCl-4L in humans, it exerts a broader range of control of vascular function by increasing the range of ligand binding to CEACAM proteins. Hence, CEACAM proteins may play a critical role in maintaining this function (as compared to PECAM-1 and other cell adhesion molecules in platelets the expression of which remains normal in either *Ceacam1* or *Ceacam2* null mice).

GPVI acts as a major platelet-collagen activating receptor and directly interacts with collagen fibrils, following a triplicate GPO sequence using glycine, proline, and hydroxyproline [136]. Integrin-$\alpha_2\beta_1$ interaction with collagen follows a GFOFER process, utilising glycine, phenylalanine, hydroxyproline, glutamic acid and arginine. Thus, *in vitro* studies used CRP as the GPVI-selective agonist because it contains 10 repeat GPO sequences, activates GPVI-mediated signalling and does not react with integrin-$\alpha_2\beta_1$ [160, 228, 251]. These attributes make it easier to differentiate between GPVI-mediated and integrin $\alpha_2\beta_1$-mediated platelet responses.

In common with members of the Ig-ITIM superfamily, GPVI/FcRγ-chain ITAM-dependent pathway signalling may reach a dynamic equilibrium in the presence of proteins with ITIM motifs. Because previous research suggested that mouse platelets lack low-affinity FcγRIIa, but contain the GPVI/FcRγ-chain ITAM-dependent pathway, we explored the possibility that CEACAM2 is an important inhibitory co-receptor that negatively regulates collagen-GPVI–mediated platelet responses. Essentially, $Cc1^{-/-}$ and $Cc2^{-/-}$ have similar phenotypes in platelet GPVI-collagen interactions. Moreover, CEACAM2 deletion was associated with CRP-stimulated platelets producing hyper-tyrosine phosphorylation of PLC-gamma2, Src and Syk, all components upstream and downstream of GPVI ITAM-associated signalling pathways (Figure 3-12B). This would be consistent with CEACAM2 acting as an ITIM-bearing receptor in platelets to down-modulate ITAM-associated

signalling, similar to CEACAM1 the ITIM-containing tail of which is almost identical to that of CEACAM2.

To compare any potential differences between responses in the wild-type and *Ceacam2*-deficient platelets, we administered a broad range of agonists, including collagen and CRP, across a dose-dependent range. To test the specificity of platelet responses, different agonists stimulated a number of receptor signalling pathways, including G-protein–coupled receptors, using PAR-4 agonist peptide and ADP; calcium ion channels, using CI; and collagen-coupled receptors, using acid soluble collagen and CRP. In the presence of PAR-4 agonist peptide, ADP, and CI, platelets displayed a normal, dose-dependent response. In contrast, $Cc2^{-/-}$ platelets displayed higher aggregation responses over the entire dose range tested with collagen and CRP as agonists (Figure 3-6). This hyper-responsiveness was particularly notable at sub-threshold concentrations, supporting the notion that CEACAM2 negatively regulates collagen-GPVI–mediated ITAM platelet responses. This contrasts with the responses in the presence of PAR-4 agonist peptide, ADP, and CI and further suggests that the $Cc2^{-/-}$ platelet defect is restricted to GPVI-mediated platelet-collagen interactions.

Many previous studies dispute this idea and argue that the GPVI-regulated platelet response merely assists coagulation and that, *in vivo*, a number of alternative platelet responses significantly influence the process [252, 253]. As a result, although there is a consensus that platelets play a major role in the production of thrombin and coagulation in plasma and whole blood, platelets derived from $Cc2^{-/-}$ and $Cc1^{-/-}$ mice display normal procoagulant PS exposure (Figure 3-11). More studies are needed to define the mechanisms and interaction between the different platelet coagulation responses.

The hyper-responsiveness of $Cc2^{-/-}$ platelets also fits the observed phenotypes of PECAM-$1^{-/-}$ *and* $Cc1^{-/-}$ [187, 219, 233]. The peak manifestation of the $Cc1^{-/-}$ phenotype

occurred at lower and higher concentrations of collagen (1.5-4.0 µg/mL; respectively). A similar low dose hyper-responsiveness occurred when CRP was the GPVI-selective agonist. At sub-threshold collagen and CRP concentrations, of 1.5 and 0.625 µg/mL respectively, *Cc1*$^{-/-}$ generated a platelet aggregation response of approximately 60%, unlike the low response of wild-type platelets [187]. At higher concentrations of CRP, 5-10 µg/mL, both wild-type and PECAM-1$^{-/-}$ platelets responded at an equivalent level [219, 233].

Platelets derived from *Cc2*$^{-/-}$ mice displayed enhanced, hyper-responsive adhesion to type I fibrillar collagen. The hyper-response was evident at all time points, and the *Cc2*$^{-/-}$ platelets, when stimulated with GPVI-selective ligands CRP (Figure 3-8B and 3-9B), displayed a lower threshold for alpha and dense granule release than wild-type platelets. This response did not occur if platelets were stimulated with the GPCR agonists, thrombin, and PAR-4 agonist peptide (Figure 3-8A and 3-9A). The results suggest the notion that, without these inhibitory co-receptors, collagen agonists stimulate higher levels of response, especially for collagen-GPVI receptor–mediated signalling. Thus, CEACAM2 negatively regulates interactions between platelets and collagen.

In conclusion, this study demonstrates the presence of a new ITIM-bearing receptor, CEACAM2 (predominantly CC2-2L), in murine platelets that negatively regulates collagen GPVI signalling *in vitro*. Moreover, it shows the importance of CEACAM2 as an inhibitory co-receptor in murine platelets when expressed on the cell surface and within intracellular pools. CEACAM2 is a negative regulator of platelet-collagen interactions, because *Cc2*$^{-/-}$ platelets induced sub-threshold hyper-responses during collagen- and CRP-mediated platelet aggregation; increased adhesion to type I collagen, enhanced alpha and dense granule release and hyper-tyrosine phosphorylation of PLCγ2, Src and Syk by stimulation with GPVI-selective ligand, CRP.

4 Chapter Four: *In vitro* studies of CEACAM2 regulation of CLEC-2 signalling pathway in platelets

4.1 Introduction

Structural determination of CLEC-2 has shown that it is a 32-kDa C-type lectin-like receptor. In platelets, it acts as a receptor for rhodocytin, a venom extracted from the Malayan Pit Viper (*Calloselasma rhodostoma*), and podoplanin (PDPN, also known as gp38 and T1α), a specific marker for lymphatic endothelium [142, 254]. The CLEC-2 signalling process involves the activation of the Src and Syk tyrosine kinases in sequence, which, in turn, activate PLCγ2. This progression is almost identical to the sequential process used by GPVI that is coupled with FcR γ-chain signalling pathway in human platelets [142]. However, there is one notable difference between the two processes: CLEC-2's regulating function for PLCγ2 uses only its single YxxL sequences and does not fully rely upon the adaptor, SLP-76, while GPVI uses both of its YxxL sequences with partial reliance on SLP-76 [142, 156].

It has long been understood that platelet activation follows a signalling pathway involving CLEC-2. This pathway emulates the processes used by collagen receptor GPVI, an ITAM, despite the fact that the CLEC-2 receptor contains only a single YxxL sequence in its cytosolic tail [142, 156]. When point mutations are engineered in the ITAM of the CLEC-2 receptor or one of the pair of Syk SH2 domains, their ability to bind with phosphotyrosine residues is compromised, disrupting CLEC-2 signalling [156]. In addition, research suggests that the specific fusion protein responsible for encoding the tandem Syk SH2 domains is the only one with the ability to cause the precipitation of cellular CLEC-2 from platelet lysates stimulated with rhodocytin [142, 156]. These processes suggest that the CLEC-2 YxxL sequence and tandem SH2 domains are an essential component of the CLEC-2 signalling process.

In murine platelets, there are two hemi ITAM associated signalling pathways including collagen GPVI/FcR γ-chain and CLEC-2. The snake venom protein rhodocytin is

a CLEC-2 ligand, which plays a crucial role in CLEC-2 clustering and platelet activation [255]. CLEC-2 receptor induces activation-dependent signalling through a process similar to the GPVI-FcR γ chain pathway. However, CLEC-2 signalling relies more on Syk rather than Src tyrosine kinases and PLCγ2-dependent mechanism of platelet activation [142, 255].

Previous studies have highlighted that homophilic binding in *trans* of Ig-ITIM superfamily members, PECAM-1 and CEACAM1 negatively regulates platelet-collagen interactions and modulates thrombus growth and stability *in vivo* [178, 187]. However, it is unknown if the Ig-ITIM superfamily member, CEACAM2 modulates CLEC-2-mediated platelet activation in a similar manner to collagen GPVI. Other mechanisms have been proposed where ligands are secreted (Gas6) or shed (Semaphorin 4D) from platelets during activation to act as bioactive molecules in the platelet gap [256]. Studies of the interaction of the platelet receptor CD72, with its ligand, Semaphorin 4D show that this receptor does not negatively regulate GPVI-dependent platelet responses [210]. While CD72 constitutively associates with SHP-1, this phosphatase dissociates from the receptor upon platelet activation to negatively regulate GPVI-dependent platelet responses [210]. This is in contrast to PECAM-1 where SHP-2 recruitment occurs upon induction of tyrosine phosphorylation of PECAM-1 that requires platelet activation and/or aggregation events followed by dephosphorylation of ITAM-signalling elements [215]. In immunological systems, SHP-1 PTP is classified as a negative regulator, while in collagen GPVI platelet responses it has been proposed to act as a positive regulator but this is controversial [245]. Given this controversy, it will be informative to test the role of CEACAM2 that preferentially recruits SHP-1 in murine platelets using a novel mouse model of CEACAM2 knockout platelets. In addition, unlike CEACAM1, CEACAM2 is a heterophilic binding receptor that may have differing roles in regulating platelet activation. Furthermore, as

CEACAM2 is expressed as the CC2-2L isoform in platelets and CEACAM1 is predominantly CC1-4L isoform, they may have different vascular functions.

The key issue to be addressed is: 1) Does CEACAM2 positively or negatively attenuate CLEC-2-mediated platelet responses?.

4.2 Results

4.2.1 *Cc2*$^{-/-}$ platelets are hyper-responsive to the CLEC-2 selective agonist, rhodocytin

In order to test that CEACAM2 normally functions to attenuate CLEC-2-mediated platelet activation, a comparison of the ability of platelets derived from wild-type and *Cc2*$^{-/-}$ mice in platelet aggregation responses over a dose-dependent range of the snake venom protein, rhodocytin (0.12-0.48 µg/mL) was undertaken. This was compared with the aggregation responses to the GPVI selective agonist, collagen-related peptide, CRP (0.625-2.5 µg/mL); the G-protein coupled agonists, PAR-4 agonist peptide (125-500 µM) and ADP (2.5-10 µM); and calcium ionophore (1.25-5 µg/mL). Platelet aggregation was determined using PRP at $100x10^9$/L containing 1 mM $CaCl_2$ and 100 µg/mL fibrinogen. PRP was stimulated using the CLEC-2 selective agonist, rhodocytin at 0.12-0.48 µg/mL (Figure 4.1A-B). As described previously in Chapter 3, comparable platelet aggregation were observed in both wild-type versus *Cc2*$^{-/-}$ platelets upon GPCRs agonists thrombin, PAR-4 agonist peptide, ADP and calcium ion channel agonist, CI-A23187 (Figure 3-3A-B). However, platelet aggregation profiles were increased in *Cc2*$^{-/-}$ platelets upon stimulation with the CLEC-2 selective agonist, rhodocytin compared to wild-type platelets. This data is similar that was obtained with GPVI agonists, type I collagen and CRP (Figure 3-4A-B). Therefore, this data suggests that absence of CEACAM2 leads to hyper-responsive GPVI- and CLEC-2-mediated platelet aggregation.

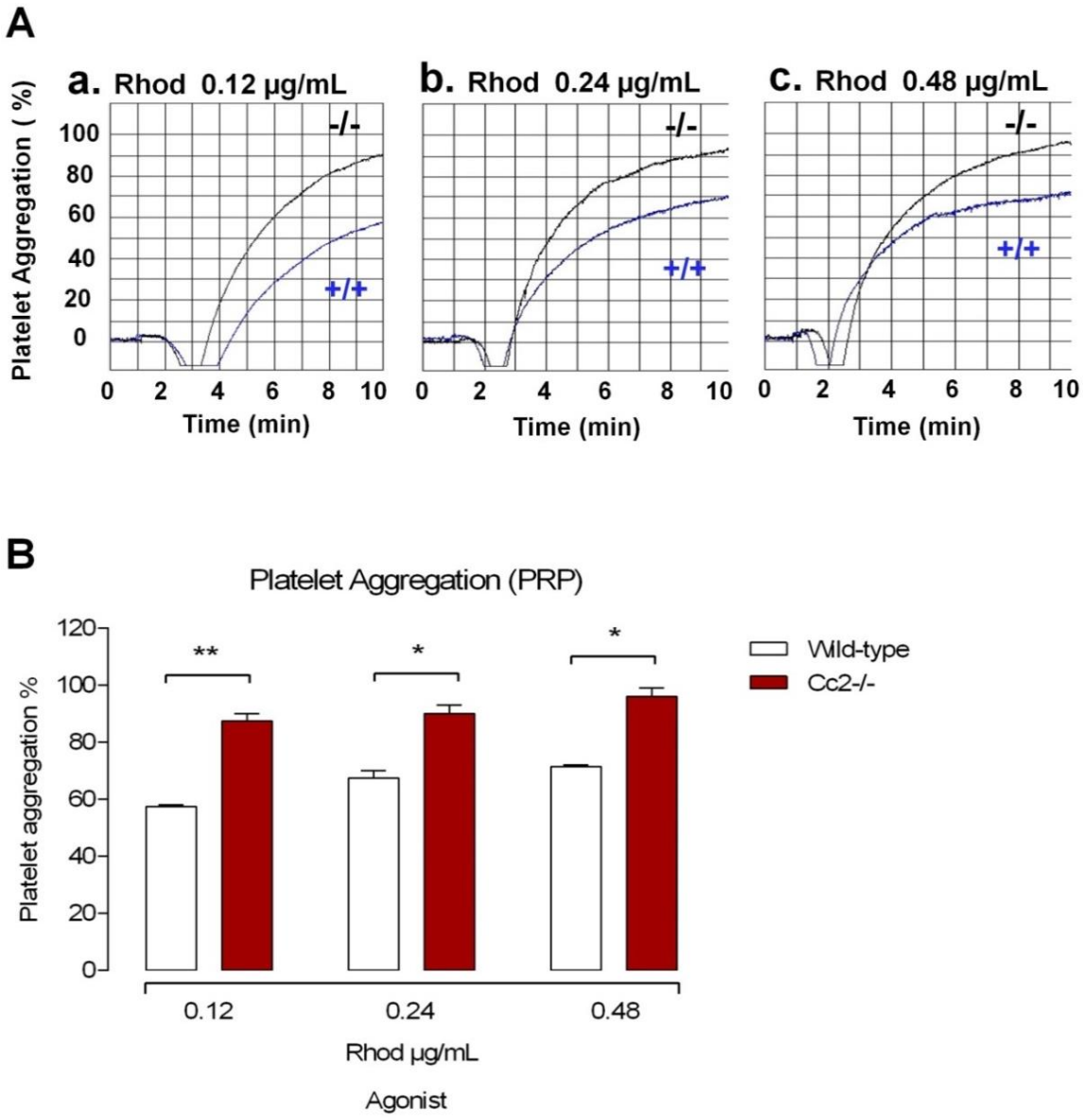

Figure 4-1: *Cc2*$^{-/-}$ platelets show hyper-responsive aggregation to stimulation with the CLEC-2 selective agonist, rhodocytin (Rhod). (A-B) Platelet aggregation responses (PRP; 100x10^9/L) for wild-type (+/+) and *Cc2*$^{-/-}$ mice were determined. PRP was stimulated with rhodocytin (Rhod; 0.12-0.48 µg/mL). *Cc2*$^{-/-}$ platelets are hyper-responsive to stimulation with CLEC-2-selective agonist, rhodocytin compared to wild-type platelets. These data are representative of at least four independent experiments performed (**P*<0.05 and ***P*<0.01; n=4).

4.2.2 *Cc2*$^{-/-}$ platelets are hyper-responsive in alpha and dense granule secretion following rhodocytin stimulation

As hyper-responsive CLEC-2-mediated platelet aggregation responses were observed in *Cc2*$^{-/-}$ platelets, the second phase is to examine whether the presence or absence of CEACAM2 affected platelet granule release. In order to examine the influence on alpha and dense granule platelet release reaction of wild-type versus *Cc2*$^{-/-}$ platelets, washed platelets ($100x10^9$/L) were stimulated with rhodocytin (0.4-1.2 µg/mL) and the secretion of alpha and dense granules was determined. *Cc2*$^{-/-}$ platelets displayed a significant increase in both P-selectin exposure (alpha granules) and dense granule release (quinacrine) compared to wild-type platelets (Figure 4-2 and 4-3). We have previously examined the influence of *Cc2*$^{-/-}$ on alpha and dense granule platelet release reaction using the G-protein coupled agonists, thrombin (0.1-0.2 U/mL) and PAR-4 agonist peptide (100-300 µM) along with the tyrosine kinase-dependent GPVI-selective agonist, CRP (0.5-2.5 µg/mL) as shown in chapter 3 (Figure 3-6 and 3-7). Therefore, *Cc2*$^{-/-}$ platelets release comparable alpha and dense granules upon GPCR agonist stimulation, but an increase in response to the tyrosine kinase dependent GPVI and CLEC-2 receptor stimulation. Therefore, these studies support the hypothesis that CEACAM2 negatively attenuates hemi (ITAM associated) CLEC-2-mediated responses in murine platelets.

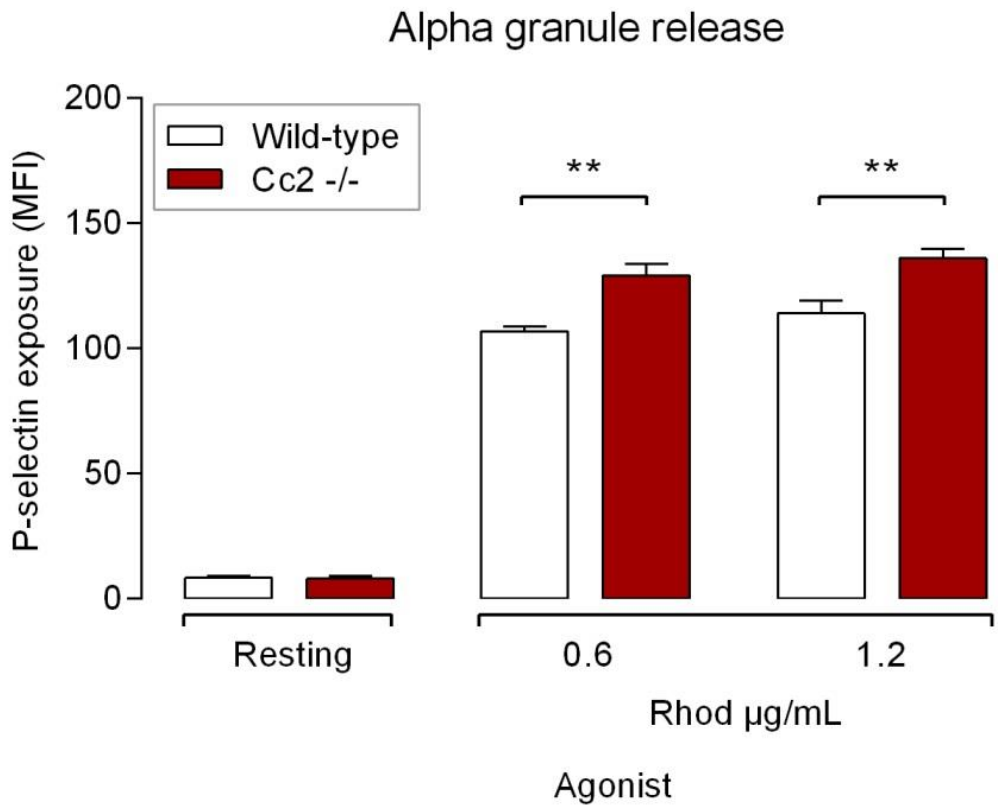

Figure 4-2: *Cc2*$^{-/-}$ platelets showed increased alpha granule release upon CLEC-2 selective agonist, rhodocytin stimulation. P-selectin exposure of wild-type and *Cc2*$^{-/-}$ washed platelets ($100x10^9$/L) was determined following stimulation with CLEC-2 selective agonist, rhodocytin (0.6-1.2 µg/mL). Platelets were stained with either control or FITC-conjugated CD62P mAb for both wild-type and *Cc2*$^{-/-}$ platelets. Samples were analysed on a FACS Canto II flow cytometer. Data are representative of four independent experiments (**P<0.01 n=4).

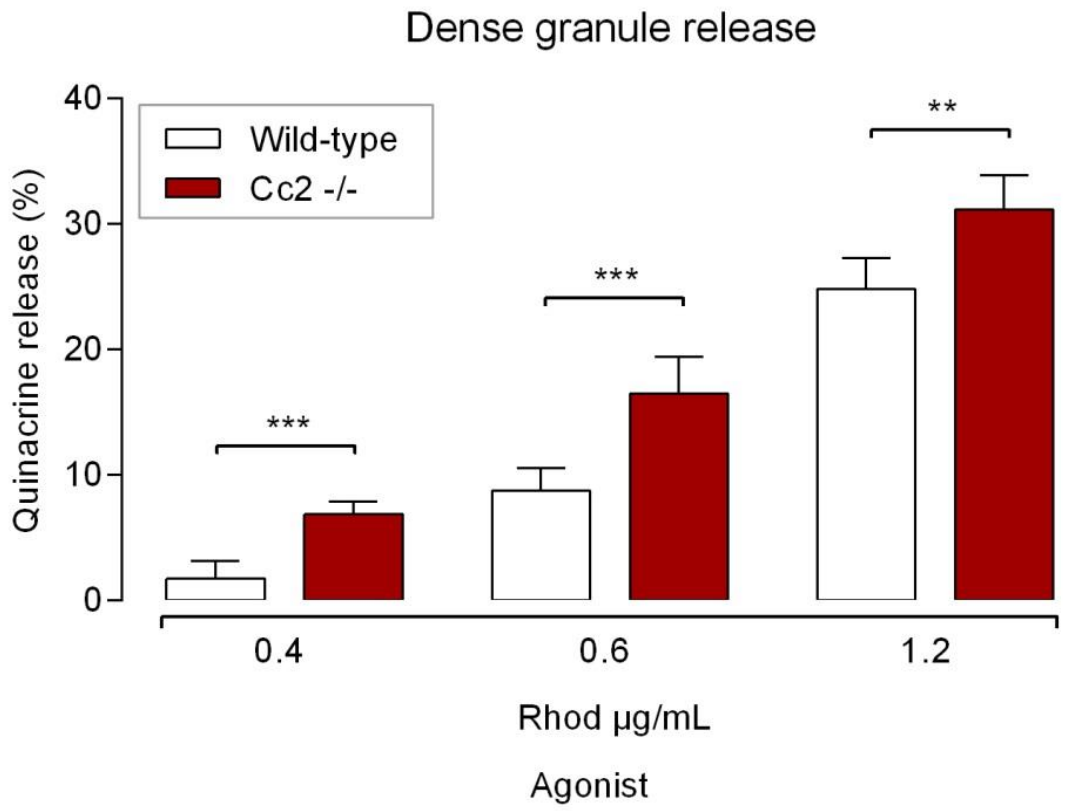

Figure 4-3: *Cc2*$^{-/-}$ platelets display more dense granule release upon CLEC-2 selective agonist, rhodocytin stimulation. Quinacrine as dense granule release fluorescent marker was measured by flow cytometry. Wild-type and *Cc2*$^{-/-}$ washed platelets ($100x10^9$/L) were stimulated with rhodocytin at 0.4-1.2 µg/mL. Samples were analysed on a FACS Canto II flow cytometer. Data are representative of four independent experiments (***P*<0.01 and ****P*<0.001; n=4).

4.2.3 *Cc1*$^{-/-}$ platelets are hyper-responsive in alpha and dense granule secretion following rhodocytin stimulation

Next, to determine if CEACAM1 similarly to CEACAM2 can attenuate hemi (ITAM associated) CLEC-2-mediated responses in murine platelets, alpha and dense granules platelet secretion was examined. Furthermore, to examine the cross-talk between CEACAM1 and rhodocytin and compare it with CEACAM2 data, washed platelets were derived from wild-type and *Cc1*$^{-/-}$ mice ($100x10^9$/L) followed by CLEC-2-selective agonist, rhodocytin stimulation (0.4-1.2 µg/mL). The alpha and dense granule release upon rhodocytin stimulation was determined for both wild-type and *Cc1*$^{-/-}$ platelets. *Cc1*$^{-/-}$ platelets exhibited higher levels of alpha (P-selectin) and dense granule (Quinacrine) release at all doses compared to wild-type platelets (Figure 4-4 and 4-5). These results are comparable with *Cc2*$^{-/-}$ platelets upon stimulation with rhodocytin and support the idea that CEACAM2 could negatively regulate hemi (ITAM-mediated) CLEC-2 signalling pathways in platelets.

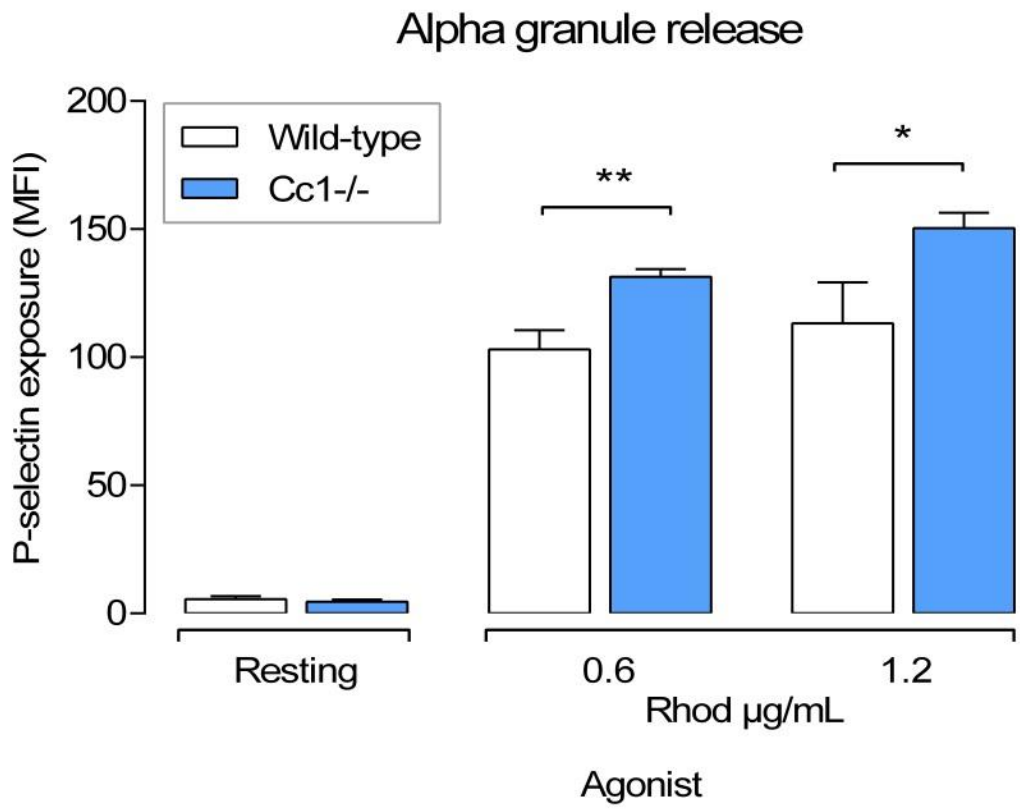

Figure 4-4: *Cc1*$^{-/-}$ platelets show increased alpha granule release upon CLEC-2 selective agonist, rhodocytin stimulation. P-selectin exposure of wild-type and *Cc1*$^{-/-}$ washed platelets ($100x10^9$/L) was determined following stimulation with CLEC-2 selective agonist, rhodocytin (0.6-1.2 µg/mL). Platelets were stained with either control or FITC-conjugated CD62P mAb for both wild-type and *Cc1*$^{-/-}$ platelets. Samples were analysed on a FACS Canto II flow cytometer. Data are representative of four independent experiments (**P*<0.05 and ***P*<0.01; n=4).

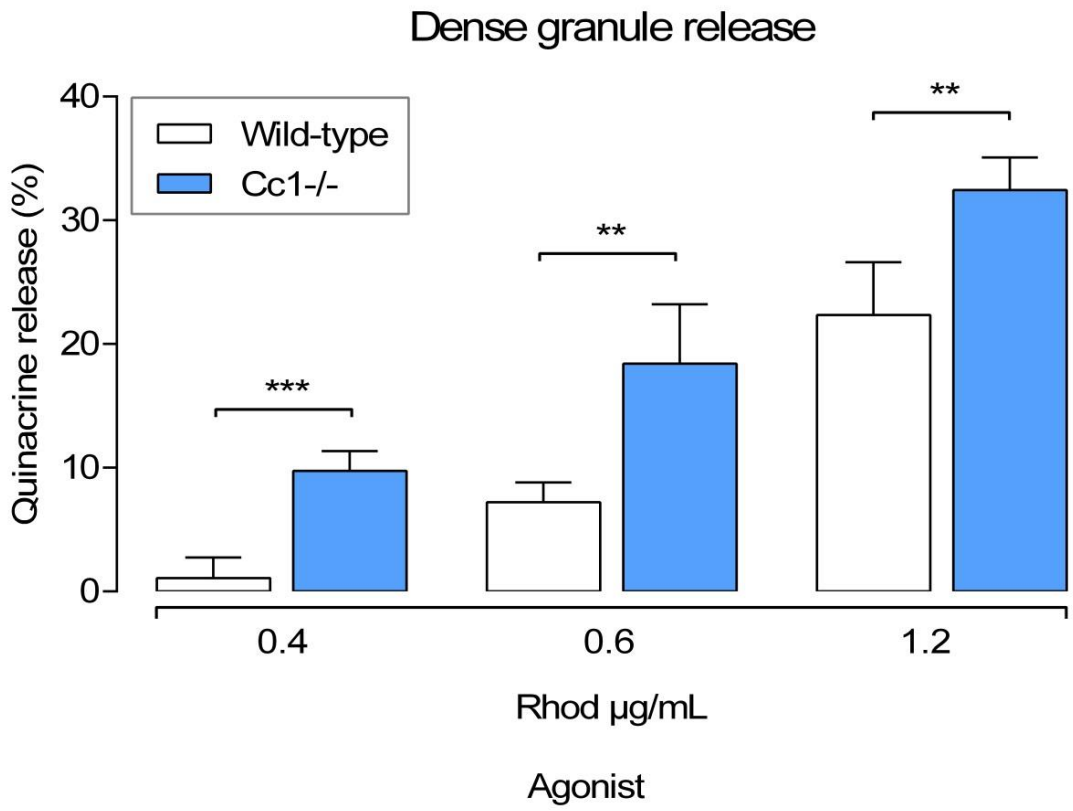

Figure 4-5: *Cc1*$^{-/-}$ platelets display enhanced dense granule release upon CLEC-2 selective agonist, rhodocytin stimulation. Quinacrine as fluorescent marker of dense granule release was measured by flow cytometry. Wild-type and *Cc1*$^{-/-}$ washed platelets (100x10^9/L) were stimulated with rhodocytin at 0.4 and 1.2 µg/mL. Samples were analysed on a FACS Canto II flow cytometer. Data are representative of four independent experiments (***P*<0.01 and ****P*<0.001; n=4).

4.2.4 Tyrosine phosphorylation in *Cc2*$^{-/-}$ platelets upon CLEC-2 selective agonist, rhodocytin stimulation

As CEACAM2 has an identical ITIM to CEACAM1, we would predict similar features including SHP-1 recruitment [244]. To examine the influence on tyrosine phosphorylation and key substrates in ITAM-coupled signalling pathways, platelets derived from wild-type and *Cc2*$^{-/-}$ mice were stimulated with rhodocytin (1.2 µg/mL) at T=0 and at T=90 seconds. The tyrosine phosphorylation profiles of immunoprecipitated ITAM-coupled signalling elements, PLCγ2, Syk and Src of wild-type and *Cc2*$^{-/-}$ platelets were determined using anti-phosphotyrosine antibody. As shown in Figure 4-6, rhodocytin-stimulated, *Cc2*$^{-/-}$ platelets showed a 3.5-fold increase in PLCγ2 tyrosine phosphorylation (0.4063±0.014 vs 0.1093±0.034; $^{**}P<0.01$; n=3; Figure 4-6), in the presence of equivalent PLCγ2 antigen (bottom panel) compared to wild-type platelets. Moreover, *Cc2*$^{-/-}$ platelets displayed a 3-fold increase in Syk tyrosine phosphorylation upon rhodocytin activation (0.4050±0.060 vs 0.1508±0.029; $^{**}P<0.01$; n=3; Figure 4-7), in the presence of equivalent Syk antigen compared to wild-type platelets. However, *Cc2*$^{-/-}$ platelets showed similar Src tyrosine phosphorylation compared to wild-type platelets, in the presence of equivalent Src antigen (0.276±0.087 vs 0.258±0.077; $P>0.05$ n=3; Figure 4-8). These data suggest that platelet CEACAM2 plays a role in attenuating tyrosine phosphorylation of key elements, PLCγ2 and Syk, but not Src in CLEC-2 ITAM-coupled signalling pathway.

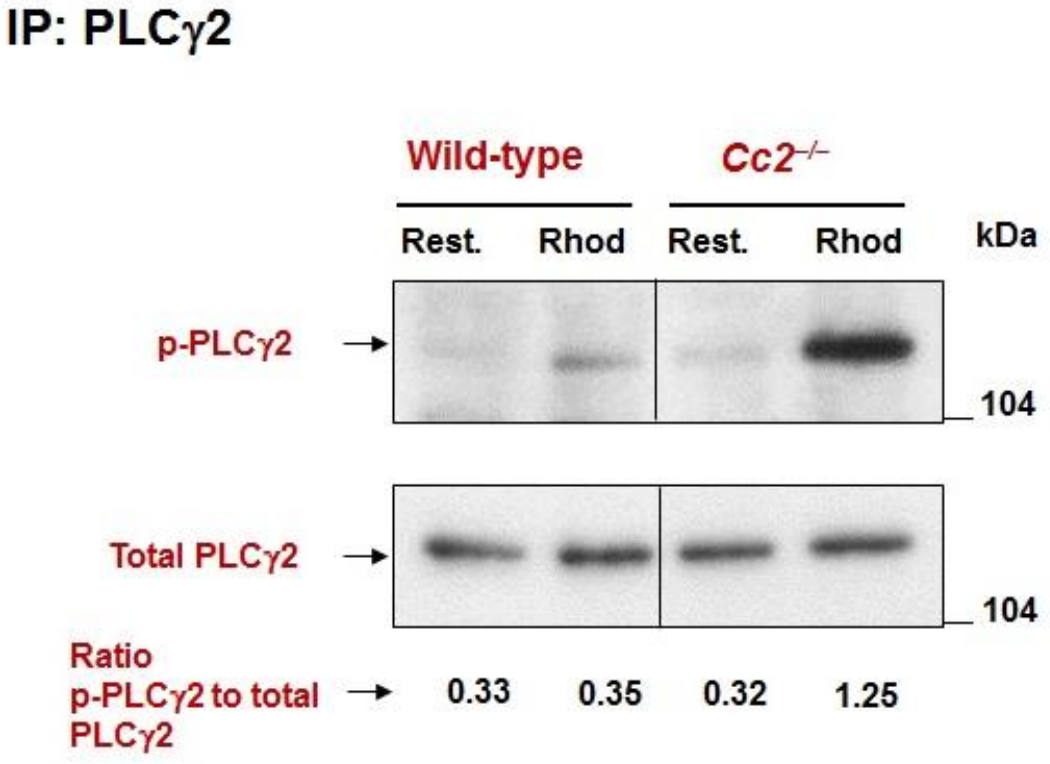

Figure 4-6: *Cc2*$^{-/-}$ platelets display hyper tyrosine phosphorylation of PLCγ2 upon CLEC-2 selective agonist, rhodocytin stimulation. Washed platelets (300x10^9/L) were isolated from wild-type and *Cc2*$^{-/-}$ mice, and then immunoprecipitation of PLCγ2 was performed from platelet lysates at resting versus activation with 1.2 µg/mL of rhodocytin for 90 seconds at 37^{o}C. Immunoblotting was performed to detect phospho-PLCγ2 using 1/20,000 of a HRP-conjugated anti-phosphotyrosine 4G10 antibody. Equivalence of loading control (PLCγ2 antigen; bottom panel) was confirmed by re-probing with a polyclonal anti-PLCγ2 (1/5000), followed by HRP-anti-rabbit at 1/20,000 antibodies. The relative intensity of tyrosine phospho-PLCγ2 was determined using ImageJ software Version 1.46r. The data shown are a representative blot of similar results for 3 independent experiments.

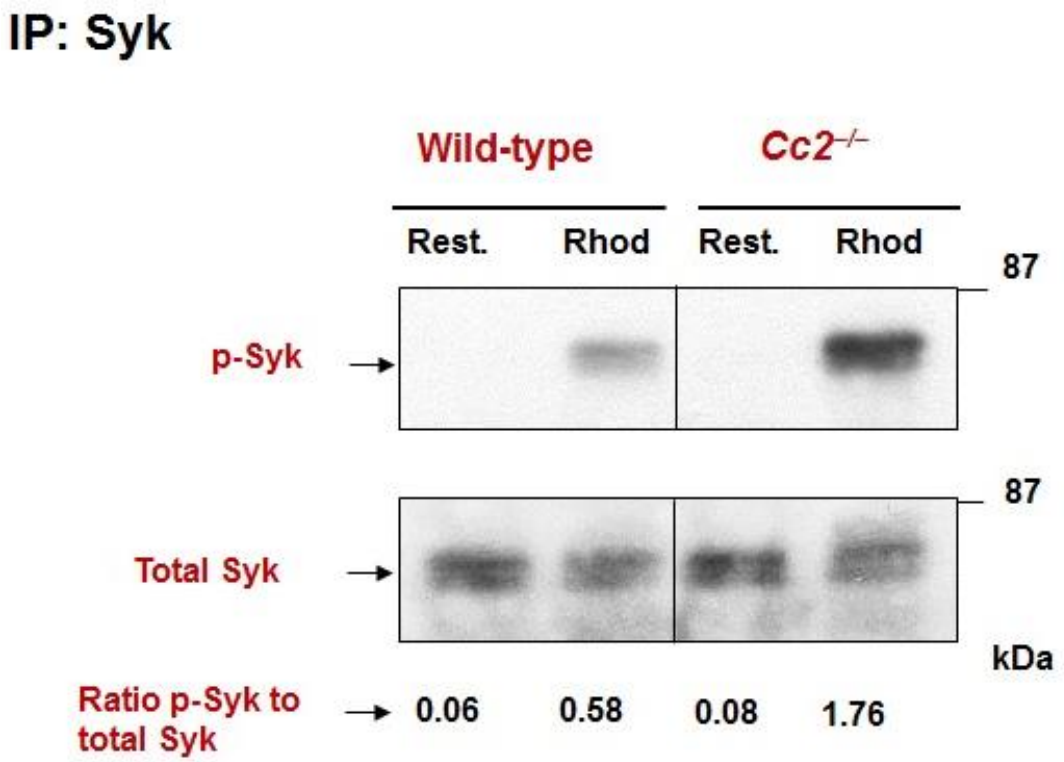

Figure 4-7: *Cc2*$^{-/-}$ platelets display hyper tyrosine phosphorylation of Syk upon CLEC-2 selective agonist, rhodocytin stimulation. Washed platelets (300x10^9/L) were isolated from wild-type and *Cc2*$^{-/-}$ mice, and then immunoprecipitation of Syk was performed from platelet lysates at resting versus activation with 1.2 µg/mL of rhodocytin for 90 seconds at 37^{o}C. Immunoblotting was performed to detect phospho-Syk using 1/20,000 of a HRP-conjugated anti-phosphotyrosine 4G10 antibody. Syk antigen (bottom panel), equivalence of loading control was confirmed by re-probing with a polyclonal anti-Syk (1/2000) antibody, followed by HRP-anti-rabbit at 1/20,000 antibody. The relative intensity of tyrosine phospho-Syk was determined using ImageJ software Version 1.46r. The data shown are a representative blot of similar results for 3 independent experiments.

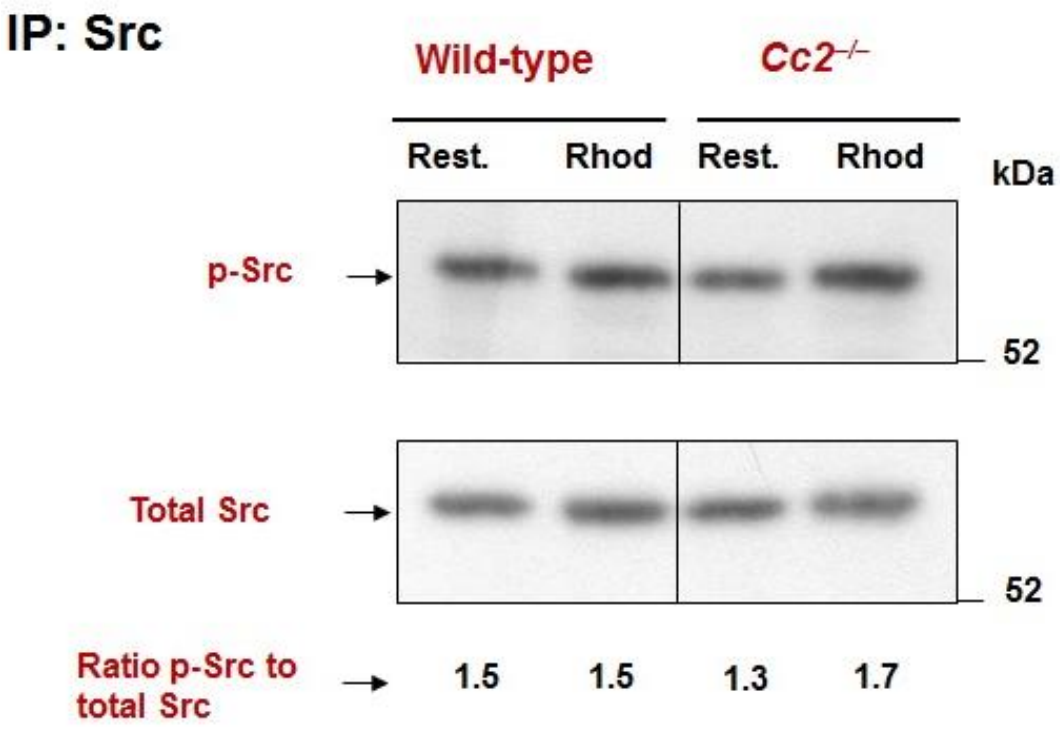

Figure 4-8: *Cc2*$^{-/-}$ platelets displays similar tyrosine phosphorylation of Src upon CLEC-2 selective agonist, rhodocytin stimulation. Washed platelets (300x10^9/L) were isolated from wild-type and *Cc2*$^{-/-}$ mice, and then immunoprecipitation of Src was performed from platelet lysates at resting versus activation with 1.2 µg/mL of rhodocytin for 90 seconds at 37^{o}C. Immunoblotting was performed to detect phospho-Src using 1/2000 of anti-phospho Src followed by 1/20,000 of anti-rabbit antibodies. Equivalence of loading control (Src antigen; bottom panel) was confirmed by re-probing with a polyclonal anti-Src (1/2000) antibody, followed by HRP-anti-rabbit at 1/20,000 antibody. The relative intensity of tyrosine phospho-Src was determined using ImageJ software Version 1.46r. The data shown are a representative blot of similar results for 3 independent experiments.

4.3 Discussion

This chapter aimed to investigate the main hypothesis that CEACAM2 could regulate CLEC-2-mediated signalling pathway in murine platelets. In the absence of CEACAM2, rhodocytin mediated platelet aggregation (Figure 4-1), together with alpha granule release and dense granule release (Figure 4-2 and 4-3; respectively) were enhanced suggesting that when present CEACAM2 negatively regulate CLEC-2 ITAM-mediated signalling pathway in murine platelets. This is also supported by examination of downstream CLEC-2 ITAM-mediated signalling components in the absence of CEACAM2 where phospho-Syk and phospho-PLC-gamma 2 but not phospho-Src were hyper-tyrosine phosphorylated following rhodocytin stimulation compared to wild-type murine platelets (Figure 4-6, 4-7 and 4-8; respectively). Similarly, deletion of CEACAM1 resulted in enhanced rhodocytin-mediated alpha and dense granule release compared to wild-type (Figure 4-4 and 4-5; respectively).

To my knowledge there is no report in the literature that indicates that Ig-ITIM superfamily members negatively regulate hemi-ITAM CLEC-2 mediated signalling pathway in murine platelets. This study provides the first report of CEACAM1 and CEACAM2 serving to negatively regulate hemi-ITAM associated CLEC-2 signalling pathway in murine platelets. This is also likely to be the case in human platelets. Further studies will be required to address this issue.

Often found operating in tandem, with a separation of between 15 and 30 amino acid residues, ITIM contains the consensus sequence (L/I/V/S)xYxx(L/V). Upon tyrosine phosphorylated, ITIMs recruit SH2-domain containing protein-tyrosine phosphatases, including SHP-1 and SHP-2. This has the effect of inhibiting ITAM-receptor-mediated signalling components. ITIM bearing receptors containing an ITIMs and an ITSMs can create activation signals, and also restrict activation signals regulated by GPCR [257]. At least five ITIM-containing receptors of the immunoglobulin superfamily occur in platelets:

PECAM-1, CEACAM1, G6B-b, a triggering receptor expressed on myeloid cell (TREM)-like transcript-1 and SIRPα [179, 187, 258, 259]. Previous studies have suggested that PECAM-1 and CEACAM1 negatively regulate GPVI signalling in murine platelets [178, 187, 219, 235]. Likewise, cell line modelling using a nuclear factor of activated T-cells (NFAT) transcriptional reporter assay showed Syk and Src inhibition by G6B-b and this resulted in both GPVI-FcR gamma-chain and CLEC-2 signalling pathways inhibition [180].

Previous studies by May et al. indicated that antibody-mediated depletion of CLEC-2 from mouse platelets resulted in normal platelet adhesion under flow. However, *in vitro* and *in vivo* thrombus formation was severely impaired [260]. In contract, other workers did not confirm this finding [261] and suggested that the genetic background of the mice used may be a predetermining factor. The results of May et al. raised the possibility of CLEC-2 playing an important role in thrombus formation and stabilisation. As the CLEC-2 knockout mouse was embryonically lethal, it would be difficult to create a double knockout of CLEC-2 and CEACAM2 [262]. However, for future studies, it would be informative to study the synergy between CEACAM2 knockout compared to wild-type mice with and without anti-CLEC-2 mediated depletion in thrombus formation and stabilisation.

In conclusion, if CLEC-2 proves to be important in thrombus formation and stabilisation, its functional relationship with CEACAM2 could provide a novel target for antiplatelet drug therapies to impair pathological thrombus formation.

5 Chapter five: *In vivo* studies of CEACAM2 negative regulation of platelet-collagen interactions and thrombus formation

5.1 Introduction

Platelet thrombus formation during normal physiological functioning occurs when the sub-endothelial matrix component of type I collagen is exposed, facilitating platelet adhesion. Matrix exposure can arise from physical trauma, cardiovascular disease, and atherosclerotic plaque formation. The '2-site, 2-step' model framework describes the processes guiding the complex platelet-collagen interactions. This model assumes that the high affinity receptor, integrin-$\alpha_2\beta_1$, controls the initial collagen engagement, and GPVI, a low-affinity collagen receptor, activates the interaction [263, 264]. The model proposes a secondary function for integrin-$\alpha_2\beta_1$, of facilitating the process rather than acting as the primary adhesive collagen receptor.

There are several mechanisms associated with regulation of platelet thrombus growth and stability *in vivo*. These include the role of thrombin, fibrin and Ig ITIM superfamily members linked to Src-domain containing protein tyrosine phosphatases such as SHP-2. Thrombin and fibrin exert their effects in the potentiation of the coagulation cascade and platelet activation. In contrast, Ig ITIM bearing receptors exert their effect through regulation of the initial adhesion and signalling events where their presence would limit the surface coverage of platelets to reduce thrombus formation *in vivo*.

Platelet- and coagulation-activating factors can induce the formation of thrombi. For platelets, collagen found in the extracellular matrix and vascular layers is a major factor, and exposure through injury initiates platelet activation and provides a surface for vWF mediated adhesion [137]. The main factor prompting coagulation is the tissue factor exposed by damage to vascular walls [252]. The arterial and venous systems display different modes of thrombosis: arterial thrombus formation is largely induced by platelet aggregation through collagen and vWF adhesion, while venous thrombosis is mainly initiated by tissue factor instigated coagulation.

An important Ig-ITIM immunoreceptor, GPVI, clusters with the FcRγ-chain on the platelet membrane to form the GPVI/FcRγ complex. FcRγ also has the ability to interact with other receptors expressed on the surface, such as GPIb [3]. Ligation in the presence of collagen or related ligands activates this platelet-specific receptor and initiates a sequential process involving the tyrosine phosphorylation of a number of signalling molecules [230, 265]. This process involves predominantly two protein tyrosine kinases belonging to the Src family, Fyn and Lyn, where the FcRγ-chain undergoes tyrosine phosphorylation. At the next stage of the immunoreceptor signalling pathway, the GPVI-FcRγ-chain-complex activates Syk, a tyrosine kinase, which activates a number of downstream signalling proteins, including the adaptor or 'scaffolding' proteins, LAT and SLP-76; and Vav, a guanine nucleotide exchange factor (GEF) regulation G-protein [266]. In the same way, phosphoinositide 3-kinase (Pi3K), a protein kinase, activates the Btk/Tec subfamily, which stimulates a downstream target, PLCγ2, a phospholipase enzyme. Other downstream protein kinases activated as part of the GPVI-activated signalling chain include protein kinase C (PKC), Erk-1/2, and focal adhesion kinase (FAK). This signalling event chain induces integrin activation in platelets, prompting a number of changes that facilitate a response to vascular injury. Integrin activation causes an increase in intracellular free Ca^{2+} levels, stimulating increased platelet aggregation, cytoskeletal reorganisation, and granular secretion, ultimately leading to coagulation. In conclusion, GPVI is the main activating agent for the eventual procoagulant activity of platelets exposed to collagen, both *in vitro* and *in vivo* [69], but the exact nature and role of the downstream signalling molecules are not fully understood.

A number of *in vivo* studies on mice support the hypothesis that GPVI may be the central receptor during platelet aggregation and thrombus formation in the arterial system. Evidence includes recent *in vivo* studies with mice, where platelet aggregation was assayed following the exposure of vascular collagen through arterial ligation [137, 267]. For FcR γ-

chain deficient mice with no GPVI, or where JAQ1 antibody treatment down-regulated GPVI, *in vivo* platelet aggregation process was restricted. Previous *in vitro* studies have suggested that GPVI is a powerful procoagulant agent that is a central receptor for thrombus formation *in vivo*.

Previous research suggests that the interaction between collagen and GPVI occurs at two separate sites [268]. Platelet activation by GPO-rich peptide CRP is severely inhibited by JAQ1, thus it is possible to propose that the antibody binds to the CRP site on the receptor, and that this is the main site for collagen binding. As JAQ1 inhibition is reduced at higher concentrations of collagen, there may also be a secondary site for interaction between GPVI and collagen. By cross-relating this finding with the observation that platelets deficient in FcRγ do not interact with collagen, due to absence of GPVI from the platelet surface. Previous *in vivo* studies found that platelets lacking GPVI following JAQ1 treatment do not respond to collagen. It is possible that there may be binding to an alternate GPVI site [267]. It is also possible that there is only a single collagen binding site on GPVI, with JAQ1's inhibiting action moderated by an allosteric effect that lowers GPVI's affinity for collagen and CRP. This would produce exactly the same effect as reducing the number of GPVI receptors expressed on the surface of platelets, an effect noted to be greater for CRP/GPVI interactions than collagen/GPVI interactions [269].

A multi-faceted approach revealed a previously unknown function of CEACAM2, as an inhibitory co-receptor found on the surface and in intracellular pools of murine platelets. CEACAM2 is a novel platelet immunoreceptor that shown negatively regulates collagen-GPVI-mediated platelet responses, and regulates type I collagen-mediated platelet *in vitro* (Chapter 3). Therefore, the potential involvement of CEACAM2 in regulating platelet-collagen interactions and platelet thrombus formation and growth under *in vitro* flow conditions and *in vivo* is unknown. The aim of this chapter was therefore to examine the

contribution of CEACAM2 role in contact-dependent platelet adhesion under *in vitro* flow conditions and *in vivo* platelet thrombus formation.

5.2 Results

5.2.1 CEACAM2 regulation of platelet thrombus formation is dependent on platelet–collagen interactions under arterial flow *in vitro*

As *Cc2*$^{-/-}$ platelets displayed strong adhesion on immobilised type I collagen (Figure 2-8), *in vitro* flow studies were performed to determine the functional role of CEACAM2 in modulating platelet thrombus formation. Rhodamine-labelled whole blood from both wild-type and *Cc2*$^{-/-}$ mice was perfused onto immobilised type I fibrillar collagen at arterial shear rate of 1800 seconds^{-1}. Six minutes of blood perfusion was monitored, thrombi images were recorded in real-time for wild-type and *Cc2*$^{-/-}$ platelets (Figure 5-1A). Z-stacks were deconvolved and thrombus parameters of thrombus area, height and volume were determined. *Cc2*$^{-/-}$ platelets exhibited a significant increase in thrombus area compared to wild-type platelets (2303±470.6 vs 907.2±87.26 µm^2; ***P<0.001; n=10; Figure 5-1B; at 4 minutes). Similarly, *Cc2*$^{-/-}$ platelets showed increased kinetics of thrombus volume over time compared to wild-type platelets (30480±3822 vs 12480±588.2 µm^3; ***P<0.001; n=10; at 4 minutes; Figure 5-1C). As *Cc2*$^{-/-}$ females are obese and insulin resistant [188] and *Cc2*$^{-/-}$ males are lean and insulin sensitive [241] and platelet activation is associated with diabetes, we sex-stratified the *in vitro* thrombus formation to investigate a potential sexual dimorphic effect. Based upon sex stratified data, *Cc2*$^{-/-}$ platelets showed increased thrombus volume to a similar extent in both male and female mice compared to wild-type platelets (*P<0.05; Figure 5-1D). Collectively, platelet adhesion onto immobilised type I collagen under arterial flow demonstrated that CEACAM2 is important in regulating platelet thrombus formation *in vitro* under flow on type I collagen.

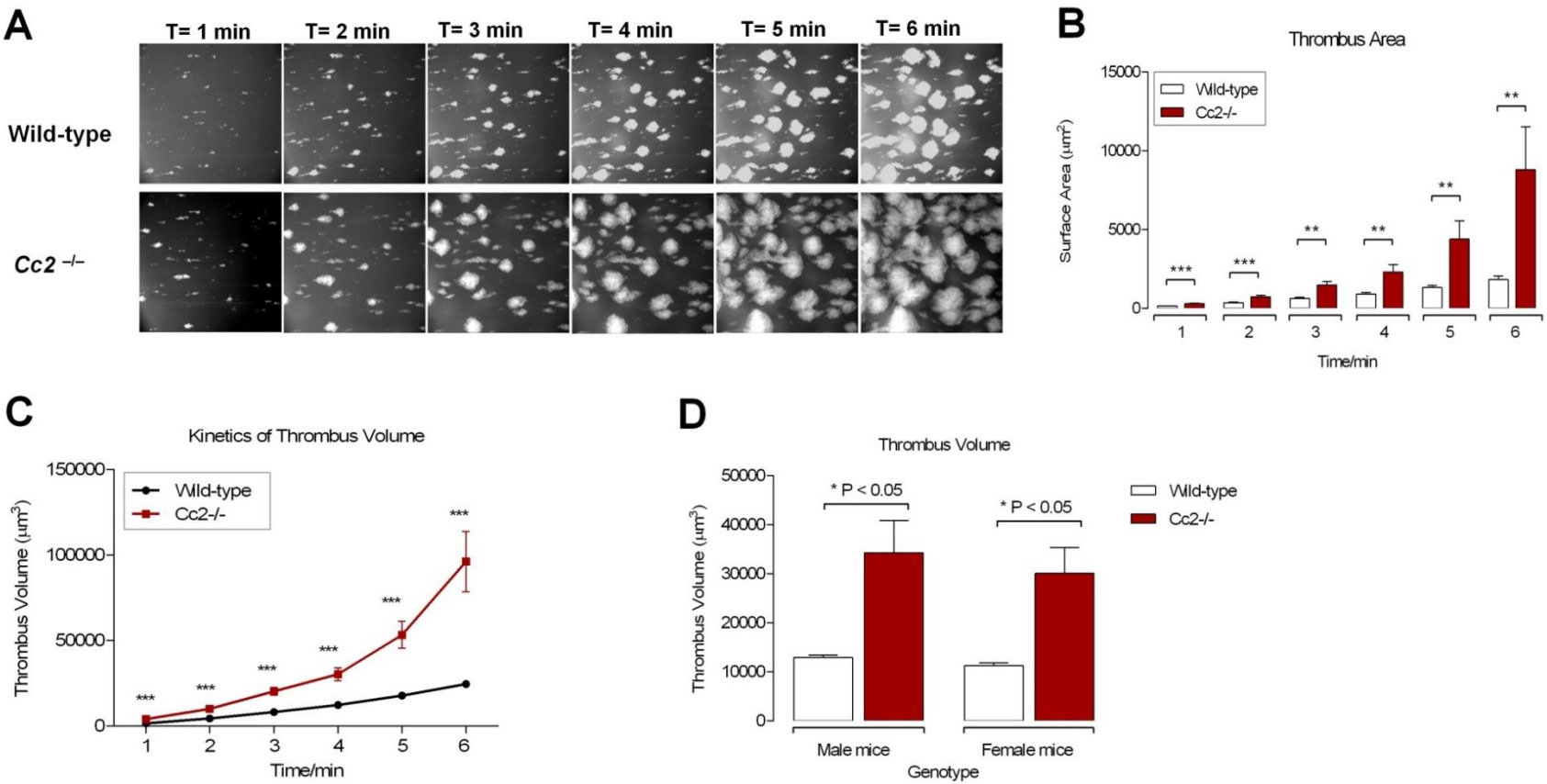

Figure 5-1: *Cc2*$^{-/-}$ platelets display greater adhesion and thrombus formation under arterial flow on immobilised type I collagen. (A-D) Rhodamine-labelled whole blood of wild-type and *Cc2*$^{-/-}$ mice was perfused over 500 µg/mL type I fibrillar collagen-coated µ-slide III$^{0.1}$ at a shear wall flow rate of 1800 seconds^{-1}. Z-stack images were recorded over 6 minutes with a Zeiss Axiovert microscope captured with Axiocam MRm camera and analysed using Zeiss Axiovision Rel4.6 software. Thrombi formed were analysed by deconvolution and 3D reconstructions. **(A)** Images of *in vitro* thrombus formation under arterial flow on immobilised type I fibrillar collagen for both wild-type and *Cc2*$^{-/-}$ platelets over 6 minutes. **(B)** Thrombus area (µm^2) over time was calculated based on surface area measurement of thrombi. **(C)** Kinetics of thrombus volume (µm^3) over time was derived by multiplying thrombus area (µm^2) with thrombus height (µm) for both wild-type and *Cc2*$^{-/-}$ (■) platelets (30480±3822 vs 12480±588.2 µm^3; ***P<0.001; at 4 minutes; n=10). **(D)** Thrombus volume (µm^3) data from panel C was stratified according to sex, male and female for both wild-type and *Cc2*$^{-/-}$ platelets at the 4 minutes time point (*P<0.05; n=5/group). These data are representative of at least ten independent experiments performed and results represent mean ± SEM.

5.2.2 CEACAM2 role in $FeCl_3$–induced vascular injury of mesenteric arterioles

Next, to determine whether CEACAM2 plays a similar role to PECAM-1 or CEACAM1 in platelet thrombus formation *in vivo*, the $FeCl_3$-induced vascular injury model of mesenteric arterioles was utilised for wild-type and *Cc2*$^{-/-}$ mice. This method used to induce vascular injuries and encourage thrombus formation is exposure to $FeCl_3$ solution [270]. This compound physically damages blood vessels by ablating the endothelium to reveal the subendothelial matrix proteins [207]. To explore the effects of $FeCl_3$-induced injury on *in vivo* mouse arterioles, a 7.5% (w/v) $FeCl_3$ solution was administered to the mesentery adventitial surface for a four minute period, causing an injury. Thrombus growth characteristics were observed by measuring the fluorescently labelled platelets bound at injury sites. In anaesthetised mice, the appropriate size of mesenteric arterioles (80-100 µm) was identified and the animal was infused with rhodamine 6G dye. Thrombus formation was monitored in real time in wild-type and *Cc2*$^{-/-}$ murine arterioles over 10 minutes period. Z-stack images were deconvolved and analysed using the Zeiss Axiovert microscope and Axiovision Rel4.6 software. The thrombus formation parameters of thrombus area, height and volume, percentage of vessel occlusion and stability score were determined. Representative images of *Cc2*$^{-/-}$ arterioles display an increase in thrombus formation particularly at 2-4 and 4-6 minutes compared to wild-type arterioles (Figure 5-2A). The kinetics of thrombus area, height and volume were increased gradually in *Cc2*$^{-/-}$ arterioles compared to wild-type arterioles (Figure 5-2B-D).

Thrombus formation parameters were quantified at all time points (0-2, 2-4, 4-6, 6-8 and 8-10 minutes) using Z-stack deconvolved images. Following Z-stack analysis at 4-6 minutes of thrombus formation, *Cc2*$^{-/-}$ arterioles showed increased thrombus growth and stability over ten-minutes, and they had a larger surface coverage of platelets (thrombus area) than wild-type arterioles (6145±125.6 vs 5627±117.7 µm^2; $^{**}P<0.001$; n=30/group;

Figure 5-3A). Moreover, thrombus height in *Cc2*$^{-/-}$ arterioles was greater compared to wild-type arterioles (27.33±0.926 vs 19.95±0.406 µm; ****P*<0.0001; n=30/group; Figure 5-3B). Furthermore, thrombus volume in *Cc2*$^{-/-}$ arterioles was significantly larger (166900±7601 vs 120500±2390 µm^3; ****P*<0.0001; n=30/group; Figure 5-3C), and the percentage of vessel occlusion was larger compared to wild-type arterioles (67.77±1.363 vs 29.79±1.239; ****P*<0.0001; n=30/group; Figure 5-3D). The stability score of thrombi formed in *Cc2*$^{-/-}$ arterioles was higher than in wild-type arterioles (7.267±0.143 vs 3.493±0.136; ****P*<0.0001; n=30/group; Figure 5-3E). *Cc2*$^{-/-}$ arterioles showed no difference in the time to first thrombus larger than 20 µm^2, and time to vessel occlusion (P > 0.05; n=30), when compared to wild-type arterioles. These differences suggest that GPVI, for $FeCl_3$-induced arteriole injuries, plays a significant role in encouraging platelet aggregation.

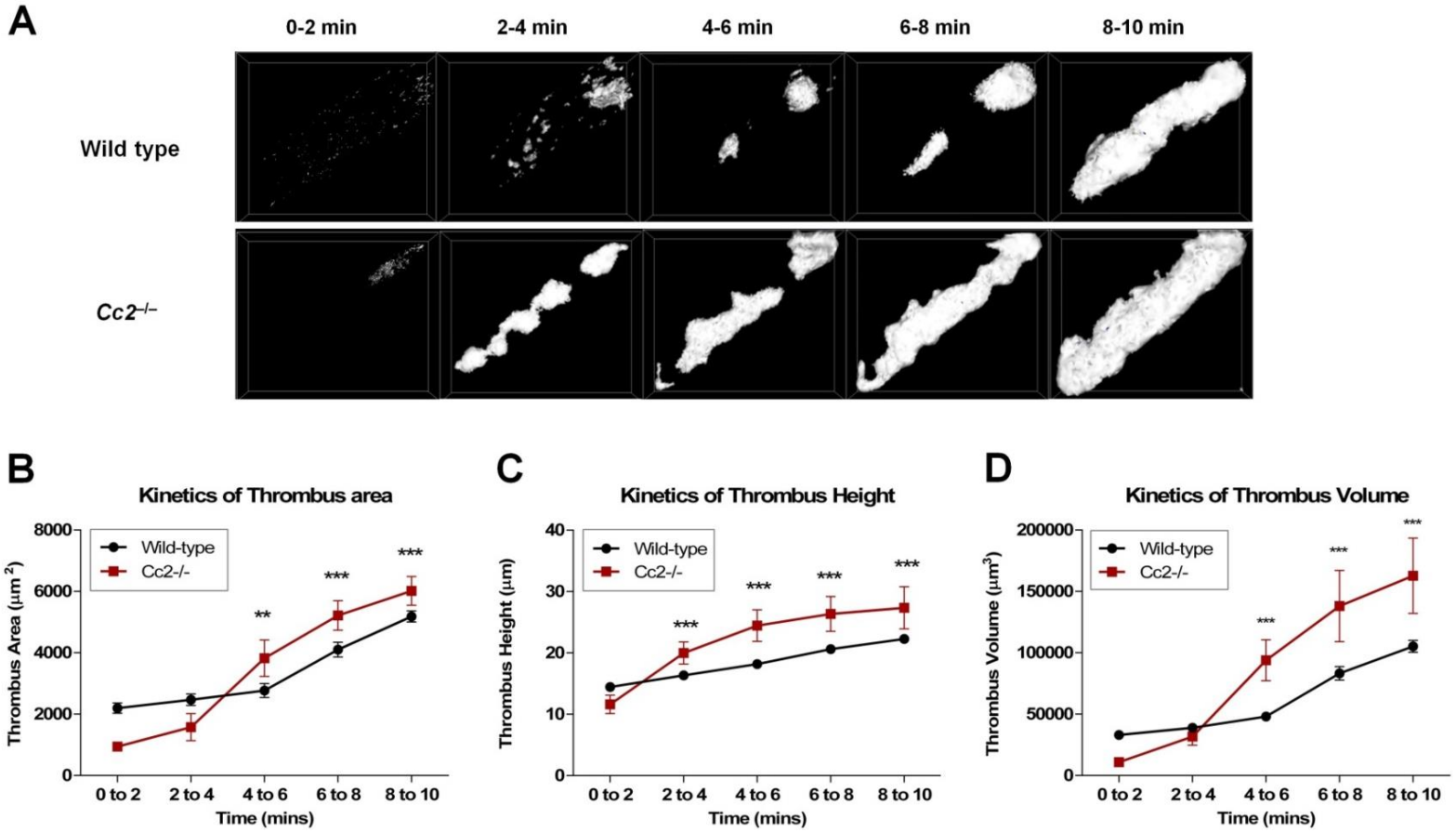

Figure 5-2: *Cc2*$^{-/-}$ mice display larger and more stable thrombi *in vivo*. (A) Z-stack thrombus formation images of $FeCl_3$-induced vascular injury were monitored in arterioles of wild-type versus *Cc2*$^{-/-}$ mice over 0-2, 2-4, 4-6, 6-8 and 8-10 minutes. The different lengths of time after $FeCl_3$ application are specified. Note that thrombi are larger in *Cc2*$^{-/-}$ arterioles over time compared to wild-type control arterioles (n=30 per group). **(B-D)** Quantitative analysis of arterial thrombogenesis of wild-type (●) versus *Cc2*$^{-/-}$ (■) arterioles. **(B)** The kinetics of thrombus area (surface area of thrombi) in µm^2 and height in µm were measured (***P*<0.001 and ****P*<0.0001; n=30). **(C)** The kinetics of thrombus height was also calculated. *Cc2*$^{-/-}$ arterioles displayed a significantly larger thrombus height at 2-4, 4-6, 6-8 and 8-10 minutes compared to wild-type arterioles (****P*<0.0001; n=30 per group). **(D)** The kinetics of thrombus volume of wild-type versus *Cc2*$^{-/-}$ arterioles over time was reliably measured. *Cc2*$^{-/-}$ arterioles was significantly increased at 4-6 minutes compared to wild-type arterioles (166900±7601 vs 120500±2390 µm^3; ****P*<0.0001; n=30 per group). These data are representative of at least 30 independent experiments performed and results represent mean ± SEM. Each symbol represents one arteriole of three examined per mouse.

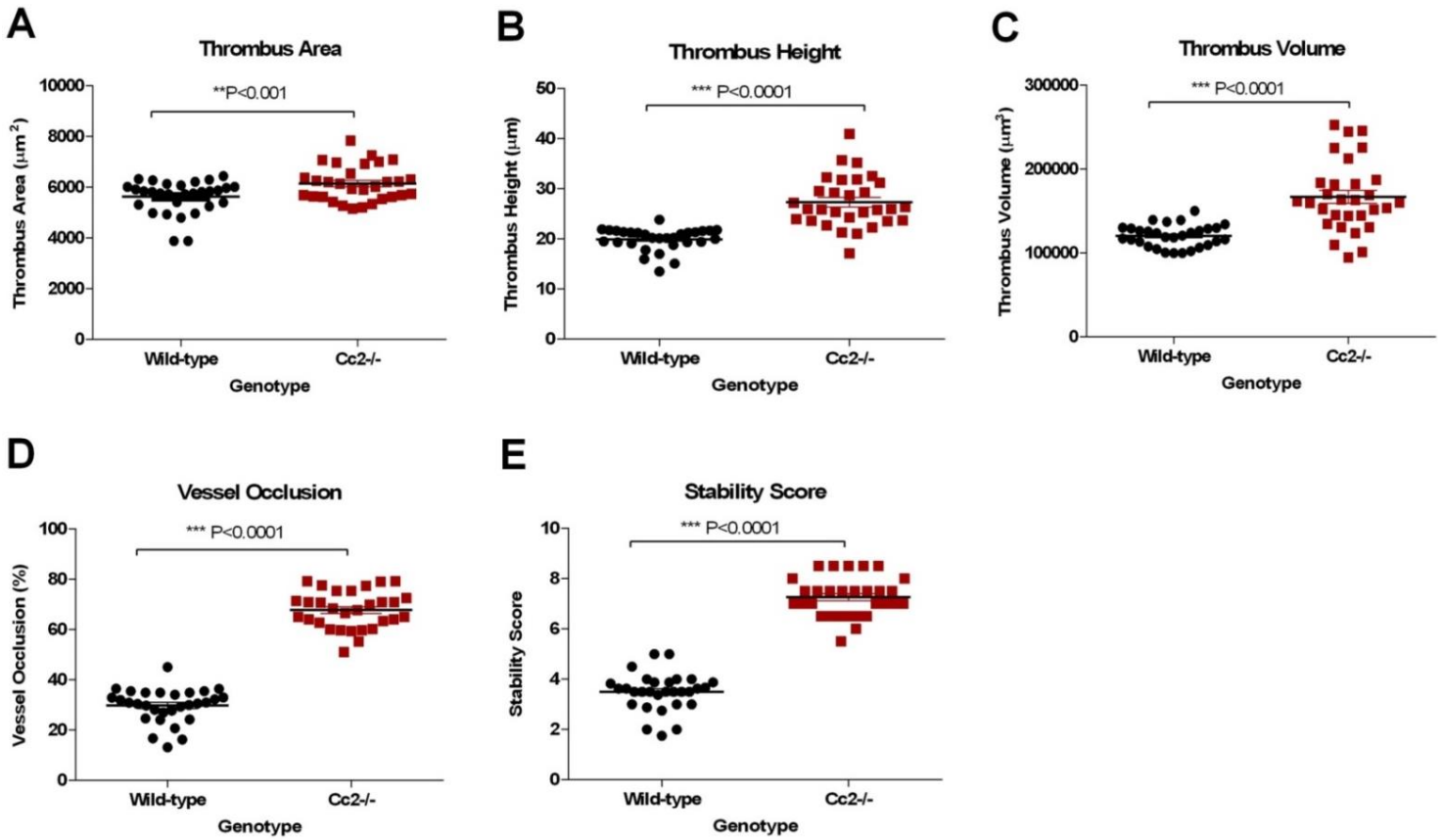

Figure 5-3: *Cc2*$^{-/-}$ mice display larger and more stable thrombi *in vivo*. (A-E) Thrombus formation images of $FeCl_3$-induced vascular injury were monitored in arterioles of wild-type versus *Cc2*$^{-/-}$ mice over 10 minutes. Quantitative analysis of arterial thrombogenesis of wild-type (●) versus *Cc2*$^{-/-}$ (■) arterioles at time 4-6 minutes were calculated. Note that thrombi are larger in *Cc2*$^{-/-}$ arterioles over time compared to wild-type control arterioles (n=30 per group). **(A)** Thrombus area in µm^2, **(B)** thrombus height in µm, **(C)** thrombus volume in µm^3, **(D)** Average percentage (%) of vessel occlusion and **(E)** The thrombus stability was scored from 1 to 10, with 1 being 0% to 10% occupancy and 10 being 91% to 100% occupancy (i.e. complete vessel occlusion) visualised over time. *Cc2*$^{-/-}$ arterioles showed greater stability in thrombi formed (7.267±0.143 vs 3.493±0.136; ****P*<0.0001; n=30 per group). *Cc2*$^{-/-}$ arterioles displayed a significantly larger thrombus area, height, volume and % vessel occlusion at 4-6 minutes compared to wild-type arterioles (****P*<0.0001; n=30 per group). These data are representative of at least 30 independent experiments performed and results represent mean ± SEM. Each symbol represents one arteriole of three examined per mouse.

5.2.3 CEACAM2 role in Laser-induced vascular injury of cremaster arterioles

The Ig-ITIM superfamily members, PECAM-1 and CEACAM1, negatively regulates platelet GPVI-collagen interactions and thrombus growth, *in vitro* and *in vivo* [187, 219]. Thus, we tested whether CEACAM2 plays a similar role in platelet thrombus formation *in vivo*. The $FeCl_3$-induced vascular injury model of mesenteric arterioles and laser-induced vascular injury of cremaster arterioles were utilised for wild-type and *Cc2*$^{-/-}$ mice. Thrombus growth characteristics were observed by measuring the fluorescently labelled platelets bound at injury sites.

It has long been established that platelet aggregation is the main precursor of arterial thrombosis, making it important to understand the processes behind platelet activation and thrombus formation. To study the stability of thrombi *in vivo*, a direct visualisation technique was used, which allowed a detailed examination of the kinetics of *Cc2*-deficient platelets during thrombus formation. This temporal, three-dimensional observation uses confocal microscopy, with high-resolution imaging providing detailed representations of how individual platelets behave in mesenteric arterioles [271, 272]. The laser technique utilises precise thermal injury with lasers to generate highly reactive oxygen molecules and free radicals that physically damage the arteriole endothelium. A number of studies have examined *in vivo* thrombus formation after laser-induced exposure of the arteriole subendothelial matrix in the cremaster muscle microcirculatory system of mice [206, 273, 274]. Building upon these findings, this research suggested that *Ceacam2*-null mice displayed a higher accumulation of platelets than the wild type control group (Figure 5-4).

Thrombus formation parameters were analysed at 2-4 minutes using Z-stack deconvolved images. Following laser-induced vascular injury of cremaster arterioles, *Cc2*$^{-/-}$ and *Cc1*$^{-/-}$ arterioles had greater thrombus volume compared to wild-type arterioles (37355±702.6 vs 31956±785.1 vs 15578±543.7, respectively; ***P<0.0001; n=30/group; at

2-4 minutes; Figure 5-4D). Furthermore, the stability score of thrombi formed in *Cc2*$^{-/-}$ arterioles was more stable than *Cc1*$^{-/-}$ and wild-type arterioles (5.733±0.143 vs 4.80±0.010 vs 2.967±0.0894, respectively; ****P*<0.0001; n=30/group; Figure 5-4F). Likewise, *Cc2*$^{-/-}$ platelets showed increased the kinetics of thrombus area, height, volume, vessel occlusion and stability over time compared to wild-type platelets (Figure 5-5). The visualisation showed that over time more *Cc2*-deficient platelets aggregated at the injury site and form more stable thrombi than wild-type platelets (Figure 5-4 and 5-5). This significant difference suggests that CEACAM2 plays a major role in stabilising thrombus formation at sites of laser-induced vascular injury of cremaster arterioles. Overall, the results suggest that, for vascular wall injuries caused by laser, *Cc2*-deficient cremaster arterioles develop larger thrombi that are more stable over time.

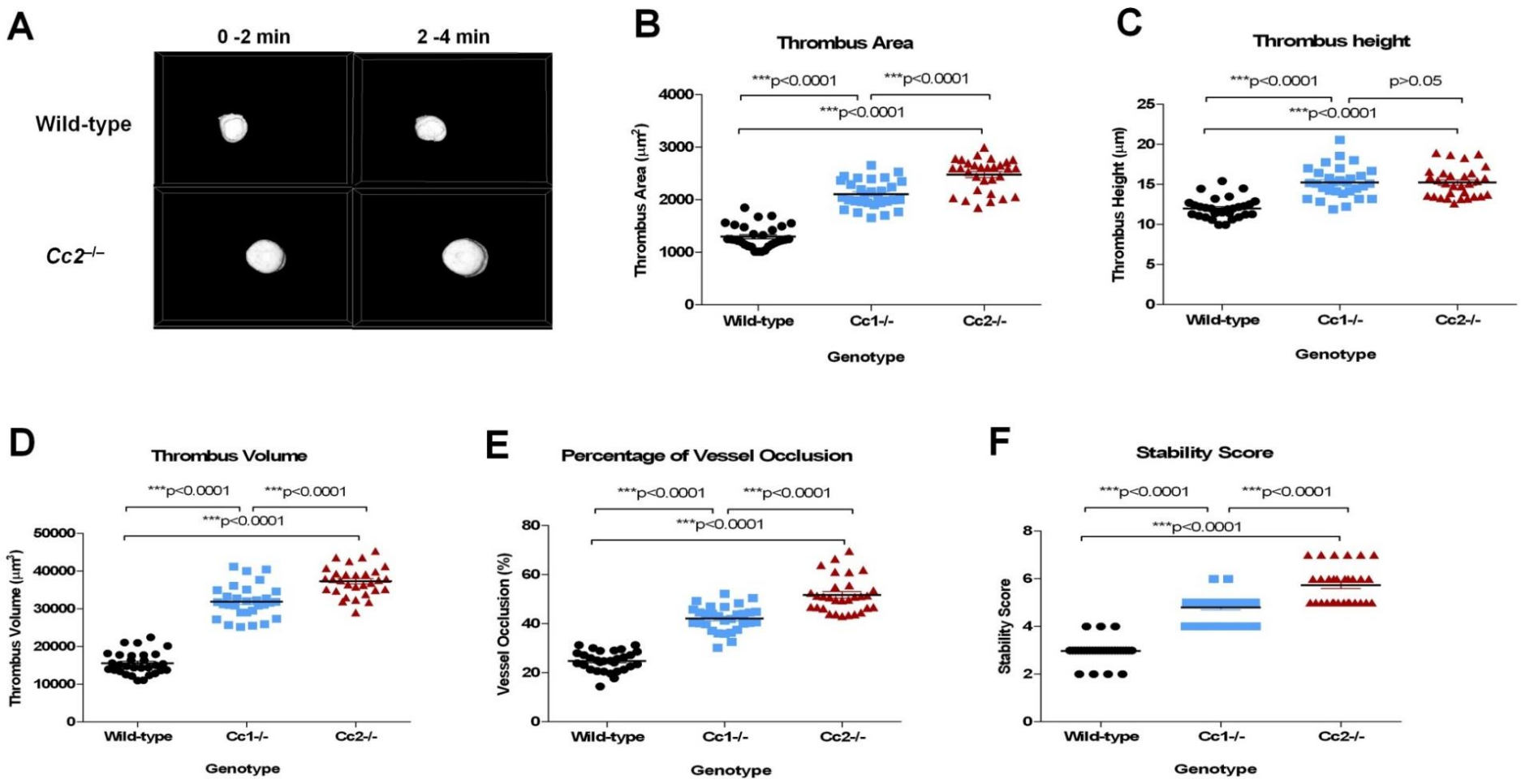

Figure 5-4: *In vivo* imaging of thrombus formation after laser-induced injury of cremaster muscle arterioles. (A-F) Platelet thrombus formation in response to laser induced injury in wild-type (●), *Cc1*$^{-/-}$ (■) and *Cc2*$^{-/-}$ (▲) arterioles. Thrombus volume in *Cc2*$^{-/-}$ and *Cc1*$^{-/-}$ arterioles was significantly greater than wild-type arterioles (37355±702.6 vs 31956±785.1 vs 15578±543.7, respectively; ****P*<0.0001; n=30 per group) and displayed greater stability in thrombi formed (5.733±0.143 vs 4.80±0.010 vs 2.967±0.0894, respectively; ****P*<0.0001; n=30 per group). These data are representative of at least 30 independent experiments performed and results represent mean ± SEM. Each symbol represents one arteriole of three examined per mouse.

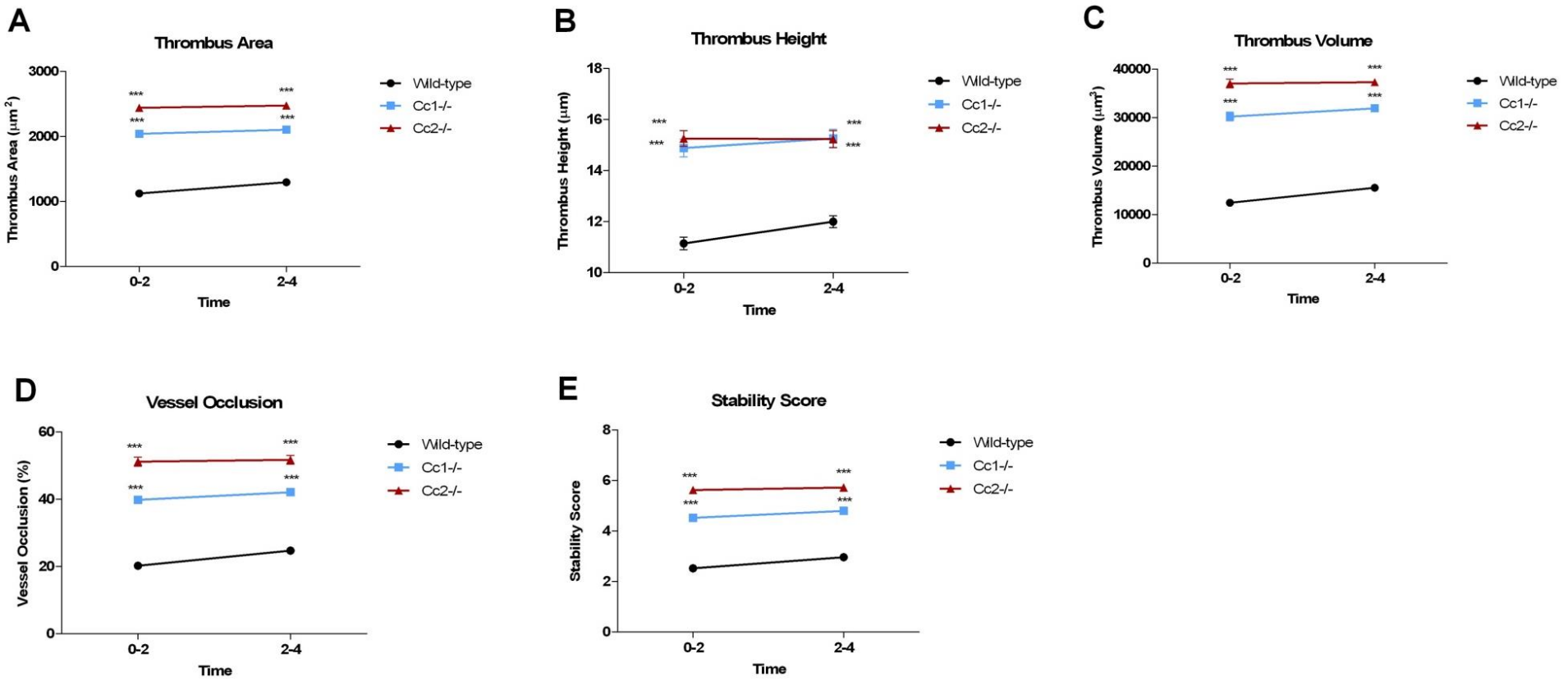

Figure 5-5: *In vivo* kinetics of thrombus formation after laser-induced injury of cremaster muscle arterioles. (A-E) Kinetic of platelet thrombus formation in response to laser induced injury in wild-type (●), *Cc1*$^{-/-}$ (■) and *Cc2*$^{-/-}$ (▲) arterioles. Thrombus area, height, volume, % of vessel occlusion and stability score in *Cc2*$^{-/-}$ and *Cc1*$^{-/-}$ arterioles was significantly greater than wild-type arterioles. These data are representative of at least 30 independent experiments performed and results represent mean ± SEM. Each symbol represents one arteriole of three examined per mouse.

5.2.4 The role of CEACAM2 in GPVI-depleted platelets in thrombus formation *in vivo*

As GPVI collagen receptors interact directly with type I collagen during thrombus formation, GPVI was depleted *in vivo* for five days prior to $FeCl_3$ injury treatment with the GPVI neutralising antibody, JAQ1 (100 µg/mouse) [137]. GPVI depletion was confirmed using Western blotting of wild-type and *Cc2*$^{-/-}$ platelet lysate (not shown). Different cohorts of wild-type and *Cc2*$^{-/-}$ mice were treated with negative isotype control IgG (100 µg/mouse). Compared to wild-type isotype control treated or untreated wild-type arterioles, JAQ1-treated *Cc2*$^{-/-}$ arterioles displayed significant differences for a two-fold reduction in thrombus volume and stability score (***P<0.001; n=10/group; Figure 5-6C). Importantly, upon JAQ1 treatment, *Cc2*$^{-/-}$ arterioles displayed reversal of the increased thrombus stability and growth phenotype compared to wild-type arterioles (4.80±0.359 vs 3.30±0.213; ***P<0.001; n=10/group; Figure 5-6E). In general, these results suggest that CEACAM2, in tandem with GPVI, contributes to the more stable thrombus phenotype.

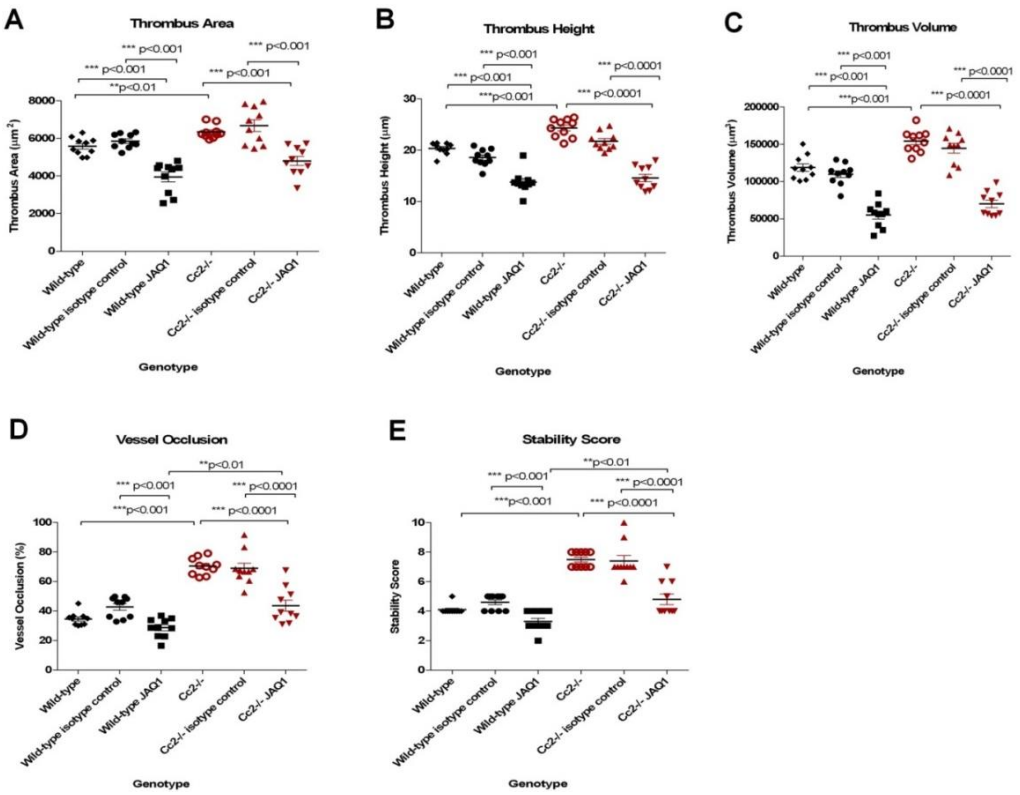

Figure 5-6: Reversal of more stable thrombus growth phenotype in *Cc2*$^{-/-}$ arterioles following GPVI depletion. (A-E) Thrombus formation in response to $FeCl_3$ after inhibition of mouse GPVI with specific monoclonal antibody (mAb) JAQ1 administration to wild-type and *Cc2*$^{-/-}$ mice compared with control IgG-treated wild-type and *Cc2*$^{-/-}$ or untreated wild-type and *Cc2*$^{-/-}$ mice. Thrombus parameters including **(A)** thrombus area, **(B)** thrombus height, **(C)** thrombus volume, **(D)** % of vessel occlusion and **(E)** stability score were calculated at 10 minutes of thrombus formation. Compared with untreated *Cc2*$^{-/-}$ or control IgG-treated *Cc2*$^{-/-}$ arterioles, JAQ1-treated *Cc2*$^{-/-}$ arterioles displayed around 2-fold smaller thrombus volume at 10 minutes (154300±4741 vs 144600±6613 vs 70050±5077 µm^3, respectively; ***P<0.0001; n=10 arterioles from 3 mice/group) and **(E)** around 2-fold lower stability score at 10 minutes (7.500±0.166 vs 7.400±0.371 vs 4.800±0.359, respectively; ***P<0.0001; n=10 arterioles from 3 mice/group). In contrast, compared with untreated wild-type or control IgG-treated wild-type arterioles, JAQ1-treated wild-type arterioles displayed around 3-fold smaller thrombus volume at 10 minutes (118700±5102 vs 109800±4497 vs 55080±5269 µm^3, respectively; ***P<0.0001; n=10 arterioles from 3 mice/group) and a moderately lower stability score at 10 minutes (4.100±0.100 vs 4.600±0.163 vs 3.300±0.213, respectively; **P<0.01; n=10 arterioles from 3 mice/group). These data are representative of at least ten independent experiments performed and results represent mean ± SEM. Each symbol represents one arteriole of three examined per mouse.

5.3 Discussion

It is known that atherosclerotic plaque rupture exposes high levels of type I collagen which induces localised thrombus formation via the adhesion of platelets to exposed subendothelial matrix components in vascular walls. This initiates a cascade process that leads to coagulation. To examine how CEACAM2 contributes to platelet aggregation and pathological thrombus formation, two methods for inducing arterial injury were used, for wild type and *Cc2*-deficient mice, and for two types of vascular beds. $FeCl_3$ was added, to induce injury and expose the subendothelial matrix in mesenteric arterioles and laser was utilised to induce injury in cremaster arterioles. The resulting formation of thrombi was examined over a 10 minute time period, using *in vivo* intravital microscopy and Z-stack images to provide a spatial context.

Unlike CEACAM1, the physiologic role of platelet CEACAM2 in thrombus formation *in vivo* had not been determined. These two receptors share some structural similarities, but differ in the number of extracellular Ig-Domains and in the ligand binding properties of their distal variable N-terminal Ig-Domain. The fact that CEACAM2 has different ligand properties than CEACAM1 would suggest unique biological roles as the avidity of ligand interactions (activation versus clustering) appears fundamental to drive cell signalling responses. In recent studies, CEACAM2 appears to function in a similar way as CEACAM1, at least in the context of insulin metabolism [188]. A more recent study has demonstrated that a closely related Ig-ITIM superfamily member, CEACAM1 serves as a negative regulator of platelet collagen GPVI-FcR γ-chain mediated signalling [187]. Using intravital microscopy to $FeCl_3$-injured mesenteric arterioles, we have shown that thrombi in *Cc2*$^{-/-}$ mice are larger and are more stable over time than wild-type mice providing evidence that CEACAM2 negatively regulates platelet-collagen interactions and thrombus growth *in vivo*. Collectively, this study has highlighted that these cell surface receptors interact with

their ligands and have the ability to negatively modulate downstream signalling events and thrombus formation.

This chapter describes real time observation via intravital microscopy to reveal how CEACAM2 influences thrombus formation *in vitro* and *in vivo*, and highlights the importance of CEACAM2 in regulating thrombus formation on immobilised collagen under arterial flow conditions produced *in vitro*. Under *in vitro* conditions of physiological arterial shear flow, absence of CEACAM2 results in increased surface coverage of platelets on immobilised type I collagen (Figure 5-1). There was no evidence of sexual dimorphism in this enhanced thrombus growth phenotype of *Cc2*$^{-/-}$ platelets. Moreover, to observe the processes under different conditions, we included vascular injury of mesenteric arterioles induced by $FeCl_3$ and laser-induced vascular injury of cremaster arterioles. $FeCl_3$-induced injury exposed a number of sub-endothelial collagen types, allowing collagen-GPVI platelets to interact with the exposed type I collagen. Thus, $FeCl_3$-induced injury led to larger thrombi, in terms of area and volume, among mice lacking CEACAM2 than in wild-type mice (Figure 5-2). Importantly, these differences were consistent over time, and the thrombi in *Cc2*$^{-/-}$ null mice were more stable than in the wild-type control group (Figure 5-3). The *in vivo* thrombus stability phenotype observed in *Cc2*$^{-/-}$ mice required platelets with GPVI receptor sites (Figure 5-6). Using the laser-induced vascular injury model, *Cc2*$^{-/-}$ cremaster muscular arterioles displayed an increase in thrombus volume and thrombi that were more stable compared to wild-type arterioles (Figure 5-4D, F). Therefore, using several models of microvascular thrombosis *in vivo,* we have shown that CEACAM2 deletion results in larger and more stable thrombi than wild-type mice and that this is at least partly depends on the presence of GPVI (Figure 5-6). This suggests that CEACAM2 negatively regulates thrombus growth, *in vivo,* in both mesenteric and cremaster muscle arterioles. Future studies could compare the relative importance of platelet-expressed

CEACAM2 with the endothelial type in regulating the *in vivo* growth of thrombi. CEACAM2 is a third example of the Ig-ITIM superfamily that negatively regulates the stationary adhesive signalling of platelet-collagen interactions and thrombus growth *in vivo*.

Previous research into arteriole thrombus formation in PECAM-1 and CEACAM1–deficient mice, using the $FeCl_3$ vascular injury model, revealed slight differences in the time taken to reach the 75% vessel occlusion level [178, 187]. Overall, the mean rate of vessel occlusion in PECAM-$1^{-/-}$ and *Cc1*$^{-/-}$ mice was slightly shorter than for the control group. By contrast, the laser-induced injury model, which does not expose type I collagen but promotes tissue factor generated platelet/fibrin thrombi, produced a larger response [178]. This suggests that PECAM-1, CEACAM1 and CEACAM2 all contribute to negative regulation during *in vivo* platelet-collagen interactions and thrombus formation.

Whether CEACAM2 regulates thrombin signalling in platelets remains unknown. In response to thrombin (at 0.25-1.0 U/mL), *Cc2*$^{-/-}$ platelets had comparable amplitude and slope of thrombin-mediated aggregation responses compared to wild-type platelets (Figure 3-5). In addition, GPCR platelet aggregation mediated by ADP, thrombin and PAR-4 agonist peptide were comparable in *Cc2*$^{-/-}$ and wild-type platelets (Figure 3-3). Moreover, *Cc2*$^{-/-}$ platelets had similar alpha and dense granules release upon thrombin and PAR-4 agonist peptide stimulation compared to wild-type platelets (Figure 3-6A and 3-7A). While these results would argue against CEACAM2 regulating thrombin signalling, more studies using thrombin at subthreshold concentrations are needed to fully address this question. Moreover, the laser injury model used in this study is mediated by thrombin:tissue factor inflammatory process and the *Cc2*$^{-/-}$ arterioles had increased thrombi that were more stable under these conditions (Figure 5-5). Thus, more studies are needed to investigate whether CEACAM2 affects thrombin signalling pathway.

Unlike human platelets, murine platelets lack the low-affinity IgG receptor, FcgammaRIIa, but contain two ITAM-bearing receptors, GPVI/FcR gamma chain and CLEC-2. Based on our *in vivo* mouse thrombus models, we show that *Cc2*$^{-/-}$ arterioles have larger thrombi that are more stable in response to type I collagen exposure (i.e: $FeCl_3$-induced vascular injury of mesenteric arterioles; Figure 5-2) and thrombin-driven processes without type I collagen exposure (i.e: laser induced injury of cremaster muscle arterioles [224, 275]; Figure 5-5). This was also the case for *Cc1*$^{-/-}$ (in this Chapter) and PECAM-1$^{-/-}$ arterioles [178]. While GPVI depletion resulted in the reversal of thrombus growth, thrombus stability was less affected indicating the involvement of other potential mechanisms regulating thrombus stability (Figure 5-3E).

Like CEACAM1, CEACAM2 plays a role in limiting thrombi formed under conditions of type I collagen exposure such as in the pathological process of atherosclerotic plaque rupture. Further studies are required to decipher its role in other mechanisms in platelet function, thrombus stabilisation and wound healing.

In conclusion, the chapter has defined the importance of CEACAM2 as an inhibitory co-receptor in murine platelets in platelet-collagen interactions *in vivo*. CEACAM2 is a negative regulator of platelet-collagen interactions and platelet thrombus formation and growth *in vivo*. CEACAM2 restricts arteriolar thrombus growth and postpones the development of thrombosis linked to type I collagen. Ultimately, this could be beneficial as it could lower the rate of thrombus formation in vessels with disease or with ruptured atherosclerotic plaques that expose the type I collagen matrix.

6 Chapter Six: *In vitro* studies of CEACAM2 positive regulation of integrin $\alpha_{IIb}\beta_3$-mediated platelet functions

6.1 Introduction

The process of platelet aggregation at sites of vascular injury is complex and the exact roles of CEACAM2 and integrin $\alpha_{IIb}\beta_3$ are not known. During normal haemostasis and thrombogenesis, platelets aggregate and adhere to damaged vascular surfaces, creating a haemostatic plug [276]. By contrast, under diseased conditions such as those created by atherosclerotic lesions, vascular rupture leads to exposure of type I collagen resulting in platelet aggregation and formation of pathological thrombi [277]. *In vivo*, platelets rarely react with inactivated endothelial surfaces, but become more active in the presence of stimulated or injured vascular surfaces, and will undergo rolling, adherence, translocation or detachment processes [276, 278-280].

The processes governing platelet adhesion and aggregation at sites of vascular injury are complex and involve a number of stages and substrates, including vWF and collagen. Under different flow conditions, numerous receptors are involved, including integrin $\alpha_{IIb}\beta_3$, integrin $\alpha_2\beta_1$, collagen GPVI and GPIb/IX/V complex. Under conditions of high flow and shear stress, the initial platelet tethering requires vWF to interact with the amino-terminal domain of the GPIbα subunit [276, 278]. In turn, this leads to integrin $\alpha_{IIb}\beta_3$ activation, a precursor for the mediation of (i) irreversible stable adhesion, (ii) cytoskeletal reorganisation, (iii) platelet spreading, (iv) platelet aggregation, and (v) stable thrombus formation and growth [277]. To promote cytoskeletal reorganisation, fibrinogen and integrin $\alpha_{IIb}\beta_3$ bind and stimulate platelet adhesion and activation, creating intracellular signals that nucleate the reorganisation process. Finally, integrin-agitating receptors undergo conformational changes when integrin $\alpha_{IIb}\beta_3$ is stimulated by agonist-induced activation. During this process, the receptor converts from a resting, low-affinity state to an active, high-affinity state, where it binds its soluble ligand, fibrinogen.

To facilitate bidirectional signalling, integrin $\alpha_{IIb}\beta_3$ uses two types of signalling event, an 'inside-out' process, usually under conditions of agonist induced stimulation, and an 'outside-in' process, which incorporates fibrinogen-occupied integrin $\alpha_{IIb}\beta_3$ post-ligand integrin $\alpha_{IIb}\beta_3$ binding. These signalling events are responsible for stimulating irreversible stable platelet adhesion and thrombus growth, by influencing processes such as cytoskeleton reorganisation, the retraction of clots, platelet aggregation and microvesicle formation. A genetic abnormality in integrin $\alpha_{IIb}\beta_3$ leads to defects in ligand binding, prolonged bleeding time and platelet aggregation in Glanzmann's Thrombasthaenia patients [281].

Prototypic platelet ITIM-bearing receptors, PECAM-1 and CEACAM1, have previously been shown to be negative regulators of platelet-collagen-GPVI interactions and positive regulators of integrin $\alpha_{IIb}\beta_3$-mediated platelet functional responses [187, 219]. As earlier discussed in chapters 3 and 5, CEACAM2 has also been confirmed as a negative regulator of platelet collagen GPVI interactions *in vitro* and *in vivo*. Importantly, CEACAM2 and CEACAM1 share some similarity in structure, but differ in their number of extracellular Ig-Domains and in the ligand binding properties of their distal variable N-terminal Ig-Domain. CEACAM2 contains 2 Ig-Domains while CEACAM1 contains 4 extracellular Ig-Domains. Furthermore, CEACAM2 N-terminal variable Ig-Domain 1 does not allow homophilic binding, while CEACAM1 N-terminal variable Ig-Domain 1 mediates homophilic binding [186]. At this stage the only ligand identified for CEACAM2 is the murine coronavirus mouse hepatitis virus spike glycoprotein (s). Both CEACAM2 and CEACAM1 contain transmembrane receptors and contain identical ITIMs in their cytoplasmic domains. The role of CEACAM2 genes in platelet function is not clearly defined but it is important to study CEACAM2 in murine platelets in terms of integrin $\alpha_{IIb}\beta_3$ responses because it will help understand the function of human CEACAM1 in platelets as it represents the sum of mouse CEACAM2 and CEACAM1.

As CEACAM1 has been reported to have a physiological relationship with β_3 integrin, it raises the possibility that CEACAM2 might also have a relationship with integrin $\alpha_{IIb}\beta_3$ in murine platelets. This chapter aimed to assess if CEACAM2 has any functional association with integrin $\alpha_{IIb}\beta_3$, the major glycoprotein present in platelets. Therefore, this chapter aimed to investigate the functional properties of *Cc2*$^{-/-}$ platelets during integrin $\alpha_{IIb}\beta_3$-dependent events; and differences in the roles of platelet CEACAM2 during the adhesive and signalling events connected to haemostasis and thrombosis.

6.2 Results

6.2.1 *In vivo* tail bleeding analysis

Murine platelets and other cell types, including intestinal tissue crypt epithelia, kidney cells and testis, express CEACAM2, so a series of *in vivo* tail bleeding assays allowed a thorough examination of the mice for abnormal vascular or platelet-mediated haemostasis. In order to test if CEACAM2 plays a role in primary haemostasis *in vivo*, tail bleeding times and volume of blood lost were tested for *Cc2*$^{-/-}$ mice compared to wild-type mice. As shown in Figure 6-1A, a significant difference in the mean tail bleeding times between the wild-type and *Cc2*$^{-/-}$ groups was observed. In addition, the data-spread further revealed longer bleeding times for CEACAM2-deficient mice (***P<0.001, n=20). Overall, the *Cc2*$^{-/-}$ mice lost double the mean volume of blood during tail bleeding (*P<0.05, n=20; Figure 6-1B).

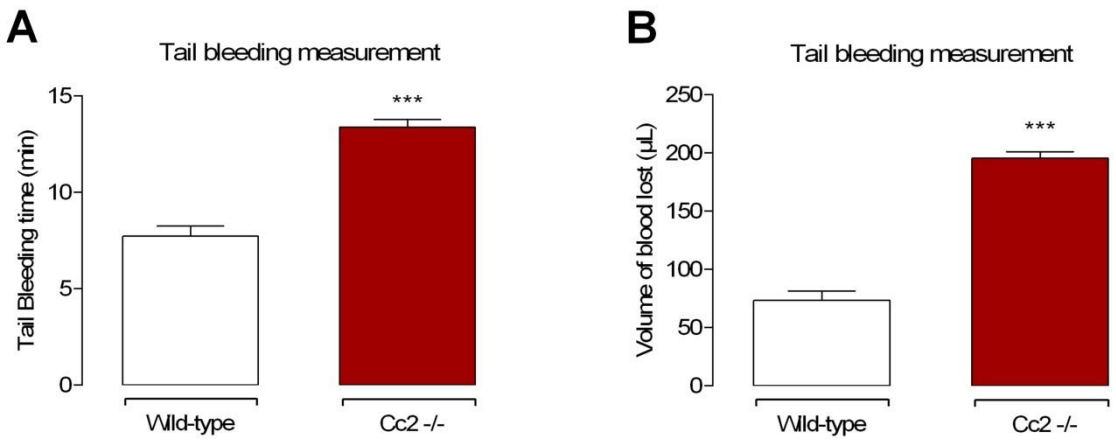

Figure 6-1: *Cc2*$^{-/-}$ mice displayed prolonged tail bleeding times and increased volume of blood lost. Tail bleeding measurement of wild-type and *Cc2*$^{-/-}$ mice was assessed using 6-8 week old age and sex-matched mice **(A)** Tail bleeding time was recorded from the time of initial tail cessation (***P<0.001, n=20/group). **(B)** The volume of blood lost during tail bleeding time was measured in both mice (***P<0.001, n=20/group). Both tail bleeding time and blood lost are greater in *Cc2*$^{-/-}$ mice compared to wild-type mice. Data are representative of at least of 20 independent experiments per group and presented as mean ± SEM.

6.2.2 *Cc2*$^{-/-}$ platelets display delayed kinetics of clot retraction *in vitro*

The main scope of this chapter involved detecting any significant differences in the clot retraction processes and dynamics of *Cc2*$^{-/-}$ and wild-type platelets, preceding a multi-stage investigation of the potential reasons behind any dissimilarity. To operationalise the experiment and reduce the impact of potential confounding variables, it was important to highlight any physiological differences between the two mice genotypes from the outset. An initial examination showed that the CEACAM2-deficient mice were otherwise healthy and had normal Mendelian inheritance characteristics [188, 241]. In addition, haematological parameters were examined in *Cc2*$^{-/-}$ mice and revealed a normal range, including platelet production (Chapter 3). *In vitro* evidence suggested that modulation of integrin $\alpha_{IIb}\beta_3$–mediated functions was influenced by engagement of PECAM-1 and CEACAM1 receptors, so the next stage involved testing if a fundamental integrin $\alpha_{IIb}\beta_3$ platelet abnormality existed in the CEACAM2 deficient platelets. Integrin $\alpha_{IIb}\beta_3$ is crucial for normal platelet aggregation, platelet spreading and clot retraction functionality, so the research involved examining any significant differences in the kinetic properties of the clot retraction process in *Cc2*$^{-/-}$ compared to wild-type platelets.

To initiate clotting, 2.5U/mL thrombin was added to the wild-type and *Cc2*$^{-/-}$ normalised platelet count (PRP; $100x10^9$/L) groups, at a temperature of 37°C. For the first hour, clots were observed at ten minute intervals, with further observation over a 24-hour period. To display the clotting process in detail, digital camera technology was used and imaged were captured at various time points (0-24 hours). The *Cc2*$^{-/-}$ platelets revealed a significant delay in the kinetics of clot retraction when compared to wild-type platelets (Figure 6-2A). After 30 minutes, *Cc2*$^{-/-}$ platelets showed no clot retraction (data not shown), with partial retraction after four hours, and nearly complete retraction after 10-24 hours. In contrast, wild-type platelets showed faster clot retraction, with partial retraction after 30

minutes and complete retraction after 4 hours. To further investigate this observation, the remaining volume of serum, after the removal of the fibrin clots, was measured as described in the methodology section. The *Cc2*$^{-/-}$ platelets revealed a 2-fold reduction in serum volume compared to the wild-type group after 4-10 hours (P<0.05, n=4; Figure 6-2B) To exclude the possibility that the expression level of integrin $\alpha_{IIb}\beta_3$ could affect the clot retraction process, surface expression of integrin $\alpha_{IIb}\beta_3$ was measured on the *Cc2*$^{-/-}$ platelets by flow cytometry and displayed normal expression. This suggested that the defect in the clot process was not related to the reduced expression of integrin $\alpha_{IIb}\beta_3$ on the surface of the *Cc2*$^{-/-}$ platelets (Figure 6-2C). This data was further supported by the normal expression of CD9 and CD44 on *Cc2*$^{-/-}$ platelets, making it possible to conclude that CEACAM2 is essential for optimal 'outside-in' integrin $\alpha_{IIb}\beta_3$–mediated signalling events in murine platelets.

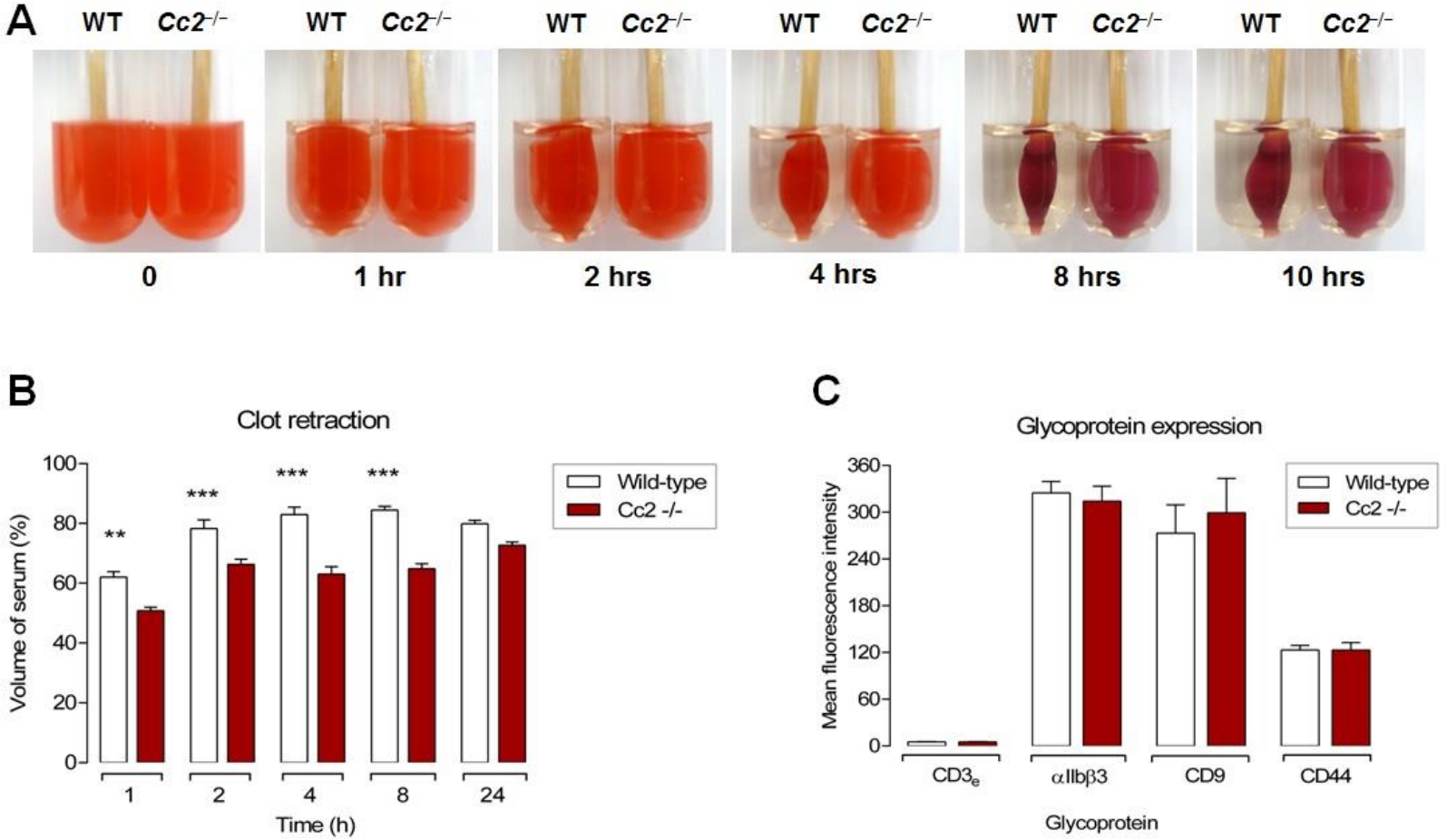

Figure 6-2: *Cc2*$^{-/-}$ platelets display delayed kinetics of clot retraction compared to wild-type platelets. Normalised PRP from wild-type and *Cc2*$^{-/-}$ mice was stimulated with 2.5 U/mL of thrombin over time points. (**A)** Digital photographs display *in vitro* kinetics of clot retraction over a 10-hour time period. Each photograph is representative of at least 4 independent experiments. (**B)** Following a 2.5 U thrombin stimulation, serum volume was also recorded from wild-type and *Cc2*$^{-/-}$ platelets after clot retraction at 1, 2, 4 , 8 and 24 hours. **(C)** Surface expression of several glycoproteins was measured on platelet surface including integrin $\alpha_{IIb}\beta_3$, CD9 and CD44. Data shown are representative of at least 4 independent experiments and presented as mean ± SEM.

6.2.3 *Cc2*$^{-/-}$ platelets display normal static platelet adhesion to integrin $\alpha_{IIb}\beta_3$-mediated matrices

Clot retraction is an integrin $\alpha_{IIb}\beta_3$-mediated function involving cytoskeletal reorganisation as part of the process. Therefore, in order to investigate the role of CEACAM2 in cytoskeletal reorganisation, the spreading of *Cc2*$^{-/-}$ platelets on immobilised fibrinogen was compared to that of wild-type platelets. The next stage determined if CEACAM2 deficiency modulates integrin $\alpha_{IIb}\beta_3$–mediated adhesive events, by evaluating the static platelet adhesion responses of wild-type and *Cc2*$^{-/-}$ platelets in the presence of immobilised fibrinogen (100 µg/mL), as an ECM protein, over a 0-60 minute period. A negative control was performed using adhesion to RCD buffer, pH 7.4. After the washing steps, the number of platelets adhering to fibrinogen was quantified using DIC microscopy (x63 oil lens). Under static conditions, *Cc2*$^{-/-}$ platelets displayed decreased kinetics of platelet adhesion to fibrinogen when measured at 30, 45 and 60 minute intervals compared to wild-type platelets (***P*<0.01; n=4; Figure 6-3). However, as shown in chapter 3, *Cc2*$^{-/-}$ platelets demonstrated increased platelet adhesion to type I fibrillar collagen when measured at intervals of 15, 30, 45 and 60 minutes (Chapter 3; Figure 3-8). Further emphasising this variation, without agonist stimulation, *Cc2*$^{-/-}$ platelets displayed reduced spreading surface area on both fibrinogen and type I collagen in comparison to the wild-type group (****P*<0.001 and ***P*<0.01; n=100 platelets). As shown in Figures 6-4A-C, the delay in spreading was corrected when the platelets underwent agonist stimulation at concentrations of 20 µM ADP, 0.5 mM PAR-4 agonist peptide, or 100 nM PMA.

In conclusion, the differing static platelet adhesion responses suggest that absence of CEACAM2 had no noticeable effect on platelet adhesive properties where inactive integrin $\alpha_{IIb}\beta_3$ binds to an immobilised ligand, fibrinogen. In addition, when platelets are undergoing adhesion to immobilised fibrinogen and type I collagen, *Cc2*$^{-/-}$ platelets displayed reduced

cytoskeletal reorganisation capability compared to wild-type platelets. This lends credence to the idea that *Cc2*$^{-/-}$ platelets have a moderately defective integrin $\alpha_{IIb}\beta_3$-mediated functionality.

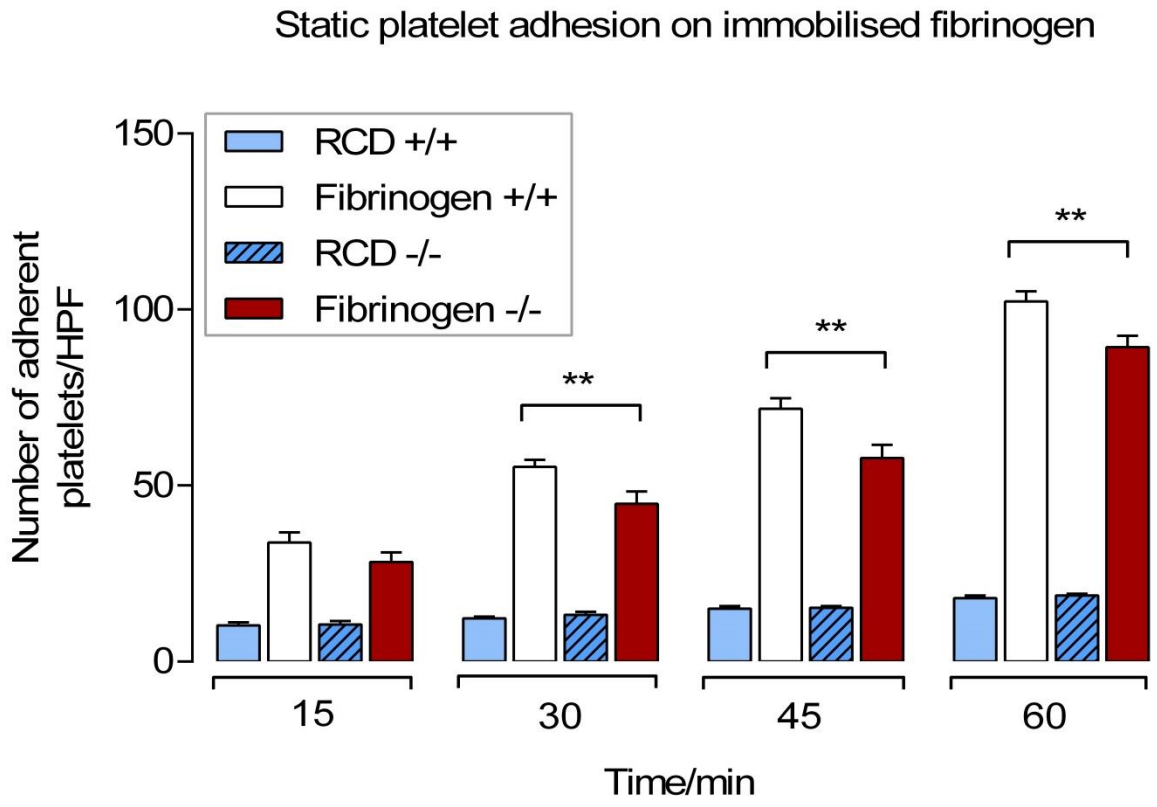

Figure 6-3: *Cc2*$^{-/-}$ platelets demonstrate a reduction in platelet adhesion on fibrinogen. Time course of wild-type and *Cc2*$^{-/-}$ platelet adhesion to either buffer control or fibrinogen (100 µg/mL) for 15, 30, 45 and 60 minutes at 37^{o}C. Non-adherent platelets were removed and adherent platelets were measured as described in methods and materials. A mild reduction in platelet adhesion on fibrinogen was observed in *Cc2*$^{-/-}$ platelets compared to wild-type platelets (**P< 0.01; n=4). Each data were performed in duplicate and represents mean ± SEM of four independent experiments.

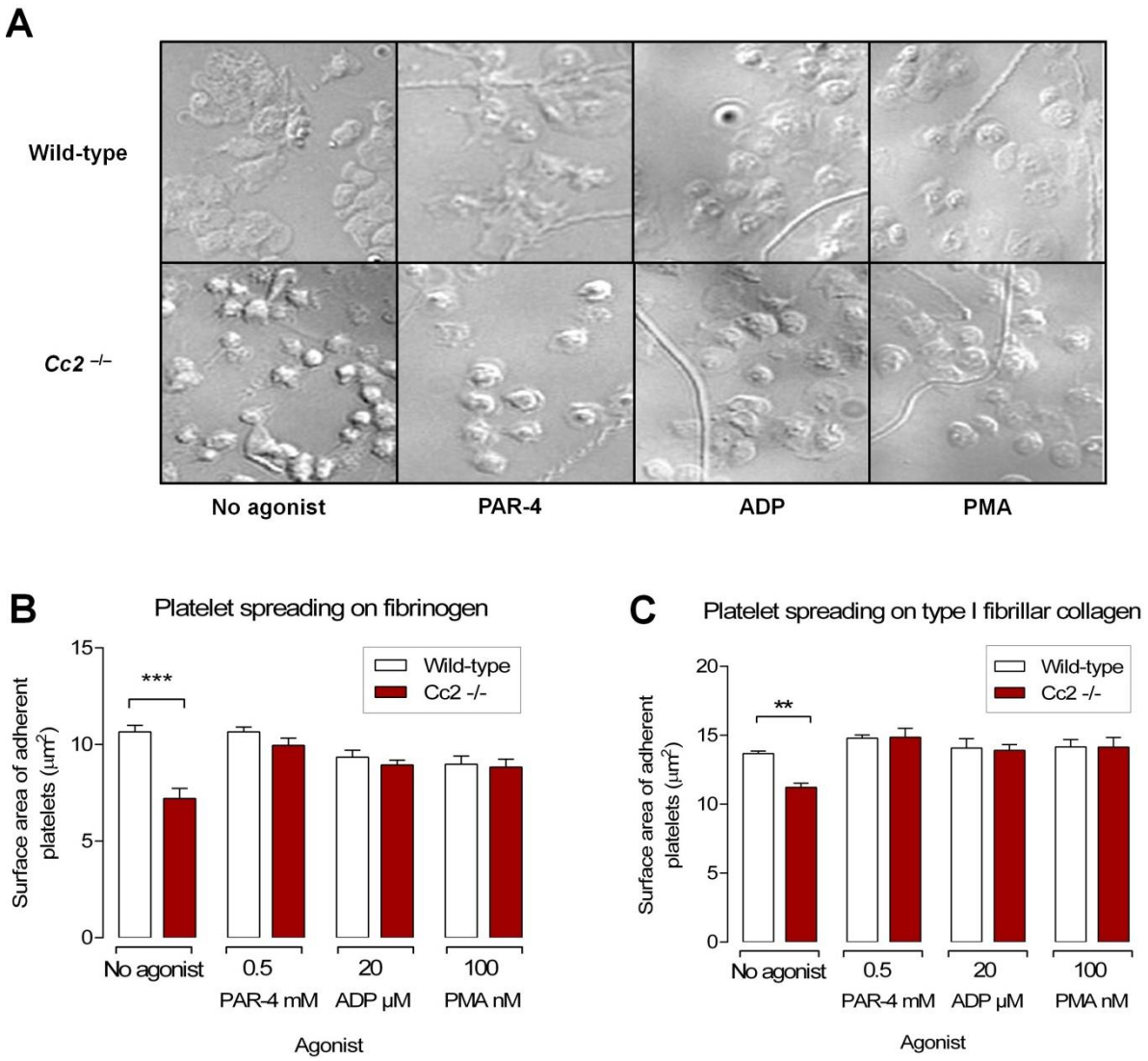

Figure 6-4: *Cc2*$^{-/-}$ platelets showed a reduction in platelet spreading on fibrinogen and type I collagen. Platelet spreading on fibrinogen (100 μg/mL) was assessed for wild-type, and *Cc2*$^{-/-}$ platelets at 60 minutes at 37°C under certain conditions. Spread surface area of adhered platelets was measured in μm^2 without agonist, with PAR-4 (0.5 mM), ADP (20 μM), and PMA (100 nM). **(A)** Representative images of platelet spreading on fibrinogen under resting conditions or upon activation with agonists. **(B)** A reduction in platelet spreading on fibrinogen was observed in *Cc2*$^{-/-}$ platelets but not wild-type platelets (***P<0.001; n=3). Each bar represents at least 100 platelets analysed. Data represent mean ± SEM of three independent experiments. **(C)** Platelet show a delay in platelet spreading on Type I fibrillar collagen (**P<0.01; n=3). Each bar represents at least 100 platelets analysed. Data represent mean ± SEM of three independent experiments.

6.2.4 Restricted cytoskeletal reorganisation of *Cc2*$^{-/-}$ platelets

The next phase of this chapter focused upon physical changes in the shape and spreading properties of platelets, testing if CEACAM2 inhibited post-ligand occupancy and the formation of filopodia in *Cc2*$^{-/-}$ platelets and whether this could be responsible for the defect in clotting properties. When platelets adhere to fibrinogen, they undergo reorganisation of the cytoskeleton, which alters their shape and spreading action. This occurrence, known as post-ligand occupancy, occurs when integrin $\alpha_{IIb}\beta_3$ complex clusters upon the membrane of the platelets, where it initiates a downstream process of 'outside-in' integrin $\alpha_{IIb}\beta_3$–mediated signalling events. To determine if CEACAM2 deficiency altered this process, high resolution SEM was used to look for platelet filopodia formation and spreading properties over 60 minutes at 37°C. *Cc2*$^{-/-}$ platelets showed a reduction in their adhesion to fibrinogen compared to wild-type platelets (Figure 6-5A-B). In addition, unstimulated *Cc2*$^{-/-}$ platelets had limited cytoskeletal reorganisation and ability to extend filopodia compared to wild-type platelets. *Cc2*$^{-/-}$ platelets extended fewer filopodia, with a small quantity having only 1-3 filopodia and fewer still with more than 3 filopodia (***P<0.001, n=4; Figure 6-5C). This data suggests that, when adhering to immobilised fibrinogen, *Cc2*$^{-/-}$ platelets have a defective ability to reorganise the cytoskeleton.

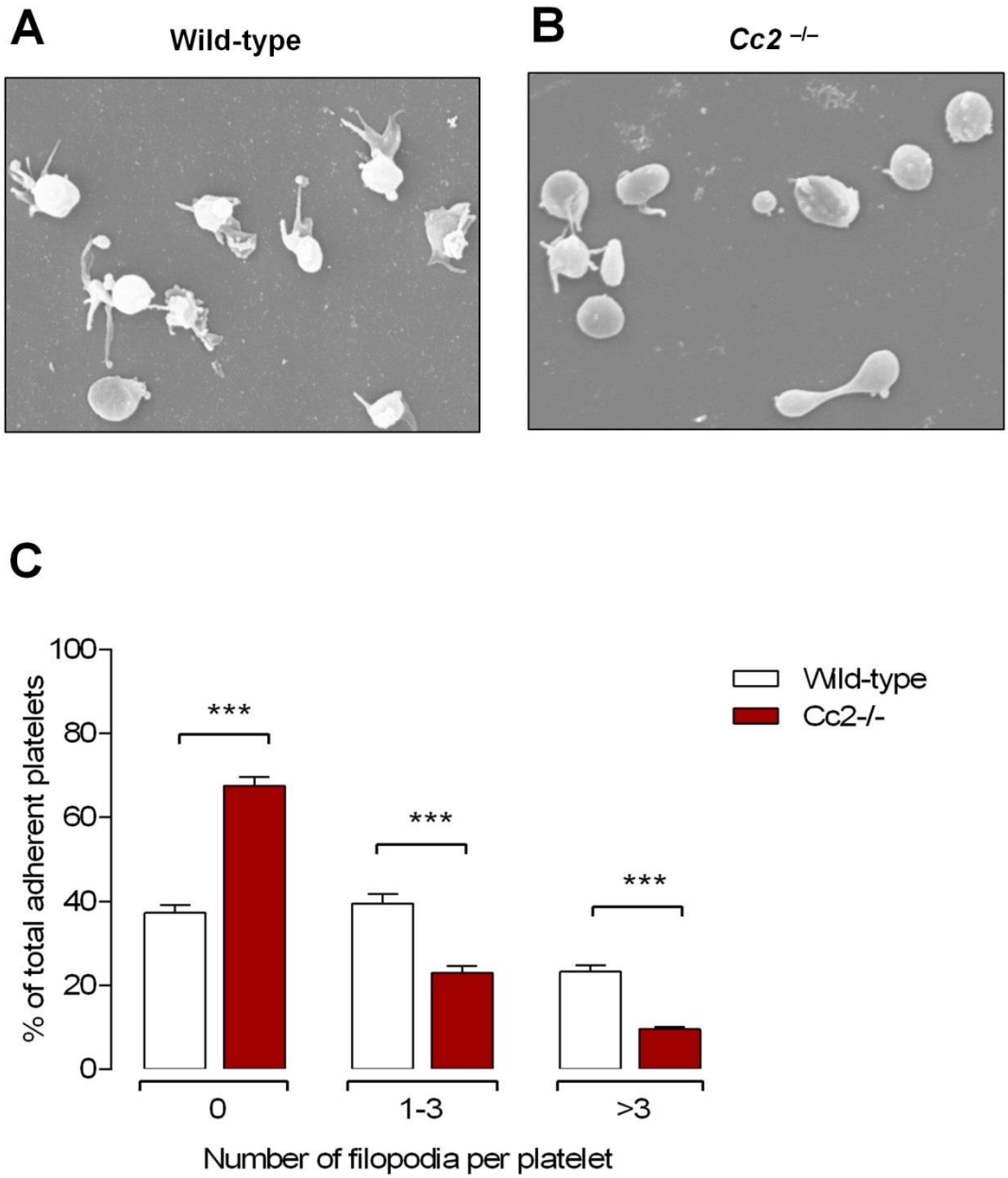

Figure 6-5: *Cc2*$^{-/-}$ platelets show restricted cytoskeleton reorganisation upon spreading on fibrinogen. Wild-type and *Cc2*$^{-/-}$ washed platelets (100x10^9/L) were allowed to adhere to fibrinogen (100 µg/mL) for 60 minutes at 37°C, then fixed and examined using SEM. **(A-B)** Representative images of platelet spreading on immobilised fibrinogen for wild-type versus *Cc2*$^{-/-}$ platelets. **(C)** Filopodia per platelet were analysed on SEM images from random fields involving 100 platelets counted. The number of filopodia demonstrating each category was expressed as a percentage of the total adherent platelets counted. Platelet filopodia were classified into 3 independent groups including 0, 1-3, and >3 filopodia (***P<0.001; n=4). Images were captured using a JCM-6000 scanning electron microscope (10 kV). Data shown are representative of at least of 4 independent experiments and presented as mean ± SEM.

6.2.5 *Cc2*$^{-/-}$ platelets display normal 'inside-out' integrin $\alpha_{IIb}\beta_3$-mediated signalling properties

Cc2$^{-/-}$ platelets display a number of defects during post-ligand occupancy processes, so the next phase involved establishing if their 'inside-out' integrin $\alpha_{IIb}\beta_3$–mediated signalling properties were normal. Testing integrin $\alpha_{IIb}\beta_3$ activation on *Cc2*$^{-/-}$ platelets involved comparing the ability of the wild-type versus *Cc2*$^{-/-}$ platelets to bind to soluble FITC-fibrinogen and JON/A-PE mAb. Flow cytometry was used to assess the binding ability of soluble FITC-fibrinogen and JON/A-PE binding under resting conditions, using a range of platelet agonists: thrombin (0.12-1 U/mL); PAR-4 agonist peptide (100-300 µM); ADP (10 µM); ADP (10 µM) plus epinephrine (20 µM); and PMA (20 µM) stimulation (Figure 6-6A-D). When subjected to agonist stimulation, the wild-type and *Cc2*$^{-/-}$ platelets displayed equivalency in their ability to bind soluble FITC-fibrinogen. In addition, they showed a similar ability to bind with JON/A mAb, which detects the active conformation of integrin $\alpha_{IIb}\beta_3$ complex on murine platelets. In summary, the above results show that *Cc2*$^{-/-}$ platelets possess normal 'inside-out' integrin $\alpha_{IIb}\beta_3$ signalling properties.

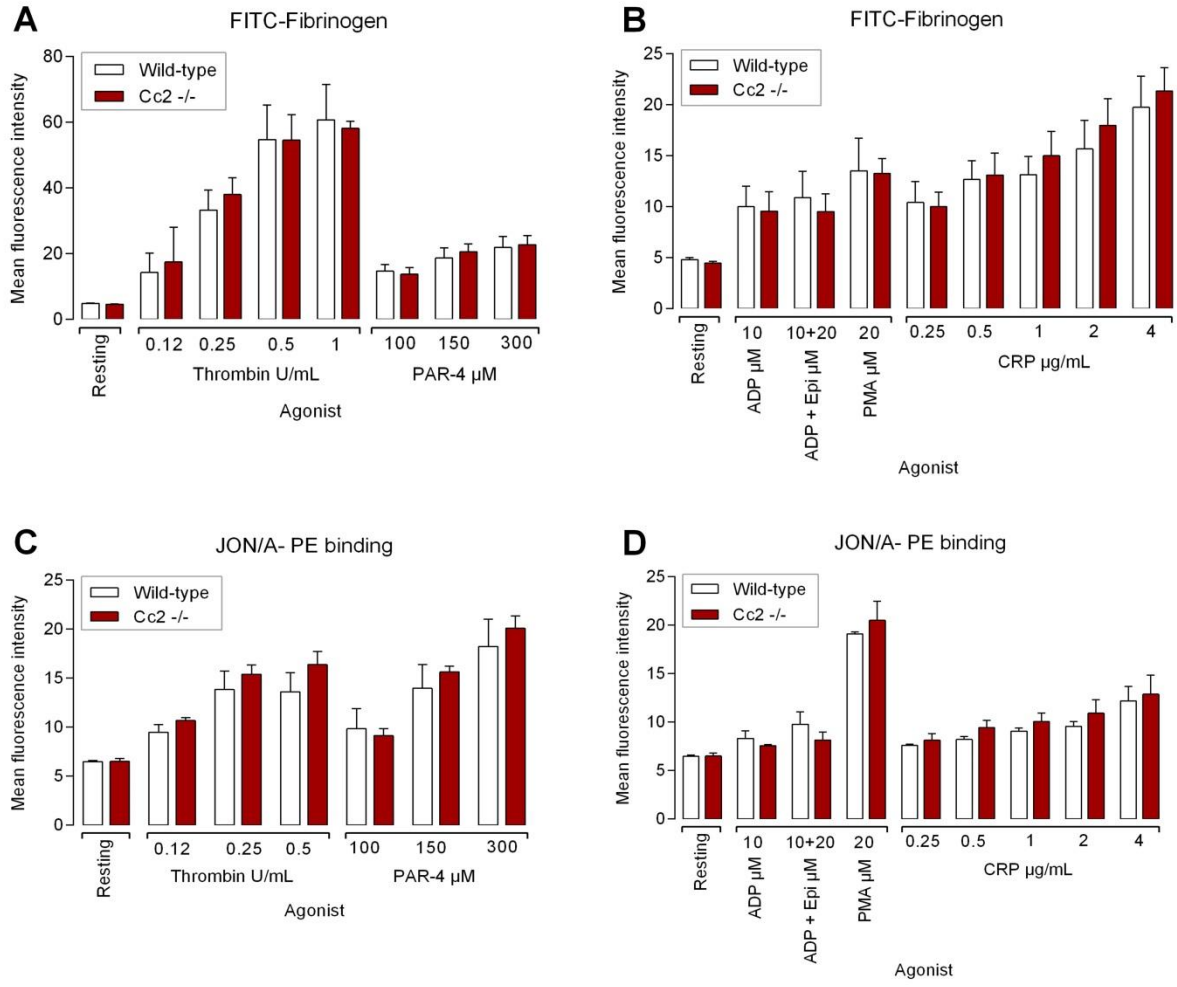

Figure 6-6: *Cc2*$^{-/-}$ platelets show normal soluble FITC-fibrinogen and JON/A mAb binding. (A-B) Flow cytometric analysis on a FACS Canto II analyser of FITC-conjugated fibrinogen binding to washed wild-type and *Cc2*$^{-/-}$ platelets stimulated by varying agonists including thrombin (0.12, 0.25, 0.5, 1 U/mL), PAR-4 agonist peptide (100, 150, 300 µM), 10 µM ADP, 10 µM ADP + 20 µM Epinephrine, 20 µM PMA or CRP (0.25, 0.5, 1, 2, 4, 8 µg/mL). Unstimulated platelets were used as control (resting). The assay samples were run in triplicates, and the data shown are representative of at least 4 independent experiments, and presented as MFI ± SEM. **(C-D)** JON/A-PE mAb binding in the absence or presence of agonists on wild-type and *Cc2*$^{-/-}$ platelets was also determined as described in panel A-B (With the only exception that thrombin was used at 0.12-0.5 U/mL). The assay samples were run in triplicate, and the data shown are representative of at least 4 independent experiments, and presented as MFI ± SEM.

6.3 Discussion

Previous studies have demonstrated a possible functional relationship between PECAM-1 or CEACAM1 with β_3 integrins in platelets or even other cell types [174, 282-284]. However, there is no direct evidence to support CEACAM2 roles in modulation of integrin functions in any cell type including platelets. Therefore, this chapter looked for evidence of any physiological relationship between CEACAM2 and integrin $\alpha_{IIb}\beta_3$ in platelets. This chapter has examined the functional properties of *Cc2*$^{-/-}$ platelets during a number of processes dependent on integrin $\alpha_{IIb}\beta_3$, and examined *Cc2*$^{-/-}$ platelets during the adhesion and signalling phases of haemostasis. The results suggested that CEACAM2 works in a comparable way to PECAM-1 and CEACAM1. This chapter shows that CEACAM2 can positively regulate platelet functions that incorporate integrin $\alpha_{IIb}\beta_3$-mediated processes. In addition, *Cc2*$^{-/-}$ mice had significantly longer tail bleed times and a higher volume of blood loss, indicating an underlying vascular or platelet defect compared to wild-type mice (Figure 6-1A-B). Finally, this chapter demonstrates that CEACAM2 is essential for optimal integrin $\alpha_{IIb}\beta_3$-mediated functioning in platelets (Figure 6-4). In conclusion, it is possible to propose that CEACAM2 appears to play an important role during thrombosis and haemostasis, by mediating adhesion and signalling events.

Platelets derived from *Cc2*$^{-/-}$ mice were used for identifying and defining the regulating function of CEACAM2 during integrin $\alpha_{IIb}\beta_3$-mediated processes. The data showed that *Cc2*$^{-/-}$ platelets contributed to a number of defects in the post-ligand occupancy events of integrin $\alpha_{IIb}\beta_3$. These included delays in kinetics of clot retraction and impeded cytoskeletal reorganisation associated with platelet spreading on immobilised fibrinogen matrix (Figures 6-3 and 6-4). However, as described in chapter 3, *Cc2*$^{-/-}$ platelets showed increased binding to type I collagen (Figure 3-8). Further analysis showed that these spreading defects were largely negated during stimulation by agonists such as PAR-4 agonist peptide, ADP and PMA (Figure

6-4C-D). In contrast, the equivalent binding of soluble FITC-fibrinogen and JON/A monoclonal antibody showed that 'inside-out' integrin $\alpha_{IIb}\beta_3$-mediated signalling processes were normal in *Cc2*$^{-/-}$ platelets (Figure 6-6). These results further support the notion that CEACAM2 expressed on platelets influences optimal integrin $\alpha_{IIb}\beta_3$-mediated functions during haemostasis and thrombosis. Overall, it is possible to suggest that CEACAM2 regulates lateral integrin clustering (avidity) events during the cell adhesion process, rather than moderating the conformation during integrin activation (affinity).

Previous studies have demonstrated that PECAM-1 or CEACAM1 (unpublished data) modulates integrin functions, and the exact mechanism behind this regulation is known [8]. However, because no previous studies used *Ceacam2*–deficient mice to search for abnormalities in the integrin $\alpha_{IIb}\beta_3$ function or activation processes, this chapter could provide a unique and detailed insight into how deletion of CEACAM2 affects integrin $\alpha_{IIb}\beta_3$ function properties in murine platelets. To separate 'outside-in', integrin $\alpha_{IIb}\beta_3$ clustering mechanisms from 'inside-out', integrin $\alpha_{IIb}\beta_3$ conformation changes, and eliminate the confounding effects of nuclear signalling, this study used terminally differentiated anucleate platelets. Contrary to the initial premise, CEACAM2–deficient platelets displayed no integrin activation defects. 'Outside-in' integrin $\alpha_{IIb}\beta_3$ function events were affected, and the *Ceacam2*–deficient platelet defects caused restricted filopodia extension and spreading on integrin $\alpha_{IIb}\beta_3$–dependent matrix, fibrinogen (Figure 6-5). In addition, *Ceacam2*–deficient platelets displayed inhibited clot retraction (Figure 6-2), a process that uses retractile forces to bind the active integrin $\alpha_{IIb}\beta_3$ complex to actin-myosin cytoskeletal proteins.

Previous studies showed that PECAM-1 or CEACAM1, a related member of the Ig-ITIM superfamily, negatively regulate collagen GPVI-FcR γ-chain signalling pathways [187, 219].

Under *in vitro* flow physiological condition, when blood perfused across a type I collagen matrix, PECAM-$1^{-/-}$ platelets formed a larger thrombus over time than wild-type platelets [219]. The PECAM-1 and CEACAM1–deficient mice also developed larger thrombi *in vivo*, when subjected to laser-induced vascular injury [178, 187, 219, 233, 234, 285, 286]. In contrast, PECAM-1 plays a positive modulation role during platelet integrin $\alpha_{IIb}\beta_3$-mediated functions [8]. These studies suggested the presence of at least two PECAM-1 and CEACAM1 regulation mechanisms in platelets. The first mechanism involves negative modulation for ITAM-coupled signalling pathways that involve the collagen GPVI-FcR γ-chain and low-affinity IgG receptor, FcγRIIa. The second mechanism is positive modulation of integrin $\alpha_{IIb}\beta_3$-mediated processes. However, it is unclear if these mechanisms are general Ig-ITIM receptor signalling processes in platelets. This chapter revealed an alternative Ig-ITIM bearing receptor in platelets, CEACAM2, which positively modulates integrin $\alpha_{IIb}\beta_3$-mediated functions. The results also implied a functional connection between Ig-ITIM bearing receptors and integrin $\alpha_{IIb}\beta_3$ in platelets, although the exact nature of the molecular interactions between CEACAM2 and integrin $\alpha_{IIb}\beta_3$ in platelets remains unclear. In addition, it is possible to propose that, because CEACAM2-2L is a heterophilic adhesion molecule while CEACAM1-4L is both homophilic and heterophilic, it may have a function in mediating platelet interactions.

These research results suggest an interesting anomaly. The previous study implied that CEACAM2 negatively modulates interactions between platelets and collagen/GPVI-FcR γ-chain interaction (Chapter 3) [287]. This is in distinct contrast to this research, which found that CEACAM2 is a positive regulator during integrin $\alpha_{IIb}\beta_3$-mediated processes. However, it is important to note that CEACAM-2 has very similar ITIM properties to PECAM-1 and CEACAM1, related Ig-ITIM superfamily members. For example, PECAM-$1^{-/-}$ mice also displayed prolonged bleeding times due to the deficiency in endothelial PECAM-1 [288].

Likewise, platelet PECAM-1 acted as a positive regulator of integrin $\alpha_{IIb}\beta_3$-mediated functions *in vitro* [8]. Moreover, *Cc1*$^{-/-}$ mice have prolonged bleeding time due to the deficiency in platelet *Ceacam1*. CEACAM1 acts as a positive regulator of integrin $\alpha_{IIb}\beta_3$-mediated functions (Unpublished data). As a result, the active functions of PECAM-1, CEACAM1 or CEACAM2, three members of the Ig-ITIM superfamily, may be moderated by homophilic or heterophilic ligand interactions, higher rates of expression, or modifications to the process of cellular distribution to areas of cellular contact in platelets. These changes could modulate the adhesion and signalling events in platelets that affect *in vivo* thrombogenesis.

The mechanism is not known as to why *Cc2*$^{-/-}$ platelets show a delay in the kinetics of 'outside-in' integrin $\alpha_{IIb}\beta_3$ signalling event. The possible reasons for that could be related to ligand clustering interactions or receptor engagement being compromised in some way or signalling strength being reduced that downregulated integrin $\alpha_{IIb}\beta_3$-dependent events.

Previous studies did not reveal any integrin abnormality in *Ceacam2*-deficient mice, so it was important to establish if CEACAM2 played a significant role in regulating platelet integrin $\alpha_{IIb}\beta_3$. This would involve assessing how CEACAM2 deletion affects the modulation, conformation and clustering properties of integrin $\alpha_{IIb}\beta_3$ in murine platelets. This research revealed a new role for CEACAM2, as a positive modulator of integrin $\alpha_{IIb}\beta_3$-mediated function, and confirmed that platelet CEACAM2 plays a crucial role throughout the adhesion and signalling events that affect haemostasis and thrombosis.

7 Chapter Seven: General discussion and future directions

7.1 General discussion

In this thesis, evidence is provided for a unique platelet function regulator model for CEACAM2 which was defined as a novel platelet immunoreceptor that negatively regulates GPVI platelet-collagen interactions and thrombus formation both *in vitro* and *in vivo*. In addition, CEACAM2 was also defined as a negative regulator of the rhodocytin-CLEC-2-mediated signalling pathway in platelets. Furthermore, CEACAM2 promotes as a positive regulator of integrin $\alpha_{IIb}\beta_3$-mediated platelet functions.

As described in Chapter 3, CEACAM2 shares some similarities with CEACAM1 in structure, but differs in the number of extracellular Ig-Domains (CEACAM1 contains 4 Ig-Domains while CEACAM2 contains 2 Ig-Domains) and in the ligand binding properties of their distal variable N-terminal Ig-Domain. There are two CEACAM genes in mouse (CEACAM1 and CEACAM2) but their role in humans appears to be carried by the CEACAM1 gene [185]. Both CEACAM2 and CEACAM1 are transmembrane receptors and contain identical ITIMs in their cytoplasmic domains.

In this thesis, CEACAM2 was shown to be expressed on the surface and in intracellular pools as the CEACAM-2L (CC2-2L) isoform in murine platelets (Figure 3-1B). As CEACAM1 and CEACAM2 genes are located within 50 centimorgan distal on the mouse chromosome 7, it was important that CEACAM1 expression was confirmed to be unaffected by deletion of CEACAM2 (Figure 3-2A), including upregulation of CEACAM1 surface expression following agonist stimulation using thrombin, PAR-4 agonist peptide and CRP (Figure 3-2D).

In this thesis, it has been shown that deletion of CEACAM2 resulted in GPVI/FcRγ-chain signalling pathway enhancement by enhanced collagen- and CRP-mediated platelet aggregation but not GPCR agonist signalling pathways (Figure 3-3, Figure 3-4 and Figure 3-5).

Furthermore, deletion of CEACAM2 also enhanced CRP-mediated alpha and dense granule release but not thrombin or PAR-4 agonist peptide alpha or dense granule release (Figure 3-6 and Figure 3-7). However, the procoagulant potential of platelet exposure of phosphatidyl serine was unaffected as shown by Annexin V-FITC binding (Figure 3-9). Likewise, CEACAM2 deficiency enhanced static adhesion of platelets to immobilised type I collagen (Figure 3-8). Finally, as shown in Figure 3-10B, deletion of CEACAM2 demonstrated hyper-tyrosine phosphorylation of collagen GPVI/FcRγ-chain signalling pathway components downstream including p-PLCγ2, p-Src (Tyr416) and p-Syk (Tyr352).

Based upon the results of this study, there does not appear to be evidence of redundancy as deletion of CEACAM2 from murine platelets resulted in a clear phenotype of enhanced collagen GPVI/FcRγ-chain signalling pathway. The phenotype observed could not be explained by alteration in any other platelet glycoproteins or alteration in expression of other Ig-ITIM inhibitory molecules in platelets, such as CEACAM1 and PECAM-1. Therefore, the global CEACAM2 knockout showed no compensatory mechanisms to account for the phenotype.

In a physiological setting, the presence of CEACAM2 will limit platelet-collagen adhesion signalling events to reduce the formation of thrombi on type I collagen. In the clinical setting of atherosclerotic plaque rupture where type I collagen is exposed, CEACAM2 along with other Ig-ITIM inhibitory receptors, CEACAM1 and PECAM-1 will limit the development of pathological thrombi. The vascular endothelium releases negative regulators, NO and PGI_2 but if injury or disease occurs the bioactive mediators NO and PGI_2 are reduced [74]. These compounds inhibit platelet aggregation through auto-regulation, but influence the subsequent platelet-platelet binding rather than the initial interaction with exposed collagen. Therefore, the natural negative inhibitory mechanisms of adhesion are provided in platelets molecules by CEACAM2, CEACAM1 and PECAM-1 [74]. On the other hand, in the absence of CEACAM2

at the site of injury, excessive thrombus formation will be formed faster, larger and even more stable (Figure 7-1). As a result, this thesis is one of the few projects that identifies a potential natural inhibitor of platelet activation in the presence of collagen. Because collagen is a powerful instigator of platelet adhesion and thrombus growth, this research could be used to develop a CEACAM2 based approach to clinically mitigate thrombotic complications associated with CVD.

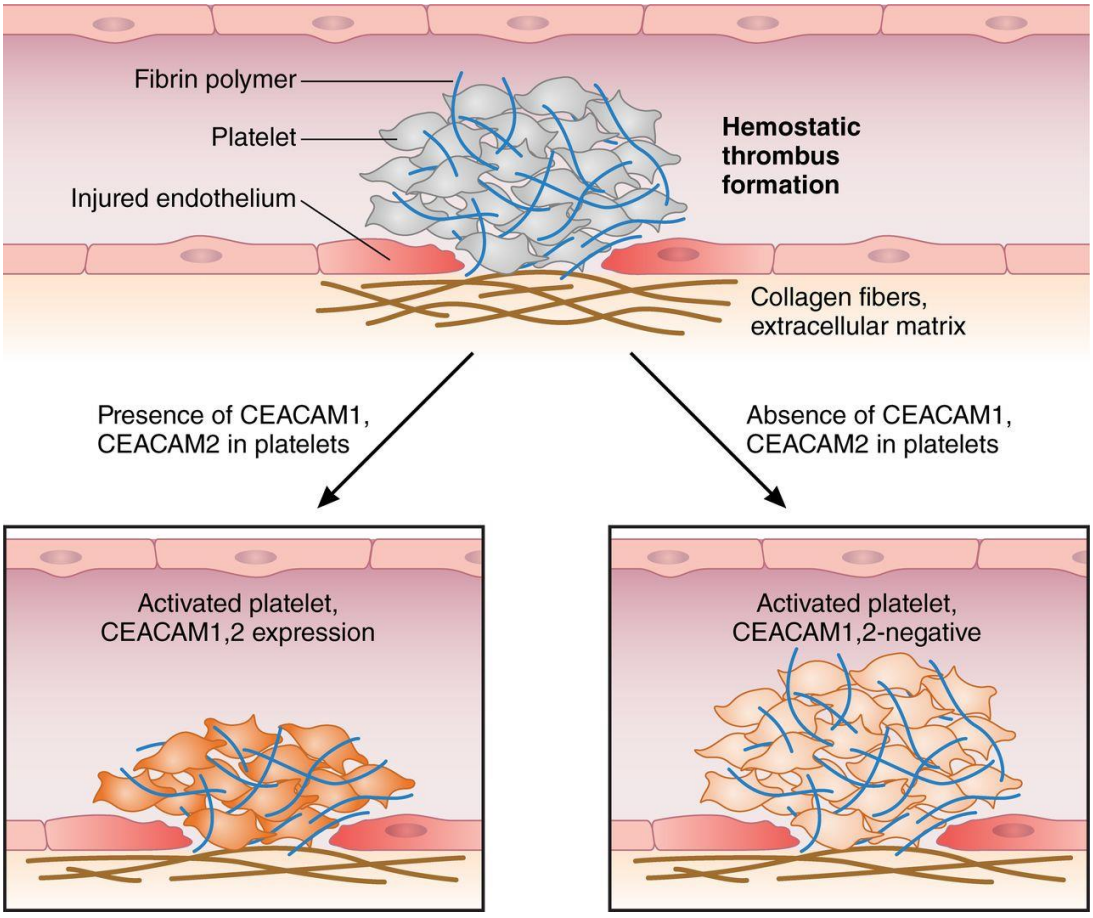

Figure 7-1: Haemostatic thrombus formation. Thrombus formation is initiated by platelet-collagen interactions at the site of endothelium injury or trauma. In the presence of Ig-ITIM receptors such as CEACAM2 or CEACAM1, thrombus formation is reduced while in the absence of CEACAM2 or CEACAM1, thrombus growth and stability is enhanced. CEACAM2 negatively regulate platelet-collagen interaction and thrombus growth *in vitro* and *in vivo*. Adapted from [289].

Chapter 4 of this thesis discusses the role of CEACAM2 in CLEC-2 contact-dependent platelet activation and signalling pathway in platelets. The results showed that in the absence of CEACAM2, hyper-responsiveness to the CLEC-2 selective agonist, rhodocytin which induced amplified platelet aggregation responses (Figure 4-1). Likewise, deletion of CEACAM2 enhanced rhodocytin induced alpha and dense granule release (Figure 4-2 and Figure 4-3; respectively). Similarly, deletion of CEACAM1 also enhanced rhodocytin induced alpha and dense granule release (Figure 4-4 and Figure 4-5; respectively). Furthermore, deletion of CEACAM2 enhanced tyrosine phosphorylation of CLEC-2 signalling pathway components including p-PLCγ2 and p-Syk (Tyr352) (Figure 4-6 and Figure 4-7; respectively) but not p-Src (Tyr416) (Figure 4-8). Thus, CEACAM2 and CEACAM1 negatively regulate the CLEC-2 signalling pathway in murine platelets. Further studies would be required to show whether human CEACAM1 also regulates the CLEC-2 signalling pathway, although as CEACAM2 in mouse platelets is thought to be analogous to CEACAM1-2L in human platelets, this may well be the case.

The results in Chapter 5 of this thesis discuss in great detail the role of CEACAM2 in contact-dependent platelet adhesion under *in vitro* and *in vivo* flow conditions. Previous research was unclear about which of these collagen receptors adopts the primary role during platelet activation, but studies using platelets lacking GPVI have proposed that GPVI is a potent agent for enhancing platelet activation and the growth of stable thrombi [290]. The idea that CEACAM2 can restrict thrombus growth was further supported by a series of *in vitro* studies assessing platelet adhesion. CEACAM2 deficiency enhanced *in vitro* thrombus formation growth over time on immobilised type I collagen under arterial flow conditions (Figure 5-1). By using $FeCl_3$ induced vascular injury of mesenteric arterioles, deletion of CEACAM2 displayed enhanced thrombus growth and stability *in vivo* (Figure 5-2 and Figure 5-3). Similarly, deletion

of CEACAM2 showed enhanced thrombus growth and stability *in vivo* using laser induced vascular injury of cremaster muscle arterioles (Figure 5-4 and Figure 5-5). Antibody depletion of GPVI in conjunction with absence of CEACAM2 displayed a reversal in the thrombus stability phenotype (Figure 5-6E).

In our study of microvascular thrombosis, $FeCl_3$-induced vascular injury was used to expose type I collagen, so that platelet-collagen interactions could be studied in the absence of CEACAM2 *in vivo.* Therefore, deletion of CEACAM2 enhanced thrombus growth and stability indicating that it can negatively regulate platelet-collagen interactions *in vivo* and that it is partially dependent on the collagen GPVI/FcRγ-chain. In contrast, the laser induced injury model is an inflammatory thrombin: tissue factor model that does not expose type I collagen [223, 224, 275]. This issue was first highlighted by Rosen et al. during studies that used laser-induced injury on blood vessels located in the mouse ear [291]. Therefore, based on the results of this study raises the possibility that CEACAM2 may also negatively regulate the thrombin signalling pathway. Conversely, as shown in Chapter 3, washed platelets showed equivalent thrombin aggregation, alpha and dense granule release at different concentrations in the presence or absence of CEACAM2 (Figure 3-5; 3-6 and 3-7). Further studies will be required to examine this possible mechanism in platelets.

To highlight the main similarity and differences between Ig-ITIM receptors in literature, laser induced injury of cremaster muscle arterioles in the PECAM-1 knockout mice revealed larger thrombi that were more stable [178]. Likewise, Cicmil et al. demonstrated that PECAM-1 could negatively regulate thrombin signalling pathway in human platelets [234]. This may highlight a role for CEACAM2 in regulating the thrombin signalling pathway. Previously, an *in vitro* flow studies on type I collagen under arterial flow was done by Jones et al. who found that in the absence of PECAM-1 there was increased kinetics thrombus formation over time [219].

Similarly, *in vitro* flow studies by Wong et al. displayed larger thrombus volume on type I collagen in the absence of CEACAM1 than in control wild-type mice [187]. Therefore, the results for *Cc2*$^{-/-}$ mice correlate with the previous studies on PECAM-1$^{-/-}$ and *Cc1*$^{-/-}$ mice. Thus, these studies highlight the importance of Ig-ITIM receptors in relation to negative regulation of platelet-collagen interactions and thrombus formation *in vitro* and *in vivo*. Apart from platelet CEACAM2 regulating collagen interactions involving collagen GPVI, thrombus growth and stabilisation, it also appears to negatively regulate the CLEC-2 signalling pathway. Further studies with antibody depletion of platelet CLEC-2 to examine thrombus formation and stabilisation will be required.

The results in Chapter 6 presented some interesting findings about the role of CEACAM2 in 'outside-in' integrin $\alpha_{IIb}\beta_3$-mediated signalling pathways. The major findings in the absence of CEACAM2 were that *Cc2*$^{-/-}$ mice had increased *in vivo* tail bleeding times, and volume of blood lost (Figure 6-1), delayed kinetics of clot retraction (Figure 6-2A-B) and delayed static adhesion on immobilised fibrinogen over time (Figure 6-3). Furthermore, lack of CEACAM2 restricted cytoskeletal reorganisation that delayed platelet spreading on fibrinogen without agonist stimulation (Figure 6-4). In fact, this spreading defect was corrected by agonist stimulation with PAR-4 agonist peptide, ADP and PMA (Figure 6-4). Therefore, CEACAM2 deficiency leads to an 'outside-in' integrin $\alpha_{IIb}\beta_3$-mediated functional defect but not 'inside-out' integrin $\alpha_{IIb}\beta_3$-mediated functional defect. Thus, this suggests that when CEACAM2 is normally present it acts as a positive regulator to optimise 'outside-in' integrin $\alpha_{IIb}\beta_3$-mediated functions in platelets. Similar findings have been observed with *Cc1*$^{-/-}$ mice (Unpublished data). Furthermore, a study by Wee et al. demonstrated that PECAM-1 act as a positive regulator to optimise 'outside-in' integrin $\alpha_{IIb}\beta_3$-mediated functions in platelets [8].

This defect may suggest that the clustering of integrin $\alpha_{IIb}\beta_3$ (fibrinogen ligand occupied state) is compromised to a certain extent by the absence of CEACAM2, CEACAM1 or PECAM-1. The exact mechanism is not clearly understood at this stage and warrants further investigation.

7.2 Conclusion

In this thesis, several studies have demonstrated the presence of a novel and new ITIM-bearing receptor, CEACAM2 in murine platelets. It has been shown that using an innovative tool of a *Ceacam2*-deficiency mouse model has revealed how CEACAM2 negatively regulates hemi (ITAM-bearing) GPVI and CLEC-2 pathways and thrombus growth *in vitro* and *in vivo*. This may potentially have therapeutic ramifications for the treatment of CVD. The presence of CEACAM2 can restrict adhesive signalling events and thrombus formation to diminish the risk of atherosclerosis by reducing the thrombus volume, size of thrombi, delaying the rate of thrombus growth and promoting thrombus instability. The *Ceacam2*-deficient murine platelets also suggested that the Ig-ITIM member, CEACAM2 is a crucial component of platelet adhesion, activation and aggregation, influencing the 'outside-in' integrin $\alpha_{IIb}\beta_3$-mediated function events. Overall, the results highlight the crucial function of CEACAM2 in platelet-collagen interactions, thrombus growth, CLEC-2 signalling, and integrin $\alpha_{IIb}\beta_3$-mediated platelet functions. Therefore, upregulating Ig-ITIM superfamily member expression in the context of atherosclerosis may offer an avenue for targeting treatments and lowering the risk of CVD problems.

7.3 Future directions

The studies carried out in this thesis demonstrate that CEACAM2 negatively regulates CLEC-2 signalling pathway in murine platelets. As in human platelets the role of CEACAM2 is

carried by CEACAM1 gene, therefore, further studies will be required to examine the role of CEACAM1 via the CLEC-2 mediated signalling pathway in murine and human platelets. Moreover, further studies will be required involving depletion of platelet CLEC-2 using specific anti-CLEC-2 antibody INUI (200 µg) to examine the role of CEACAM2 or CEACAM1 in thrombus formation and stabilisation under *in vitro* flow and *in vivo* in the presence of control wild-type mice.

Based upon the results of this thesis, the deletion of CEACAM2 showed normal platelet aggregation responses, alpha and dense granule secretion following thrombin stimulation compared to control wild-type mice. Interestingly and conversely, the deletion of CEACAM2 enhanced thrombus growth compared to wild-type arterioles. Based on the fact that laser induced injury is involves the inflammatory thrombin: tissue factor pathway, more work is required to understand the role of CEACAM2 regulation of thrombin signalling pathways in *Cc1*$^{-/-}$ and *Cc2*$^{-/-}$ mice platelets. In addition, further work at cellular level will be required involving measurement of global tyrosine phosphorylation over time or PLCγ2, Src and Syk tyrosine phosphorylation upon thrombin-stimulation for 0-90 seconds by immunoprecipitation and Western blot analysis with anti-phosphotyrosine antibodies.

Future work on how CEACAM2 and the integrin $\alpha_{IIb}\beta_3$ tyrosine phosphorylation signalling mechanism influence 'outside-in' integrin $\alpha_{IIb}\beta_3$-mediated signalling events will be warranted. The integrin β_3 cytoplasmic domain undergoes tyrosine phosphorylation which, in turn, prompts the activation of cytosolic proteins myosin and adaptor protein Src homology collagen (Shc), together with linkage with actin which are necessary for clot retraction and platelet stimulation respectively. However, exactly how ^{125}FAK undergoes tyrosine phosphorylation after the integrin $\alpha_{IIb}\beta_3$ clustering prompted by platelet aggregation is unclear.

This crucial stage of the process occurs early during integrin β_3 tyrosine phosphorylation and the recruitment of Src family kinase members, particularly c-Src and Syk. Intensive studies need to be performed to examine the role of CEACAM during 'outside-in' integrin $\alpha_{IIb}\beta_3$-mediated signalling pathways upon activation or adhered on immobilised fibrinogen (100 µg/mL). Measurement of PLCγ2, Src and Syk tyrosine phosphorylation are the hardest experiments because when integrin $\alpha_{IIb}\beta_3$ bind to fibrinogen leads to ligand clustering interactions or receptor engagement being compromised or the strength of signalling being reduced in some way. Furthermore, a number of potential physical associations and functions: the physical interaction of CEACAM2 and integrin $\alpha_{IIb}\beta_3$ in murine platelets is subject to further studies.

8 Chapter Eight: Bibliography

References

1. National Heart Foundation of Australia. Cardiovascular disease (CVD) Data and statistics [cited 2014 30/10]; Available from: http://www.heartfoundation.org.au/information-for-professionals/data-and-statistics/Pages/default.aspx.

2. Bergmeier, W., K. Rackebrandt, W. Schröder, H. Zirngibl, and B. Nieswandt, Structural and functional characterization of the mouse von Willebrand factor receptor GPIb-IX with novel monoclonal antibodies. Blood, 2000. **95**(3): p. 886-893.

3. Nieswandt, B., W. Bergmeier, V. Schulte, K. Rackebrandt, J.E. Gessner, and H. Zirngibl, Expression and function of the mouse collagen receptor glycoprotein VI is strictly dependent on its association with the FcRγ chain. Journal of Biological Chemistry, 2000. **275**(31): p. 23998-24002.

4. Australian Institute of Health Welfare. Heart, Stroke and Vascular Diseases-Australian Facts 2011 [cited 2014 30/10]; Available from: http://www.aihw.gov.au/publication-detail/?id=10737418510.

5. Highlander, P. and G.P. Shaw, Current pharmacotherapeutic concepts for the treatment of cardiovascular disease in diabetics. Therapeutic Advances in Cardiovascular Disease, 2010. **4**(1): p. 43-54.

6. Kostyak, J.C., M.U. Naik, and U.P. Naik, Calcium- and integrin-binding protein 1 regulates megakaryocyte ploidy, adhesion, and migration. Blood, 2012. **119**(3): p. 838-46.

7. Jones, C.I., N.E. Barrett, L.A. Moraes, J.M. Gibbins, and D.E. Jackson, Endogenous inhibitory mechanisms and the regulation of platelet function, J.M. Gibbins and M.P. Mahaut-Smith, Editors. 2012. p. 341-366.

8. Wee, J.L. and D.E. Jackson, The Ig-ITIM superfamily member PECAM-1 regulates the "outside-in" signaling properties of integrin αIIbβ3 in platelets. Blood, 2005. **106**(12): p. 3816-3823.

9. Michelson, A.D., Platelets. 2nd ed. 2007, MA, USA: Elsevier Science & Technology Books: Burlington.

10. Thon, J.N. and J.E. Italiano, Platelet formation. Seminars in Hematology, 2010. **47**(3): p. 220-226.

11. Brill, A., H. Elinav, and D. Varon, Differential role of platelet granular mediators in angiogenesis. Cardiovascular Research, 2004. **63**(2): p. 226-235.

12. Scheld, W. and M. Sande, Endocarditis and intravascular infections. Principles and Practice of Infectious Diseases, 1995. **1**: p. 740-783.

13. Vinter, D.W., T.W. Wakefield, W.E. Burkel, L.M. Graham, W.M. Whitehouse Jr, J.W. Ford, et al., Radioisotope-labeled platelet studies and infection of vascular grafts. Journal of Vascular Surgery, 1984. **1**(6): p. 921-923.

14. Osler, W., An account of certain organisms occurring. Proceedings of the Royal Society of London, 1874. **22**: p. 391–398.

15. Bizzozero, G., Su di un nuovo elemento morfologico del sangue dei mammiferi e della sua importanza nella trombosi e nella coagulazione. L'Osservatore, 1881. **17**: p. 785–787.

16. Bizzozero, J., On a new blood particle and its role in thrombosis and blood coagulation. Arch Pathol Anat Physiol Klin Med., 1882. **90**: p. 261–332.

17. Wright, J.H., The origin and nature of blood plates. Boston Medical and Surgical Journal, 1906. **154**: p. 643–645.

18. O'Connell SM, Impeduglia T, Hessler K, Wang XJ, Carroll RJ, and D. H, Autologous platelet-rich fibrin matrix as cell therapy in the healing of chronic lower-extremity ulcers. Wound Repair and Regeneration, 2008. **16**(6): p. 749–756.

19. Sánchez M, Anitua E, Azofra J, Andía I, Padilla S, and M. I, Comparison of surgically repaired Achilles tendon tears using platelet-rich fibrin matrices. American Journal of Sports Medicine, 2007. **35**(2): p. 245–251.

20. Kaushansky, K., Historical review: megakaryopoiesis and thrombopoiesis. Blood, 2008. **111**(3): p. 981-986.

21. Machlus, K.R. and J.E. Italiano Jr, The incredible journey: From megakaryocyte development to platelet formation. Journal of Cell Biology, 2013. **201**(6): p. 785-796.

22. Italiano, J.J. and J.H. Hartwig, Megakaryocyte Development and Platelet Formation, in Platelets, 3rd edition. 2007, Elsevier: Amsterdam. p. 23-44.

23. Long, M.W., Megakaryocyte differentiation events. Seminars in Hematology, 1998. **35**(3): p. 192-199.

24. Coller, B.S., Foreword: A Brief History of Ideas about Platelets in Health and Disease, in Platelets, 3rd edition. 2007, Elsevier: Amsterdam. p. xxiii-xlii.

25. de Botton, S., S. Sabri, E. Daugas, Y. Zermati, J. Guidotti, O. Hermine, et al., Platelet formation is the consequence of caspase activation within megakaryocytes. Blood, 2002. **100**(4): p. 1310-1317.

26. Gordge, M.P., Megakaryocyte apoptosis: Sorting out the signals. British Journal of Pharmacology, 2005. **145**(3): p. 271-273.

27. Radley, J.M. and C.J. Haller, Fate of senescent megakaryocytes in the bone marrow. British Journal of Haematology, 1983. **53**(2): p. 277-287.

28. Falcieri, E., A. Bassini, S. Pierpaoli, F. Luchetti, L. Zamai, M. Vitale, et al., Ultrastructural characterization of maturation, platelet release, and senescence of human cultured megakaryocytes. Anatomical Record, 2000. **258**(1): p. 90-99.

29. Zauli, G., M. Vitale, E. Falcieri, D. Gibellini, A. Bassini, C. Celeghini, et al., In vitro senescence and apoptotic cell death of human megakaryocytes. Blood, 1997. **90**(6): p. 2234-2243.

30. Kaluzhny, Y. and K. Ravid, Role of apoptotic processes in platelet biogenesis. Acta Haematologica, 2004. **111**(1-2): p. 67-77.

31. De Botton, S., S. Sabri, E. Daugas, Y. Zermati, J.E. Guidotti, O. Hermine, et al., Platelet formation is the consequence of caspase activation within megakaryocytes. Blood, 2002. **100**(4): p. 1310-1317.

32. Kaluzhny, Y., G. Yu, S. Sun, P.A. Toselli, B. Nieswandt, C.W. Jackson, et al., BclxL overexpression in megakaryocytes leads to impaired platelet fragmentation. Blood, 2002. **100**(5): p. 1670-1678.

33. Sanz, C., I. Benet, C. Richard, B. Badia, E.J. Andreu, F. Prosper, et al., Antiapoptotic protein Bcl-xL is up-regulated during megakaryocytic differentiation of CD34+ progenitors but is absent from senescent megakaryocytes. Experimental Hematology, 2001. **29**(6): p. 728-735.

34. Battinelli, E. and J. Loscalzo, Nitric oxide induces apoptosis in megakaryocytic cell lines. Blood, 2000. **95**(11): p. 3451-3459.

35. Battinelli, E., S.R. Willoughby, T. Foxall, C.R. Valeri, and J. Loscalzo, Induction of platelet formation from megakaryocytoid cells by nitric oxide. Proceedings of the National Academy of Sciences of the United States of America, 2001. **98**(25): p. 14458-14463.

36. Kim, J.A., Y.J. Jung, J.Y. Seoh, S.Y. Woo, J.S. Seo, and H.L. Kim, Gene expression profile of megakaryocytes from human cord blood CD34+ cells ex vivo expanded by thrombopoietin. Stem Cells, 2002. **20**(5): p. 402-416.

37. Clarke, M.C.H., J. Savill, D.B. Jones, B.S. Noble, and S.B. Brown, Compartmentalized megakaryocyte death generates functional platelets committed to caspase-independent death. Journal of Cell Biology, 2003. **160**(4): p. 577-587.

38. Brown, S.B., M.C.H. Clarke, L. Magowan, H. Sanderson, and J. Savill, Constitutive death of platelets leading to scavenger receptor-mediated phagocytosis. A caspase-independent cell clearance program. Journal of Biological Chemistry, 2000. **275**(8): p. 5987-5996.

39. Kerrigan, S.W., M. Gaur, R.P. Murphy, S.J. Shattil, and A.D. Leavitt, Caspase-12: A developmental link between G-protein-coupled receptors and integrin αIIbβ3 activation. Blood, 2004. **104**(5): p. 1327-1334.

40. White, J.G., Platelet Stucture, in Platelets, 2nd edition. 2007, Elsevier: Amsterdam. p. 45-74.

41. Tocantins, L., The Mammalian Blood Platelet in Health and Disease. Medicine, 1938. **17**(2): p. 155-260.

42. White, J.G. and J.M. Gerrard, Ultrastructural features of abnormal blood platelets: a review. American Journal of Pathology, 1976. **83**(3): p. 589-632.

43. Zarbock, A., R.K. Polanowska-Grabowska, and K. Ley, Platelet-neutrophil-interactions: Linking hemostasis and inflammation. Blood Reviews, 2007. **21**(2): p. 99-111.

44. Rendu, F. and B. Brohard-Bohn, The platelet release reaction: Granules' constituents, secretion and functions. Platelets, 2001. **12**(5): p. 261-273.

45. Heinritz, D. (Wisc-Online). Platelet Structure [cited 2014 01/10]; Available from: https://www.wisc-online.com/learn/career-clusters/health-science/clt504/platelet-structure.

46. Rao, L.V.M. and Nigel Mackman, Factor VIIa and tissue factor – from cell biology to animal models. Thrombosis Research, 2010. **125**: p. S1-S3.

47. White, J.G. and W. Krivit, An ultrastructural basis for the shape change induced in platelets by chilling. Blood, 1967. **30**: p. 625-635.

48. White, J.G., Effects of colchicine and vinca alkaloidson human platelets: I. Influence on platelet microtubules and contractile function. American Journal of Pathology, 1968. **53**: p. 281-291.

49. White, J.G., Platelet glycosomes. Platelets, 1999. **10**(4): p. 242-246.

50. Reed, G.L., Platelet Secretion, in Platelets, 2nd edition. 2007. p. 309-318.

51. White, J.G., N.S. Key, R.A. King, and G.M. Vercellotti, The White platelet syndrome: a new autosomal dominant platelet disorder. Platelets, 2004. **15**(3): p. 173-84.

52. White, J.G., Ultrastructural studies of the gray platelet syndrome. Am J Pathol, 1979. **95**(2): p. 445-62.

53. Raccuglia, G. and Raccuglia, Gray platelet syndrome. American Journal of Medicine, 1971. **51**(6): p. 818-828.

54. van Nispen tot Pannerden, H., F. de Haas, W. Geerts, G. Posthuma, S. van Dijk, and H.F.G. Heijnen, The platelet interior revisited: electron tomography reveals tubular α-granule subtypes. Blood, 2010. **116**(7): p. 1147-1156.

55. Israels, S., E. McMillan, C. Robertson, S. Singhory, and A. McNicol, The lysosomal granule membrane protein, LAMP-2, is also present in platelet dense granule membranes. Thrombosis and Haemostasis, 1996. **75**(4): p. 623–629.

56. Febbraio, M. and R.L. Silverstein, Identification and characterization of LAMP-1 as an activation-dependent platelet surface glycoprotein. Journal of Biological Chemistry, 1990. **265**: p. 18531–18537.

57. Huizing, M., Y. Anikster, and W.A. Gahl, Pudlak syndrome and Chediak–Higashi syndrome: Disorders of vesicle formation and trafficking. Journal of Thrombosis and Haemostasis, 2001. **86**: p. 233-245.

58. Jobe, S.M., K.M. Wilson, L. Lorie Leo, A. Raimondi, J.D. Molkentin, S.R. Lentz, et al., Critical role for the mitochondrial permeability transition pore and cyclophilin D in platelet activation and thrombosis. Blood, 2008. **111**(3): p. 1257-1265.

59. White, J.G., N.S. Key, R.A. King, and G.M. Vercellotti, The white platelet syndrome: A new autosomal dominant disorder I. Structural abnormalities. Platelets, 2004. **15**: p. 173-184.

60. Ebbeling, L., C. Robertson, A. McNicol, and J.M. Gerrard, Rapid ultrastructural changes in the dense tubular system following platelet activation. Blood, 1992. **80**(3): p. 718-723.

61. Ezumi Y, Uchiyama T, and T. H, Molecular cloning, genomic structure, chromosomal localization, and alternative splice forms of the platelet collagen receptor glycoprotein VI. Biochemical and Biophysical Research Communications, 2000. **277**(1): p. 27–36.

62. Jackson, S.P., Arterial thrombosis-insidious, unpredictable and deadly. Nature Medicine, 2011. **17**(11): p. 1423-1436.

63. Veklich, Y. and J.W. Weisel. A Better Understanding of Clot Physiology Can Lead to More Effective Therapies. [cited 2014 01/10]; Available from: http://www.uphs.upenn.edu/news/News_Releases/jun05/clotfiber_photo.htm.

64. Cattaneo, M., The Platelet P2 Receptors, in Platelets, 2nd edition. 2007, Elsevier: Amsterdam. p. 201-220.

65. Hirsch, E., O. Bosco, P. Tropel, M. Laffargue, R. Calvez, F. Altruda, et al., Resistance to thromboembolism in PI3Kgamma-deficient mice. Federation of American Societies for Experimental Biology, 2001. **15**(11): p. 2019-2021.

66. Lopez-Vilchez, M. Diaz-Ricart, J.G. White, G. Escolar, and A. Galan, The platelet interior revisited: electron tomography reveals tubular α-granule subtypes. Cardiovascular Research, 2009. **84**(2): p. 309-316.

67. Garcia, A., S. Kim, K. Bhavaraju, S.M. Schoenwaelder, and S.P. Kunapuli, Role of phosphoinositide 3-kinase beta in platelet aggregation and thromboxane A2 generation mediated by Gi signalling pathways. Biochemical Journal, 2010. **429**(2): p. 369-377.

68. Hirata, T., F. Ushikubi, A. Kakizuka, M. Okuma, and S. Narumiya, Two thromboxane A2 receptor isoforms in human platelets. Opposite coupling to adenylyl cyclase with different sensitivity to Arg60 to Leu mutation. Journal of Clinical Investigation, 1996. **97**(4): p. 949-956.

69. Heemskerk, J.W.M., E.M. Bevers, and T. Lindhout, Platelet activation and blood coagulation. Thrombosis and Haemostasis, 2002. **88**(2): p. 186-193.

70. Doolittle, R.F., Step-by-step evolution of vertebrate blood coagulation. Cold Spring Harbor Symposia on Quantitative Biology, 2009. **74**: p. 35-40.

71. Bombeli, T. and D.R. Spahn, Updates in perioperative coagulation: Physiology and management of thromboembolism and haemorrhage. British Journal of Anaesthesia, 2004. **93**(2): p. 275-287.

72. Bhattacharjee, P. and D. Bhattacharyy, An Insight into the Abnormal Fibrin Clots-Its Pathophysiological Roles in Fibrinolysis and Thrombolysis, D.K.K. (Ed.), Editor. 2014, InTech.

73. Siemens. Full Hemostasis Cascade Overview. [cited 2014 02/10]; Available from: http://www.healthcare.siemens.com/hemostasis/hemostasis-online-campus/interactive-hemostasis-cascade.

74. Jones, C.I., N.E. Barrett, L.A. Moraes, J.M. Gibbins, and D.E. Jackson, Endogenous inhibitory mechanisms and the regulation of platelet function, in Platelets and Megakaryocytes, J.M. Gibbins and M.P. Mahaut-Smith, Editors. 2012, Springer. p. 341-366.

75. Rex, S. and J.E. Freedman, Inhibition of Platelet Function by the Endothelium, in Platelets, 2nd edition. 2007, Elsevier: Amsterdam. p. 251-280.

76. Bellamy, T.C. and J. Garthwaite, The receptor-like properties of nitric oxide-activated soluble guanylyl cyclase in intact cells. Molecular and Cellular Biochemistry, 2002. **230**(1-2): p. 165-176.

77. Freedman, J.E., J. Loscalzo, M.R. Barnard, C. Alpert, J.F. Keaney, and A.D. Michelson, Nitric oxide released from activated platelets inhibits platelet recruitment. Journal of Clinical Investigation, 1997. **100**(2): p. 350-356.

78. Aji, W., S. Ravalli, M. Szabolcs, X.C. Jiang, R.R. Sciacca, R.E. Michler, et al., L-arginine prevents xanthoma development and inhibits atherosclerosis in LDL receptor knockout mice. Circulation, 1997. **95**(2): p. 430-7.

79. Vane, J.R. and R.M. Botting, Pharmacodynamic profile of prostacyclin. American Journal of Cardiology, 1995. **75**: p. 3A–10A.

80. Atkinson, B., K. Dwyer, K. Enjyoji, and S.C. Robson, Ecto-nucleotidases of the CD39/NTPDase family modulate platelet activation and thrombus formation: Potential as therapeutic targets. Blood Cells, Molecules and Diseases, 2006. **36**(2): p. 217-222.

81. Robson, S.C., J. Sévigny, and H. Zimmermann, The E-NTPDase family of ectonucleotidases: Structure function relationships and pathophysiological significance. Purinergic Signalling, 2006. **2**(2): p. 409-430.

82. Davì, G. and C. Patrono, Platelet Activation and Atherothrombosis. New England Journal of Medicine, 2007. **357**(24): p. 2482-2494.

83. Bhatt, D.L. and E.J. Bhatt, Scientific and therapeutic advances in antiplatelet therapy. Nature Reviews Drug Discovery, 2003. **2**(1): p. 15-28.

84. Berent, R. and H. Sinzinger, "Aspirin - resistance"? A few critical considerations on definition, terminology, diagnosis, clinical value, natural course of atherosclerotic disease, and therapeutic consequences. Journal for Vascular Diseases, 2011. **40**(6): p. 429-38.

85. Topol, E., D.J. Moliterno, H.C. Herrmann, E.R. Powers, C.L. Grines, D.J. Cohen, et al., Comparison of Two Platelet Glycoprotein IIb/IIIa Inhibitors, Tirofiban and Abciximab, for the Prevention of Ischemic Events with Percutaneous Coronary Revascularization. The New England Journal of Medicine, 2001. **344**(25): p. 1888-1894.

86. Jones, J.L. and R.A. Walker, Integrins: A role as cell signalling molecules. Journal of Clinical Pathology-Molecular Pathology, 1999. **52**(4): p. 208-213.

87. Hynes, R.O., Integrins: Bi-Directional Signalling Machines. Cell, 2002. **110**(6): p. 673-687.

88. Shattil, S.J. and P.J. Newman, Integrins: dynamic scaffolds for adhesion and signaling in platelets. Blood, 2004. **104**(6): p. 1606-1615.

89. Plow, E.F., M.M. Pesho, and Y.Q. Ma, Integrin Alpha II-Beta b3, in Platelets, 2nd edition. 2007, Elsevier: Amsterdam. p. 165-178.

90. Plow, E.F., T.A. Haas, L. Zhang, J. Loftus, and J.W. Smith, Ligand binding to integrins. Journal of Biological Chemistry, 2000. **275**(29): p. 21785-21788.

91. Kloczewiak, M., S. Timmons, and J. Hawiger, Recognition site for the platelet receptor is present on the 15-residue carboxy-terminal fragment of the γ chain of human fibrinogen and is not involved in the fibrin polymerization reaction. Thrombosis Research, 1983. **29**(2): p. 249-254.

92. Plow, E.F., G. Marguerie, and M. Ginsberg, Fibrinogen, fibrinogen receptors, and the peptides that inhibit these interactions. Biochemical Pharmacology, 1987. **36**(23): p. 4035-4040.

93. Tranqui, L., A. Andrieux, G. Hudry Clergeon, J.J. Ryckewaert, S. Soyez, A. Chapel, et al., Differential structural requirements for fibrinogen binding to platelets and to endothelial cells. Journal of Cell Biology, 1989. **108**(6): p. 2519-2527.

94. Zhu, J., B.-H. Zhu, T. Luo, C. Xiao, N. Zhang, T. Nishida, et al., Structure of a Complete Integrin Ectodomain in a Physiologic Resting State and Activation and Deactivation by Applied Forces. Molecular Cell, 2008. **32**(6): p. 849-861.

95. Raborn, J., W. Wang, and B.H. Luo, Regulation of integrin αiIbβ3 ligand binding and signaling by the metal ion binding sites in the β i domain. Biochemistry, 2011. **50**(12): p. 2084-2091.

96. Campbell, I.D. and M.J. Humphries, Integrin structure, activation, and interactions. Cold Spring Harbor perspectives in biology, 2011. **3**(3).

97. Xiong, J.P., T. Stehle, B. Diefenbach, R. Zhang, R. Dunker, D.L. Scott, et al., Crystal structure of the extracettutar segment of integrin αVβ3. Science, 2001. **294**(5541): p. 339-345.

98. Xie, C., M. Shimaoka, T. Xiao, Schwab P, Klickstein L.B, and S. TA, The integrin alpha-subunit leg extends at a Ca2+ -dependent epitope in the thigh/genu interface upon activation. Proceedings of the National Academy of Sciences, 2004. **101**(43): p. 5422–5427.

99. Goschnick, M.W., L.-M. Lau, J.L. Wee, Y.S. Liu, P.M. Hogarth, L.M. Robb, et al., Impaired "outside-in" integrin αIIbβ3 signaling and thrombus stability in TSSC6-deficient mice. Blood, 2006. **108**(6): p. 1911-1918.

100. Calderwood, D.A., R. Zent, R. Grant, D.J. Rees, R.O. Hynes, and M.H. Ginsberg, The talin head domain binds to integrin beta subunit cytoplasmi ctails and regulates integrin activation. Journal of Biological Chemistry, 1999. **274**(40): p. 28071–28074.

101. Prévost, N. and S.J. Shattil, Outside-In Signaling by Integrin aIIbb3, in Platelets, 2nd edition. 2007, Elsevier: Amsterdam. p. 347-358.

102. Hantgan, R., D. Lyles, T.C. Mallett, M. Rocco, C. Nagaswami, and J. Weisel, Ligand binding promotes the entropy-driven oligomerization of integrin αIIbβ3. Journal of Biological Chemistry, 2003. **278**(5): p. 3417–3426.

103. Coller, B.S., Blockade of platelet GPIIb/IIIa receptors as an antithrombotic strategy. Circulation, 1995. **92**(9): p. 2373-2380.

104. Zucker, M.B., J.H. Pert, and M.W. Hilgartner, Platelet function in a patient with thrombasthenia. Blood, 1966. **28**(4): p. 524-534.

105. Flood, V., F.L. Flood, L. Johnson, G. Boshkov, D. Thomas, A. Nugent, et al., Sustained engraftment post bone marrow transplant despite anti-platelet antibodies in Glanzmann thrombasthenia. Pediatric Blood & Cancer, 2005. **45**(7): p. 971-975.

106. Hodivala-Dilke, K.M., K.P. McHugh, D.A. Tsakiris, H. Rayburn, D. Crowley, M. Ullman-Cullere, et al., Beta3-integrin-deficient mice are a model for Glanzmann thrombasthenia showing placental defects and reduced survival. Journal of Clinical Investigation, 1999. **103**(2): p. 229-238.

107. Nurden, A.T. and P. Nurden, Inherited Disorders of Platelet Function, in Platelets, 2nd editiion. 2007, Elsevier: Amsterdam. p. 1029-1150.

108. Knight, C.G., L.F. Morton, A.R. Peachey, D.S. Tuckwell, R.W. Farndale, and M.J. Barnes, The collagen-binding A-domains of integrins alpha(1)beta(1) and alpha(2)beta(1) recognize the same specific amino acid sequence, GFOGER, in native (triple-helical) collagens. Journal of Biological Chemistry, 2000. **275**(1): p. 35-40.

109. Clemetson, K.J. and J.M. Clemetson, Platelet Receptors, in Platelets, 2nd edition. 2007, Elsevier: Amsterdam. p. 117-144.

110. Luo, B.-H., C. Carman, and T. Springer, Structural basis of integrin regulation and signaling. Annual Review of Immunology, 2007. **25**: p. 619-647.

111. Miller, M.W., S. Basra, D.W. Kulp, P.C. Billings, S. Choi, M.P. Beavers, et al., Small-molecule inhibitors of integrin α2β1 that prevent pathological thrombus formation via an allosteric mechanism. Proceedings of the National Academy of Sciences of the United States of America, 2009. **106**(3): p. 719-724.

112. Piguet, P.F., C. Vesin, and A. Rochat, β2 Integrin modulates platelet caspase activation and life span in mice. European Journal of Cell Biology, 2001. **80**: p. 171-177.

113. Andrews, R.K., M.C. Berndt, and J.A. López, The Glycoprotein Ib-IX-V Complex, in The Platelets, 2nd edition. 2007, Elsevier: Amsterdam. p. 145-164.

114. Andonegui, G., S.M. Kerfoot, K. McNagny, K.V. Ebbert, K.D. Patel, and P. Kubes, Platelets express functional Toll-like receptor-4. Blood, 2005. **106**(7): p. 2417-2423.

115. Vassilatis, D.K., J.G. Hohmann, H. Zeng, F. Li, J.E. Ranchalis, M.T. Mortrud, et al., The G protein-coupled receptor repertoires of human and mouse. Proceedings of the National Academy of Sciences of the United States of America, 2003. **100**(8): p. 4903-4908.

116. The Medical Biochemistry G-Protein Coupled Receptors [cited 2014 10/10]; Available from: http://themedicalbiochemistrypage.org/signal-transduction.php#gpcr.

117. Coughlin, S. and Coughlin, Thrombin signalling and protease-activated receptors. Nature, 2000. **407**(6801): p. 258-264.

118. Griffin, C.T., Y. Srinivasan, Y.W. Zheng, W. Huang, and S.R. Coughlin, A role for thrombin receptor signaling in endothelial cells during embryonic development. Science, 2001. **293**(5535): p. 1666-1670.

119. Nakanishi-Matsui, S.R., M. Coughlin, Y.-W. Nakanishi Matsui, D. Zheng, E. Sulciner, M. Weiss, et al., PAR3 is a cofactor for PAR4 activation by thrombin. Nature, 2000. **404**(6778): p. 609–610.

120. Vandendries, E., J. Hamilton, S. Coughlin, and B. Furie, Par4 is required for platelet thrombus propagation but not fibrin generation in a mouse model of thrombosis. Proceedings of the National Academy of Sciences of the United States of America, 2007. **104**(1): p. 288-292.

121. Bar-Shavit, R., A. Eldor, and I. Vlodavsky, Binding of thrombin to subendothelial extracellular matrix. Protection and expression of functional properties. Journal of Clinical Investigation, 1989. **84**(4): p. 1096-1104.

122. Jandrot-Perrus, M., S. Busfield, A.H. Lagrue, X. Xiong, N. Debili, T. Chickering, et al., Cloning, characterization, and functional studies of human and mouse glycoprotein VI: A platelet-specific collagen receptor from the immunoglobulin superfamily. Blood, 2000. **96**(5): p. 1798-1807.

123. Kahner, B.N., H. Shankar, S. Murugappan, G.L. Prasad, and S.P. Kunapuli, Nucleotide receptor signaling in platelets. Journal of Thrombosis and Haemostasis, 2006. **4**(11): p. 2317-2326.

124. Ohlmann, P., A. Eckly, M. Freund, J.P. Cazenave, S. Offermanns, and C. Gachet, ADP induces partial platelet aggregation without shape change and potentiates collagen-induced aggregation in the absence of Galphaq. Blood, 2000. **96**(6): p. 2134–2139.

125. Foster, C.J., D.M. Prosser, J.M. Agans, Y. Zhai, M.D. Smith, J.E. Lachowicz, et al., Molecular identification and characterization of the platelet ADP receptor targeted by thienopyridine antithrombotic drugs. Journal of Clinical Investigation, 2001. **107**(12): p. 1591-8.

126. Bos, C.L., D.J. Richel, T. Ritsema, M.P. Peppelenbosch, and H.H. Versteeg, Prostanoids and prostanoid receptors in signal transduction. International Journal of Biochemistry & Cell Biology, 2004. **36**(7): p. 1187-205.

127. Wilson, S.J., A.M. Roche, E. Kostetskaia, and E.M. Smyth, Dimerization of the human receptors for prostacyclin and thromboxane facilitates thromboxane receptor-mediated cAMP generation. Journal of Biological Chemistry, 2004. **279**(51): p. 53036-53047.

128. Thomas, D.W., R.B. Mannon, P.J. Mannon, A. Latour, J.A. Oliver, M. Hoffman, et al., Coagulation defects and altered hemodynamic responses in mice lacking receptors for thromboxane A2. Journal of Clinical Investigation, 1998. **102**(11): p. 1994-2001.

129. Coyle, A., S. Coyle, B.T. Miggin, and Kinsella, Characterization of the 5′ untranslated region of α and β isoforms of the human thromboxane A2 receptor (TP). European Journal of Biochemistry, 2002. **269**(16): p. 4058-4073.

130. Abbate, R., P.A. Modesti, A. Fortini, A. Lombardi, M. Matucci, G.F. Gensini, et al., Decreased number of PGD2 binding sites on platelets from patients with type IIa hyperlipoproteinemia. Atherosclerosis, 1985. **54**(2): p. 167-175.

131. Iyú D, J.M., Glenn JR, White AE, Johnson AJ, Fox SC, Heptinstall S., PGE1 and PGE2 modify platelet function through different prostanoid receptors. Prostaglandins & Other Lipid Mediators, 2011. **94**(1-1): p. 9-16.

132. Kowalska, M.A., M.Z. Ratajczak, M. Majka, J. Jin, S. Kunapuli, L. Brass, et al., Stromal cell-derived factor-1 and macrophage-derived chemokine: 2 chemokines that activate platelets. Blood, 2000. **96**(1): p. 50-7.

133. Schafer, A., C. Schulz, M. Eigenthaler, D. Fraccarollo, A. Kobsar, M. Gawaz, et al., Novel role of the membrane-bound chemokine fractalkine in platelet activation and adhesion. Blood, 2004. **103**(2): p. 407-412.

134. Barrow, A.D. and J. Trowsdale, You say ITAM and I say ITIM, let's call the whole thing off: The ambiguity of immunoreceptor signalling. European Journal of Immunology, 2006. **36**(7): p. 1646-1653.

135. Gardiner, E.E., D. Karunakaran, J.F. Arthur, F.T. Mu, M.S. Powell, R.I. Baker, et al., Dual ITAM-mediated proteolytic pathways for irreversible inactivation of platelet receptors: de-ITAM-izing FcgammaRIIa. Blood, 2008. **111**(1): p. 165-174.

136. Watson, S.P., J.M. Auger, O.J. McCarty, and A.C. Pearce, GPVI and integrin alphaIIb beta3 signaling in platelets. Journal of Thrombosis and Haemostasis, 2005. **3**(8): p. 1752-1762.

137. Massberg, S., M. Gawaz, S. Gruner, V. Schulte, I. Konrad, D. Zohlnhofer, et al., A crucial role of glycoprotein VI for platelet recruitment to the injured arterial wall in vivo. Journal of Experimental Medicine, 2003. **197**(1): p. 41-49.

138. Suzuki-Inoue, K., O. Inoue, J. Frampton, and S.P. Watson, Murine GPVI stimulates weak integrin activation in PLCgamma2-/- platelets: involvement of PLCgamma1 and PI3-kinase. Blood, 2003. **102**(4): p. 1367-1373.

139. Uckun, F.M., A. Vassilev, S. Bartell, Y. Zheng, S. Mahajan, and H.E. Tibbles, The anti-leukemic Bruton's tyrosine kinase inhibitor alpha-cyano-beta-hydroxy-beta-methyl-N-(2,5-dibromophenyl) propenamide (LFM-A13) prevents fatal thromboembolism. Leuk Lymphoma, 2003. **44**(9): p. 1569-1577.

140. Sardjono, C.T., P.L. Mottram, N.C. van de Velde, M.S. Powell, D. Power, R.F. Slocombe, et al., Development of spontaneous multisystem autoimmune disease and hypersensitivity to antibody-induced inflammation in Fc gamma receptor IIa-transgenic mice. Arthritis and Rheumatism, 2005. **52**(10): p. 3220-3229.

141. Chong, B.H. and J.J. Chong, Heparin-induced thrombocytopenia. Expert Review of Cardiovascular Therapy, 2004. **2**(4): p. 547-559.

142. Suzuki-Inoue, K., G.L. Fuller, A. Garcia, J.A. Eble, S. Pohlmann, O. Inoue, et al., A novel Syk-dependent mechanism of platelet activation by the C-type lectin receptor CLEC-2. Blood, 2006. **107**(2): p. 542-549.

143. Chaipan, C., E.J. Soilleux, P. Simpson, H. Hofmann, T. Gramberg, A. Marzi, et al., DC-SIGN and CLEC-2 mediate human immunodeficiency virus type 1 capture by platelets. Journal of Virology, 2006. **80**(18): p. 8951-8960.

144. Kerrigan, A.M., K.M. Dennehy, D. Mourão-Sá, I. Faro-Trindade, J.A. Willment, P.R. Taylor, et al., CLEC-2 is a phagocytic activation receptor expressed on murine peripheral blood neutrophils. Journal of Immunology, 2009. **182**(7): p. 4150-4157.

145. Colonna, M., J. Samaridis, and L. Angman, Molecular characterization of two novel C-type lectin-like receptors, one of which is selectively expressed in human dendritic cells. European Journal of Immunology, 2000. **30**(2): p. 697-704.

146. Weis, W.I., M.E. Taylor, and K. Drickamer, The C-type lectin superfamily in the immune system. Immunological Reviews, 1998. **163**: p. 19-34.

147. Drickamer, K. and Drickamer, C-type lectin-like domains. Current Opinion in Structural Biology, 1999. **9**(5): p. 585-590.

148. Pamuk, O.N. and G.C. Tsokos, Spleen tyrosine kinase inhibition in the treatment of autoimmune, allergic and autoinflammatory diseases. Arthritis Research and Therapy, 2010. **12**(6): p. 1-11.

149. Huang, T.F., C.Z. Liu, and S.H. Yang, Aggretin, a novel platelet-aggregation inducer from snake (Calloselasma rhodostoma) venom, activates phospholipase C by acting as a glycoprotein Ia/IIa. Biochemical Journal, 1995. **309**(3): p. 1021-1027.

150. Shin, Y. and T. Morita, Rhodocytin, a functional novel platelet agonist belonging to the heterodimeric C-type lectin family, induces platelet aggregation independently of glycoprotein Ib. Biochemical and Biophysical Research Communications, 1998. **245**(3): p. 741-745.

151. Suzuki-Inoue, K., Y. Ozaki, M. Kainoh, Y. Shin, Y. Wu, Y. Yatomi, et al., Rhodocytin induces platelet aggregation by interacting with glycoprotein Ia/IIa (GPIa/IIa, integrin α2β1). Involvement of GPIa/IIa-associated Src and protein tyrosine phosphorylation. Journal of Biological Chemistry, 2001. **276**(2): p. 1643-1652.

152. Eble, J.A., B. Beermann, H.J. Hinz, and A. Schmidt-Hederich, α2β1 Integrin Is Not Recognized by Rhodocytin but Is the Specific, High Affinity Target of Rhodocetin, an RGD-independent Disintegrin and Potent Inhibitor of Cell Adhesion to Collagen. Journal of Biological Chemistry, 2001. **276**(15): p. 12274-12284.

153. Navdaev, A., J.M. Clemetson, J. Polgár, B.E. Kehrel, M. Glauner, E. Magnenat, et al., Aggretin, a Heterodimeric C-type Lectin from Calloselasma rhodostoma (Malayan Pit Viper), Stimulates Platelets by Binding to α2β1 Integrin and Glycoprotein Ib, Activating Syk and Phospholipase Cγ2, but Does Not Involve the Glycoprotein VI/Fc Receptor γ Chain Collagen Receptor. Journal of Biological Chemistry, 2001. **276**(24): p. 20882-20889.

154. Bergmeier, W., D. Bouvard, J.A. Eble, R. Mokhtari-Nejad, V. Schulte, H. Zirngibl, et al., Rhodocytin (Aggretin) Activates Platelets Lacking α2β1 Integrin, Glycoprotein VI, and the Ligand-binding Domain of Glycoprotein Ibα. Journal of Biological Chemistry, 2001. **276**(27): p. 25121-25126.

155. Watson, A.A., C.M. Christou, J.R. James, A.E. Fenton-May, G.E. Moncayo, A.R. Mistry, et al., The platelet receptor CLEC-2 is active as a dimer. Biochemistry, 2009. **48**(46): p. 10988-10996.

156. Fuller, G.L.J., J.A.E. Williams, M.G. Tomlinson, J.A. Eble, S.L. Hanna, S. Pöhlmann, et al., The C-type lectin receptors CLEC-2 and Dectin-1, but not DC-SIGN, signal via a novel YXXL-dependent signaling cascade. Journal of Biological Chemistry, 2007. **282**(17): p. 12397-12409.

157. Hughes, C.E., A.Y. Pollitt, J. Mori, J.A. Eble, M.G. Tomlinson, J.H. Hartwig, et al., CLEC-2 activates Syk through dimerization. Blood, 2010. **115**(14): p. 2947-2955.

158. Geijtenbeek, T.B.H., D. Geijtenbeek, R. Kwon, S. Torensma, G.C.F. van Vliet, J. van Duijnhoven, et al., DC-SIGN, a Dendritic Cell–Specific HIV-1-Binding Protein that Enhances trans-Infection of T Cells. Cell, 2000. **100**(5): p. 587-597.

159. Suzuki-Inoue, K., Y. Kato, O. Inoue, K.K. Mika, K. Mishima, Y. Yatomi, et al., Involvement of the snake toxin receptor CLEC-2, in podoplanin-mediated platelet activation, by cancer cells. Journal of Biological Chemistry, 2007. **282**(36): p. 25993-26001.

160. Kato, K., T. Kanaji, S. Russell, T.J. Kunicki, K. Furihata, S. Kanaji, et al., The contribution of glycoprotein VI to stable platelet adhesion and thrombus formation illustrated by targeted gene deletion. Blood, 2003. **102**(5): p. 1701-1707.

161. Nash, G.F., L.F. Nash, M.F. Turner, A.K. Scully, and Kakkar, Platelets and cancer. Lancet Oncology, 2002. **3**(7): p. 425-430.

162. Gupta, G.P. and J. Massagué, Platelets and metastasis revisited: A novel fatty link. Journal of Clinical Investigation, 2004. **114**(12): p. 1691-1693.

163. Kaneko, M., Y. Kato, A. Kunita, N. Fujita, T. Tsuruo, and M. Osawa, Functional sialylated O-glycan to platelet aggregation on Aggrus (T1α/podoplanin) molecules expressed in Chinese hamster ovary cells. Journal of Biological Chemistry, 2004. **279**(37): p. 38838-38843.

164. Kaneko, M.K., Y. Kato, A. Kameyama, H. Ito, A. Kuno, J. Hirabayashi, et al., Functional glycosylation of human podoplanin: Glycan structure of platelet aggregation-inducing factor. FEBS Letters, 2007. **581**(2): p. 331-336.

165. Sweeney, M.C., A.S. Wavreille, J. Park, J.P. Butchar, S. Tridandapani, and D. Pei, Decoding protein-protein interactions through combinatorial chemistry: sequence specificity of SHP-1, SHP-2, and SHIP SH2 domains. Biochemistry, 2005. **44**(45): p. 14932-14947.

166. Newman, P.J., M.C. Berndt, J. Gorski, G.C. White, S. Lyman, C. Paddock, et al., PECAM-1 (CD31) cloning and relation to adhesion molecules of the immunoglobulin gene superfamily. Science, 1990. **247**(4947): p. 1219-1222.

167. Bieber, A.J., P.M. Snow, M. Hortsch, N.H. Patel, J.R. Jacobs, Z.R. Traquina, et al., Drosophila neuroglian: A member of the immunoglobulin superfamily with extensive homology to the vertebrate neural adhesion molecule L1. Cell, 1989. **59**(3): p. 447-460.

168. Sachs, U.J., C.L. Andrei-Selmer, A. Maniar, T. Weiss, C. Paddock, V.V. Orlova, et al., The neutrophil-specific antigen CD177 is a counter-receptor for platelet endothelial cell adhesion molecule-1 (CD31). Journal of Biological Chemistry, 2007. **282**(32): p. 23603-23612.

169. Bayat, B., S. Werth, U.J. Sachs, D.K. Newman, P.J. Newman, and S. Santoso, Neutrophil transmigration mediated by the neutrophil-specific antigen CD177 is influenced by the endothelial S536N dimorphism of platelet endothelial cell adhesion molecule-1. Journal of Immunology, 2010. **184**(7): p. 3889-3896.

170. Mazurov, A.V., D.V. Vinogradov, N.V. Kabaeva, G.N. Antonova, Y.A. Romanov, T.N. Vlasik, et al., A monoclonal antibody, VM64 reacts with a 130 kDa glycoprotein common to platelets and endothelial cells: Heterogeneity in antibody binding to human aortic endothelial cells. Thrombosis and Haemostasis, 1991. **66**(4): p. 494-499.

171. Moraes, L.A., N.E. Barrett, C.I. Jones, L.M. Holbrook, M. Spyridon, T. Sage, et al., Platelet endothelial cell adhesion molecule-1 regulates collagen-stimulated platelet function by modulating the association of phosphatidylinositol 3-kinase with Grb-2-associated binding protein-1 and linker for activation of T cells. Journal of Thrombosis and Haemostasis, 2010. **8**(11): p. 2530-2541.

172. Newman, P.J., The role of PECAM-1 in vascular cell biology. Ann N Y Acad Sci, 1994. **714**: p. 165-174.

173. Novinska, M.S., B.C. Pietz, T.M. Ellis, D.K. Newman, and P.J. Newman, The alleles of PECAM-1. Gene, 2006. **376**(1): p. 95-101.

174. Varon, D., D.E. Jackson, B. Shenkman, R. Dardik, L. Tamarin, N. Savion, et al., Platelet/endothelial cell adhesion molecule-1 serves as a costimulatory agonist receptor that modulates integrin-dependent adhesion and aggregation of human platelets. Blood, 1998. **91**(2): p. 500-507.

175. Maeda, A., M. Kurosaki, and T. Kurosaki, Paired immunoglobulin-like receptor (PIR)-A is involved in activating mast cells through its association with Fc receptor gamma chain. Journal of Experimental Medicine, 1998. **188**(5): p. 991-995.

176. Gao, C., W. Sun, M. Christofidou-Solomidou, M. Sawada, D.K. Newman, C. Bergom, et al., PECAM-1 functions as a specific and potent inhibitor of mitochondrial-dependent apoptosis. Blood, 2003. **102**(1): p. 169-179.

177. O'Brien, C., G. Cao, A. Makrigiannakis, and H. DeLisser, Role of immunoreceptor tyrosine-based inhibitory motifs of PECAM-1 in PECAM-1-dependent cell migration. American Journal of Physiology-Cell Physiology, 2004. **287**(4): p. C1103-13.

178. Falati, S., S. Patil, P.L. Gross, M. Stapleton, G. Merrill-Skoloff, N.E. Barrett, et al., Platelet PECAM-1 inhibits thrombus formation in vivo. Blood, 2006. **107**(2): p. 535-541.

179. Newland, S.A., I.C. Macaulay, A.R. Floto, E.C. de Vet, W.H. Ouwehand, N.A. Watkins, et al., The novel inhibitory receptor G6B is expressed on the surface of platelets and attenuates platelet function in vitro. Blood, 2007. **109**(11): p. 4806-4809.

180. Mori, J., A.C. Pearce, J.C. Spalton, B. Grygielska, J.A. Eble, M.G. Tomlinson, et al., G6b-B inhibits constitutive and agonist-induced signaling by glycoprotein VI and CLEC-2. Journal of Biological Chemistry, 2008. **283**(51): p. 35419-35427.

181. Washington, A.V., L. Quigley, and D.W. McVicar, Initial characterization of TREM-like transcript (TLT)-1: a putative inhibitory receptor within the TREM cluster. Blood, 2002. **100**(10): p. 3822-3824.

182. Washington, A.V., R.L. Schubert, L. Quigley, T. Disipio, R. Feltz, E.H. Cho, et al., A TREM family member, TLT-1, is found exclusively in the alpha-granules of megakaryocytes and platelets. Blood, 2004. **104**(4): p. 1042-1047.

183. Washington, A.V., S. Gibot, I. Acevedo, J. Gattis, L. Quigley, R. Feltz, et al., TREM-like transcript-1 protects against inflammation-associated hemorrhage by facilitating platelet aggregation in mice and humans. Journal of Clinical Investigation, 2009. **119**(6): p. 1489-1501.

184. Li, T.T., S. Larrucea, S. Souza, S.M. Leal, J.A. Lopez, E.M. Rubin, et al., Genetic variation responsible for mouse strain differences in integrin alpha 2 expression is associated with altered platelet responses to collagen. Blood, 2004. **103**(9): p. 3396-3402.

185. Nedellec, P., G.S. Dveksler, E. Daniels, C. Turbide, B. Chow, A.A. Basile, et al., Bgp2, a new member of the carcinoembryonic antigen-related gene family, encodes an alternative receptor for mouse hepatitis viruses. Journal of Virology, 1994. **68**(7): p. 4525-4537.

186. Robitaille, J., L. Izzi, E. Daniels, B. Zelus, K.V. Holmes, and N. Beauchemin, Comparison of expression patterns and cell adhesion properties of the mouse biliary glycoproteins Bbgp1 and Bbgp2. European Journal of Biochemistry-FEBS, 1999. **264**(2): p. 534-544.

187. Wong, C., Y. Liu, J. Yip, R. Chand, J.L. Wee, L. Oates, et al., CEACAM1 negatively regulates platelet-collagen interactions and thrombus growth in vitro and in vivo. Blood, 2009. **113**(8): p. 1818-1828.

188. Heinrich, G., S. Ghosh, A.M. DeAngelis, J.M. Schroeder–Gloeckler, P.R. Patel, T.R. Castaneda, et al., Carcinoembryonic Antigen-Related Cell Adhesion Molecule 2 Controls Energy Balance and Peripheral Insulin Action in Mice. Gastroenterology, 2010. **139**(2): p. 644-652.

189. Janowska-Wieczorek, A., M. Wysoczynski, J. Kijowski, L. Marquez-Curtis, B. Machalinski, J. Ratajczak, et al., Microvesicles derived from activated platelets induce metastasis and angiogenesis in lung cancer. International Journal of Cancer, 2005. **113**(5): p. 752-760.

190. Markel, G., R. Gruda, H. Achdout, G. Katz, M. Nechama, R.S. Blumberg, et al., The critical role of residues 43R and 44Q of carcinoembryonic antigen cell adhesion molecules-1 in the protection from killing by human NK cells. Journal of Immunology, 2004. **173**(6): p. 3732-3739.

191. Najjar, S.M., D. Accili, N. Philippe, J. Jernberg, R. Margolis, and S.I. Taylor, pp120/ecto-ATPase, an endogenous substrate of the insulin receptor tyrosine kinase, is expressed as two variably spliced isoforms. Journal of Biological Chemistry, 1993. **268**(2): p. 1201-1206.

192. Lin, S.H., W. Luo, K. Earley, P. Cheung, and D.C. Hixson, Structure and function of C-CAM1: Effects of the cytoplasmic domain on cell aggregation. Biochemical Journal, 1995. **311**(1): p. 239-245.

193. Öbrink, B., CEA adhesion molecules: Multifunctional proteins with signal-regulatory properties. Current Opinion in Cell Biology, 1997. **9**(5): p. 616-626.

194. Luo, W., K. Earley, V. Tantingco, D.C. Hixson, T.C. Liang, and S.H. Lin, Association of an 80 kDa protein with C-CAM1 cytoplasmic domain correlates with C-CAM1-mediated growth inhibition. Oncogene, 1998. **16**(9): p. 1141-1147.

195. Liu, Q., J.C. Docherty, J.C.T. Rendell, A.S. Clanachan, and G.D. Lopaschuk, High levels of fatty acids delay the recovery of intracellular pH and cardiac efficiency in post-ischemic hearts by inhibiting glucose oxidation. Journal of the American College of Cardiology, 2002. **39**(4): p. 718-725.

196. Nagaishi, T., L. Pao, S.H. Lin, H. Iijima, A. Kaser, S.W. Qiao, et al., SHP1 Phosphatase-Dependent T Cell Inhibition by CEACAM1 Adhesion Molecule Isoforms. Immunity, 2006. **25**(5): p. 769-781.

197. Han, E., D. Phan, P. Lo, M.N. Poy, R. Behringer, S.M. Najjar, et al., Differences in tissue-specific and embryonic expression of mouse Ceacam1 and Ceacam2 genes. Biochemical Journal, 2001. **355**(Pt 2): p. 417-423.

198. Kuespert, K., S. Pils, and C.R. Hauck, CEACAMs: their role in physiology and pathophysiology. Curr Opin Cell Biol, 2006. **18**(5): p. 565-571.

199. Chen, Z., L. Chen, S.W. Qiao, T. Nagaishi, and R.S. Blumberg, Carcinoembryonic antigen-related cell adhesion molecule 1 inhibits proximal TCR signaling by targeting ZAP-70. Journal of Immunology, 2008. **180**(9): p. 6085-6093.

200. Newman, D.K., The Y's that bind: negative regulators of Src family kinase activity in platelets. Journal of Thrombosis and Haemostasis, 2009. **7 Suppl 1**: p. 195-199.

201. Blann, A.D., Angiogenesis and platelets: the clot thickens further. Cardiovascular Research, 2004. **63**(2): p. 192-193.

202. Carramolino, L., J. Fuentes, C. Garcia-Andres, V. Azcoitia, D. Riethmacher, and M. Torres, Platelets play an essential role in separating the blood and lymphatic

vasculatures during embryonic angiogenesis. Circulation Research, 2010. **106**(7): p. 1197-1201.

203. Peterson, J.E., D. Zurakowski, J.E. Italiano, Jr., L.V. Michel, L. Fox, G.L. Klement, et al., Normal ranges of angiogenesis regulatory proteins in human platelets. American Journal of Hematology, 2010. **85**(7): p. 487-493.

204. Klement, G.L., T.T. Yip, F. Cassiola, L. Kikuchi, D. Cervi, V. Podust, et al., Platelets actively sequester angiogenesis regulators. Blood, 2009. **113**(12): p. 2835-2842.

205. Celi, A., G. Merrill-Skoloff, P. Gross, S. Falati, D.S. Sim, R. Flaumenhaft, et al., Thrombus formation: direct real-time observation and digital analysis of thrombus assembly in a living mouse by confocal and widefield intravital microscopy. Journal of Thrombosis and Haemostasis, 2003. **1**(1): p. 60-68.

206. Falati, S., P. Gross, G. Merrill-Skoloff, B.C. Furie, and B. Furie, Real-time in vivo imaging of platelets, tissue factor and fibrin during arterial thrombus formation in the mouse. Nature Medicine, 2002. **8**(10): p. 1175-1181.

207. Ni, H., C.V. Denis, S. Subbarao, J.L. Degen, T.N. Sato, R.O. Hynes, et al., Persistence of platelet thrombus formation in arterioles of mice lacking both von Willebrand factor and fibrinogen. Journal of Clinical Investigation, 2000. **106**(3): p. 385-392.

208. Denis, C., N. Methia, P.S. Frenette, H. Rayburn, M. Ullman-Culleré, R.O. Hynes, et al., A mouse model of severe von Willebrand disease: Defects in hemostasis and thrombosis. Proceedings of the National Academy of Sciences of the United States of America, 1998. **95**(16): p. 9524-9529.

209. Bergmeier, W., C.L. Piffath, T. Goerge, S.M. Cifuni, Z.M. Ruggeri, J. Ware, et al., The role of platelet adhesion receptor GPIbα far exceeds that of its main ligand, von Willebrand factor, in arterial thrombosis. Proceedings of the National Academy of Sciences of the United States of America, 2006. **103**(45): p. 16900-16905.

210. Zhu, L., W. Bergmeier, J. Wu, H. Jiang, T.J. Stalker, M. Cieslak, et al., Regulated surface expression and shedding support a dual role for semaphorin 4D in platelet responses to vascular injury. Proceedings of the National Academy of Sciences of the United States of America, 2007. **104**(5): p. 1621-1626.

211. Denis, C.V. and D.D. Wagner, Platelet adhesion receptors and their ligands in mouse models of thrombosis. Arteriosclerosis, Thrombosis, and Vascular Biology, 2007. **27**(4): p. 728-739.

212. Brass, L.F., H. Jiang, J. Wu, T.J. Stalker, and L. Zhu, Contact-dependent signaling events that promote thrombus formation. Blood Cells, Molecules, and Diseases, 2006. **36**(2): p. 157-161.

213. Mendrick, D.L., D.M. Kelly, S.S. DuMont, and D.J. Sandstrom, Glomerular epithelial and mesangial cells differentially modulate the binding specificities of VLA-1 and VLA-2. Laboratory Investigation, 1995. **72**(3): p. 367-375.

214. Yuan, Y., S. Kulkarni, P. Ulsemer, S.L. Cranmer, C.L. Yap, W.S. Nesbitt, et al., The von Willebrand factor-glycoprotein Ib/V/IX interaction induces actin polymerization and cytoskeletal reorganization in rolling platelets and glycoprotein Ib/V/IX-transfected cells. Journal of Biological Chemistry, 1999. **274**(51): p. 36241-36251.

215. Jackson, D.E., C.M. Ward, R. Wang, and P.J. Newman, The protein-tyrosine phosphatase SHP-2 binds platelet/endothelial cell adhesion molecule-1 (PECAM-1) and forms a distinct signaling complex during platelet aggregation. Evidence for a mechanistic link between PECAM-1- and integrin-mediated cellular signaling. Journal of Biological Chemistry, 1997. **272**(11): p. 6986-6993.

216. André, P., S.M. Delaney, T. LaRocca, D. Vincent, F. DeGuzman, M. Jurek, et al., P2Y12 regulates platelet adhesion/activation, thrombus growth, and thrombus stability in injured arteries. Journal of Clinical Investigation, 2003. **112**(3): p. 398-406.

217. Azam, M., S.S. Andrabi, K.E. Sahr, L. Kamath, A. Kuliopulos, and A.H. Chishti, Disruption of the mouse μ-calpain gene reveals an essential role in platelet function. Molecular and Cellular Biology, 2001. **21**(6): p. 2213-2220.

218. Lau, L.M., J.L. Wee, M.D. Wright, G.W. Moseley, P.M. Hogarth, L.K. Ashman, et al., The tetraspanin superfamily member CD151 regulates outside-in integrin alphaIIbbeta3 signaling and platelet function. Blood, 2004. **104**(8): p. 2368-2375.

219. Jones, K.L., S.C. Hughan, S.M. Dopheide, R.W. Farndale, S.P. Jackson, and D.E. Jackson, Platelet endothelial cell adhesion molecule-1 is a negative regulator of platelet-collagen interactions. Blood, 2001. **98**(5): p. 1456-1463.

220. Kazal, L.A., S. Amsel, O.P. Miller, and L.M. Tocantins, The Preparation and Some Properties of Fibrinogen Precipitated from Human Plasma by Glycine. Proceedings of the Society for Experimental Biology and Medicine, 1963. **113**: p. 989-994.

221. Bradford, M.M., A rapid and sensitive method for the quantitation of microgram quantities of protein utilizing the principle of protein dye binding. Analytical Biochemistry, 1976. **72**(1-2): p. 248-254.

222. Orlowski, E., R. Chand, J. Yip, C. Wong, M.W. Goschnick, M.D. Wright, et al., A platelet tetraspanin superfamily member, CD151, is required for regulation of thrombus growth and stability in vivo. Journal of Thrombosis and Haemostasis, 2009. **7**(12): p. 2074-2084.

223. Dubois, C., L. Panicot-Dubois, J.F. Gainor, B.C. Furie, and B. Furie, Thrombin-initiated platelet activation in vivo is vWF independent during thrombus formation in a laser injury model. Journal of Clinical Investigation, 2007. **117**(4): p. 953-960.

224. Dubois, C., L. Panicot-Dubois, G. Merrill-Skoloff, B. Furie, and B.C. Furie, Glycoprotein VI-dependent and -independent pathways of thrombus formation in vivo. Blood, 2006. **107**(10): p. 3902-3906.

225. Savage, B., E. Saldívar, and Z.M. Ruggeri, Initiation of platelet adhesion by arrest onto fibrinogen or translocation on von Willebrand factor. Cell, 1996. **84**(2): p. 289-297.

226. Moroi, M., S.M. Jung, M. Okuma, and K. Shinmyozu, A patient with platelets deficient in glycoprotein VI that lack both collagen-induced aggregation and adhesion. Journal of Clinical Investigation, 1989. **84**(5): p. 1440-1445.

227. Santoro, S.A., Identification of a 160,000 dalton platelet membrane protein that mediates the initial divalent cation-dependent adhesion of platelets to collagen. Cell, 1986. **46**(6): p. 913-920.

228. Nieswandt, B., C. Brakebusch, W. Bergmeier, V. Schulte, D. Bouvard, R. Mokhtari-Nejad, et al., Glycoprotein VI but not α2β1 integrin is essential for platelet interaction with collagen. EMBO Journal, 2001. **20**(9): p. 2120-2130.

229. Clemetson, J.M., J. Polgar, E. Magnenat, T.N.C. Wells, and K.J. Clemetson, The platelet collagen receptor glycoprotein VI is a member of the immunoglobulin superfamily closely related to FcαR and the natural killer receptors. Journal of Biological Chemistry, 1999. **274**(41): p. 29019-29024.

230. Nieswandt, B. and S.P. Watson, Platelet-collagen interaction: Is GPVI the central receptor? Blood, 2003. **102**(2): p. 449-461.

231. Gibbins, J., J. Asselin, R. Farndale, M. Barnes, C.L. Law, and S.P. Watson, Tyrosine phosphorylation of the Fc receptor γ-chain in collagen- stimulated platelets. Journal of Biological Chemistry, 1996. **271**(30): p. 18095-18099.

232. Watson, S.P., N. Asazuma, B. Atkinson, O. Berlanga, D. Best, R. Bobe, et al., The role of ITAM- and ITIM-coupled receptors in platelet activation by collagen. Thrombosis and Haemostasis, 2001. **86**(1): p. 276-288.

233. Patil, S., D.K. Newman, and P.J. Newman, Platelet endothelial cell adhesion molecule-1 serves as an inhibitory receptor that modulates platelet responses to collagen. Blood, 2001. **97**(6): p. 1727-1732.

234. Cicmil, M., J.M. Thomas, M. Leduc, C. Bon, and J.M. Gibbins, Platelet endothelial cell adhesion molecule-1 signaling inhibits the activation of human platelets. Blood, 2002. **99**(1): p. 137-144.

235. Dhanjal, T.S., E.A. Ross, J.M. Auger, O.J.T. McCarty, C.E. Hughes, Y.A. Senis, et al., Minimal regulation of platelet activity by PECAM-1. Platelets, 2007. **18**(1): p. 56-67.

236. Pao, L.I., K. Badour, K.A. Siminovitch, and B.G. Neel, Nonreceptor protein-tyrosine phosphatases in immune cell signaling, W.E. Paul, Editor. 2007. p. 473-523.

237. Chemnitz, J.M., R.V. Parry, K.E. Nichols, C.H. June, and J.L. Riley, SHP-1 and SHP-2 associate with immunoreceptor tyrosine-based switch motif of programmed death 1 upon primary human T cell stimulation, but only receptor ligation prevents T cell activation. Journal of Immunology, 2004. **173**(2): p. 945-954.

238. Okazaki, T., A. Maeda, H. Nishimura, T. Kurosaki, and T. Honjo, PD-1 immunoreceptor inhibits B cell receptor-mediated signaling by recruiting src homology 2-domain-containing tyrosine phosphatase 2 to phosphotyrosine. Proceedings of the National Academy of Sciences of the United States of America, 2001. **98**(24): p. 13866-13871.

239. Hamerman, J.A. and L.L. Lanier, Inhibition of immune responses by ITAM-bearing receptors. Science's STKE: Signal Transduction Knowledge Environment, 2006. **2006**(320): p. re1. 1-7.

240. Abram, C.L. and C.A. Lowell, The expanding role for ITAM-based signaling pathways in immune cells. Science's STKE: Signal Transduction Knowledge Environment, 2007. **2007**(377): p. re2. 1-6.

241. Patel, P.R., S.K. Ramakrishnan, M.K. Kaw, C.K. Raphael, S. Ghosh, J.S. Marino, et al., Increased metabolic rate and insulin sensitivity in male mice lacking the carcino-embryonic antigen-related cell adhesion molecule 2. Diabetologia, 2012. **55**(3): p. 763-772.

242. Salaheldeen, E., H. Kurio, A. Howida, and H. Iida, Molecular cloning and localization of a CEACAM2 isoform, CEACAM2-L, expressed in spermatids in mouse testis. Molecular Reproduction and Development, 2012. **79**(12): p. 843-852.

243. Beauchemin, N., T. Kunath, J. Robitaille, B. Chow, C. Turbide, E. Daniels, et al., Association of biliary glycoprotein with protein tyrosine phosphatase SHP-1 in malignant colon epithelial cells. Oncogene, 1997. **14**(7): p. 783-790.

244. Huber, M., L. Izzi, P. Grondin, C. Houde, T. Kunath, A. Veillette, et al., The carboxyl-terminal region of biliary glycoprotein controls its tyrosine phosphorylation and association with protein-tyrosine phosphatases SHP-1 and SHP-2 in epithelial cells. Journal of Biological Chemistry, 1999. **274**(1): p. 335-344.

245. Pasquet, J.M., L. Quek, S. Pasquet, A. Poole, J.R. Matthews, C. Lowell, et al., Evidence of a role for SHP-1 in platelet activation by the collagen receptor glycoprotein VI. Journal of Biological Chemistry, 2000. **275**(37): p. 28526-28531.

246. Kunicki, T.J., The role of platelet collagen receptor (glycoprotein Ia/IIa; integrin α2β1) polymorphisms in thrombotic disease. Current Opinion in Hematology, 2001. **8**(5): p. 277-285.

247. Siljander, P.R., I.C. Munnix, P.A. Smethurst, H. Deckmyn, T. Lindhout, W.H. Ouwehand, et al., Platelet receptor interplay regulates collagen-induced thrombus formation in flowing human blood. Blood, 2004. **103**(4): p. 1333-1341.

248. Heemskerk, J.W.M., M.J.E. Kuijpers, I.C.A. Munnix, and P.R.M. Siljander, Platelet collagen receptors and coagulation. A characteristic platelet response as possible target for antithrombotic treatment. Trends in Cardiovascular Medicine, 2005. **15**(3): p. 86-92.

249. Bevers, E.M., P. Comfurius, and R.F.A. Zwaal, Regulatory mechanisms in maintenance and modulation of transmembrane lipid asymmetry: Pathophysiological implications. Lupus, 1996. **5**(5): p. 480-487.

250. Nouvion, A.L., M. Oubaha, S. LeBlanc, E.C. Davis, H. Jastrow, R. Kammerer, et al., CEACAM1: A key regulator of vascular permeability. Journal of Cell Science, 2010. **123**(24): p. 4221-4230.

251. Asselin, J., J.M. Gibbins, M. Achison, Y.H. Lee, L.F. Morton, R.W. Farndale, et al., A collagen-like peptide stimulates tyrosine phosphorylation of syk and phospholipase Cγ2 in platelets independent of the integrin α2β1. Blood, 1997. **89**(4): p. 1235-1242.

252. Butenas, S., K.M. Cawthern, C. Van't Veer, M.E. DiLorenzo, J.B. Lock, and K.G. Mann, Antiplatelet agents in tissue factor-induced blood coagulation. Blood, 2001. **97**(8): p. 2314-2322.

253. Monroe, D.M., M. Hoffman, and H.R. Roberts, Platelets and thrombin generation. Arteriosclerosis, Thrombosis, and Vascular Biology, 2002. **22**(9): p. 1381-1389.

254. Christou, C.M., A.C. Pearce, A.A. Watson, A.R. Mistry, A.Y. Pollitt, A.E. Fenton-May, et al., Renal cells activate the platelet receptor CLEC-2 through podoplanin. Biochemical Journal, 2008. **411**(1): p. 133-140.

255. Severin, S., A.Y. Pollitt, L. Navarro-Nunez, C.A. Nash, D. Mourao-Sa, J.A. Eble, et al., Syk-dependent phosphorylation of CLEC-2: a novel mechanism of hem-immunoreceptor tyrosine-based activation motif signaling. Journal of Biological Chemistry, 2011. **286**(6): p. 4107-4116.

256. Brass, L.F., L. Zhu, and T.J. Stalker, Novel therapeutic targets at the platelet vascular interface. Arteriosclerosis, Thrombosis, and Vascular Biology, 2008. **28**(3): p. s43-s50.

257. Suzuki-Inoue, K., O. Inoue, and Y. Ozaki, Novel platelet activation receptor CLEC-2: from discovery to prospects. Journal of Thrombosis and Haemostasis, 2011. **9 Suppl 1**: p. 44-55.

258. Barrow, A.D., E. Astoul, A. Floto, G. Brooke, I.A.M. Relou, N.S. Jennings, et al., Cutting Edge: TREM-Like Transcript-1, a Platelet Immunoreceptor Tyrosine-Based Inhibition Motif Encoding Costimulatory Immunoreceptor that Enhances, Rather than Inhibits, Calcium Signaling via SHP-2. Journal of Immunology, 2004. **172**(10): p. 5838-5842.

259. Ravetch, J.V. and L.L. Lanier, Immune inhibitory receptors. Science, 2000. **290**(5489): p. 84-89.

260. May, F., I. Hagedorn, I. Pleines, M. Bender, T. Vogtle, J. Eble, et al., CLEC-2 is an essential platelet-activating receptor in hemostasis and thrombosis. Blood, 2009. **114**(16): p. 3464-3472.

261. Hughes, C.E., L. Navarro-Núñez, B.A. Finney, D. Mourão-Sá, A.Y. Pollitt, and S.P. Watson, CLEC-2 is not required for platelet aggregation at arteriolar shear. Journal of Thrombosis and Haemostasis, 2010. **8**(10): p. 2328-2332.

262. Suzuki-Inoue, K., O. Inoue, G. Ding, S. Nishimura, K. Hokamura, K. Eto, et al., Essential in vivo roles of the C-type lectin receptor CLEC-2: Embryonic/neonatal lethality of CLEC-2-deficient mice by blood/lymphatic misconnections and impaired thrombus formation of CLEC-2-deficient platelets. Journal of Biological Chemistry, 2010. **285**(32): p. 24494-24507.

263. Santoro, S.A., J.J. Walsh, W.D. Staatz, and K.J. Baranski, Distinct determinants on collagen support alpha 2 beta 1 integrin-mediated platelet adhesion and platelet activation. Cell Regulation, 1991. **2**(11): p. 905-913.

264. Morton, L.F., P.G. Hargreaves, R.W. Farndale, R.D. Young, and M.J. Barnes, Integrin α2β1-independent activation of platelets by simple collagen-like peptides: Collagen tertiary (triple-helical) and quaternary (polymeric) structures are sufficient alone for α2β1-independent platelet reactivity. Biochemical Journal, 1995. **306**(2): p. 337-344.

265. Ezumi, Y., K. Shindoh, M. Tsuji, and H. Takayama, Physical and functional association of the Src family kinases Fyn and Lyn with the collagen receptor glycoprotein VI-Fc receptor γ chain complex on human platelets. Journal of Experimental Medicine, 1998. **188**(2): p. 267-276.

266. Wonerow, P., A.C. Pearce, D.J. Vaux, and S.P. Watson, A critical role for phospholipase Cγ2 in αIIbβ 3-mediated platelet spreading. Journal of Biological Chemistry, 2003. **278**(39): p. 37520-37529.

267. Nieswandt, B., V. Schulte, W. Bergmeier, R. Mokhtari-Nejad, K. Rackebrandt, J.P. Cazenave, et al., Long-term antithrombotic protection by in vivo depletion of platelet glycoprotein VI in mice. Journal of Experimental Medicine, 2001. **193**(4): p. 459-469.

268. Schulte, V., D. Snell, W. Bergmeier, H. Zirngibl, S.P. Watson, and B. Nieswandt, Evidence for two distinct epitopes within collagen for activation of murine platelets. Journal of Biological Chemistry, 2001. **276**(1): p. 364-368.

269. Snell, D.C., V. Schulte, G.E. Jarvis, K. Arase, D. Sakurai, T. Saito, et al., Differential effects of reduced glycoprotein VI levels on activation of murine platelets by glycoprotein VI ligands. Biochemical Journal, 2002. **368**(1): p. 293-300.

270. Kurz, K.D., B.W. Main, and G.E. Sandusky, Rat model of arterial thrombosis induced by ferric chloride. Thrombosis Research, 1990. **60**(4): p. 269-280.

271. Nishimura, S., I. Manabe, M. Nagasaki, K. Seo, H. Yamashita, Y. Hosoya, et al., In vivo imaging in mice reveals local cell dynamics and inflammation in obese adipose tissue. Journal of Clinical Investigation, 2008. **118**(2): p. 710-721.

272. Takizawa, H., S. Nishimura, N. Takayama, A. Oda, H. Nishikii, Y. Morita, et al., Lnk regulates integrin αIIbβ3 outside-in signaling in mouse platelets, leading to stabilization

of thrombus development in vivo. Journal of Clinical Investigation, 2010. **120**(1): p. 179-190.

273. Chou, J., N. Mackman, G. Merrill-Skoloff, B. Pedersen, B.C. Furie, and B. Furie, Hematopoietic cell-derived microparticle tissue factor contributes to fibrin formation during thrombus propagation. Blood, 2004. **104**(10): p. 3190-3197.

274. Sim, D.S., G. Merrill-Skoloff, B.C. Furie, B. Furie, and R. Flaumenhaft, Initial accumulation of platelets during arterial thrombus formation in vivo is inhibited by elevation of basal cAMP levels. Blood, 2004. **103**(6): p. 2127-2134.

275. Atkinson, B.T., R. Jasuja, V.M. Chen, P. Nandivada, B. Furie, and B.C. Furie, Laser-induced endothelial cell activation supports fibrin formation. Blood, 2010. **116**(22): p. 4675-4683.

276. Savage, B., F. Almus-Jacobs, and Z.M. Ruggeri, Specific synergy of multiple substrate-receptor interactions in platelet thrombus formation under flow. Cell, 1998. **94**(5): p. 657-666.

277. Ruggeri, Z.M., Old concepts and new developments in the study of platelet aggregation. Journal of Clinical Investigation, 2000. **105**(6): p. 699-701.

278. Ruggeri, Z.M., J.A. Dent, and E. Saldívar, Contribution of distinct adhesive interactions to platelet aggregation in flowing blood. Blood, 1999. **94**(1): p. 172-178.

279. Savage, B., J.J. Sixma, and Z.M. Ruggeri, Functional self-association of von Willebrand factor during platelet adhesion under flow. Proceedings of the National Academy of Sciences of the United States of America, 2002. **99**(1): p. 425-430.

280. Kisucka, J., C.E. Butterfield, D.G. Duda, S.C. Eichenberger, S. Saffaripour, J. Ware, et al., Platelets and platelet adhesion support angiogenesis while preventing excessive hemorrhage. Proceedings of the National Academy of Sciences of the United States of America, 2006. **103**(4): p. 855-860.

281. Coller, B.S., U. Seligsohn, and P.A. Little, Type I Glanzmann thrombasthenia patients from the Iraqi-Jewish and Arab populations in Israel can be differentiated by platelet glycoprotein IIIa immunoblot analysis. Blood, 1987. **69**(6): p. 1696-1703.

282. Berman, M.E. and W.A. Muller, Ligation of platelet/endothelial cell adhesion molecule 1 (PECAM-1/CD31) on monocytes and neutrophils increases binding capacity of leukocyte CR3 (CD11D/CD18). Journal of Immunology, 1995. **154**(1): p. 299-307.

283. Horst, A.K., W.D. Ito, J. Dabelstein, U. Schumacher, H. Sander, C. Turbide, et al., Carcinoembryonic antigen-related cell adhesion molecule 1 modulates vascular remodeling in vitro and in vivo. Journal of Clinical Investigation, 2006. **116**(6): p. 1596-1605.

284. Nair, K.S. and S.M. Zingde, Adhesion of neutrophils to fibronectin: Role of the CD66 antigens. Cellular Immunology, 2001. **208**(2): p. 96-106.

285. Rathore, V., M.A. Stapleton, C.A. Hillery, R.R. Montgomery, T.C. Nichols, E.P. Merricks, et al., PECAM-1 negatively regulates GPIb/V/IX signaling in murine platelets. Blood, 2003. **102**(10): p. 3658-3664.

286. Thai, L.M., L.K. Ashman, S.N. Harbour, P.M. Hogarth, and D.E. Jackson, Physical proximity and functional interplay of PECAM-1 with the Fc receptor FcγRIIa on the platelet plasma membrane. Blood, 2003. **102**(10): p. 3637-3645.

287. Alshahrani, M.M., E. Yang, J. Yip, S.S. Ghanem, S.L. Abdallah, A.M. deAngelis, et al., CEACAM2 negatively regulates hemi (ITAM-bearing) GPVI and CLEC-2 pathways and thrombus growth in vitro and in vivo. Blood, 2014. **124**(15): p. 2431-2441.

288. Mahooti, S., D. Graesser, S. Patil, P. Newman, G. Duncan, T. Mak, et al., PECAM-1 (CD31) expression modulates bleeding time in vivo. American Journal of Pathology, 2000. **157**(1): p. 75-81.

289. Horst, A., CEA a thrombus CAM: CEACAM2, a twin of CEACAM1? Blood, 2014. **124**(15): p. 2323-2324.

290. Moroi, M., S. Jung, K. Shinmyozu, Y. Tomiyama, A. Ordinas, and M. Diaz-Ricart, Analysis of platelet adhesion to a collagen-coated surface under flow conditions: the involvement of glycoprotein VI in the platelet adhesion. Blood, 1996. **88**(6): p. 2081-2092.

291. Rosen, E.D., S. Raymond, A. Zollman, F. Noria, M. Sandoval-Cooper, A. Shulman, et al., Laser-induced noninvasive vascular injury models in mice generate platelet- and coagulation dependent thrombi. American Journal of Pathology, 2001. **158**(5): p. 1613-1622.

9 Chapter Nine: Appendix

9.1 Published scientific paper (Blood journal)

CEACAM2 negatively regulates hemi (ITAM-bearing) GPVI and CLEC-2 pathways and thrombus growth *in vitro* and *in vivo*